D4.2 Underground simulations of the HOCLOOP concept at the selected pilot sites

Deliverable No.: D4.2

Deliverable lead: VITO

Authors: E. Hernandez (VITO), J. Pogacnik (VITO), V. Leontidis (IFPEN)

Dissemination level: PU

Due date : 31.03.2025

Submission date: 31.03.2025

Funded by the European Union. Views and opinions expressed are however those of the author(s) only and do not necessarily reflect those of the European Union or CINEA. Neither the European Union nor the granting authority can be held responsible for them.

PROJECT INFORMATION

PROJECT ACRONYM	HOCLOOP
Call ID	HORIZON- CL5-2021-D3-03-15
Project title	A circular by design environmentally friendly geothermal energy solution based on a horizontal closed loop - HOCLOOP
Grant Agreement No	101083558
Start of Project	01.10.2022
Project Duration	42 Months
Type of Action	HORIZON Research and Innovation Actions
Coordinator	IFE

DOCUMENT INFORMATION

Deliverable No.	D4.2
Work Package	WP2
Deliverable Lead	VITO
Deliverable Authors	E. Hernandez (VITO), J. Pogacnik (VITO), V. Leontidis (IFPEN), Hung Pham (TUD), P. Wojnarowski (AGH), L. Pająk (AGH), M. Kaczmarczyk (AGH), Daniele Fiaschi (UNIFI), Pietro Ungar (UNIFI), Federico Gigliotti (UNIFI), Edoardo Falchini (UNIFI)
Issue	1/1
Due date	31.03.2025
Submission date	31.03.2025
Dissemination level[1]	PU

[1] Dissemination level: **PU** = Public, **SEN** = Sensitive, **R-UE/EU-R** = EU classified, **C-UE/EU-C** = EU classified, **S-UE/EU-S** – EU classified

This project has received funding from the European Union's Horizon Europe research and innovation program under grant agreement No 101083558

Nature[2]	R
Copyright	© 2023 Consortium

DOCUMENT HISTORY

DATE	VERSION	MODIFIED BY	COMMENT
18.02.2025	0.1	E. Hernandez (VITO), J. Pogacnik (VITO), V. Leontidis (IFPEN), Hung Pham (TDA), Federico Gigliotti (UNIFI), Paweł Wojnarowski (AGH), Leszek Pająk (AGH), Michał Kaczmarczyk (AGH)	First draft for internal revision
25.02.2025	0.2	V. Harcouët-Menou (VITO)	First internal revision
14.03.2025	0.3	E. Hernandez (VITO), J. Pogacnik (VITO), V. Leontidis (IFPEN), Hung Pham (TDA), Federico Gigliotti (UNIFI), Paweł Wojnarowski (AGH), Leszek Pająk (AGH), Michał Kaczmarczyk (AGH)	Distributed for review to authors
20.03.2025	0.4	V. Harcouët-Menou (VITO)	Second internal review
21.03.2025	1.0	E. Hernandez (VITO), J. Pogacnik (VITO), V. Leontidis (IFPEN), Hung Pham (TDA), Federico Gigliotti (UNIFI), Paweł Wojnarowski (AGH), Leszek Pająk (AGH), Michał Kaczmarczyk (AGH)	Review addressed
31.03.2025	2.0	Mario Silva (IFE)	Final version (approval)

[2] Nature of the deliverable: deliverable: **R** = Document, report; **DEM** – Demonstrator, pilot, prototype; **DEC** – Websites, patent, filings, videos etc; **DATA** – data sets, microdata, etc; **DMP** – Data Management Plan; **ETHICS**; **SECURITY**; **OTHER**

This project has received funding from the European Union's Horizon Europe research and innovation program under grant agreement No 101083558

TABLE OF CONTENT

PROJECT INFORMATION 2
DOCUMENT INFORMATION 2
DOCUMENT HISTORY 3
TABLE OF CONTENT 4
LIST OF TABLES 6
LIST OF FIGURES 8
EXECUTIVE SUMMARY 16
Scope of the deliverable 16
Main conclusions 16
1. Introduction 18
2. Methodology 19
3. Results 20
3.1. Belgium case study 20
3.1.1. Introduction 20
3.1.2. Collected available data 20
3.1.3. Simulation procedure 25
3.1.4. Integration scenarios 27
3.1.5. Simulation of the integration scenarios and results 28
3.1.6. Conclusions of the Belgium case 45
3.2. German case study 46
3.2.1. Introduction 46
3.2.2. Collected available data 49
3.2.3. Simulation procedure 50
3.2.4. Integration scenarios 52
3.2.5. Simulation of the integration scenarios and results 53
3.2.6. Conclusion and outlook 56
3.3. French case study 57
3.3.1. Introduction 57
3.3.2. Collected available data 57
3.3.3. Simulation procedure 59
3.3.4. Integration scenarios 60
3.3.5. Simulation of the integration scenarios and results 60
3.3.6. Conclusion of the French case 68
3.4. Italian case study 69
3.4.1. Introduction 69
3.4.2. Collected available data 69
3.4.3. Simulation procedure 71

This project has received funding from the European Union's Horizon Europe research and innovation program under grant agreement No 101083558

3.4.4. Integration scenarios 74
3.4.5. Simulation of the integration scenarios and results 82
3.4.6. Conclusions of the Italian cases 89
3.5. Polish case study 89
3.5.1. Introduction 89
3.5.2. Geological and well-characteristic 89
3.5.3. Simulation procedure 95
3.5.4. Integration scenarios 101
3.5.5. Simulation of the integration scenarios and results 103
3.5.6. Conclusions of the case of Poland 125
4. Conclusions 126
5. References 128
Annex 1- MOL-GT-03 well trajectory 130
Annex 2- Fluid flow rate optimization procedure 131
Annex 3- Detailed results of the simulations for the Polish case 133

This project has received funding from the European Union's Horizon Europe research and innovation program under grant agreement No 101083558

LIST OF TABLES

Table 1. Geometrical characteristics of the casings, liners, open-hole section and cemented layers in well MOL-GT-03 21

Table 2. Thermal properties of the completion elements in well MOL-GT-03 23

Table 3. Rock thermal conductivity, rock heat capacity, temperature gradient and surface temperature 23

Table 4. Comparison of model's thermal parameters and referential measured values used for modelling MOL-GT-03 25

Table 5. Definition of the average properties of well's wall for GTW simulator. The well's walls are defined in Table 1. 26

Table 6. Characteristics of HOCLOOP completion tubing 27

Table 7. Thermal properties of HOCLOOP tubing 27

Table 8. Properties of the recirculating fluid for the HOCLOOP application 27

Table 9. Description of simulated cases for Scenario a: Pre-heating the working fluid of VITO geothermal plant 29

Table 10. HOCLOOP Well injection conditions at the wellhead 31

Table 11. Description of cases with a horizontal section 34

Table 12. Resume of injection conditions and main outputs – Pre-heating working fluid of VITO geothermal plant. W: winter, S: summer 35

Table 13. Heat requirements for the heating network of the new buildings 37

Table 14. Cases considered for simulation of scenario b: Integration of HOCLOOP system with the new buildings 38

Table 15. Well control conditions for integration scenario b 39

Table 16. Seasonal usage scenario results for MOL-GT-03 as drilled. 39

Table 17. 7-month seasonal usage results for MOL-GT-03 with 500 m horizontal sidetrack 40

Table 18. Different studied scenarios for MD-BTES system of Darmstadt site with 19 boreholes scenario 47

Table 19. Geological properties for modelling – Darmstadt site 51

Table 20 Different studied scenarios for integrating HOCLOOP concept in Darmstadt site 53

Table 21. Technical characteristics of the three well in Fresnes, France geothermal site. 57

Table 22. Thermal properties of all geological layers for the Paris basin. 58

Table 23. Characteristics of the GFR-3 well completion in Fresnes, France. 59

Table 24. Properties of the materials in the wellbore for the Fresnes site in France. 60

Table 25. Thermal properties of all geological layers for the three Italian cases 69

This project has received funding from the European Union's Horizon Europe research and innovation program under grant agreement No 101083558

Table 26. System Model Parameters 75
Table 27. Interpolation parameters for EP_{li} 76
Table 28. Estimated overall residential heating consumption 76
Table 29. Values of the parameters used in the calculations 81
Table 30. Simplified chroostratigraphic profile for Goleniów IG-1 (based on CBDG, access: 12.2024) 93
Table 31: Simplified lithostratigraphic profile Goleniów IG-1 (based on CBDG, access: 12.2024) 93
Table 32. Estimated stratigraphic profile for well – salt dome case 96
Table 33. Well stratigraphy 97
Table 34. Geometrical characteristics of the casings. and cemented layers - salt dome cases 98
Table 35. Geometrical characteristics of the casings. and cemented layers - salt pillow cases 99
Table 36. Rock properties – salt dome cases 100
Table 37. Rock properties – salt pillow cases 100
Table 38. Properties of the recirculating fluid for the HOCLOOP application in Goleniów site study 101
Table 39. Injection pressure depend on flow rates 104

This project has received funding from the European Union's Horizon Europe research and innovation program under grant agreement No 101083558

LIST OF FIGURES

*Figure **1.** Depth map of the top of the Lower Carboniferous Limestone Group around VITO geothermal plant (left) and the projection of MOL-GT-03 well (dashed green line) on the geological cross section between wells MOL-GT-01(red line) and MOL-GT-02 (light blue) at the right figure. The trajectory of the cross section is shown as a red line in the left figure [1].* 20

*Figure **2.** Visualization of MOL-GT-03 well trajectory* 22

*Figure **3.** Description of MOL-GT-03 cased and non-cased sections and drilled geological formations.* 22

*Figure **4.** Initial temperature distribution versus depth in well MOL-GT-03* 24

*Figure **5.** Domains considered in GTW simulator for modelling closed-loop single well systems like HOCLOOP system* 25

*Figure **6.** Wellbore layers definition for computing average properties of the segments. A: area, r: radius and CP:heat capacity* 26

*Figure **7.** Possible integration schemes of HOCLOOP concept installed in well MOL-GT-03 with VITO's facilities. (a) Pre-heat the working used to carry the heat between Balmatt geothermal plant 'GEO' and VITO's research campus facilities. (b) provide heat to a new building development* 28

*Figure **8.** Illustration of well trajectories tested for Scenario a: Pre-heating the working fluid of VITO geothermal plant. Case a-1 is the original well trajectory, Case a-2 and Case a-3 consider the original well trajectory plus a horizontal section of 500 m and 1000 m respectively.* 29

Figure 9. Real operational conditions of the working fluid that transport the heat produced by the deep open-loop geothermal system to VITO's research campus. Testing phases of year 2022. 30

*Figure **10.** Sensitivity analysis result of flow rate on Gross Power.* 32

*Figure **11.** Sensitivity analysis result of flow rate on COP.* 32

*Figure **12.** Production temperature and power from well MOL-GT-03 using HOCLOOP for preheating VITO's research campus working fluid. Winter and summer periods are considered to last 6 months each. These periods imply different injection temperature while the injection rate is held constant during the year at 5 kg/sec. Case a-1: Original well trajectory of MOL-GT-03.* 33

*Figure **13.** Working fluid temperature after mixing the water injected in the well and the remaining working fluid from VITO research campus network considering original well geometry MOL-GT-03 Case a-1. Working fluid temperature before pre-heating is equal to injection temperature in the well. Injection fluid rate is 5 kg/sec (18 m^3/hr) while injection temperature is changed during winter (65 °C) and summer (70 °C).* 33

*Figure **14.** Working fluid temperature after pre-heating for two horizontals hypothetical sections in well MOL-GT-03: 500 m (left) and 1000 m (right). Injection fluid rate is 5 kg/sec (18 m^3/hr) while injection temperature is changed during winter (65 °C) and summer (70 °C)* 35

This project has received funding from the European Union's Horizon Europe research and innovation program under grant agreement No 101083558

*Figure **15.** Comparison of temperature increase of the VITO campus working fluid and produced thermal power when considering the well MOL-GT-03 with the original well geometry and by adding additional horizontal sections at the bottom. The well is continuously producing heat but injection temperature changes during summer (70°C) and winter (65°C)* 35

Figure 16: Contour plot of COP for various well horizontal lengths (0-4000 m) and flowrates (0-50 kg/s). 36

Figure 17: Gross power and pump power for horizontal well length and flowrate study. 37

*Figure **18.** Referential seasonal average demand of thermal power for the new buildings during a period of 20 years. It is assumed that the energy demand takes place during 7 months per year at constant load.* 38

*Figure **19.** Estimated 12-hour heat demand profile from the new buildings during a period of 1 year* 38

*Figure **20.** Results for seasonal usage scenario for MOL-GT-03 as drilled performed for testing the flow rate optimization methodology. Power demand is unable to be supplied when heat demand is increased from 0.49MW to 0.69MW (year 10). In this condition, the minimum production temperature of 45 °C controls the flow rate.* 40

*Figure **21.** Results for the 7-monthly heat demand scenario with a 500 m horizontal extension to the existing MOL-GT-03 well track used for testing the flow rate optimization methodology.* 41

*Figure **22.** Estimated well performance for 5 years of monthly averages, followed by a single year of 12-hourly demand values for heating the new buildings. Power output (red – top figure) in W, flowrate (blue – middle figure) in kg/s, and outflow temperature (black – bottom figure) in °C. The x-axis is years. The well is considered as drilled.* 42

*Figure **23.** Long term well performance for heating the new buildings. (a) Temperature, flow rate, and power delivered, and (b) tracking of minimum and maximum outlet temperature and flow rate for the Scenario 2 with Control 2 for 20 years of monthly demand.* 43

Figure 24 20 year monthly fluctuating demand scenario for 3000, 3500, 4000, 4500, and 4904 m MOL-GT-03 well lengths. 44

*Figure **25.** Darmstadt site – MD-BTES* 47

*Figure **26.** Darmstadt site – MD-BTES - Outlet temperature after 30 years of operation. The temperature drops from 44 degree from the beginning of extraction time to 32 degrees at the end* 48

*Figure **27.** Darmstadt site – MD-BTES - Heat power of 30 years operation, for the worst-case scenario, 1MW is expected.* 48

*Figure **28.** HOCLOOP solution replaces MD-BTES system in Darmstadt site* 49

***Figure 29.** Darmstadt site – Geological structural model with different blocks based on site investigation results. Block-1 and Block-4 are Granite type-A. Block-2, Block-5 and Block-6 are Granite type-B. Block-3 is Permian Andesite, and Block-7 is fractured rock.* 49

*Figure **30.** Finite element model – Darmstadt site* 50

*Figure **31.** Characteristics of the closed-loop string used in the simulations for the Darmstadt site.* 51

This project has received funding from the European Union's Horizon Europe research and innovation program under grant agreement No 101083558

Figure 32. HOCLOOP pipe in FEFLOW, the outlet pipe represents three layers of HOCLOOP pipe with the equivalent thermal conductivity 0.0264 W/mK 52

Figure 33. Darmstadt site - Heat output and outlet temperature depend on flow rate with two different scenarios 53

Figure 34. Darmstadt site – Different depth and different length – Extracted heat power after 30 years 54

Figure 35. Darmstadt site – Different inlet extraction temperature – Extracted heat power after 30 year 55

Figure 36. Darmstadt site – Different thermal gradient – Extracted heat power after 30 years 55

Figure 37. Schema of the geothermal plant in Fresnes, France. 57

Figure 38. Desing of the GFR-3 geothermal wellbore in the French site. 58

Figure 39. Characteristics of the closed-loop string used in the simulations for the French site. 60

Figure 40. Impact of flow rate on the temporal evolution of (a) the outlet temperature and (b) the pressure difference between outlet and inlet in the actual GFR-3 well of the French site. 61

Figure 41. Impact of inlet temperature in the temporal evolution of (a) the outlet temperature and (b) gross thermal power in the actual GFR-3 well of the French site 62

Figure 42. Comparison of the temporal evolution of the outlet temperature without and with an extension of the GFR-3 well in the French site 63

Figure 43. Comparison of the temporal evolution of the gross thermal power without and with an extension of the GFR-3 well in the French site 63

Figure 44. Comparison of the temporal evolution of the pressure difference between outlet and inlet without and with an extension of the GFR-3 well in the French site. 64

Figure 45. Evolution of inlet temperature and delivered gross thermal power for fixed outlet temperature (50 °C) and flow rate (3 kg/s) in the actual GFR-3 well of the French site. 65

Figure 46. Evolution of inlet temperature and delivered gross thermal power for fixed outlet temperature (65 °C) and flow rate (12 kg/s) with a 2 km horizontal extension of well GFR-3 of the French site. 65

Figure 47. Evolution of flow rate and delivered gross thermal power for fixed inlet (25 °C) and outlet (50 °C) temperatures in the actual GFR-3 well of the French site 66

Figure 48. Evolution of flow rate and delivered gross thermal power for fixed inlet (25 °C) and outlet (65 °C) temperatures in the actual GFR-3 well of the French site 66

Figure 49. Evolution of flow rate and delivered gross thermal power for fixed inlet (25 °C) and outlet temperatures (65 °C) in the GFR-3 well of the French site with a 2 km horizontal extension 66

Figure 50. Evolution of flow rate and delivered gross thermal power for fixed inlet (25 °C) and outlet (73 °C) temperatures in the GFR-3 well of the French site with a 4 km horizontal extension. 67

Figure 51. Evolution of flow rate and delivered gross thermal power with a seasonal variation of the inlet temperature and fixed outlet temperatures (65 °C) in the GFR-3 well of the French site with a 4 km horizontal

This project has received funding from the European Union's Horizon Europe research and innovation program under grant agreement No 101083558

extension.....67

*Figure **52.** Evolution of flow rate and delivered gross thermal power with a seasonal variation of the inlet temperature and fixed outlet temperatures (73 °C) in the GFR-3 well of the French site with a 4 km horizontal extension*.....67

*Figure **53.** Evolution of the temperature in the rock domain at (a) 1 m, (b) 5 m, (c) 10 m and (d) 50 m distance from the wellbore and in three total lengths for the GFR-3 well of the French site with a 4 km horizontal extension, and without (dashed lines) and with seasonal variation (solid lines) of the inlet temperature*.....68

*Figure **54.** Temperature profiles of two existing geothermal wells in the Amiata area with highlighted the two hydrothermal reservoir and the possible well profile that targets the low permeability section between the two*
.....70

*Figure **55.** Geothermal well model: heat transfer and discretization scheme*.....71

*Figure **56.** Benchmarking of time convolution and correlation*.....73

*Figure **57.** Benchmarking of the model considering off-design conditions and injection temperature control*.....73

Figure 58: Area selected for the case study (yellow - municipalities, bluish - industries, green - geothermal resource, orange - DHN).....74

*Figure **59.** Scheme of the proposed heating network*.....75

*Figure **60.** Calenzano power demand. The unshaded area, excluding summer operation for absorption refrigeration, has been considered to estimate the heating demand.*.....77

*Figure **61.** Annual average temperature in the Gargano region*.....77

*Figure **62.** Existing activities in the Manfredonia Area. Highlighted in the map are the targeted geothermal field (in green), residential areas (in yellow), Flat glass production plant (in blue), and Industrial fish market (in violet)*.....78

*Figure **63.** Schemes of the surface plant installation for the Gargano and Amiata Cases*.....78

*Figure **64.** Existing activities in the monte Amiata Area. Highlighted in the map are: the targeted geothermal field (in green), residential areas (in yellow), Floramiata industrial area (in blue), and Conventional geothermal power plant (in dark green). In orange is an existing DH network that provides residual heat from the geothermal power plant to Floramiata.*.....79

*Figure **65.** Historic temperatures and flow rates in the existing FLORAMIATA heating system. Notice that the flow rate is adjusted approximately on a monthly base while the dynamic adjustment to the power is handled by a variation of the injection temperature.*.....80

*Figure **66.** Off-design behaviour of the ORC. Dashed line represents the behaviour of the cycle with if the water flow rate drops to 0.75x of the design condition while dotted lines represent the behaviour of the cycle with water flow rate equal to 1.25x of the design.*.....80

*Figure **67.** Validation of the correlation for the prediction of the ORC power output for different inlet temperatures and water flow rate percentage. The absolute power refers to a 300kg/s flow rate of water.*.....81

This project has received funding from the European Union's Horizon Europe research and innovation program under grant agreement No 101083558

Figure 68. Control 1 results Top left in dashed lines are represented the injection temperature in the well while in the continuous lines are the outlet temperature, both with different number of operating wells. Bottom left graph represents the circulating mass flow rate. On the right, the graph shows the outlet temperature over time.....82

Figure 69. Control 2 results: On the top left in dashed lines are represented the injection temperature in the well while in the continuous lines are the outlet temperature, both with different number of operating wells. The graph on the bottom left represents the circulating mass flow rate. On the right, the graph shows the outlet temperature over time.....83

Figure 70. Extracted power from an HOCLOOP well installed in the Gargano area for different depths, horizontal section lengths and flow rates.....84

Figure 71. Extracted power from an HOCLOOP well installed in the Gargano area for different depths, horizontal section lengths and flow rates.....85

Figure 72. Ejection cycle cooling capacity for different depth and horizontal section (the flow rate has been chosen to maximize the cooling capacity itself).....86

Figure 73. In the figure are shown the inlet and outlet temperature of the geothermal well and the electrical power output of the ORC plant with two different configurations.....87

Figure 74. In the graphs are shown the inlet and outlet temperature of the geothermal well, the mass flow rate and the outlet temperatures of the well during the first and the tenth year of operation, respectively from the top left to the bottom.....88

Figure 75. Capacity factor and average power of the ORC power plant for each year of operation.....89

Figure 76. Location of salt structure in the Szczecin region on the Tectonic Map of the Zechstein-Mesozoic complex in the Polish Lowlands, 1:500000 (after Dadlez, 1998) with forms favorable for CGS (based on Czapowski & Tomassi-Morawiec, 2012, modified).....90

Figure 77. Geological cross-section through the salt structures of Maszewo and Grzęzno (Sowiżdżał, 2009). Cross-section location line in Figure 76.....91

Figure 78. Geological cross-section along the T0076209 seismic line passing through the Goleniów rock salt diapir deposit (based on PGI, 2014,[18]).....92

Figure 79. Temperature profile for Goleniów IG-1.....95

Figure 80. The well trajectory – salt dome case (1000 m horizontal part).....96

Figure 81. The temperature distribution with depth – salt dome case.....97

Figure 82. The well trajectory – salt pillow case (1000 m horizontal part).....97

Figure 83. The temperature distribution with depth – salt pillow case.....98

Figure 84. The general scheme of the system utilized the HOCLOOP units without heat pump utilization.....102

Figure 85. The scheme of the HOCLOOP system supplemented by a heat pump unit.....102

Figure 86. The output heat power for salt dome, horizontal part 2000 [m] case depending on the inlet temperature

This project has received funding from the European Union's Horizon Europe research and innovation program under grant agreement No 101083558

and flow rate 106

Figure 87. The output heat power for salt dome, horizontal part 2500 [m] case depending on the inlet temperature and flow rate 107

Figure 88. The output heat power for salt pillow, horizontal part 1000 [m] case depending on the inlet temperature and flow rate 108

Figure 89. The output heat power for salt pillow, horizontal part 2000 [m] case depending on the inlet temperature and flow rate 110

Figure 90. Input temperature for HOCLOOP system – installation without Heat Pump 111

Figure 91. Input temperature for HOCLOOP system – installation with Heat Pump (case 1.2) 112

Figure 92. The output temperatures and heat power for salt dome, horizontal part 2000 [m] case depending on the flow rate – without Heat Pump 113

Figure 93. The output temperatures and heat power for salt dome, horizontal part 2000 [m] case depending on the flow rate – with Heat Pump 113

Figure 94. The output temperatures and heat power for salt dome, horizontal part 2500 [m] case depending on the flow rate – without Heat Pum 114

Figure 95. The output temperatures and heat power for salt dome, horizontal part 2500 [m] case depending on the flow rate – with Heat Pump 114

Figure 96. The output temperatures and heat power for salt pillow, horizontal part 1000 [m] case depending on the flow rate – without Heat Pump 115

Figure 97. The output temperatures and heat power for salt pillow, horizontal part 1000 [m] case depending on the flow rate – with Heat Pump 115

Figure 98. The output temperatures and heat power for salt pillow, horizontal part 2000 [m] case depending on the flow rate – without Heat Pump 116

Figure 99. The output temperatures and heat power for salt pillow, horizontal part 2000 [m] case depending on the flow rate – with Heat Pump 116

Figure 100. The power changes after 20 years of HOCLOOP heat exchanger operation as a function of flow rate 117

Figure 101. The changes in power divided by the pressure difference at the input and output of the heat exchanger 118

Figure 102. The changes in power divided by the input pressure of the heat exchanger 119

Figure 103. Ordered and time-dependent demand for thermal power covered by energy source 120

Figure 104. Ordered and time-dependent way of power control used in the Goleniów district heating (defined based on system design parameters and TMY – PV GIS in the location of Goleniów) 121

Figure 105. Coverage of power demand in the case of the direct HOCLOOP units utilisation (no heat pumps), in

This project has received funding from the European Union's Horizon Europe research and innovation program under grant agreement No 101083558

Case-X2 (20 m3/hr flow of water by each HOCLOOP unit), number of units: 3, various inlet temperatures (time and power-dependent), horizontal length of the well 2 km, location the salt dome, 10th year of the system exploitation. Ordered (top) and time-dependent curves (bottom) 122

*Figure **106.** The share of energy production in lifetime of the system in the case of the direct HOCLOOP units utilisation (no heat pumps), in Case-X2 (20 m3/hr flow of water by each HOCLOOP unit), number of units: 3, various inlet temperatures (time and power-dependent), horizontal length of the well 2 km, location the salt dome (share in the lifetime: direct geothermal 43.6%, heat pumps 0.0%, peak sources 56.4%)* 123

*Figure **107.** Coverage of power demand in the case of the direct HOCLOOP units utilisation supported by heat pumps, in Case-X2 (20 m3/hr flow of water by each HOCLOOP unit), number of units: 3, various inlet temperatures (time and power-dependent), horizontal length of the well 2 km, location the salt dome, 10th year of the system exploitation. Ordered (top) and time-dependent curves (bottom)* 124

*Figure **108.** The share of energy production in the lifetime of the system in the case of the direct HOCLOOP units utilisation supported by heat pumps, in Case-X2 (20 m3/hr flow of water by each HOCLOOP unit), number of units: 3, various inlet temperatures (time and power-dependent), the horizontal length of the well 2 km, location the salt dome (share in the lifetime: direct geothermal 43.5%, heat pumps 12.9%, peak sources 43.6%. Total share of renewables, including energy obtained by heat pumps evaporators 52.4%)* 125

Figure 109: Example linear interpolation iteration technique to find minimum flowrate for required power. 132

Figure 110: The output temperatures for salt dome, horizontal part 2000 [m] case depending on the inlet temperature and flow rate 134

Figure 111: The temperature distribution in the HOCLOOP borehole heat exchanger for salt dome, horizontal part 2000 [m] case - T_{in} = 30 [°C] 135

Figure 112: The temperature distribution in the HOCLOOP borehole heat exchanger for salt dome, horizontal part 2000 [m] case - T_{in} = 60 [°C] 136

Figure 113: The output temperatures for salt dome, horizontal part 2500 [m] case depending on the inlet temperature and flow rate 137

Figure 114: The temperature distribution in the HOCLOOP borehole heat exchanger for salt pillow, horizontal part 1000 [m] case - T_{in} = 30 [°C] 139

Figure 115: The temperature distribution in the HOCLOOP borehole heat exchanger for salt pillow, horizontal part 1000 [m] case - T_{in} = 60 [°C] 140

Figure 116: The output temperatures for salt pillow, horizontal part 2000 [m] case depending on the inlet temperature and flow rate 141

Figure 117: The temperature distribution in the HOCLOOP borehole heat exchanger for salt pillow, horizontal part 2000 [m] case - T_{in} = 30 [°C] 142

Figure 118: The temperature distribution in the HOCLOOP borehole heat exchanger for salt pillow, horizontal part 2000 [m] case - T_{in} = 60 [°C] 144

This project has received funding from the European Union's Horizon Europe research and innovation program under grant agreement No 101083558

Figure 119: The temperature distribution in the HOCLOOP borehole heat exchanger for salt dome, horizontal part 2000 [m] case – variable T_{in} without Heat Pump 145

Figure 120: The temperature distribution in the HOCLOOP borehole heat exchanger for salt dome, horizontal part 2000 [m] case – variable Tin with Heat Pump 146

Figure 121: The temperature distribution in the HOCLOOP borehole heat exchanger for salt dome, horizontal part 2500 [m] case – variable T_{in} without Heat Pump 147

Figure 122: The temperature distribution in the HOCLOOP borehole heat exchanger for salt dome, horizontal part 2500 [m] case – variable T_{in} with Heat Pump 149

Figure 123: The temperature distribution in the HOCLOOP borehole heat exchanger for salt pillow, horizontal part 1000 [m] case – variable T_{in} without Heat Pump 150

Figure 124: The temperature distribution in the HOCLOOP borehole heat exchanger for salt pillow, horizontal part 1000 [m] case – variable T_{in} with Heat Pump 151

Figure 125: The temperature distribution in the HOCLOOP borehole heat exchanger for salt pillow, horizontal part 2000 [m] case – variable T_{in} without Heat Pump 152

Figure 126: The temperature distribution in the HOCLOOP borehole heat exchanger for salt pillow, horizontal part 2000 [m] case – variable T_{in} with Heat Pump 153

This project has received funding from the European Union's Horizon Europe research and innovation program under grant agreement No 101083558

EXECUTIVE SUMMARY

Scope of the deliverable

The objective of WP4 is to pave the way for future demonstration projects and assess the forward portability of the HOCLOOP solution. It includes simulation, pre-feasibility, and pre-design of the HOCLOOP concept in selected pilot sites. Within WP4, Tasks 4.2 aims at modelling of the heat extraction at the selected pilot sites using the simulation tools developed in T2.3. Deliverable 4.2 presents the conceptual closed loop systems designed specifically for each pilot as well as the different scenarios and input parameters used to assess the long-term energetic performance of the conceptual systems. The results of the dynamic simulations obtained using the simulation tools developed in T2.3 are presented and discussed. The modelling exercise contributes towards the selection of optimal combination of geological and surface conditions for the HOCLOOP concept. In addition, it supports the conceptual design of the integration of the HOCLOOP concept in the existing or future local energy system of the selected pilot sites.

Main conclusions

The Belgium case considered the potential use of the HOCLOOP concept under two integration schemes with VITO facilities: pre-heating the working fluid for the deep geothermal plant and directly heating new buildings designed for low-temperature heat sources. The reuse of the deep dry well (MOL-GT-03), with an added horizontal section, was considered for implementation. Pre-heating the working fluid could result in an extra 250–300 kW of thermal power for the plant (~10–15% of the plant's actual capacity). With an additional 1,000 m horizontal section, power could rise to 600 kW (24% of capacity), though still below 1 MW due to high injection temperatures and thermal losses. A detailed economic analysis is required, particularly for horizontal drilling feasibility. On the other hand, heating the new buildings offers advantages because the heat is required at low temperature (minimum 45°C) and the heat demand is moderate (≈2015MWy). Under these demand conditions, the well can meet the energy demand for more than 20 years, achieving this without the need for additional drilling. Heating the new building is thus the preferred option from an efficiency perspective, as it is expected to result in lower heat losses and higher heat flow rates. Additionally, this approach does not require further drilling.

The Darmstadt case compares the HOCLOOP solution with a medium-deep borehole thermal energy storage (MD-BTES) system. Due to the lower temperature gradient in Darmstadt, and excluding economic considerations, the HOCLOOP solution produces less heat than the MD-BTES system during the winter period.

The Paris case considers the repurposing of existing wells (doublet) in a low temperature geological setting. The simulations results showed that the use of closed-loop will always produce much lower thermal power when compared to the existing geothermal doublet. In addition, for the system to be able to deliver to the district heating system a fluid with constant temperature, the flow rate in the well must be controlled.

For the Italian cases, the results of the simulations show that the HOCLOOP solution is able to provide a reasonable amount of heat for the medium and high gradient areas (Gavorrano and Amiata) without interacting with the underground hydrothermal environment. In the Amiata case they also show that the predicted outlet temperature is high enough to produce some electrical power alongside providing heat to the final user. On the other hand, in the Gargano area, the extremely low gradient significantly limits the

This project has received funding from the European Union's Horizon Europe research and innovation program under grant agreement No 101083558

power that can be extracted from the well and, consequently, the cooling capacity of the ejection cycle. As a result, implementing the HOCLOOP solution at this location is likely unjustified, particularly given the high costs associated with drilling the necessary deep well.

For the Polish case, two integration options of the HOCLOOP concept were investigated at the Goleniów facilities to supply heat to the existing district heating network. The simulations enable to understand the potential benefits of HOCLOOP systems in combination with heat pumps or as stand-alone systems. The calculations show that by implementing HOCLOOP, the share of renewable energy is significant, exceeding 40% in both configurations and reaching over 50% with heat pumps. A flow rate of 20 m^3/h, as assumed in the calculations and validated by underground system analysis, ensures stable thermal power output over time, confirming the system's reliable operation. Defining the optimal solution requires establishing economic boundary conditions, with underground heat exchanger installation costs being a key factor. System optimization, including economic feasibility, will be addressed in later project stages, and the tools developed so far provide all necessary data for this process.

This project has received funding from the European Union's Horizon Europe research and innovation program under grant agreement No 101083558

1. Introduction

The HOCLOOP project aims to develop an environmentally friendly, circular-by-design geothermal energy solution based on a horizontal closed-loop system. Deliverable D4.2 focuses on simulating the performance of the HOCLOOP system at selected pilot sites in Belgium, Germany, France, Italy, and Poland. These simulations play a crucial role in understanding the concept's feasibility and optimizing the design for various geological and operational conditions.

This work builds on the data collection and site characterization performed in Task 4.1 (as reported in Deliverable D4.1), leveraging the geological, thermal, and available data obtained from each pilot location. The primary objectives of this deliverable are to:

- Assess the long-term thermal performance of the HOCLOOP system at the selected pilot sites.
- Identify optimal operational parameters such as flow rates, injection temperatures, and well configurations.
- Support future decisions regarding system design, integration with local energy networks, and potential scaling for demonstration projects.

This deliverable presents simulations conducted using advanced numerical models developed under WP2, including the GTW simulator and other tailored modeling tools that were benchmarked under WP2. Different well configurations (vertical, deviated, and horizontal extensions) and operational scenarios are explored to assess the adaptability and efficiency of the HOCLOOP system across varying geological contexts and surface uses.

By providing a comprehensive analysis of underground simulations, D4.2 contributes to the overarching goal of the HOCLOOP project: to develop a robust, scalable, and environmentally sustainable geothermal solution adaptable to diverse European geological settings.

This project has received funding from the European Union's Horizon Europe research and innovation program under grant agreement No 101083558

2. Methodology

First, for each site, the input parameters, resulting from the data collection phase in T4.1 are summarized and their quality is being discussed. Second, the simulation procedure to define the static thermal is presented. Then the conceptual closed loop systems designed specifically for each pilot is described as well as the different scenarios used to assess the long-term energetic performance of the conceptual systems. The results of the dynamic simulations obtained using the simulation tools developed in T2.3 are presented and discussed.

This project has received funding from the European Union's Horizon Europe research and innovation program under grant agreement No 101083558

3. Results

3.1. Belgium case study

3.1.1. Introduction

The Balmatt site, located in Belgium, has been selected as one of the case studies for analysing the long-term energetic performance of the HOCLOOP concept. This site includes a geothermal plant that was built for processing the brine and transferring the heat produced from a deep open-loop doublet geothermal system to VITO's research campus and nearby areas. During the plant's development and testing phases, extensive geological data was collected. This valuable information serves as the foundation for conducting a realistic analysis of the HOCLOOP concept. In addition to the two wells of the doublet in operation, the facility includes a non-productive well (MOL-GT-03). This well has been selected as a potential candidate to be utilized for deploying the HOCLOOP technology. A comprehensive description of this site and the available data is provided in deliverable D4.1 [1].

3.1.2. Collected available data

3.1.2.1. Geological data

The option that is being investigated for the Belgium case study consists in installing the HOCLOOP well completion in the existing well MOL-GT-03 shown in Figure **1**.

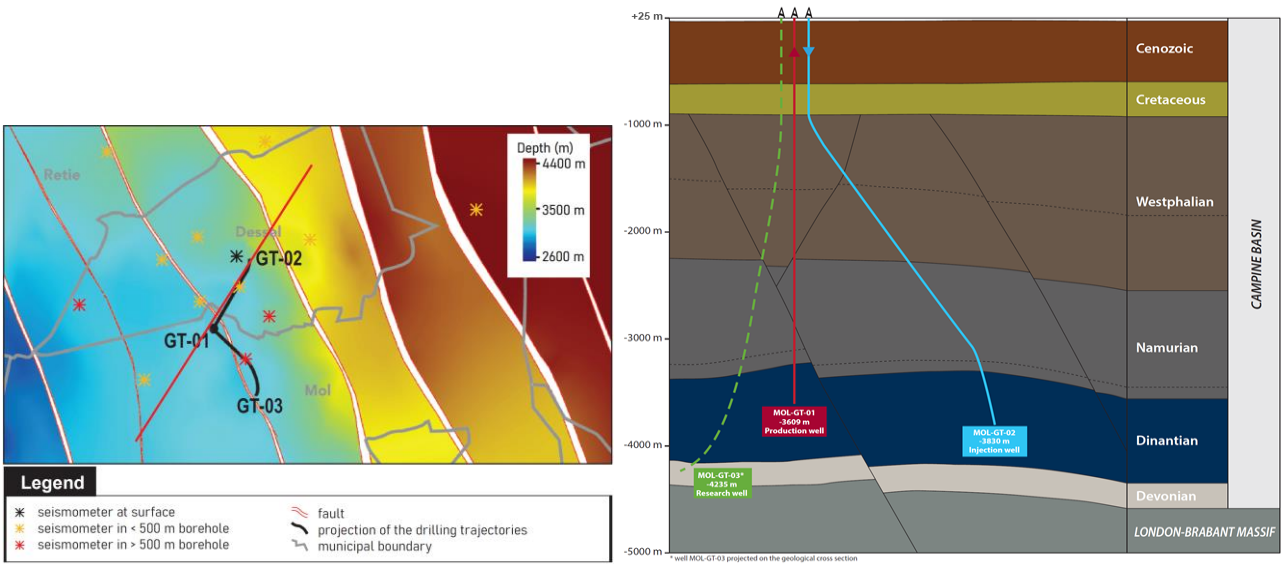

*Figure **1.** Depth map of the top of the Lower Carboniferous Limestone Group around VITO geothermal plant (left) and the projection of MOL-GT-03 well (dashed green line) on the geological cross section between wells MOL-GT-01(red line) and MOL-GT-02 (light blue) at the right figure. The trajectory of the cross section is shown as a red line in the left figure [1].*

The well was initially drilled for the open-loop deep geothermal project associated with the VITO geothermal plant. However, testing revealed poor permeability, leading to its classification as a dry well. Reusing this well could result in significant cost savings by eliminating the need for drilling a new deep well to test the HOCLOOP technology at this site.

This project has received funding from the European Union's Horizon Europe research and innovation program under grant agreement No 101083558

3.1.2.2. Data on existing well candidate for the implementation of the HOCLOOP system

MOL-GT-03 is a deviated well with a total vertical depth of 4230 m and a total trajectory of 4905 m as shown in Figure **2**. The well trajectory can be found in Annex 1. To further assess the well's thermal potential, some of the modelled scenarios included a hypothetical horizontal section at the well's bottom.

The well structure consists of both cased and uncased sections, from top to bottom as follows: a conductor pipe at the top, followed by four casing strings, a short hanging liner, and finally, an open-hole section at the bottom as shown in Figure 3. The diameters and properties of these different sections and the corresponding cemented sections are described in Table 1 and Table **2**.

*Table **1.** Geometrical characteristics of the casings, liners, open-hole section and cemented layers in well MOL-GT-03*

Casing and liner layers

Well's walls	Top depth [m MD]	Bottom Depth [m MD]	OD [inches]	ID [inches]
1	0	30	32	31.5
2	0	206	24	23.5
3	0	874	18.625	17.755
4	0	2183	13.375	12.347
5	2067	3600	9.625	8.535
6	3533.2	3750	7	6.184
7	3750	4905	8.5	

Cement Layers

	Top depth [m MD]	Bottom Depth [m MD]	OD	ID
8	0	206	31.5	24
9	0	874	23.5	18.625
10	0	2183	17.755	13.375
11	2067	3600	12.5	9.625

* MD: Measured depth, OD: Outer diameter, ID:Inner diameter, K: thermal conductivity

This project has received funding from the European Union's Horizon Europe research and innovation program under grant agreement No 101083558

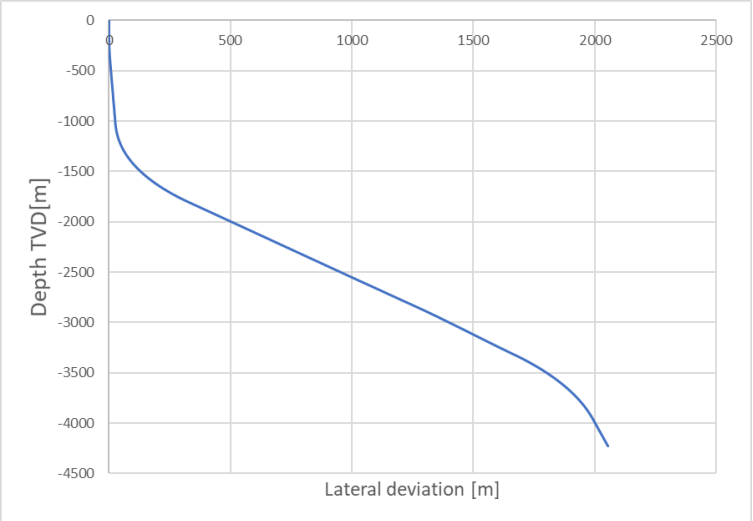

*Figure **2.** Visualization of MOL-GT-03 well trajectory*

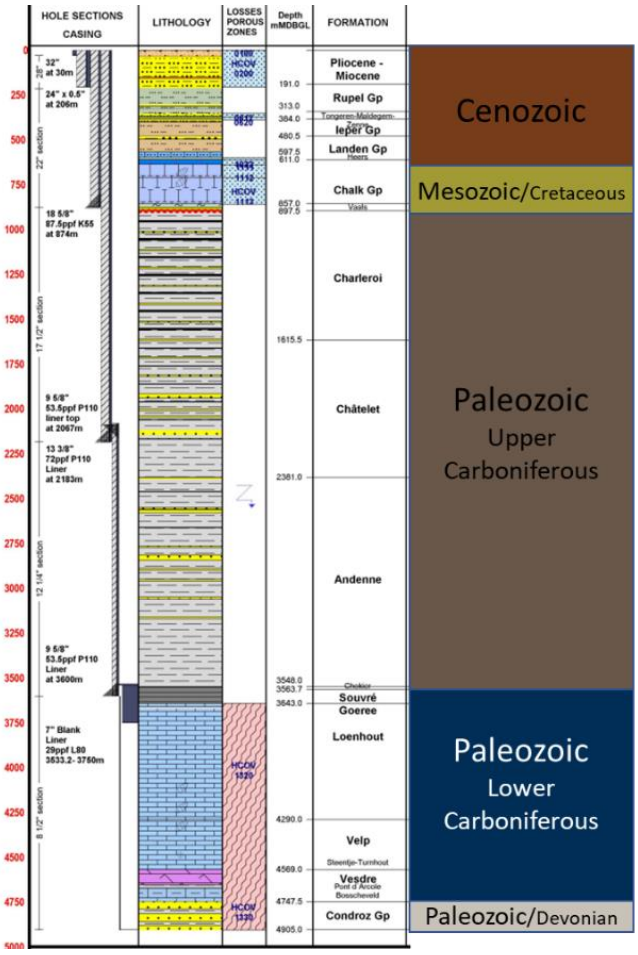

*Figure **3.** Description of MOL-GT-03 cased and non-cased sections and drilled geological formations.*

This project has received funding from the European Union's Horizon Europe research and innovation program under grant agreement No 101083558

*Table **2.** Thermal properties of the completion elements in well MOL-GT-03*

	Casing/liner	Cement
Heat conductivity [W/m*C]	45	0.896
Heat capacity [J/kg*C]	420	1400
Density [kg/m^3]	7000	3140

3.1.2.3. Thermal static model

The thermal static state of well MOL-GT-03 is based on a simplified thermal model assuming five geological layers to which thermal rock properties and corresponding temperature gradient have been assigned. The properties of the different layers are presented in Table 3. These layers were defined based on rocks of similar age and thermal properties. Due to fundamental heat diffusion, the temperature gradients are related with the thermal conductivity of the rock 'K'. Thus, the highest temperature gradient '0.043 °C/m' is found in the upper carboniferous where the rock conductivity is the lowest as shown in Table **3**. In addition, at this site the surface temperature is assumed to be 11°C. The mentioned static state or initial temperature along MOL-GT-03 well trajectory is shown in Figure **4**.

*Table **3.** Rock thermal conductivity, rock heat capacity, temperature gradient and surface temperature*

Thermal rock layer	Top trajectory [m MD]	Bottom trajectory [m MD]	K [W/m-°C]	Cp [J/Kg.K]	Temperature gradient [°C/m TVD]	Temperature at layer bottom [°C]
Cenozoic	0	636	2.00	930	0.029	29
Cretaceous - Mesozoic	636	897.5	1.89	800	0.029	37
Upper carboniferous - Paleozoic	897.5	3643	1.4	903.5	0.043	134
Lower carboniferous - Paleozoic	3643	4747	2.70	933.8	0.021	153
Devonian - Paleozoic	4747	4905	2.48	933.8	0.021	156

Surface Temperature [°C]	11

MD: Measured depth, TVD: True vertical depth, K: Thermal conductivity, Cp: Specific Heat Capacity

This project has received funding from the European Union's Horizon Europe research and innovation program under grant agreement No 101083558

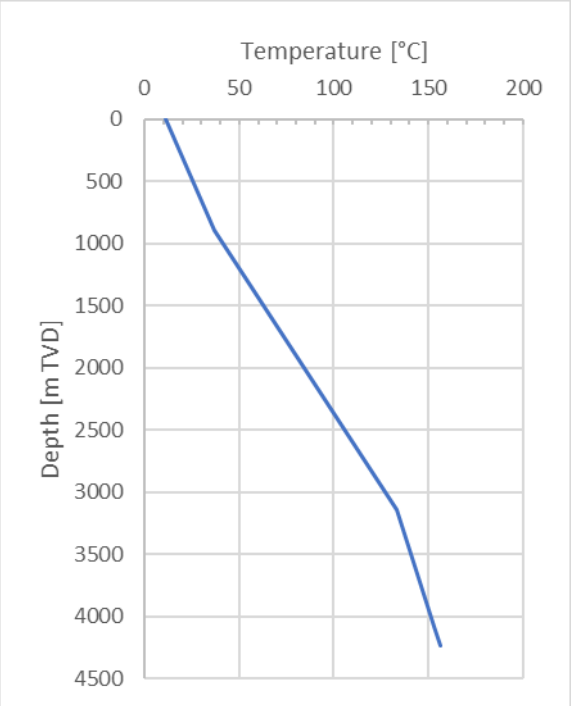

*Figure **4.** Initial temperature distribution versus depth in well MOL-GT-03*

3.1.2.4. Input data quality

The quality of the results of the simulations is directly influenced by the uncertainty of the input data. For the simulations conducted at the Belgium site considering testing of the HOCLOOP concept in well MOL-GT-03 for the, the uncertainty is lower compared to sites without drilled wells. This is because the thermal properties and temperature at this site have been either directly measured or estimated from the acquired information in the drilled wells at the VITO geothermal plant. For instance, temperature observations at different depths and rock lithology defined via logs and core samples measured not only in the well MOL-GT-03 but also in the wells MOL-GT-01 and MOL-GT-02 have allowed to formulate a robust thermal model.

Nevertheless, there are still uncertainties. For instance, the rock specific heat capacity 'Cp' has not been directly measured and cannot be inferred from static observations of temperature. Thus, correlations based on lithology and XRD-analyses were used for its estimation [1]. On the other hand, rock thermal conductivity is less uncertain than specific heat capacity as temperature observation versus depth allowed the adjustments/verification of its estimated values. The estimation of the thermal properties can be also compared with measured values in analog rocks to understand the possible degree of variation in these properties as shown in Table **4**. For the most significant rock formations in MOL-GT-03, which are associated with higher temperatures, Table **4** shows that the variation from reference values is small (equal to or less than 15%). This low level of deviation provides confidence in the reliability of the estimated parameters.

This project has received funding from the European Union's Horizon Europe research and innovation program under grant agreement No 101083558

Table 4. Comparison of model's thermal parameters and referential measured values used for modelling MOL-GT-03

Rock type	Corresponding rock formation	Corresponding Thermal rock layer	K @140°C thermal model [W/m-°C]	K @140°C reference [W/m-°C]	Cp @140°C thermal model [J/Kg.K]	Cp @140°C reference [J/Kg.K]
Limestome	Loenhout	Lower carboniferous - Paleozoic	2.7	2.8*	933.8	978*
Shale, Coals and sandstone layers	Andenne and Chockier	Upper carboniferous - Paleozoic	1.4	1.18*	903.5	800 **

* [2] ** [3]

3.1.3. Simulation procedure

3.1.3.1. Simulation tool

GTW (Geo-Thermal-Well) is a single-phase numerical geothermal simulator in cylindrical coordinates for single well applications. It was developed by IFE under open license terms. It couples the heat fluxes between the rock and the well. Heat flux is only considered in the radial direction. The simulator numerically solves the equation for transient heat conduction in the rock and well wall domain while it assumes stationary fluid flow in the internal well domain (Figure **5**). The simulator obtains the numerical solution using an energy-conservative finite volume method. This simulator was benchmarked during WP2, Task 2.1 of the present project [4].

The GTW simulator models a closed-loop single well system composed of concentric tubular and annular domains in both radial and vertical directions, as shown in Figure **5**. The innermost domain represents the flow area of the returning pipe (HOCLOOP production pipe) and the outermost corresponds to the surrounding rock. The internal rings of the model represent: the tubing wall of the returning pipe, the annular downward flow path of the recirculating fluid and the well's walls (casing and cement) that separate the rock and the mentioned fluid. The domains can vary in size along the vertical and radial directions due to differences in the well completion or rock properties.

A Python class for setting up GTW input files was created. The use of scripting provided the possibility to test different well configurations (*in* situ/as drilled vs horizontal/sidetrack options), differing material parameters/geometries, time varying production scenarios, and usage optimized scenarios in time.

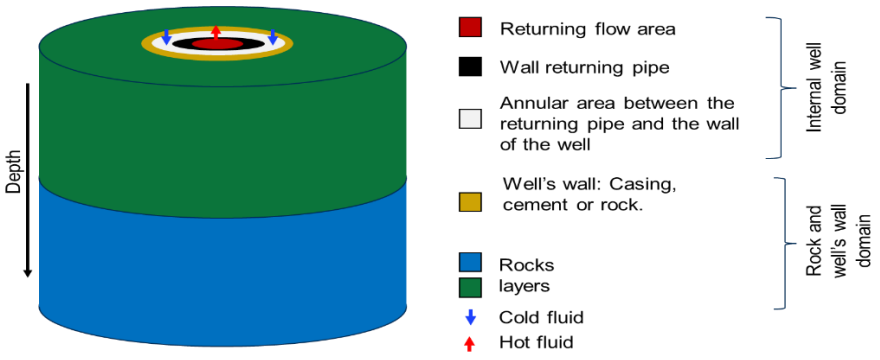

Figure 5. Domains considered in GTW simulator for modelling closed-loop single well systems like HOCLOOP system

This project has received funding from the European Union's Horizon Europe research and innovation program under grant agreement No 101083558

3.1.3.2. Well and rock properties

The well's walls (casing, cement and liner as shown in Figure **5** and defined in Table 1) are grouped into segments along the well as described in Table 5. An averaging procedure is required because the simulator can only account for a total of three well walls. Average thermal conductivity, heat capacity, and density of the segments are computed following $k_{average} = \frac{ln\left(\frac{r_1}{r_n}\right)}{\sum_{i=2}^{rn} \frac{ln\left(\frac{r_i}{r_{i-1}}\right)}{k_{i-1}}}$ Equation 1, $CP_{average} = \frac{1}{\sum_{i=1}^{n} A_i} \sum_{j=1}^{n} A_j * CP_j$ Equation 2 and $\rho = \frac{1}{\sum_{i=1}^{n} A_i} \sum_{j=1}^{n} A_j * \rho_j$ Equation 3, respectively. In these equations, r is the annular outer radius, A is the annular area of every layer, CP is the heat capacity, k is the thermal conductivity, ρ is the density and n the total number of well walls (cement, casing, liner as illustrated in Figure **6**) in a certain section. The properties of the HOCLOOP tubing used in the simulations are described in Table 6. These properties are constant along the well trajectory.

*Table **5.** Definition of the average properties of well's wall for GTW simulator. The well's walls are defined in Table **1**.*

Well walls	Top – Bottom [m MD]	$k_{average}$[W/m-K]	$CP_{average}$[J/kg-K]	ρ [kg/m^3]
1,2,3,4,8,9,10	0 – 30	1.08	1272.3	3643.1
2,3,4,8,9,10	30 - 206	1.06	1304.5	3516.2
3,4,9,10	206 – 874	1.11	1257.6	3700.9
4,10	874 – 2067	1.14	1240.8	3767
5,11	2067 – 3533.2	1.32	1156.3	4099.9
6, water layer	3533.2 - 3643	0.95	3022.1	2864.3
Lower carboniferous	3643 – 4747.5	2.7	933.8	2700
Devonian	4747.5 - 4905	2.48	933.8	2700

MD: Measured depth

$$k_{average} = \frac{ln\left(\frac{r_1}{r_n}\right)}{\sum_{i=2}^{rn} \frac{ln\left(\frac{r_i}{r_{i-1}}\right)}{k_{i-1}}} \quad \textit{Equation 1}$$

$$CP_{average} = \frac{1}{\sum_{i=1}^{n} A_i} \sum_{j=1}^{n} A_j * CP_j \quad \textit{Equation 2}$$

$$\rho = \frac{1}{\sum_{i=1}^{n} A_i} \sum_{j=1}^{n} A_j * \rho_j \quad \textit{Equation 3}$$

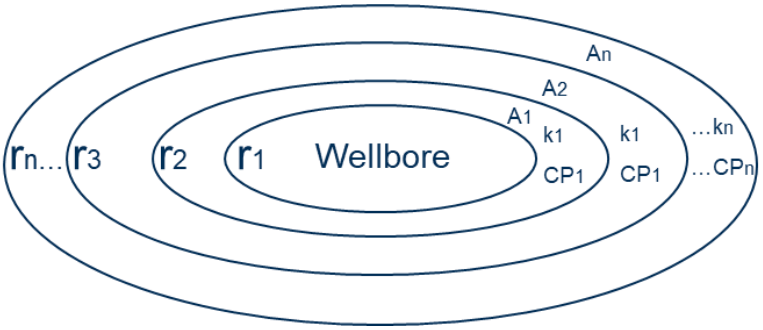

*Figure **6.** Wellbore layers definition for computing average properties of the segments. A: area, r: radius and CP:heat capacity*

This project has received funding from the European Union's Horizon Europe research and innovation program under grant agreement No 101083558

3.1.3.3. HOCLOOP production pipe

For the case study using the existing MOL-GT-03 well, the general characteristics of the HOCLOOP tubing are given in Table 6 and Table 7. In all simulations, the tubing is assumed to run from the wellhead to the bottom of the existing well.

Table 6. Characteristics of HOCLOOP completion tubing

Internal radius [mm]	Wall thickness [mm]	Top depth [m MD]	Bottom Depth [m MD]
42.5	27.5	0	4905

MD: measured depth

Table 7. Thermal properties of HOCLOOP tubing

	Insulated tubing
Heat conductivity [W/m*C]	0.0264
Heat capacity [J/kg*C]	500
Density [kg/m^3]	300

3.1.3.4. Recirculating fluid properties and initialization

The recirculating fluid chosen for this HOCLOOP application is water as it is the working fluid used between the Balmatt geothermal plant, and the research campus for heat delivery. The properties used for modelling are shown in Table 8.

Table 8. Properties of the recirculating fluid for the HOCLOOP application

Fluid	Thermal conductivity [W/m- C°]	Thermal capacity [J/kg- C°]	Density [kg/m^3]	Viscosity [cP]
Water	0.6	4200	1000	1

Temperature initialization is performed based on the temperature gradients defined in Table 3. Layer thermal properties are set in accordance with depth intervals. Those values are also reported in Table 3.

3.1.4. Integration scenarios

Two different integration options of the HOCLOOP concept at VITO's facilities were envisaged as possible ways to provide heat to the existing heating network and/or new buildings [1]. For both scenarios, the existing dry well (MOL-GT-03), with its approximate trajectory of 5000 meters, is considered for the potential installation of the HOCLOOP concept and the assessment of its thermal performance.

The integration scenarios considered in this deliverable are as follows:

a) Use of the HOCLOOP concept in well MOL-GT-03 for pre-heating the working fluid used to carry the heat between the VITO geothermal plant and VITO's research campus (Figure 7-a). The heat network of the campus is an older system that works with high temperatures (> 70°C).

This project has received funding from the European Union's Horizon Europe research and innovation program under grant agreement No 101083558

b) Use of the HOCLOOP concept in well MOL-GT-03 to provide low temperature heat to new building facilities located near the Balmatt geothermal site (Figure **7**-b). These facilities will feature modern heating systems that require lower temperature heat sources (< 50°C).

These integrations scenarios impose different operating conditions on the HOCLOOP system. A detailed analysis of the performance of the system and its impact on the heating facilities are described in the next sections.

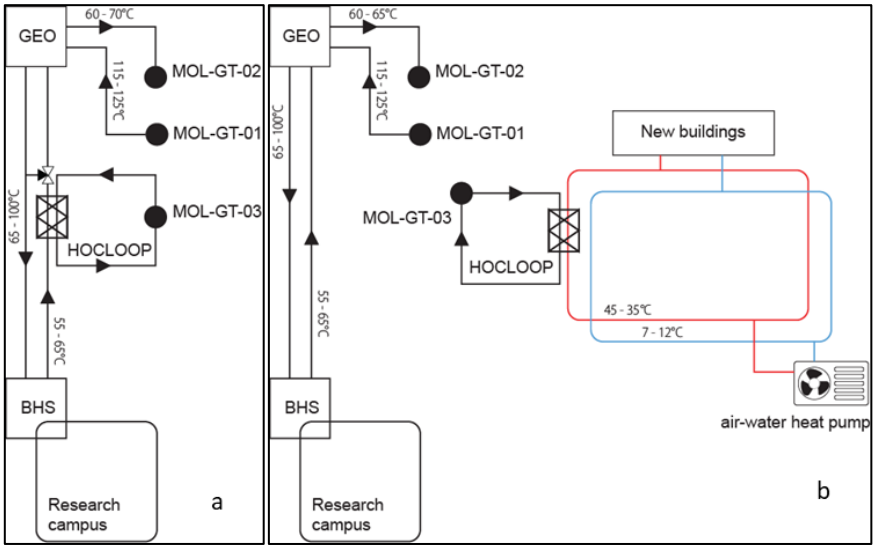

*Figure **7.** Possible integration schemes of HOCLOOP concept installed in well MOL-GT-03 with VITO's facilities. (a) Pre-heat the working used to carry the heat between Balmatt geothermal plant 'GEO' and VITO's research campus facilities. (b) provide heat to a new building development*

3.1.5. Simulation of the integration scenarios and results

3.1.5.1. Scenario a: Pre-heating the working fluid of VITO geothermal plant

3.1.5.1.1. Description of the integration scheme

The first integration scheme involves utilizing the HOCLOOP system to preheat the water ''working fluid'' used for transferring heat from the geothermal plant to VITO's research campus. The HOCLOOP system is installed in well MOL-GT-03 for this purpose. The standard heat transport process operates as follows: once the working fluid delivers heat to the research campus, it returns at a lower temperature to the geothermal plant, where it is reheated as it passes through the heat exchangers. This cycle continues as long as there is a demand for heat at the research campus. The concept of preheating the working fluid before it reaches the heat exchangers serves two main purposes: to reduce the amount of heat extracted from the open-loop system or to repurpose excess heat for other uses. By reducing heat extraction from the deep geothermal reservoir, where the open-loop system operates, this approach is expected to extend the reservoir's lifespan and increase the reinjection temperature. A higher injection temperature, in turn, lowers the risk of inducing seismic events.

To preheat the working fluid, all or a portion of it can be circulated through well MOL-GT-03 using the proposed HOCLOOP tubing completion. The final flow rate of water circulated in the well will be optimized to achieve the maximum heat transfer at the highest coefficient of performance (COP). Cold water from the research campus is injected into the annular space of the well, and after reaching the bottom, it returns to

This project has received funding from the European Union's Horizon Europe research and innovation program under grant agreement No 101083558

the surface via the HOCLOOP pipe. For this process, it is assumed that the working fluid can be directly circulated into the well. This requires the well to be fully cased for preventing contamination of the working fluid.

For the simulations of the HOCLOOP system in well MOL-GT-03, two well configurations are considered:

- The original geometry of well MOL-GT-03, which represents the most practical condition for a future testing.
- The inclusion of a horizontal section in well MOL-GT-03, if additional heat delivery is required. This horizontal section would be included at the bottom of the well.

The cases corresponding with the different well configurations are described in Table 9 and illustrated in Figure 8.

*Table **9.** Description of simulated cases for Scenario a: Pre-heating the working fluid of VITO geothermal plant*

Tested cases for scenario 'a'	Description
Case a-1	Original well trajectory of MOL-GT-03
Case a-2	Considers the original well trajectory plus an additional horizontal section of 500 m at the bottom of well MOL-GT-03
Case a-3	Considers the original well trajectory plus an additional horizontal section of 500 m at the bottom of well MOL-GT-03

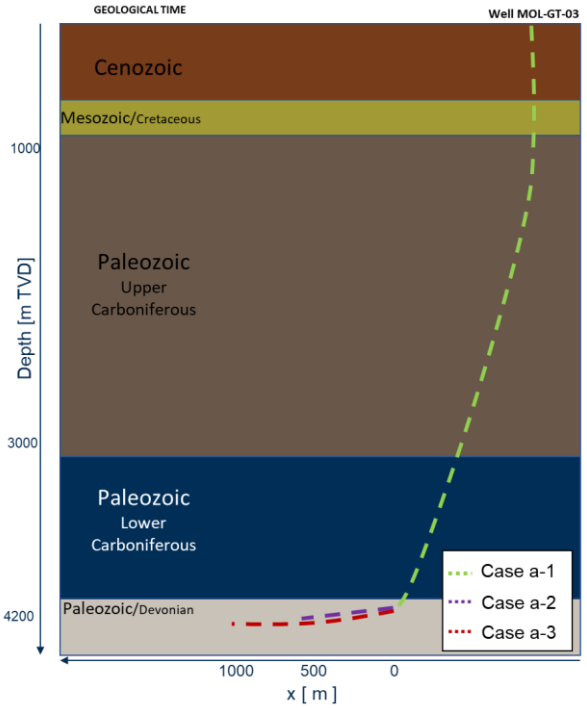

*Figure **8.** Illustration of well trajectories tested for Scenario a: Pre-heating the working fluid of VITO geothermal plant. Case a-1 is the original well trajectory, Case a-2 and Case a-3 consider the original well trajectory plus a horizontal section of 500 m and 1000 m respectively.*

This project has received funding from the European Union's Horizon Europe research and innovation program under grant agreement No 101083558

3.1.5.1.2. Well control conditions

The heating network at VITO's research campus operates at high temperatures (above 70°C), which means the working fluid also has a high temperature. For example, during the testing phases in 2022, the temperature of the working fluid returning from the research campus to the VITO geothermal plant exceeded 60°C, as illustrated by the black line in Figure 9. Thus, the injection temperature in the well was defined as 65°C during winter and 70°C during the summer for the simulations of scenario a as shown in Table 10.

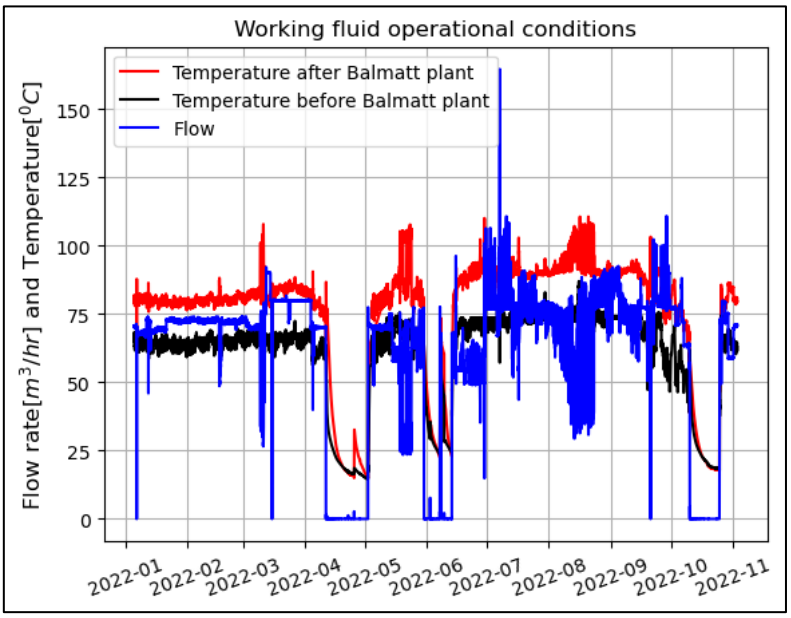

Figure 9. Real operational conditions of the working fluid that transport the heat produced by the deep open-loop geothermal system to VITO's research campus. Testing phases of year 2022.

For the definition of the injection flow rate, *a sensibility analysis* must be carried out to determine its optimum value. The optimum water flow rate in the well is the one that achieves both high thermal power output and a high coefficient of performance (COP). The COP is defined as the ratio between the thermal energy produced and the energy expended to pump the working fluid inside the well (pumping energy), as described in *Equation 4* and *Equation 5*. These equations assume that the heat transfer from the pump to the fluid is negligible. The maximum injection flow rate considered in this analysis is 72 m³/h (20 kg/sec), which is equivalent to the working fluid rate during January of 2022 (Figure 9). For the sensibility analysis the injection temperature is kept constant to 65°C. The efficiency of the pump is assumed to be 50% for these estimations.

$$COP = \frac{E_{\text{prod}}}{W_{\text{pump}} + |E_{\text{ref}} - E_{\text{prod}}|} \quad \textit{Equation 4}$$

Where: E_{prod} is the thermal energy produced by the well, E_{ref} is the reference power required, and

$$W_{pump}[kW] = \frac{q_{well} * \Delta P[Pas]}{\eta[fract.] * 1000} \quad \textit{Equation 5}$$

$where$:

q_{well}: $volumetric\ flow\ rate\ in\ the\ well$
$\left[\frac{m^3}{sec}\right]$: $Injection\ pressure\ minus\ production\ pressure\ in\ the\ well\ [Pas]$
η: $Efficiency\ of\ the\ pump\ [fract.]$

This project has received funding from the European Union's Horizon Europe research and innovation program under grant agreement No 101083558

In the sensitivity analysis cases where the injection fluid rate in the well is lower than the flow rate of the working fluid, the final temperature of the pre-heated working fluid will be computed with Equation 6.

$$T_{after\ preheating} = \frac{[(q]_{total} - q_{well}) * T_{before\ pre-heating} - q_{well} * T_P}{q_{total}} \quad for\ q_{total} > q_{well} \quad \text{Equation 6}$$

$where$:

$T_{after\ preheating}$: $temperature\ of\ the\ working\ fluid\ after\ pre-heating$ [°C]

q_{total}: $Working\ fluid\ rate\ of$ VITO research campus network

q_{well}: Injection fluid rate in the well

$T_{before\ pre-heating}$: $temperature\ of\ the\ working\ fluid\ after\ pre-heating$ [°C]

T_P: $Production\ temperature\ from\ the\ HOCLOOP\ system$ [°C]

Once an optimal injection flow rate is selected, a case with varying temperature between the summer and winter as shown in Table 10 is run for 20 years. This intends to mimic a more realistic well operation where more heat is consumed during winter than summer and that impacts the injection temperatures.

*Table **10.** HOCLOOP Well injection conditions at the wellhead*

Period	Injection temperature = Temperature before pre-heating [°C]	Heating network working fluid flow rate [m^3/h] / [kg/sec]	Tested fluid rates in the well [kg/sec]	Period duration [months]
Winter	65	72 / 20	5 - 20	6
Summer	70	72 / 20	5 - 20	6

* Fluid rate will be defined during a sensitivity scenario. This number represents the maximum but not the final conditions.

3.1.5.1.3. Results of Case a-1

Flow rate selection

The results of the flow rate sensitivity analysis, in terms of produced thermal power and COP for a 20 year production scenario, are presented in Figure **10** and Figure **11**, respectively. The produced power remains almost constant for mass flow rates above 10 kg/sec but shows a significant decline for flow rates below 5 kg/sec. Conversely, the COP dips below 1 over a flowrate of about 17 kg/sec, indicating that for every 1 kW of thermal power produced, 1kW of electricity is required. Considering the goal of achieving both high COP and high thermal power output, an optimal injection flow rate of 5 kg/sec has been selected to evaluate the pre-heating of the working fluid from VITO research campus heating network.

This project has received funding from the European Union's Horizon Europe research and innovation program under grant agreement No 101083558

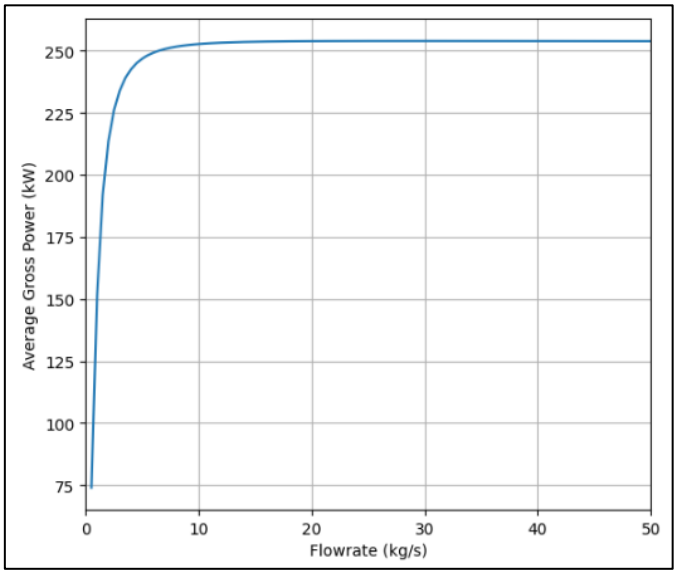

*Figure **10.** Sensitivity analysis result of flow rate on Gross Power.*

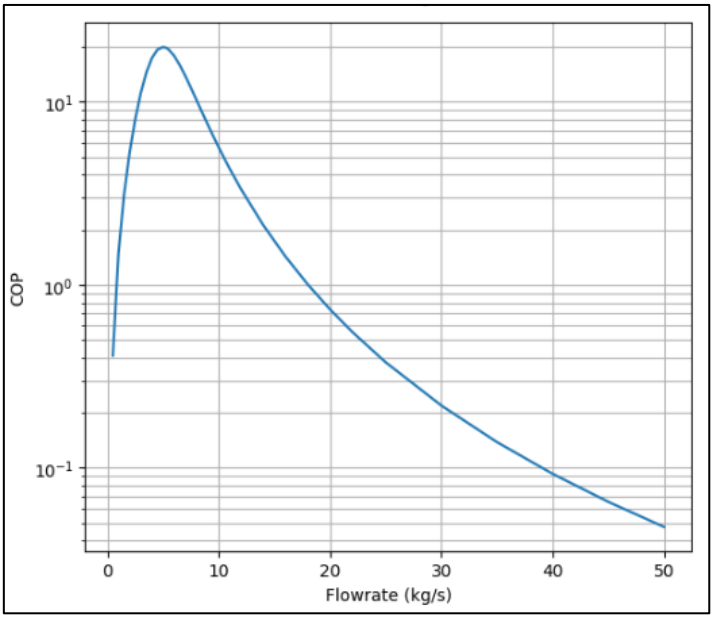

*Figure **11.** Sensitivity analysis result of flow rate on COP.*

Performance

The performance of the HOCLOOP system installed in the well MOL-GT-03 with the current well geometry (Case a-1) and the selected flow rate of 5 kg/sec for 20 years is shown in Figure 12. In this scenario the injection temperature during winter was set lower at 65°C, compared to 70°C during the summer. The output temperature of the well is expected to be above 80 °C during most of the 20 years of operation. It is important to mention that this is not the final temperature of the pre-heated working fluid as this stream must be mixed with the portion of the working fluid that was not injected in the well (15 kg/sec). Once the mixing of the 2 streams is accounted for, the final temperature of the pre-heated working fluid is estimated as shown in Figure 13. In this figure it is shown that the HOCLOOP system has the potential of increasing the working fluid temperature from 65°C to 69°C during winter and from 70°C to 73°C during summer.

This project has received funding from the European Union's Horizon Europe research and innovation program under grant agreement No 101083558

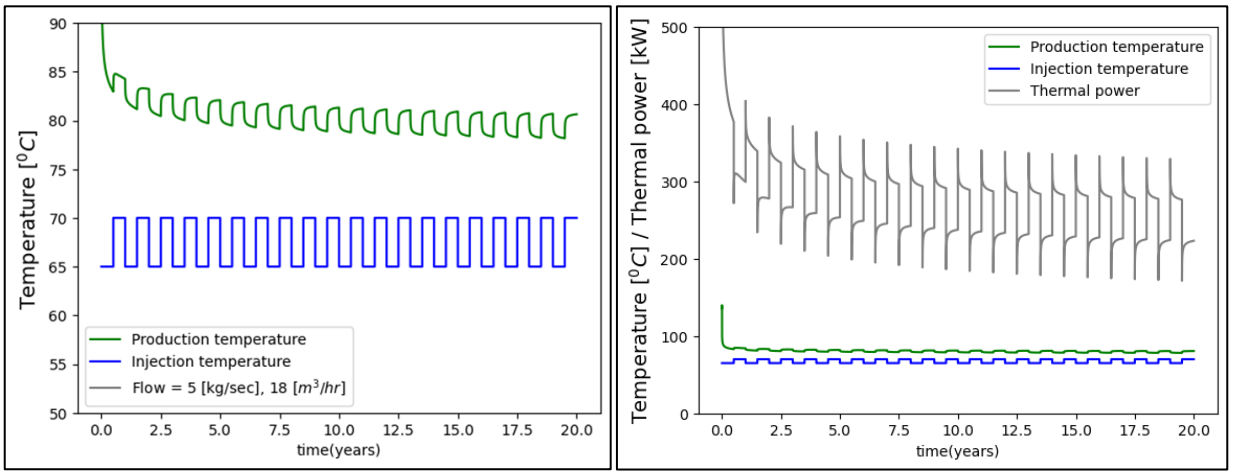

*Figure **12.** Production temperature and power from well MOL-GT-03 using HOCLOOP for preheating VITO's research campus working fluid. Winter and summer periods are considered to last 6 months each. These periods imply different injection temperature while the injection rate is held constant during the year at 5 kg/sec. Case a-1: Original well trajectory of MOL-GT-03.*

The mentioned temperature changes in the campus network working fluid (Figure **13**) are equivalent to an increase of 250 kW to 300 kW in its thermal power. This value may be considered low compared to the output of the deep geothermal power plant, which is designed to produce a minimum of 2 MW of thermal power. Thus, the preheating of the water is not expected to have a major impact on the injection temperature of the deep geothermal project and in the additional delivered heat.

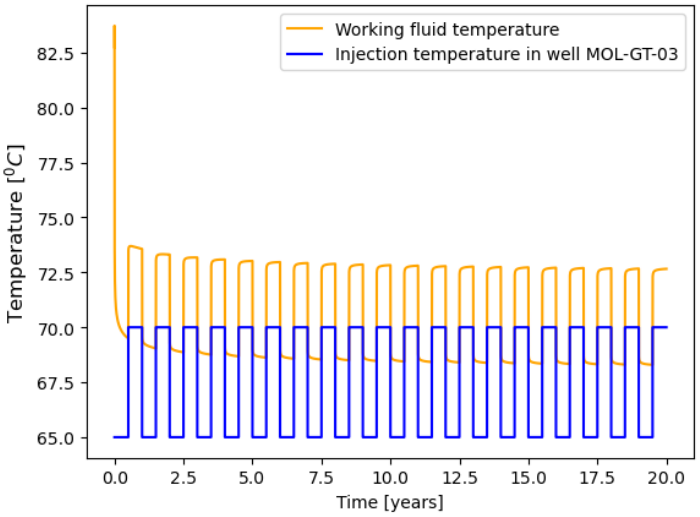

*Figure **13.** Working fluid temperature after mixing the water injected in the well and the remaining working fluid from VITO research campus network considering original well geometry MOL-GT-03 Case a-1. Working fluid temperature before pre-heating is equal to injection temperature in the well. Injection fluid rate is 5 kg/sec (18 m^3/hr) while injection temperature is changed during winter (65 °C) and summer (70 °C)*

One important observation of this scenario is that it does not allow to exploit the full thermal potential of the well.

This occurs because the injection temperature is significantly higher than the subsurface temperature in a

This project has received funding from the European Union's Horizon Europe research and innovation program under grant agreement No 101083558

considerable long section of the well, leading to energy losses not only at shallow depths but also at intermediate depths. As a result, the extraction of low temperature heat is hindered. For example, an injection temperature of 65°C leads to heat loss along the first 1550 meters of depth—a substantial section that could otherwise contribute to low-temperature heat recovery. Thus, a more efficient use of the well involves injecting fluid at temperatures closer to shallow subsurface levels, which will allow the extraction of higher thermal power.

3.1.5.1.4. Results of Case-a2 and Case-a3

Two additional hypothetical cases assuming the drilling of a horizontal section in well MOL-GT-03 were considered. The flow rate and injection temperature conditions are the same as the ones used in the previous case 'original well geometry'. The considered horizontal lengths and well control conditions are shown in Table **11**. The corresponding temperatures of the VITO campus working fluid before and after preheating are shown in Figure **14**.Table **11.**

*Table **11.** Description of cases with a horizontal section*

Case	Additional horizontal Length [m]	Fluid rate [m³/hr] / [kg/sec]	Injection temperature winter / summer*
Horizontal 1	500	18 / 5	65 / 70
Horizontal 2	1000	18 / 5	65 / 70

** Winter and summer are considered to last 6 months each*

As anticipated, adding a horizontal well section at the bottom of the well (4900 m) results in a higher final temperature of the working fluid compared to maintaining the original well geometry of well MOL-GT-03, as shown in Figure **14**.

This effect is clearly illustrated by the comparison of the temperature increase and power gain of the working fluid (Figure 15 and Table 12). The temperature increment ranges from a minimum of 3°C during summer with the original well geometry to a maximum of 6°C in winter when a 1000 m horizontal extension is added. The latter (case a-3) results in twice the power output compared to the original well geometry. Nevertheless, despite this improvement, the generated heat remains below the megawatt range. However, it could be considered significant due to the temperature range reached. Thus, an economic analysis needs to be carried to assess the overall feasibility of this solution.

This project has received funding from the European Union's Horizon Europe research and innovation program under grant agreement No 101083558

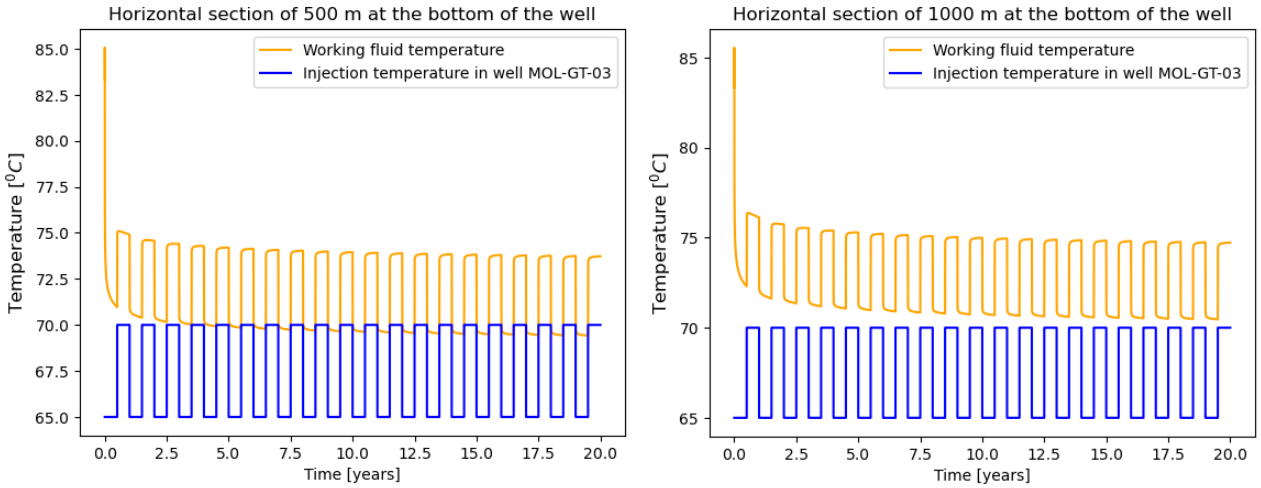

*Figure **14.** Working fluid temperature after pre-heating for two horizontals hypothetical sections in well MOL-GT-03: 500 m (left) and 1000 m (right). Injection fluid rate is 5 kg/sec (18 m³/hr) while injection temperature is changed during winter (65 ℃) and summer (70 ℃)*

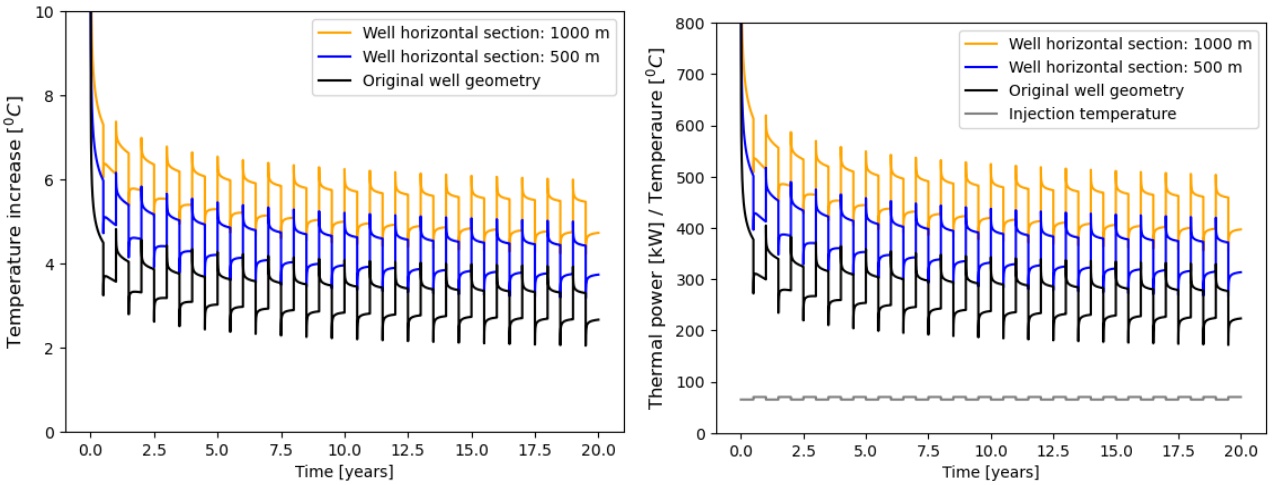

*Figure **15.** Comparison of temperature increase of the VITO campus working fluid and produced thermal power when considering the well MOL-GT-03 with the original well geometry and by adding additional horizontal sections at the bottom. The well is continuously producing heat but injection temperature changes during summer (70℃) and winter (65℃)*

*Table **12.** Resume of injection conditions and main outputs – Pre-heating working fluid of VITO geothermal plant. W: winter, S: summer*

Case	Water injection rate [kg/sec]	Injection temperature W – S [℃]	Increase in temperature W - S [℃]	Output power [kW] @ 20 years W - S
Case a-1	5	65 - 70	4 - 3	300 – 250
Case a-2	5	65 - 70	5 - 4	400 – 320
Case a-3	5	65 - 70	6 – 5	490 - 410

This project has received funding from the European Union's Horizon Europe research and innovation program under grant agreement No 101083558

To better illustrate the impact of flow rate and horizontal well length on the system's performance, Figure 16 presents a contour plot of the coefficient of performance (COP) as a function of horizontal well length and flow rate for the previously discussed seasonal temperature variation scenario. In the figure, well horizontal lengths from 0 m (original drilled well) to 4000 m were tested. Flowrates were varied from 0.5 kg/s to 50 kg/s. In general, the COP is maximized within a flowrate range of approximately 1 to 15 kg/s for all tested horizontal lengths, indicating higher system efficiency in this interval.

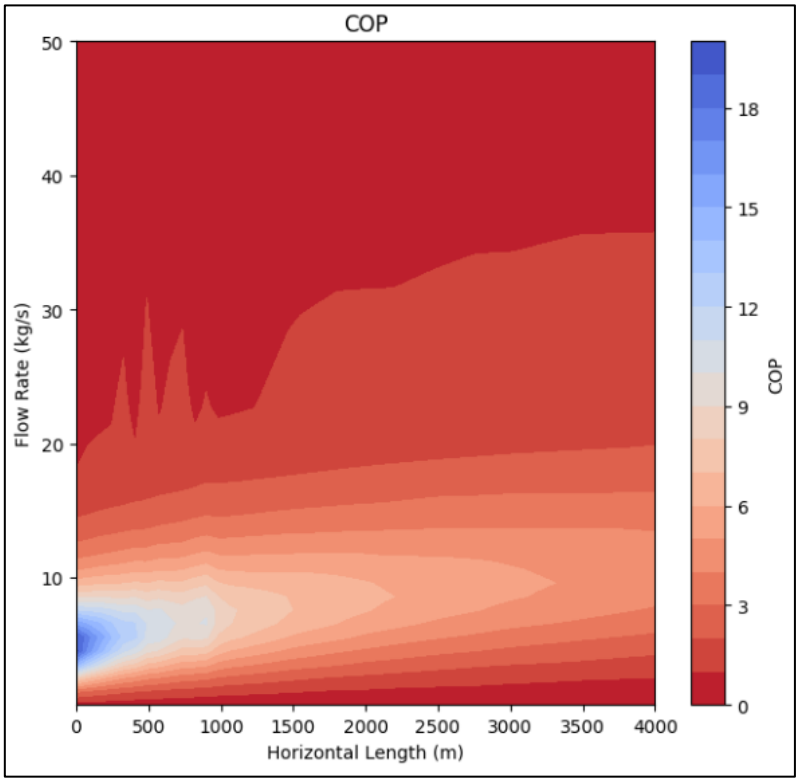

Figure 16: Contour plot of COP for various well horizontal lengths (0-4000 m) and flowrates (0-50 kg/s).

Figure 17 provides a more detailed view of these effects, displaying the gross power generated (left) and pump power required (right). Clearly, the gross power primarily depends on the well length, while the pump power is mainly influenced by the flowrate. The COP plot gives an idea of the most efficient options. However, achieving the desired gross power may not be possible with shorter well lengths. Longer horizontal sections can deliver more total gross power. This information can be used in financial planning to determine if heat pump top ups can be more efficient than longer well lengths.

This project has received funding from the European Union's Horizon Europe research and innovation program under grant agreement No 101083558

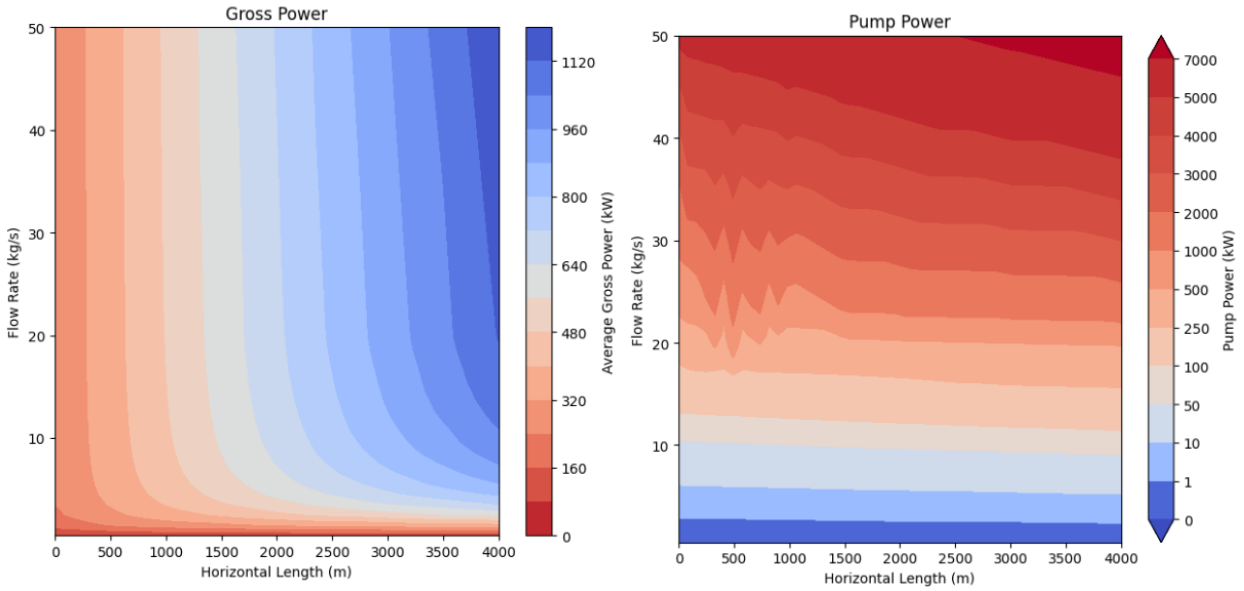

Figure 17: Gross power and pump power for horizontal well length and flowrate study.

3.1.5.2. Scenario b: Provide low temperature heating to new buildings facilities

3.1.5.2.1. Description of the integration scheme - Heat demand

The facilities that could be heated using the HOCLOOP solution include two new office buildings currently planned for construction. A seasonal heat demand, consisting of 7 months of operation and 5 months of downtime, as detailed in Table 13 and Figure **18**, will be assumed. A rate-control algorithm was specifically developed to handle irregular demands and will be tested using the considered heat demand. Finally, a case study was conducted considering the actual expected heat demand of the new buildings to assess the capacity of the well to meet both long-term heat requirements and daily peak demands, illustrated in Figure **19**. It also aims to determine the corresponding flow rate magnitudes necessary to fulfil these demands.

*Table **13.** Heat requirements for the heating network of the new buildings*

Period [Years]	Demand [MWh/y]	Seasonal demanded thermal power [MW]	Minimum input required temperature [°C]	Output temperature [°C]
0 – 10	2500	0.49	45	35
10 - 20	3400	0.67	45	35

This project has received funding from the European Union's Horizon Europe research and innovation program under grant agreement No 101083558

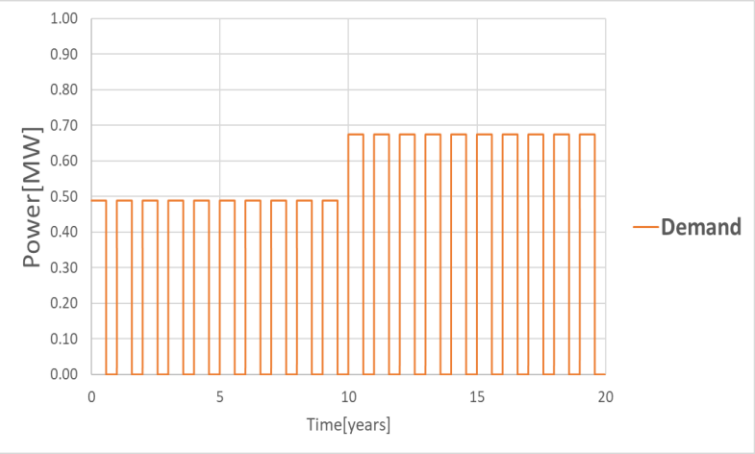

*Figure **18.** Referential seasonal average demand of thermal power for the new buildings during a period of 20 years. It is assumed that the energy demand takes place during 7 months per year at constant load.*

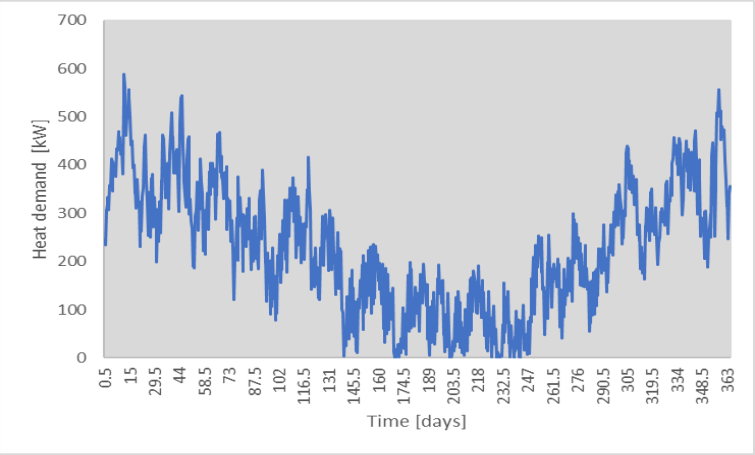

*Figure **19.** Estimated 12-hour heat demand profile from the new buildings during a period of 1 year.*

A total of three cases were modeled in integration scenario b as described in Table **14**. These cases consider different well trajectories and different demand profiles.

*Table **14.** Cases considered for simulation of scenario b: Integration of HOCLOOP system with the new buildings*

Tested cases for scenario 'a'	Description
Case b-1	The original well trajectory of MOL-GT-03 and seasonal heat demand for testing flow control algorithms and power potential of the well.
Case b-2	A 500 m horizontal section was added to the well (as case a-2 in Figure **8**) to test flow control algorithms and assess its power potential under seasonal demand.
Case b-3	The original well trajectory of MOL-GT-03 and daily heat demand expected for the new buildings and optimization of the length of the HOCLOOP production pipe.

3.1.5.2.2. Well controls conditions

The injection temperature of the system is considered equivalent to the output temperature of the building's heating network, which is 35°C (Table **13**Table **13**). A minimum temperature glide of 10°C at the heat exchangers is assumed. Thus, the minimum production temperature is set to 45°C.

This project has received funding from the European Union's Horizon Europe research and innovation program under grant agreement No 101083558

Providing constant thermal power during a certain period with single close-loop wells demands changing the injection conditions over time: flow rate and/or injection temperature. Thus, a rate-control algorithms was developed for optimizing the injection fluid rate to meet fluctuating heat demands. A detailed explanation of the optimization procedure for finding the flow rate that allow meeting the demand can be found in Annex 2. A resume of the injection conditions for evaluating the use of well MOL-GT-03 under the previously mentioned cases is given in Table 15.

*Table **15.** Well control conditions for integration scenario b*

	Injection temperature [C]	Recirculation fluid flow rate [kg/s]	Referential injection pressure for estimating dynamic properties [bar]	Minimum output temperature [C]
Heating new building development	35	To be determined based on the energy demand implementing and using an optimization procedure	10	45

3.1.5.2.3. Results of Case b-1

The optimization algorithms were tested for the 7-month seasonal usage scenario. Figure 20 Figure 20 and Table 16 display the results for MOL-GT-03 as drilled. The first 10 years, the heat demand is 0.49 MW and the well can deliver the heat, though output temperature steadily declines each year, while the required flowrate steadily increases. After 10 years, the required heat increases, and the well can no longer deliver this demand at the required output temperature over 45°C. Thus, the algorithms predicts that a slowly reduction in flowrate is required to deliver the heat at 45°C but the price is reduction of the output heat (Figure 20Figure 20-top). The fluctuations in the solutions before year 11 at the lower required heat demand are due to the transition from laminar to turbulent flow inside the annulus space.

*Table **16.** Seasonal usage scenario results for MOL-GT-03 as drilled.*

Year	1	2	3	4	5	6	7	8	9	10	11	12	13	14	15	16	17	18	19	20
Power (MW)	0.49	0.49	0.49	0.48	0.52	0.47	0.51	0.46	0.5	0.46	0.67	0.66	0.65	0.64	0.64	0.63	0.63	0.63	0.62	0.62
Flow (kg/s)	2.43	2.68	2.8	2.8	2.8	2.8	2.8	2.8	2.8	2.8	16	15.7	15.5	15.3	15.2	15.1	15	14.9	14.8	14.8
Temp (C)	83	79	76	75	79	75	78	74	78	74	45	45	45	45	45	45	45	45	45	45

This project has received funding from the European Union's Horizon Europe research and innovation program under grant agreement No 101083558

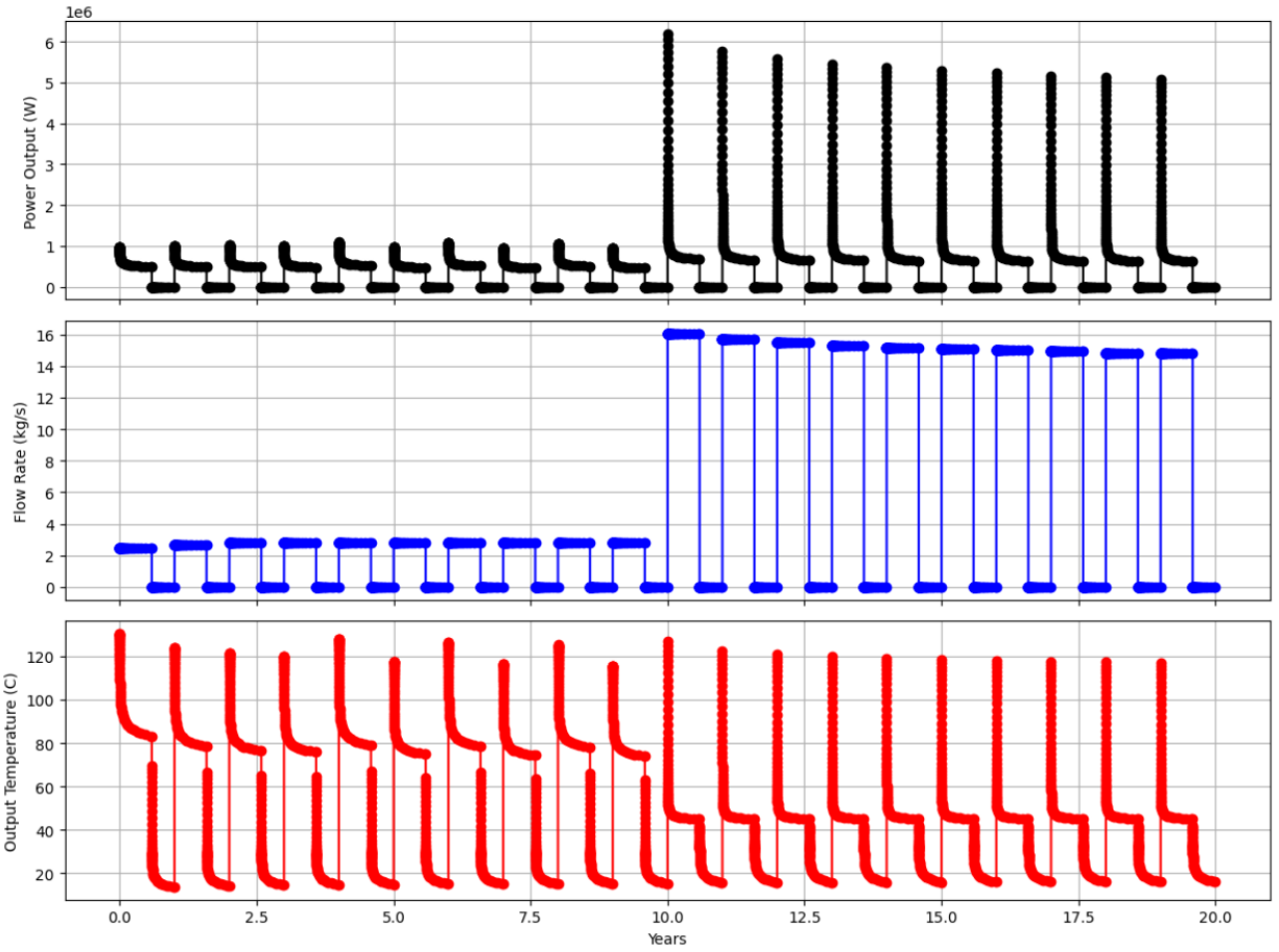

*Figure **20.** Results for seasonal usage scenario for MOL-GT-03 as drilled performed for testing the flow rate optimization methodology. Power demand is unable to be supplied when heat demand is increased from 0.49MW to 0.69MW (year 10). In this condition, the minimum production temperature of 45°C controls the flow rate.*

3.1.5.2.4. Results of Case b-2

We next tested the same 7-month seasonal usage scenario for the case if MOL-GT-03 were given a 500m horizontal sidetrack at the base of the well. We assumed the rock properties and completion did not change from that of the base of the well for the entire horizontal section and that the section was perfectly horizontal (no elevation change). This results in a higher production temperature and lower required flowrate for a given heat demand when compared with the well as drilled. In addition, the well can deliver the required heat demand for the entire 20 years. Figure 21 Figure 21 and Table 17 show that the developed optimization algorithms can predict the required flow changes to cover the energy demand.

*Table **17.** 7-month seasonal usage results for MOL-GT-03 with 500 m horizontal sidetrack.*

Year	1	2	3	4	5	6	7	8	9	10	11	12	13	14	15	16	17	18	19	20
Power (MW)	0.49	0.49	0.49	0.49	0.49	0.49	0.49	0.49	0.5	0.49	0.68	0.68	0.68	0.68	0.68	0.68	0.68	0.68	0.68	0.68
Flow (kg/s)	1.76	1.84	1.89	1.92	1.95	1.98	2	2.02	2	2.05	3.71	3.9	4.03	4.14	4.24	4.33	4.41	4.49	4.56	4.63
Temp (C)	101	99	97	96	95	94	93	93	92	92	79	77	75	74	73	72	72	71	71	70

This project has received funding from the European Union's Horizon Europe research and innovation program under grant agreement No 101083558

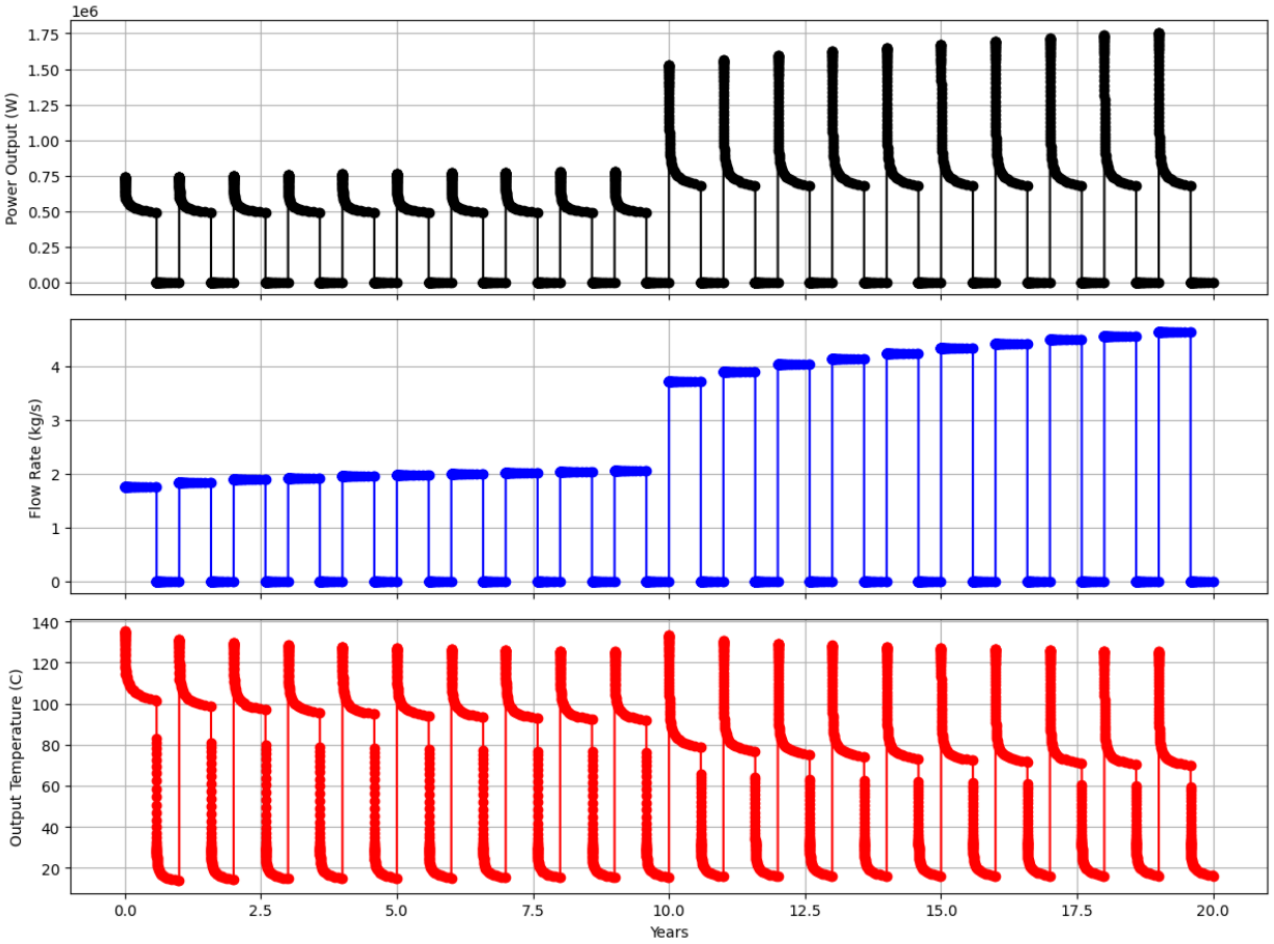

*Figure **21.** Results for the 7-monthly heat demand scenario with a 500 m horizontal extension to the existing MOL-GT-03 well track used for testing the flow rate optimization methodology.*

3.1.5.2.5. Results of Case b-3

Following the evaluation of the optimization algorithms, the well's capability to meet the expected heat demand of the new buildings—including both seasonal averages and peak requirements—is assessed.

First the capacity of the well to cover the peaks was evaluated considering the length of the HOCLOOP production pipe equivalent to the well trajectory (4905 m). To that end, 12-hourly heat demand was estimated for 1 year (Figure **19**). Those demands were averaged monthly and repeated for 5 years in order to provide some initial stress to the system. Then a single year was simulated with the 12 hourly demand data. The time discretization of 12 hours was otherwise too fine and would require a very long simulation time to obtain a result to simulate a full 5 years at that level. This hybrid approach presented runs in a more reasonable time and is able to assess the well performance well for year 5. Indeed, as shown in Figure **22**, the well was able to deliver the heat demand (top) completely for every 12 hourly period in year 5. The maximum flowrate required was under 3 kg/s.

This project has received funding from the European Union's Horizon Europe research and innovation program under grant agreement No 101083558

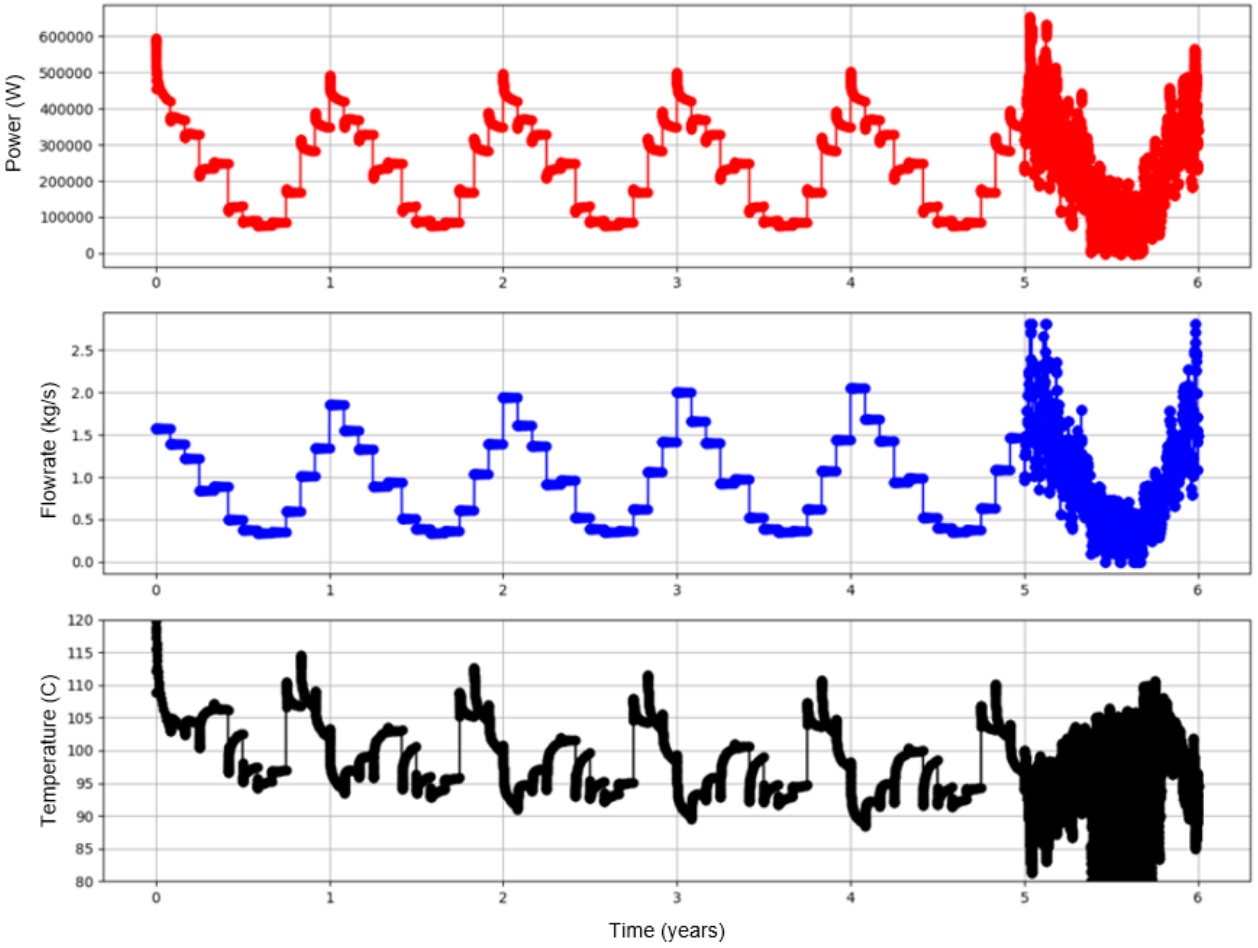

*Figure **22.** Estimated well performance for 5 years of monthly averages, followed by a single year of 12-hourly demand values for heating the new buildings. Power output (red – top figure) in W, flowrate (blue – middle figure) in kg/s, and outflow temperature (black – bottom figure) in °C. The x-axis is years. The well is considered as drilled.*

When the long-term performance of the well is evaluated for covering the heat demand, it is shown in Figure 23-a that the demanded thermal power is fully covered and the outlet temperature is above the minimum required temperature (45°C) during 20 years. Thus, there is no need of including a heat pump or another sources of additional heat. To practically achieved these results, it is required to slowly increase the flow rate from 1.5 kg/s to 2 kg/s during the evaluated period of time (Figure 23-b). Based on the high output temperature, it is expected that the well can cover the energy demand of the new building for much longer than 20 years.

This project has received funding from the European Union's Horizon Europe research and innovation program under grant agreement No 101083558

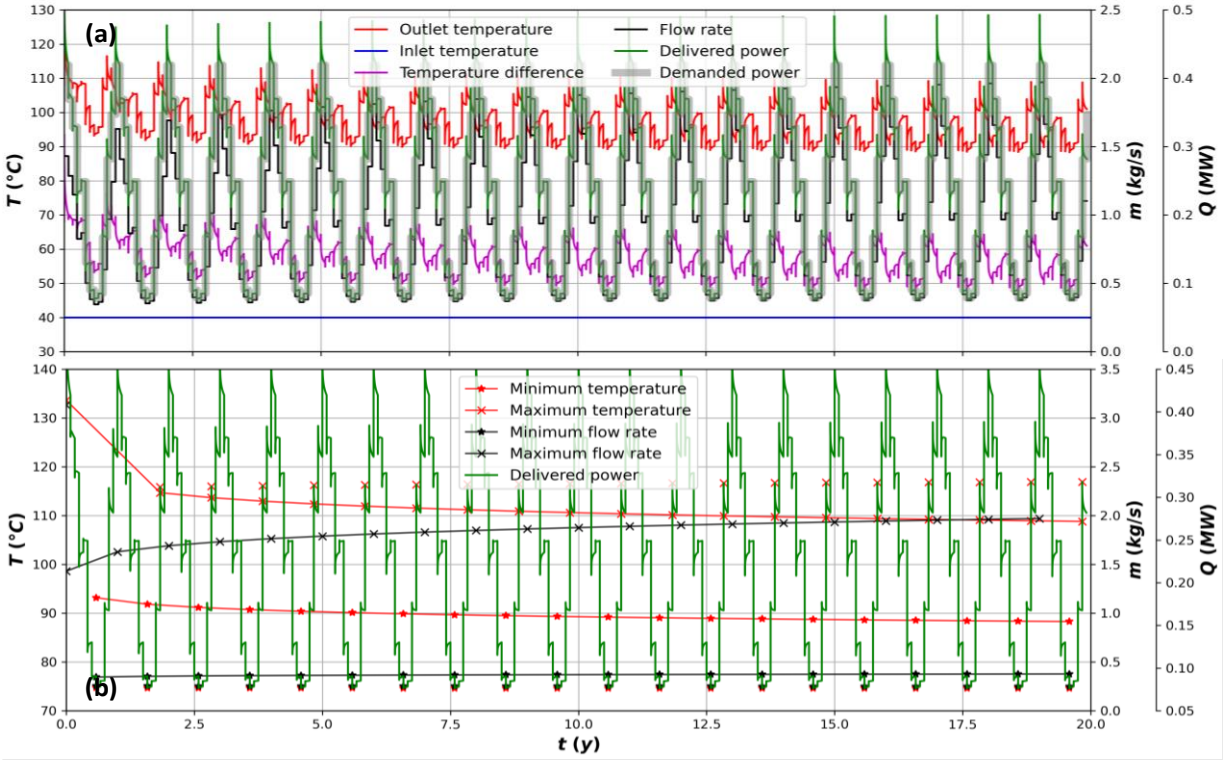

*Figure **23.** Long term well performance for heating the new buildings. (a) Temperature, flow rate, and power delivered, and (b) tracking of minimum and maximum outlet temperature and flow rate for the Scenario 2 with Control 2 for 20 years of monthly demand.*

Second, the optimal length of the HOCLOOP production pipe is determined. It is sub-optimal from a cost perspective to complete a 4904 m well with insulated pipe that is overdesigned for the heating demand as drilling and completion costs increase for each additional meter of well. Therefore, we tested the 20-year monthly fluctuating demand case from Figure 23 for a variety of production pipe lengths along the well current trajectory: 3000 m, 3500 m, 4000 m, 4500 m, and (the original drilled length) 4904 m. The purpose of this exercise was to determine the minimum well length that could completely accommodate the expected demand and, thus, compute the required well drilling/completion costs more accurately.

Figure 24 displays the results of this exercise. The plot shows the power output of the well, the output temperature, and the required flowrates. The 4000 m production pipe length fails to deliver the full requirement during winter in year 2 and continues to decline over time. The 4500 m pipe length delivers the required heat for the entire 20-year duration. So, if MOL-GT-03 were used for the new VITO buildings to meet their forecasted demand, the cost of approximately 400 m of completion could be saved and the well could still meet the required demand. By calculating the area under the power curves, we conclude that demand is met for the 4904 m and 4500 m production pipe length. However, the shorter pipe lengths do not meet the required demand. The 4000 m pipe delivers 94%; the 3500 m 67%; and the 3000 m 46% of the total required power.

This project has received funding from the European Union's Horizon Europe research and innovation program under grant agreement No 101083558

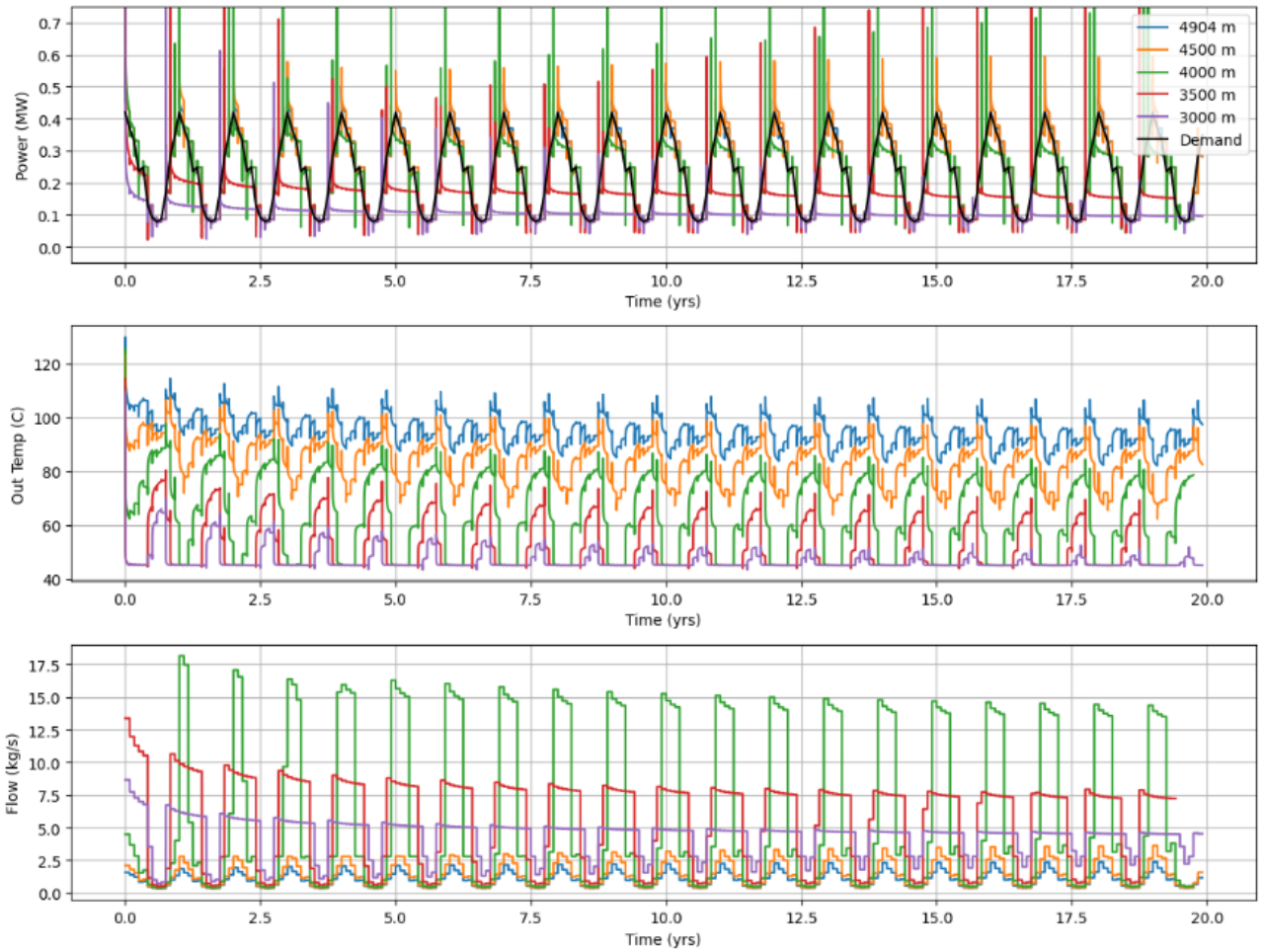

Figure 24 20 year monthly fluctuating demand scenario for 3000, 3500, 4000, 4500, and 4904 m MOL-GT-03 well lengths.

This project has received funding from the European Union's Horizon Europe research and innovation program under grant agreement No 101083558

3.1.6. Conclusions of the Belgium case

HOCLOOP concept was evaluated under two integration schemes with VITO facilities: Pre-heating the working fluid that transports the heat between the research campus and the deep geothermal plant and providing direct heating to new buildings designed to work with low temperature heat sources. The reuse of the deep dry well (MOL-GT-03), along with the addition of a horizontal section to this well, was considered for the installation of the HOCLOOP concept.

The performance of these two integration schemes is very different. On the one hand, pre-heating the working fluid resulted in an increase of temperature of 3 °C to 4 °C of this fluid corresponding to a thermal power between 250kW to 300kW when using the dry well as drilled. This thermal power represents about 10% to 15% of the current operational capacity of the open-loop deep project of VITO. If an additional 1000 m horizontal section were drilled at the bottom of the well, the delivered power could increase to 600 kW, with the working fluid temperature rising by up to 6°C at a flow rate of 72 m^3/h. This represents approximately 24% of the current plant's operational capacity, which can be considered significant. The power produced by the well in the condition as drilled and with an additional horizontal length is relatively low (lower than 1 MW). One of the reasons is the high injection temperature (> 60°C) that leads to important thermal losses and low delta temperature between the rock and the fluid which generates low heat flows. To assess the feasibility of this integration scheme, particularly when horizontal drilling is proposed, a comprehensive economic analysis is necessary.

On the other hand, heating the new buildings offers advantages because the heat is required at low temperature (minimum 45 °C) and the heat demand is moderate (≈ 2015 MWy). The low required temperature means that water can also be injected at low temperatures (40 °C), which maximises the heat flow rate (high delta temperature between the working fluid and the rock) and minimises heat losses. Under these demand conditions, the well can meet the energy demand for more than 20 years, achieving this without the need for additional drilling.

Heating the new building is the preferred option from an efficiency perspective, as it is expected to result in lower heat losses and higher heat flow rates compared to the scheme for pre-heating the working fluid of the deep geothermal plant. Additionally, this approach does not require further drilling, whereas the alternative scheme would necessitate horizontal or vertical drilling to achieve significant heat production.

This project has received funding from the European Union's Horizon Europe research and innovation program under grant agreement No 101083558

3.2. German case study

3.2.1. Introduction

The Technical University of Darmstadt is one of Germany's leading technical universities, with approximately 25,000 students and 5,000 staff members. The university operates across four primary locations: Campus Lichtwiese, Campus Stadtmitte (City Centre), Campus Botanischer Garten (Botanical Garden), and the University Stadium (Hochschulstadion).

TU Darmstadt's primary energy requirements include heating, cooling, and electricity. While electricity consumption remains relatively stable throughout the year, heating demand fluctuates significantly between the summer and winter months. In 2023, the university's energy consumption amounted to 39,300 MWh for heating and 48,200 MWh for electricity.

Electricity at TU Darmstadt is primarily supplied by three combined heat and power (CHP) modules, providing a total maximum capacity of 5.95 MW. If needed, additional electricity can be purchased from the city grid.

The three CHP engines also generate heat, with a combined thermal output of 7.0 MW. To cover higher heating demands during the winter months, six boilers, each with a thermal capacity of 9.3 MW, are available.

TU Darmstadt is committed to supporting Germany's national climate protection goals by implementing measures at the local level across its campus areas. The university aims to achieve an 80% reduction in area-specific CO2 emissions compared to 1990 levels until 2050. Therefore, different projects are being carried out to investigate different scenarios and strategies to reach this goal.

For example, heat generated by the high-performance computing center can be utilized with heat pumps to cover partially heating demands. Additionally, excess heat produced during the summer months (from sources such as solar collectors and CHPs) can be stored in medium-depth boreholes and then extracted during the winter.

In 2023, as part of the SKEWs (Seasonal crystalline borehole thermal energy storage) pilot project, three medium-deep boreholes, each 750 meters deep, were constructed. These boreholes, referred to as medium-deep borehole thermal energy storage (MD-BTES), have been undergoing testing since 2023, with the phase set to continue until early 2025. Following this, under the PUSH-IT project framework (EU Horizon research and innovation program, funding agreement No 101096566), the three boreholes will be integrated into the TU Darmstadt district heating grid for real-world operational evaluation. If results are promising, suggestions can be proposed to TU Darmstadt to expand from three to 19 or 37 boreholes.

The MD-BTES system enables efficient seasonal thermal energy storage by utilizing underground heat retention capabilities. The system operates by storing excess heat during summer and extracting it during winter to balance seasonal energy demand.

The HOCLOOP concept could be a strong alternative to the MD-BTES system. Instead of requiring multiple boreholes, such as 19 or 37, one or two boreholes may be sufficient to deliver comparable heating power.

The Darmstadt case thus focuses on this specific scenario which consists of using the HOCLOOP concept as an alternative to the MD-BTES numerous boreholes.

This project has received funding from the European Union's Horizon Europe research and innovation program under grant agreement No 101083558

3.2.1.1. *Thermal energy storage option with medium deep boreholes*

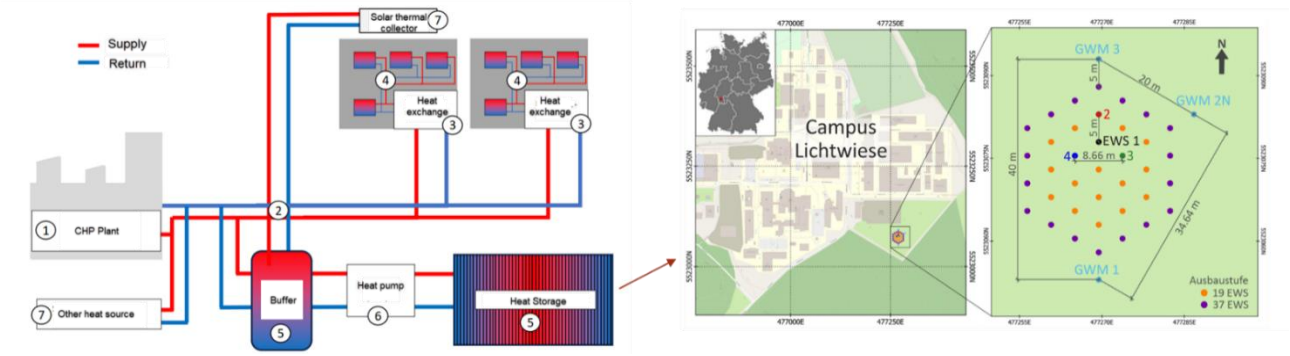

*Figure **25.** Darmstadt site – MD-BTES*

As shown in the below figure (Figure **25**), heat from CHPs, solar collectors, and other sources can be used to charge the MD-BTES system during low heat demand period. Then, during winter months, heat is extracted and temperature is raised with a heat pump. Currently, only 3 boreholes are available. The plan is to expand to 19 or 37 boreholes.

A recent study was conducted to evaluate various flow rates, inlet storage temperatures, and extraction temperatures for the 19-borehole scenario (Table **18**), with a simulation period of 30 years. Results show that, the outlet temperature drops from 44°C to 32°C (Figure **26**). The minimum heating power after 30 years is around 1MW (Figure **27**).

The following key parameters were tested:

- Flow rate per borehole: Ranging from 2 to 4 L/s.
- Inlet stored temperature in summer: 75°C to 90°C.
- Inlet extracted temperature in winter: 30°C.

These findings highlight the importance of optimizing flow rates and temperature regulation strategies to maximize system efficiency.

*Table **18.** Different studied scenarios for MD-BTES system of Darmstadt site with 19 boreholes scenario*

Parameters	Option-1	Option-2	Option-3	Option-4	Option-5	Option-6
Flow rate (l/s) of each borehole	4	2	4	2	4	2
Inlet stored temperature in summer time	90°C	90°C	80°C	80°C	75°C	75°C
Inlet extracted temperature in winter time	30°C	30°C	30°C	30°C	30°C	30°C

This project has received funding from the European Union's Horizon Europe research and innovation program under grant agreement No 101083558

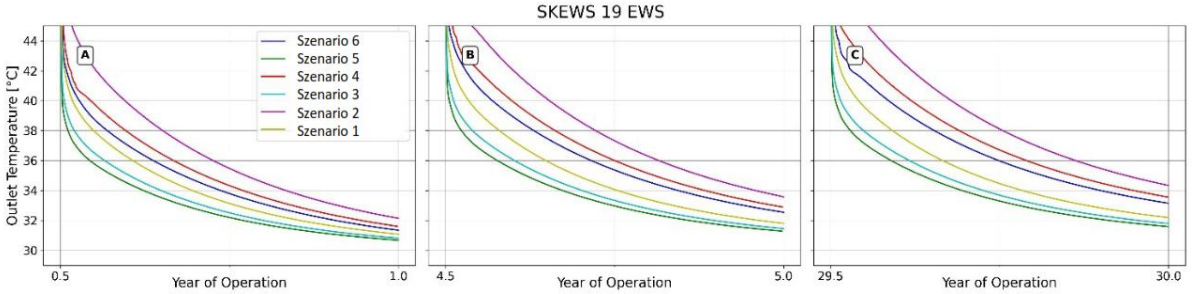

*Figure **26.** Darmstadt site – MD-BTES - Outlet temperature after 30 years of operation. The temperature drops from 44 degree from the beginning of extraction time to 32 degrees at the end*

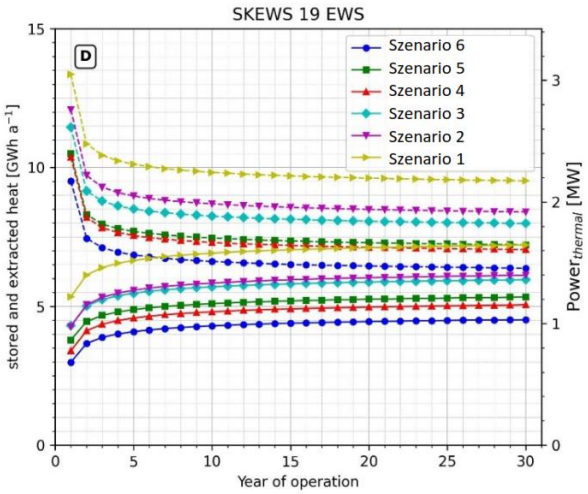

*Figure **27.** Darmstadt site – MD-BTES - Heat power of 30 years operation, for the worst-case scenario, 1MW is expected.*

HOCLOOP solution

Figure **28** shows how HOCLOOP solution can be replaced the MD-BTES system. Comparing the two systems, the HOCLOOP concept offers a more compact alternative with potentially lower land use requirements. However, deeper drilling incurs higher costs and operational risks. Extending existing boreholes for HOCLOOP solution is not planned for Darmstadt case.

This project has received funding from the European Union's Horizon Europe research and innovation program under grant agreement No 101083558

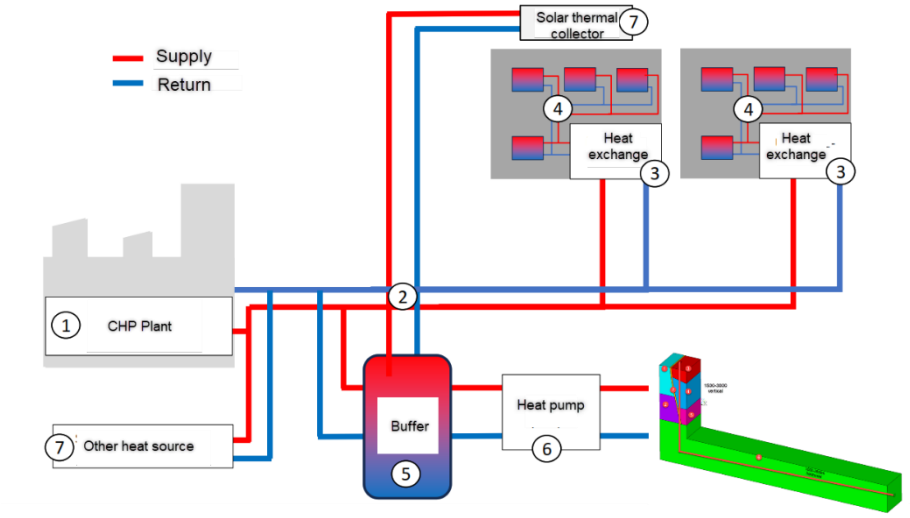

*Figure **28.** HOCLOOP solution replaces MD-BTES system in Darmstadt site*

3.2.2. Collected available data

For the Darmstadt site, during the construction of the three recently drilled boreholes, an intensive geological investigation was carried out [5]. Based on this, the geological structure model was set up (Figure 29).

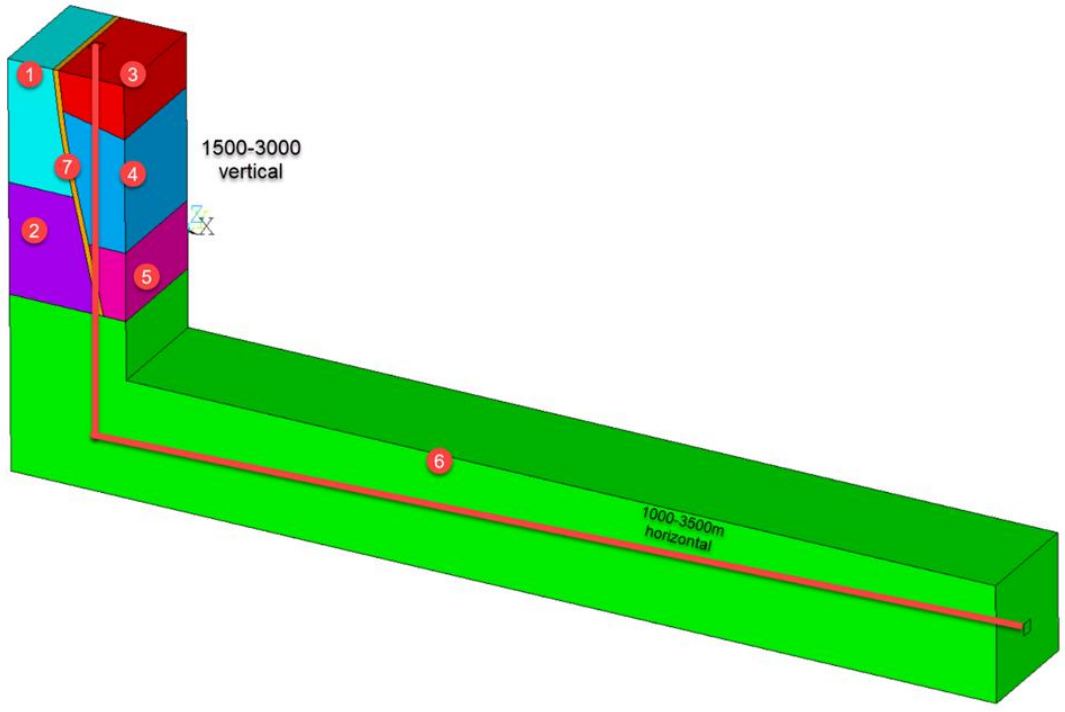

***Figure 29.** Darmstadt site – Geological structural model with different blocks based on site investigation results. Block-1 and Block-4 are Granite type-A. Block-2, Block-5 and Block-6 are Granite type-B. Block-3 is Permian Andesite, and Block-7 is fractured rock.*

This project has received funding from the European Union's Horizon Europe research and innovation program under grant agreement No 101083558

3.2.3. Simulation procedure

3.2.3.1. Simulation tool

Based on the geological structure model, finite element models were created in the FEFLOW software (Figure 30). The rock domain was discretized using an unstructured mesh. HOCLOOP well was represented by 1D elements. In FEFLOW, HOCLOOP pipe can be modelled as a coaxial pipe using the numerical method [6] or analytical method [7] [8].

To reduce model size and computational effort, only block 1000m x 1000m around the well was included in models. The mesh around the well was also refined based on recommendation of Diersch [8] to achieve high accuracy.

For all models, the following conditions are applied:

- Surface temperature: 11°C
- Geothermal gradient: 2.1°C/100m
- Ground water direction: North-South
- Ground water gradient: 0.02
- Calculation time: 30 years

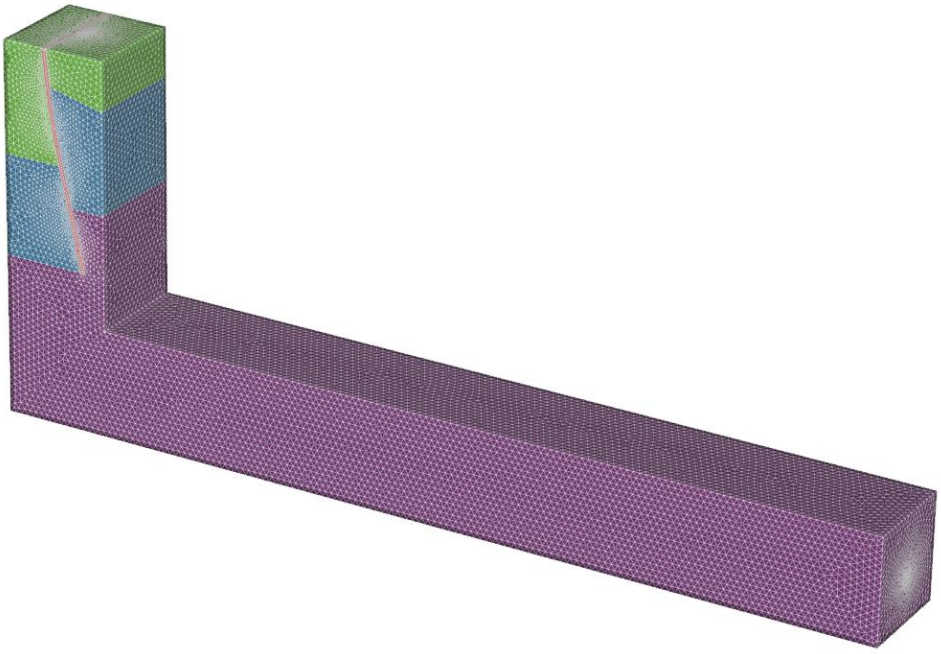

*Figure **30.** Finite element model – Darmstadt site*

3.2.3.2. Rock properties

Table 19 presents material properties used for FEFLOW model based on data obtained from laboratory measurements.

This project has received funding from the European Union's Horizon Europe research and innovation program under grant agreement No 101083558

*Table **19.** Geological properties for modelling – Darmstadt site*

Block	Description	Hydraulic conductivity (m/s)	Thermal conductivity (W/m/K)	Porosity (%)
Block-1	Granite, type A	1e-6	3.2	2.3
Block-2	Granite, type B	1e-7	3.2	0.6
Block-3	Permian Andesite	1e-5	1.58	11
Block-4	Granite, type A	1e-7	3.2	2.3
Block-5	Granite, type B	1e-8	3.2	0.6
Block-6	Granite, type B	1e-8	3.2	0.6
Block-7	Fractures	1e-5	2.0	10

3.2.3.3. HOCLOOP production pipe

The dimension of the closed-loop pipe is provided by the project partner Reelwell (Figure **31**).

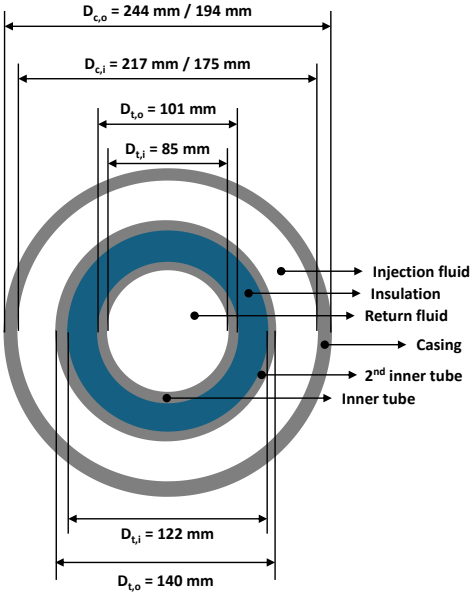

*Figure **31.** Characteristics of the closed-loop string used in the simulations for the Darmstadt site.*

In FEFLOW, it is not possible to include three different layers for the inner casing (inner tube, insulation laye, and 2nd inner tube). Therefore, those layers are merged as a single layer with an equivalent thermal conductivity 0.0264 W/mK (Figure 32).

This project has received funding from the European Union's Horizon Europe research and innovation program under grant agreement No 101083558

Property	Value
BHE Geometry	Coaxial (annular inlet)
Name	
Borehole Diameter (D)	0.3 [m]
Inlet Pipe Diameter (d-in)	0.194 [m]
Inlet Pipe Wall Thickness (b-in)	0.011 [m]
Outlet Pipe Diameter (d-out)	0.14 [m]
Outlet Pipe Wall Thickness (b-out)	0.0275 [m]
Computational Method	Quasi-stationary (Eskilson & Claesson)
Heat-transfer coefficients	Computed
Inlet Pipe Thermal Conductivity (tc-in)	43.28 [J/m/s/K]
Outlet Pipe Thermal Conductivity (tc-out)	0.0264 [J/m/s/K]
Grout volume thermal conductivity (tc-grout)	3 [J/m/s/K]
Grout to soil	nan [m s K/J]
Pipe-in to grout	nan [m s K/J]
Pipes-out to pipe-in	nan [m s K/J]
Refrigerant volumetric heat capacity (Ref. heat cap.)	4 [10+6 J/m³/K]
Refrigerant thermal conductivity (Ref. cond.)	0.48 [J/m/s/K]
Refrigerant dynamic viscosity (Therm. visc.)	3 [10-3 kg/m/s]
Refrigerant density (Ref. mass dens.)	1.052 [10+3 kg/m³]

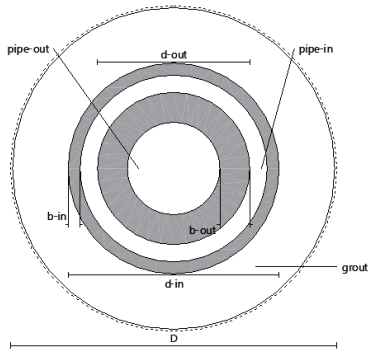

*Figure **32.** HOCLOOP pipe in FEFLOW, the outlet pipe represents three layers of HOCLOOP pipe with the equivalent thermal conductivity 0.0264 W/mK*

3.2.3.4. Recirculating fluid properties and initialization

All simulations were conducted using FEFLOW over a 30 - year operational period, with water as the sole fluid option available in the software.

3.2.4. Integration scenarios

The integration scenarios analysed aim at evaluating the potential of a system using the HOCLOOP concept as an alternative to the MD-BTES system currently planned for the site. A first scenario is run to define the optimal flow rate of the potential HOCLOOP system to be deployed. Then, several scenarios are simulated to understand the impact of various combination of depth and horizontal section length for the system, of the inlet temperature and of the temperature gradient on the thermal output of the system.

Different vertical and horizontal length scenarios were investigated (Table 20). In the MD-BTES system, the output temperature ranges from 32°C to 44°C. Assuming a temperature gradient of 2.1°C per 100 meters and a surface temperature of 11°C, from primarily simulation results, achieving a similar output temperature with the HOCLOOP system requires a vertical depth between 1500 and 3000 meters, with a horizontal length varying from 1000 to 3500 meters. Later, simulation results indicate that a relationship can be established among depth, horizontal length, and output power.

This project has received funding from the European Union's Horizon Europe research and innovation program under grant agreement No 101083558

Table 20 Different studied scenarios for integrating HOCLOOP concept in Darmstadt site

Vertical length (m)	Horizontal length (m)			
	Option-1	Option-2	Option-3	Option-4
1500	1000	2000	3000	3500
2000	1000	2000	3000	3500
2500	1000	2000	3000	3500
3000	1000	2000	3000	3500

3.2.5. Simulation of the integration scenarios and results

3.2.5.1. Definition of optimal flow rate

To determine the optimal flow rate, various flow rates were tested using two scenarios:

- Senario-1: 1500m depth, 1000m horizontal length, and inlet temperature 10°C
- Senario-2: 3000m depth, 3500m horizontal length, and inlet temperature 30°C

In FEFLOW, the pressure drop is not included in the solution of the coaxial pipe. The heat power output is calculated as $P = (T_{out} - T_{in})c\rho$ where Tout is the outlet temperature (°C), Tin is the inlet temperature (°C), c is the heat capacity of fluid (J/kg/°C), and ρ is the density (kg/m^3).

Increasing the flow rate results in a higher pressure drop and a lower outlet temperature. Conversely, heat output, calculated using the simplified method, increases as the flow rate rises. However, a lower outlet temperature negatively impacts heat pump efficiency.

Figure **33** illustrates that, in both scenarios, increasing the flow rate beyond 6 l/s provides minimal additional theoretical heat output, while causing a further decrease in temperature. Without incorporating a heat pump into the model, it is not possible to precisely determine an optimal flow rate that maximizes both the heat pump's coefficient of performance (COP) and thermal output.

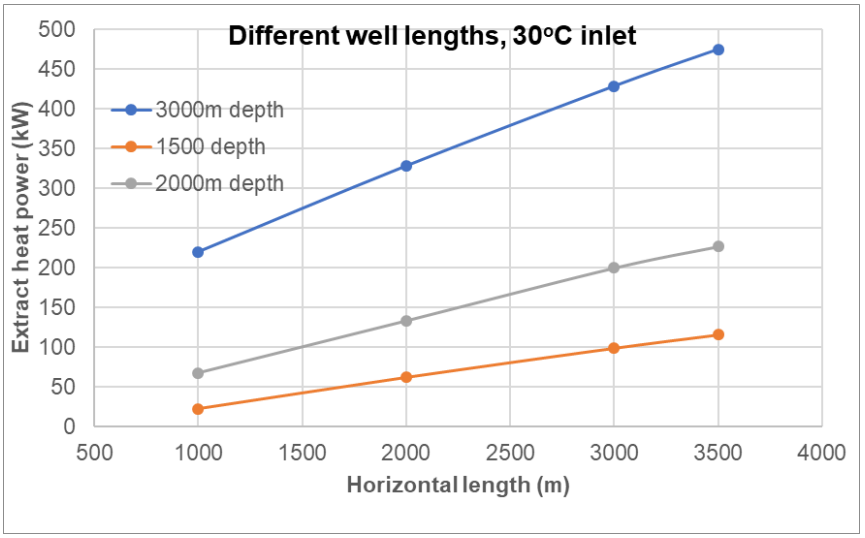

*Figure **33.** Darmstadt site - Heat output and outlet temperature depend on flow rate with two different scenarios*

This project has received funding from the European Union's Horizon Europe research and innovation program under grant agreement No 101083558

For futher investigation, 6 l/s flow rate is chosen.

3.2.5.2. Impact of depth and horizontal length

Figure **34** illustrates the heat extraction performance after 30 years, assuming an inlet temperature of 30°C and a flow rate of 6 L/s. The vertical depth varies from 1500m to 3000m, while horizontal path is from 1000m to 3500m.

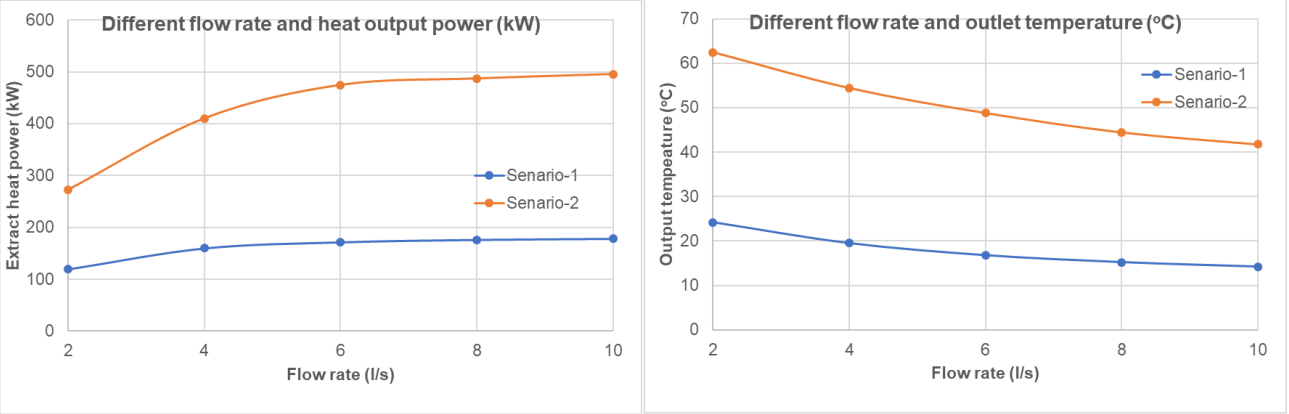

*Figure **34.** Darmstadt site – Different depth and different length – Extracted heat power after 30 years*

As shown in Figure **34**, a relationship can be established between heat output power, borehole depth, and horizontal length for a given inlet temperature. For a borehole depth of 3000 m and a horizontal length of 3500 m, the extracted heat output is approximately 460 kW, roughly half of the targeted 1 MW. Using extrapolation, it can be determined that to achieve the target of 1 MW with a borehole depth of 3000 m, the horizontal length should be extended to approximately 8000 m.

3.2.5.3. Impact of inlet temperature

In a closed system where the borehole is connected to a heat pump, the inlet temperature can be adjusted. For a simplified analysis, various inlet temperatures have been considered.

Figure **35** demonstrates that lowering the inlet temperature from 30°C to 10°C significantly boosts heat extraction power, which increases from 400 kW to 700 kW.

Theoretically, the inlet temperature can be lower. However, it is noted that, the outlet temperature also decreases when the inject temperature decreases. This affects COP of heat pump. For further analysis, coupled models between heat pump and underground model will be performed to address this, they will be presented in D4.3.

This project has received funding from the European Union's Horizon Europe research and innovation program under grant agreement No 101083558

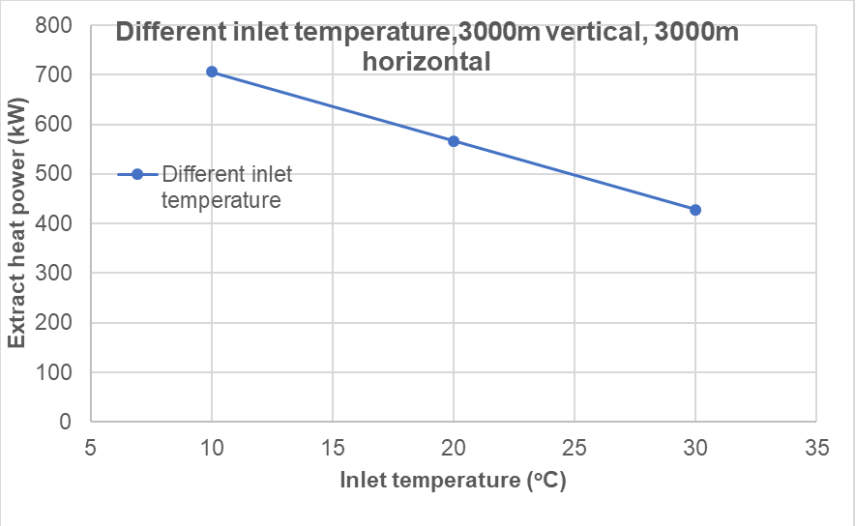

*Figure **35.** Darmstadt site – Different inlet extraction temperature – Extracted heat power after 30 year*

3.2.5.4. Impact of temperature gradient

Previous studies estimated that the temperature at a depth of 750 m at the Darmstadt site could reach up to 40°C. However, real measurement data from the SKEWs project revealed that the actual temperature at the bottom of the borehole is only 27°C, indicating a thermal gradient of 21°C/100 m, an unexpected result.

Under favorable conditions, if the borehole extends deeper and the thermal gradient increases, for example, from 2.1°C/100 m to 4°C/100 m, the extracted heat power could rise significantly, from 400 kW to over 1 MW (Figure **36**).

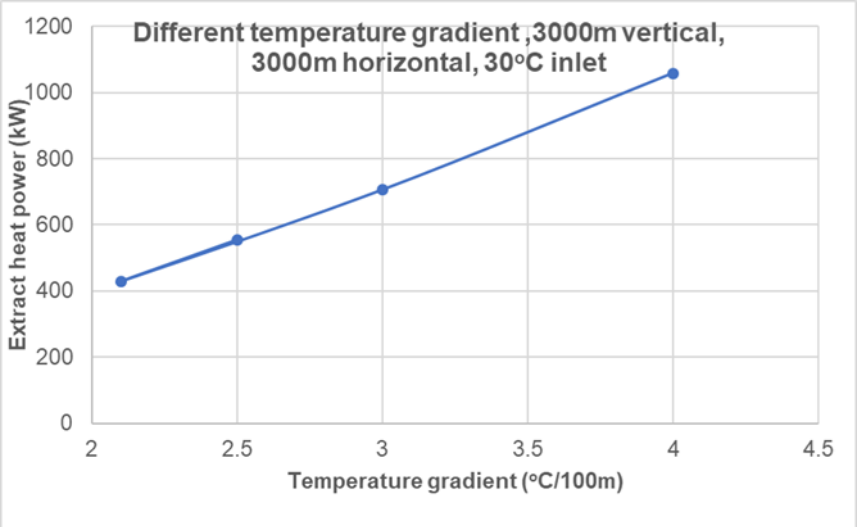

*Figure **36.** Darmstadt site – Different thermal gradient – Extracted heat power after 30 years*

This project has received funding from the European Union's Horizon Europe research and innovation program under grant agreement No 101083558

3.2.6. Conclusion and outlook

In Darmstadt, several projects are investigating various scenarios aimed at developing an efficient heating network. Specifically, the geothermal solutions HOCLOOP and MD-BTES are compared under the actual geological conditions of the area. From a purely technical perspective, without considering economic factors, the MD-BTES system currently appears more advantageous than the HOCLOOP approach. During the winter period, a single borehole using the HOCLOOP solution generates significantly less thermal energy (approximately 460 kW) compared to the minimum 1 MW of heating achievable by the MD-BTES system's 19 boreholes. However, it is important to note that the total drilling length of the MD-BTES system (approximately 14 km, with each borehole drilled to a depth of 750 m) is roughly equivalent to that required for two HOCLOOP boreholes (each 3,000 m deep with an additional 3,500 m horizontal section).

Further investigation, particularly a detailed cost analysis comparing the MD-BTES and HOCLOOP systems, will be carried out. Results of this analysis will be presented in deliverable D4.3.

This project has received funding from the European Union's Horizon Europe research and innovation program under grant agreement No 101083558

3.3. French case study

3.3.1. Introduction

The site of Fresnes, south of Paris, near Paris Orly airport, has been selected as one of the case studies for considering the HOCLOOP concept. There, a geothermal plant is already in operation producing hot water from the Dogger reservoir, and it is connected to the district heating system. At the present day, the primary fluid is produced from the GFR-3 well at 73°C with a 250 m^3/h (around 70 kg/s) flowrate. The produced fluid goes through the filtration, the heat exchangers, before being reinjected between 41 and 35°C in wells GFR-1 and GFR-2 (Figure **37**, Table **21**). If the outside temperatures fall below 8°C, a thermal heat pump is used after the heat exchangers and the temperature of the reinjected brine is falling to 25°C. Thus, a total thermal energy of around 9-14 MW, depending on the reinjection temperature, is produced. For an outside temperature below 6°C, a parallel cogeneration turbine is used. Emergency turbines are also present for maintenance or any breakdown of the installations. This study evaluates the potential of well GFR-3 for deploying the HOCLOOP concept.

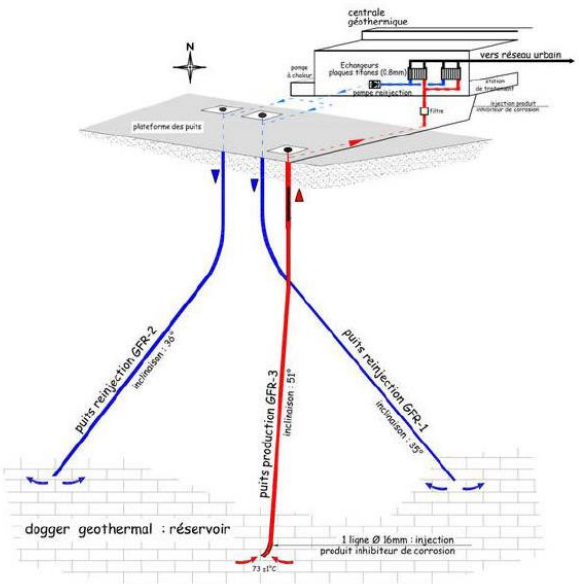

*Figure **37.** Schema of the geothermal plant in Fresnes, France.*

*Table **21.** Technical characteristics of the three well in Fresnes, France geothermal site.*

Well	GFR-1	GFR-2	GFR-3
Drilling length [m]	1740	1751	2306
Final inclination [°]	35	36	51
Reservoir temperature [°C]	71.7	74.1	73
Spacing with GFR-3 [m]	1540	1181	-

3.3.2. Collected available data

3.3.2.1. Geological data

Table 22 summarizes the properties of the geological setting of the Paris basin, as already provided in Deliverable D4.1 of the project,.

This project has received funding from the European Union's Horizon Europe research and innovation program under grant agreement No 101083558

*Table **22.** Thermal properties of all geological layers for the Paris basin.*

Layer	Bottom [m MD]	Temperature [°C]	Conductivity [W/m²/°C]	Capacity [J/°C/kg]	Density [kg/m³]
Surface	0	15	-	-	-
Albian	548	30.6	1.59	903	2380
Gault shale	608	32.6	3.16	859	2270
Barremian	754	38.3	1.63	915	2480
Oxfordian	1322	58.4	2.24	795	2390
Callovian	1623	68.1	1.73	917	2590
Lower Callovian	1727	71.7	2.14	805	2450
Bathonian	1767	73.7	2.14	806	2590
Dommerian	1963	81.0	1.74	915	2600
Rhetian	2146	88.0	2.63	887	2510
Anisian	2590	100.4	2.94	710	2370

3.3.2.2. Data on existing well candidate for the implementation of the HOCLOOP system

The geometry of the GFR-3 wellbore is given in Figure 38, and

Table **23** details the geometrical parameters.

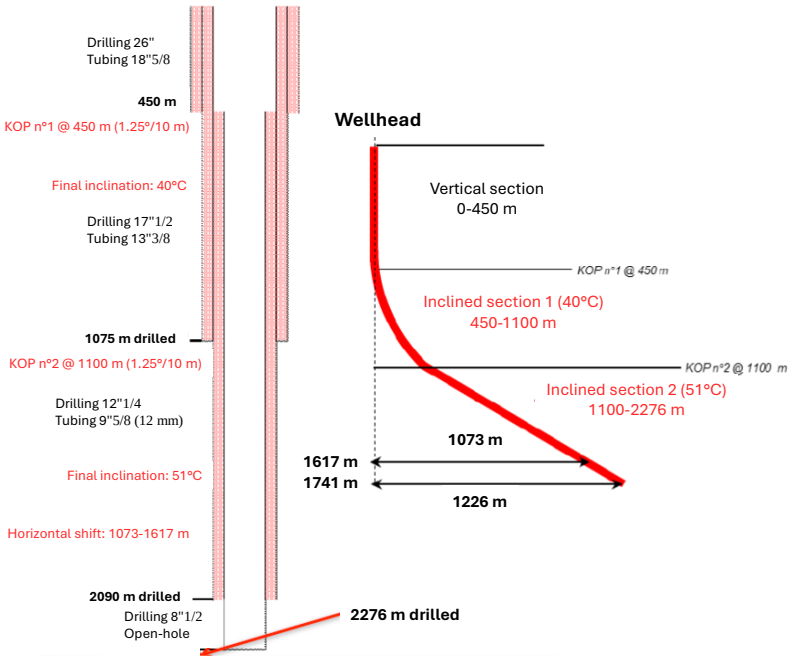

*Figure **38.** Desing of the GFR-3 geothermal wellbore in the French site.*

This project has received funding from the European Union's Horizon Europe research and innovation program under grant agreement No 101083558

*Table **23.** Characteristics of the GFR-3 well completion in Fresnes, France.*

Segment	Top [m MD]	Bottom [m MD]	Inclination [°]	Drilling [m]	Tube ID [m]	Thickness [m]			
						Tube	Cement	Casing	Cement
1	0	450	0	0.6604	0.309245	0.01524	0.0523875	0.011049	0.0936625
2	450	1100	40	0.4318	0.198755	0.01016	0.0333375	0.01524	0.0523875
3	1100	2090	51	0.3048	0.198755	0.01016	0.0333375	-	-
4	2090	2276	51	0.2159	-	-	-	-	-

3.3.3. Simulation procedure

3.3.3.1. Simulation tool

GWellFM (Geothermal Well Flow Model) is a steady-state, 1D non-isothermal axisymmetric, multicomponent, and two-phase flow simulator. The model considers the single-phase flows of liquids and gases, the hydrodynamics of the two-phase downward and upward flows, constitutive laws for mixtures and the heat exchange between the well completion and the surrounding formation. For modelling the heat flow, the heat transfer in the wellbore is considered under steady-state conditions and modelled applying the concept of thermal resistance in series until, whereas the corresponding heat transfer is the formation is modelled under transient conditions solving numerically the 2D heat conduction (Fourier's law). This simulator was benchmarked during WP2, Task 2.1 of the present project [4]

3.3.3.2. Well and rock properties

The detailed well configuration and properties of all materials as provided in Section 3.3.2 are used in the simulator.

3.3.3.3. HOCLOOP production pipe

For the extension of the existing well, the same installed casing (before the open-hole section) is considered, whereas for the horizontal drain a narrower casing is assumed. Finally, the closed-loop is created with the pipe-in-pipe string, as described in Deliverable D2.4 and according to Figure **39** [9]. In detail, the setup consists of two tubes and the space between them is under vacuum conditions for insulating the return fluid. The conductivity of all the materials is given in Table **24**.

This project has received funding from the European Union's Horizon Europe research and innovation program under grant agreement No 101083558

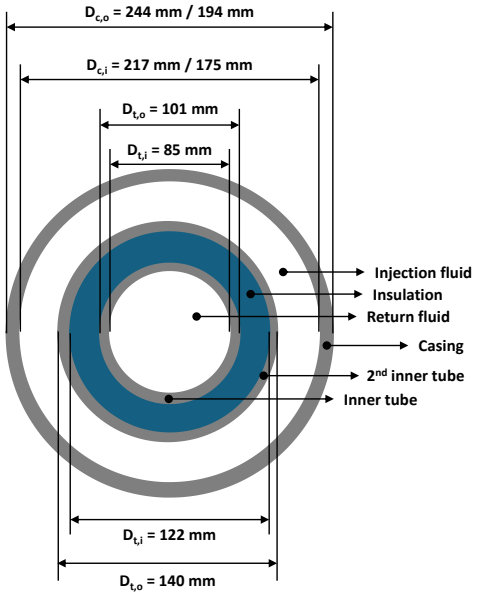

*Figure **39.** Characteristics of the closed-loop string used in the simulations for the French site.*

*Table **24.** Properties of the materials in the wellbore for the Fresnes site in France.*

Layer	Inner tube	Vacuum	2nd inner tube	Casing/tube	Cement
Thickness [m]	0.008	0.0105	0.009	-	-
Conductivity [W/m²/°C]	45	0.001	45	45	0.896

3.3.3.4. Recirculating fluid properties and initialization

All simulations are carried out with GWellFM for a 20-year operation. The thermophysical properties of the fluid (water) are pressure-temperature dependent, and the Kestin Equation-of-State is used. Details on the model could be found on the reports of WP2 [4, 10].

3.3.4. Integration scenarios

This study evaluates the potential of well GFR-3 for deploying the HOCLOOP concept. The scenarios analysed include utilizing the existing deviated wellbore or extending the well deeper into the reservoir, with the addition of a horizontal section. Initially, simulations are performed with constant flow rate inlet temperature to access the potential of the site and to investigate the impact of different parameters (flow rate, injection temperature and horizontal length). Then, the case with fixed outlet temperature is considered, while either the flow rate or the inlet temperature is controlled. Since the closed-loop solution is supposed to be connected to the existing district heating network, the outlet temperature corresponds to the temperature delivered to the district system.

3.3.5. Simulation of the integration scenarios and results

3.3.5.1. Site potential

The site potential with the existing well length is studied for different inlet conditions. Figure 40 presents the temporal evolution of the outlet temperature and pressure difference, expressed as the difference between the outlet and the inlet, in the existing GFR-3 well for different flow rates and fixed inlet

This project has received funding from the European Union's Horizon Europe research and innovation program under grant agreement No 101083558

temperature. In all cases, the outlet temperature decreases with time, with the decreasing rate being higher at the early stages of the operation. At lower flow rates, the production temperature is always higher because of the longer residence time of the fluid in the wellbore during which the fluid remains in contact with the hot rocks recovering more heat. The outlet pressure slightly changes with time, but there is a high impact of the flow rate. The higher flow rates require more injection pressure in order to overcome the pressure losses due to the high fluid velocity, thus more energy for pumping must be spent. It is worth mentioning that positive pressure difference means that the outlet pressure is higher than the injection pressure and that this pressure gain is because of the difference in density in the annular and central section of the coaxial well. In the central tube, the fluid density is slightly lower due to the higher temperature demanding less effort to raise the fluid.

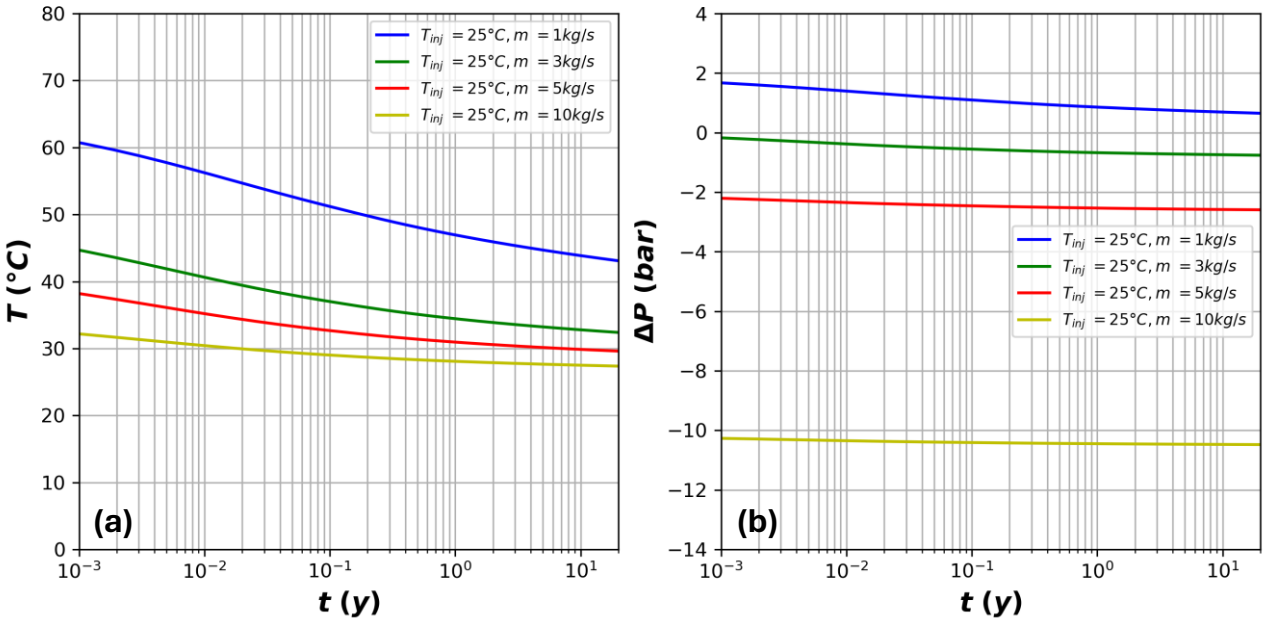

*Figure **40.** Impact of flow rate on the temporal evolution of (a) the outlet temperature and (b) the pressure difference between outlet and inlet in the actual GFR-3 well of the French site.*

Similarly, Figure **41** shows the outlet temperature and the gross thermal power for different inlet temperatures. The higher the inlet temperature, the higher the outlet temperature, with the impact being more important at higher flow rates. For higher inlet temperatures, the energy losses at shallow depths are higher, because the temperature in the well is higher than the surrounding rock temperature. On the other hand, at intermediate and deep depths, the fluid reaches higher temperatures, leading to lower heat fluxes compared to scenarios with a lower injection temperature. On the contrary, the thermal power, estimated from the enthalpy difference between outlet and inlet, is much higher for the lower injection temperatures and the same flow rate because the enthalpy of the fluid in the inlet of the system is also lower. In addition, as the gross thermal power is proportional to the flow rate, more power is produced for higher flow rates.

This project has received funding from the European Union's Horizon Europe research and innovation program under grant agreement No 101083558

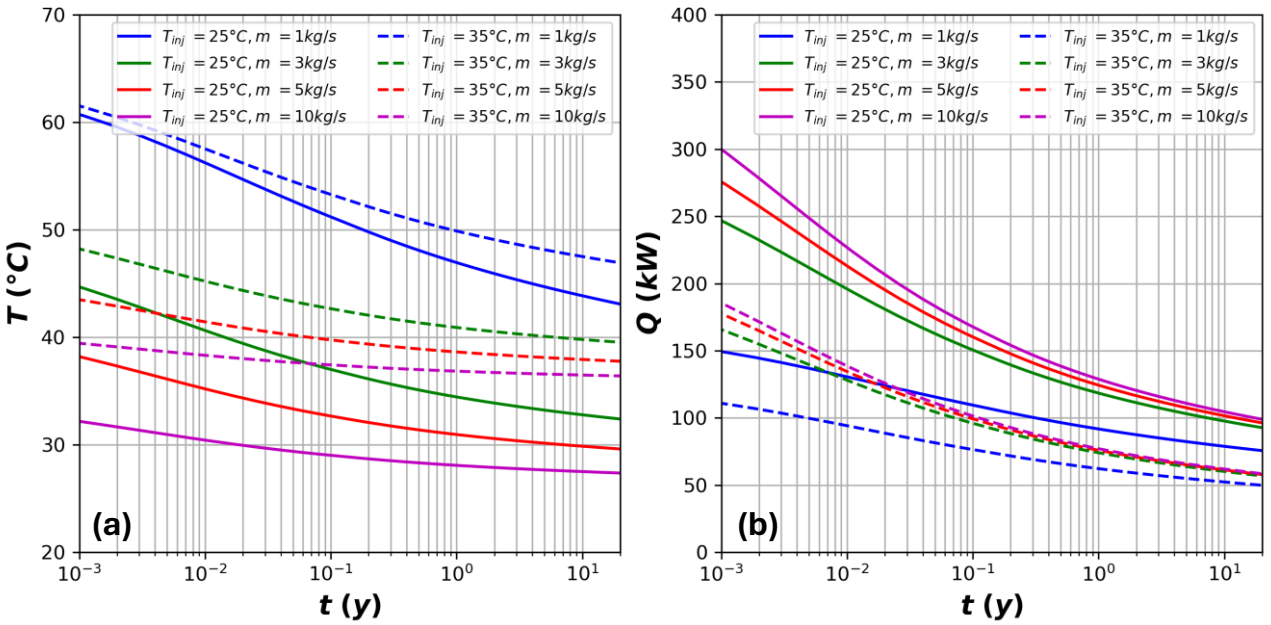

*Figure **41.** Impact of inlet temperature in the temporal evolution of (a) the outlet temperature and (b) gross thermal power in the actual GFR-3 well of the French site.*

The highly transient nature of the heat conduction transfer suggests that for the geothermal closed-loop to provide a constant temperature and to be connected to the district heating network, either the inlet temperature or the flow rate together must be controlled. The figures above also show that the outlet temperature is several degrees lower than the actual production temperature of the doublet. To increase the temperature, the wellbore could be elongated and/or extended with a horizontal section and the use of a cogeneration system (i.e., heat pump) could be needed. In addition, the flow rates for producing a fluid with relatively high temperature are very small when compared to the flow rate of the actual open-loop geothermal system, thus meaning that wider or multiple wellbores must be used to cover the same needs as the geothermal doublet.

3.3.5.2. Wellbore extension

First, a 500 m elongation of the wellbore is simulated, and then different horizontal lengths are tested. When compared to the actual wellbore, the outlet temperature is always higher, as shown in Figure **42**. In the case of the horizontal extensions, the increase caused by adding 1 km of wellbore section is substantial (35°C at the beginning of the operation, and around 20°C after 20 years). The rate of increase, however, decreases for longer wellbores with the impact above 2 km being relatively low. When compared to the inlet and outlet temperatures of the doublet, the closed-loop must be elongated by 500 m and extended for at least 2 km. But again, it is clear that the inlet temperature and flow rate have to be controlled for delivering a fluid with constant temperature. In addition, to keep the outlet temperature always around 73°C, a horizontal extension above 3 km will probably be required. The exact length depends also on the inlet temperature and the flow rate.

This project has received funding from the European Union's Horizon Europe research and innovation program under grant agreement No 101083558

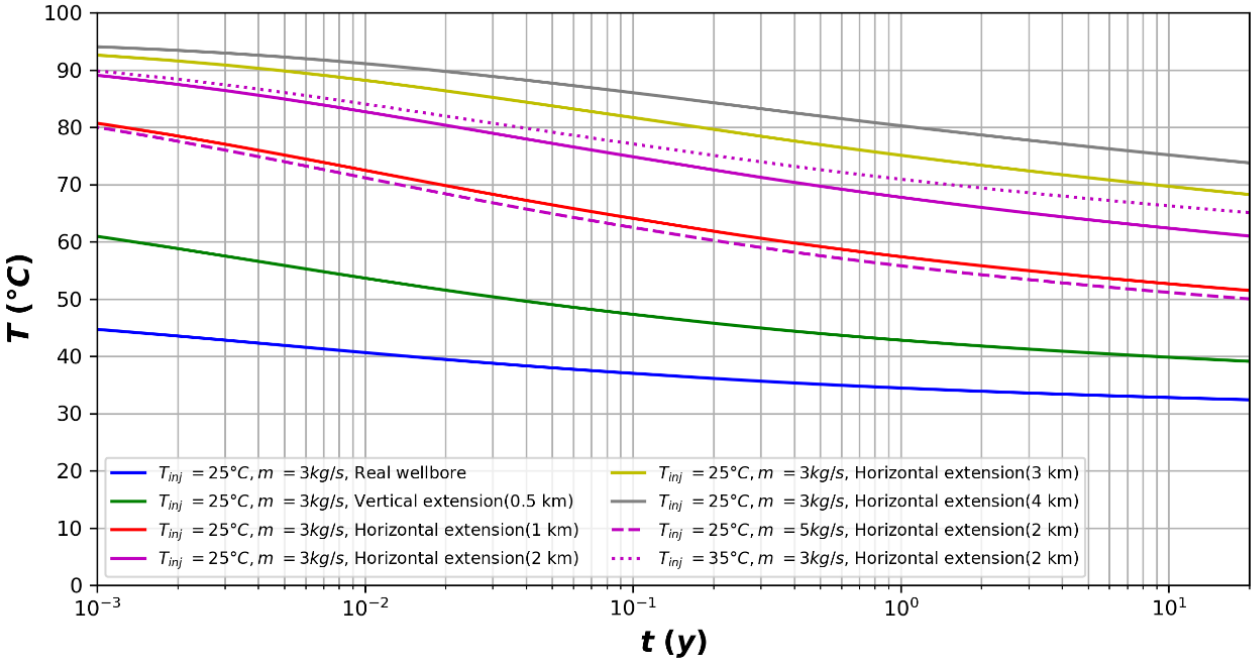

*Figure **42.** Comparison of the temporal evolution of the outlet temperature without and with an extension of the GFR-3 well in the French site.*

Even though the gross thermal power produced with the extended wellbores is much higher than the power that could be produced with the actual wellbore (Figure **43**), it still remains much lower when compared to the doublet case. The temporal trend of the power is similar with the outlet temperature evolution of Figure **42**, but much higher power is produced with higher flow rates due to the linear correlation between flow rate and power.

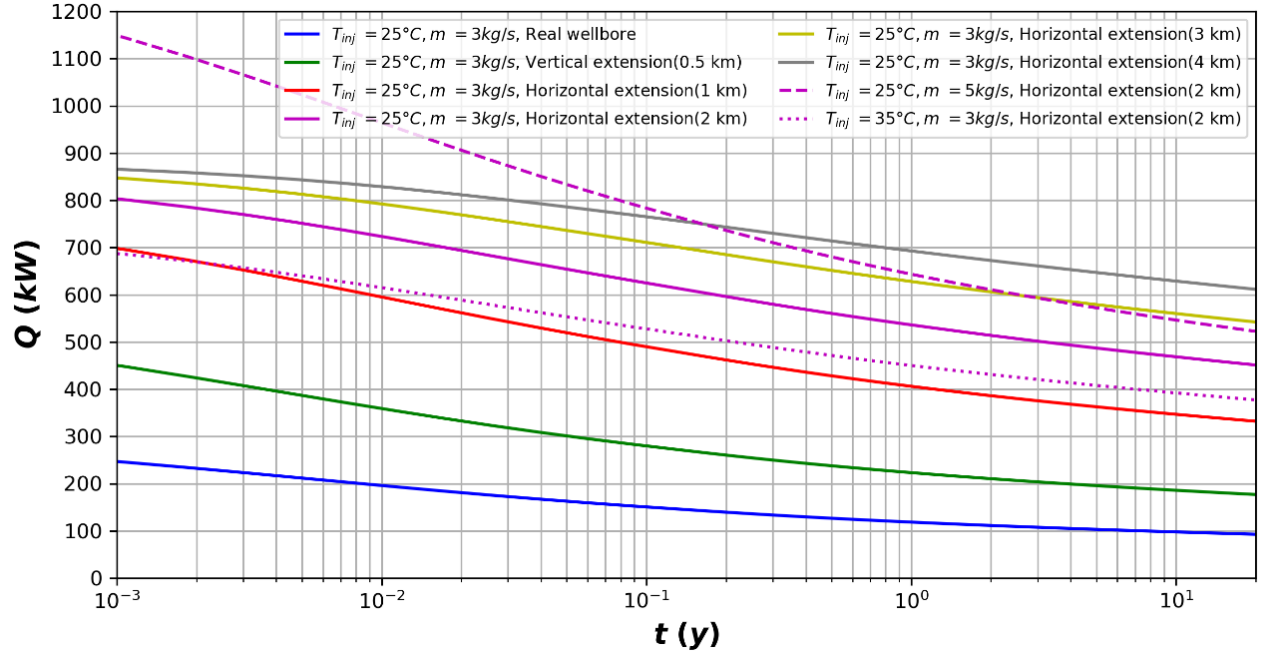

*Figure **43.** Comparison of the temporal evolution of the gross thermal power without and with an extension of the GFR-3 well in the French site.*

However, high flow rate results in higher pressure losses, according to Figure **44**, and consequently more

This project has received funding from the European Union's Horizon Europe research and innovation program under grant agreement No 101083558

pumping pressure may be required. For the actual wellbore, the pressure difference is always negative, thus meaning that pressure losses in the return tube are higher than the pressure increase in the downward part of the wellbore. On the other hand, in the elongated and extended wellbores, the outlet pressure is higher than the inlet for an initial period of time, which depends on the total wellbore length. The pressure losses in the return tube are lower than the pressure increase in the annular part. This results in a pressure gain, which is caused because the fluid in the return tube is lighter (has lower density) due to the higher temperatures. This phenomenon, which is known as thermosiphon effect, decreases with time due to the corresponding decrease of fluid's temperature. After a certain time, the effect becomes negligible, and the outlet pressure is lower than the inlet pressure.

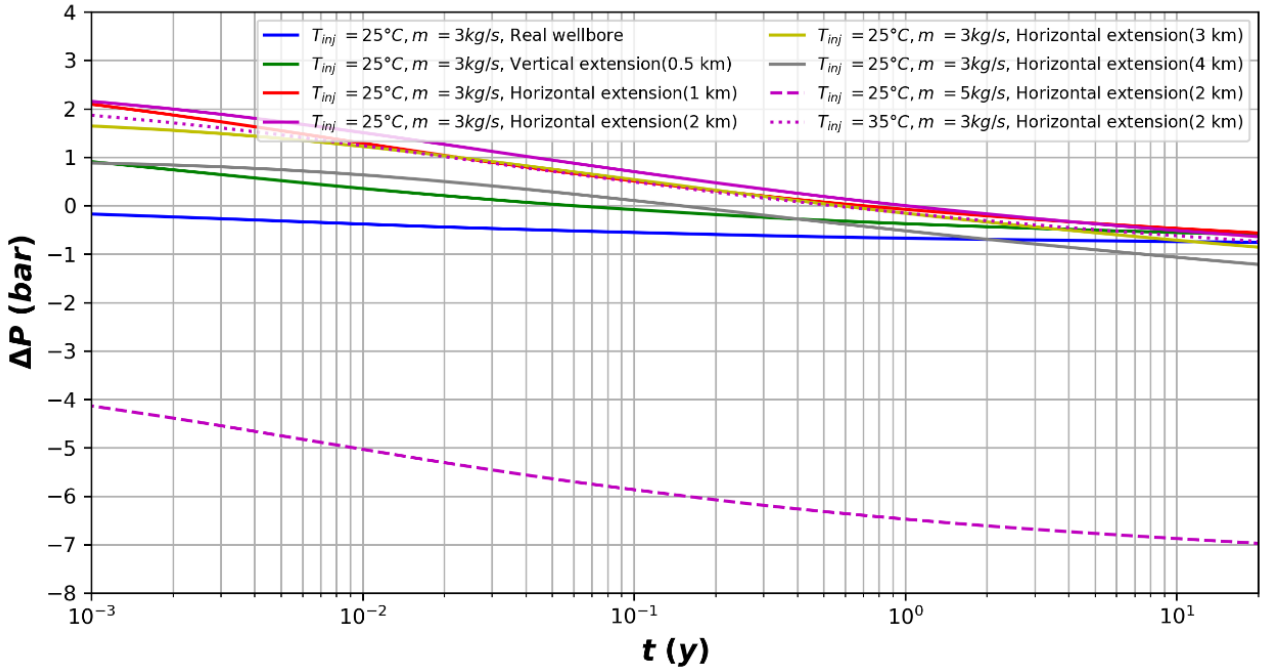

*Figure **44**. Comparison of the temporal evolution of the pressure difference between outlet and inlet without and with an extension of the GFR-3 well in the French site.*

3.3.5.3. Control of inlet conditions

As previously mentioned, to ensure the system delivers fluid at the desired temperature, the inlet conditions must be regulated (optimized) throughout its operational life. First, simulations are performed by controlling the inlet temperature and then with adjustable injection flow rate.

3.3.5.3.1. Control of inlet temperature

Figure **45** shows the evolution of the inlet temperature for the system with the actual wellbore to produce the fluid at the fix temperature of 50°C and with a constant flow rate (3 kg/s). The inlet temperature is close to the outlet temperature, and as a result the produced gross power is very low. The results are similar for a higher required outlet temperature (65°C) and higher fixed flow rate (12 kg/s), but with higher gross thermal power because of the high flow rate (Figure **46**). Both cases reveal that controlling the inlet temperature is not the appropriate method of optimization of the current application, since the inlet temperature must be high with a very low difference with the outlet temperature.

This project has received funding from the European Union's Horizon Europe research and innovation program under grant agreement No 101083558

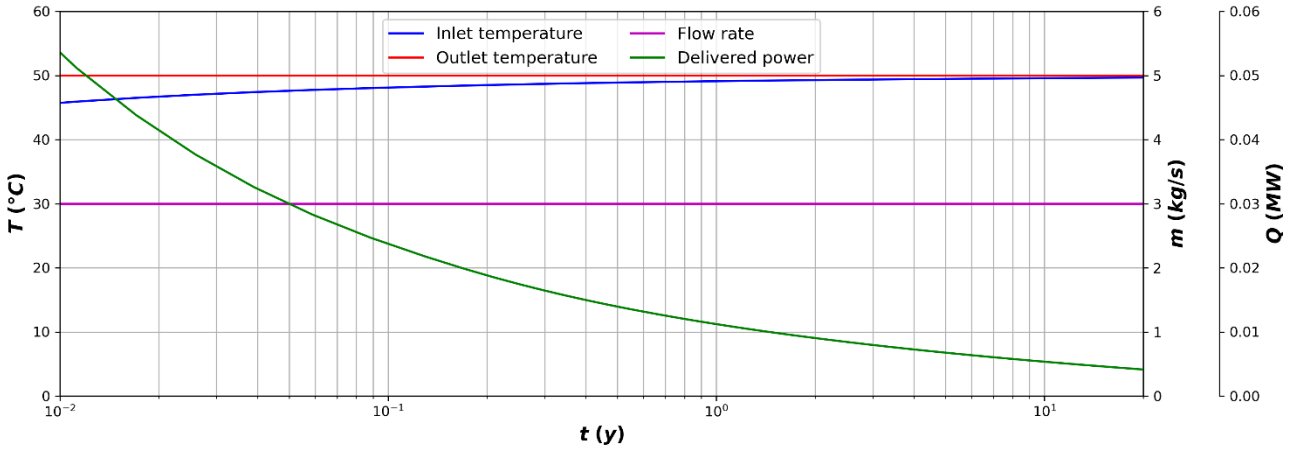

*Figure **45.** Evolution of inlet temperature and delivered gross thermal power for fixed outlet temperature (50°C) and flow rate (3 kg/s) in the actual GFR-3 well of the French site.*

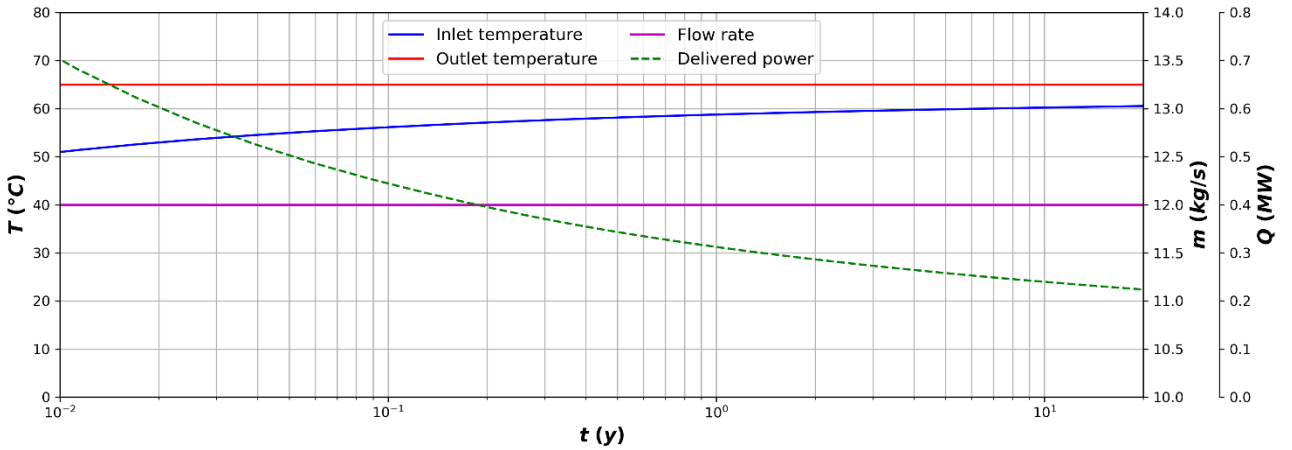

*Figure **46.** Evolution of inlet temperature and delivered gross thermal power for fixed outlet temperature (65°C) and flow rate (12 kg/s) with a 2 km horizontal extension of well GFR-3 of the French site.*

3.3.5.3.2. Control of flow rate

Controlling the flow rate for fixed inlet and outlet temperatures seems to be a more suitable methodology for the specific application. In Figure **47** and Figure **48** the evolution of the flow rate for a moderate (50°C) and higher (65°C) outlet temperature are presented, for the actual well depth. In both cases, the flow rate is relatively low resulting in a low gross thermal power output, four and three orders of magnitude lower for the 50°C and 65°C, respectively, when compared to the nominal power output of the doublet.

This project has received funding from the European Union's Horizon Europe research and innovation program under grant agreement No 101083558

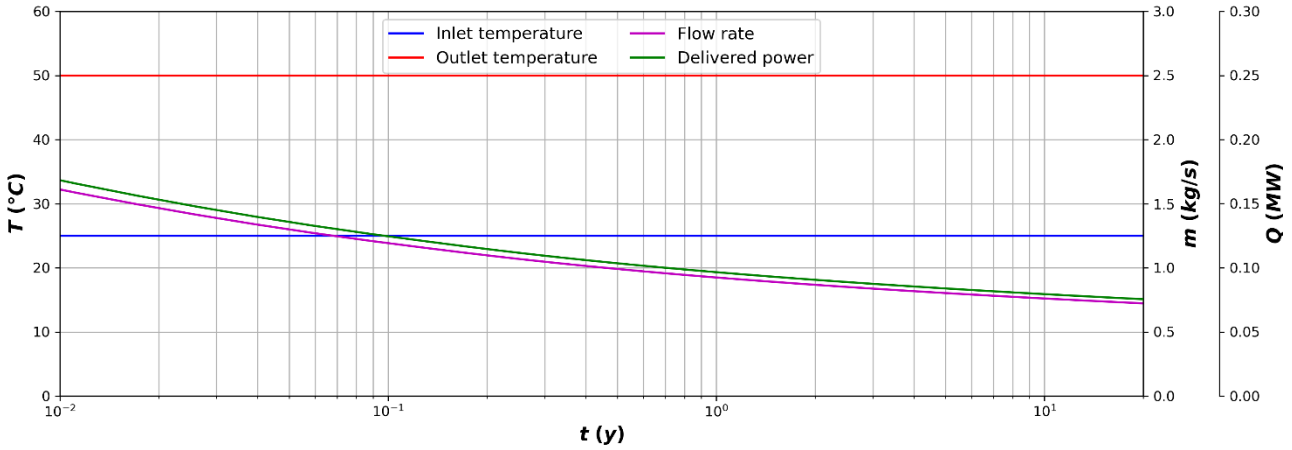

*Figure **47.** Evolution of flow rate and delivered gross thermal power for fixed inlet (25°C) and outlet (50°C) temperatures in the actual GFR-3 well of the French site.*

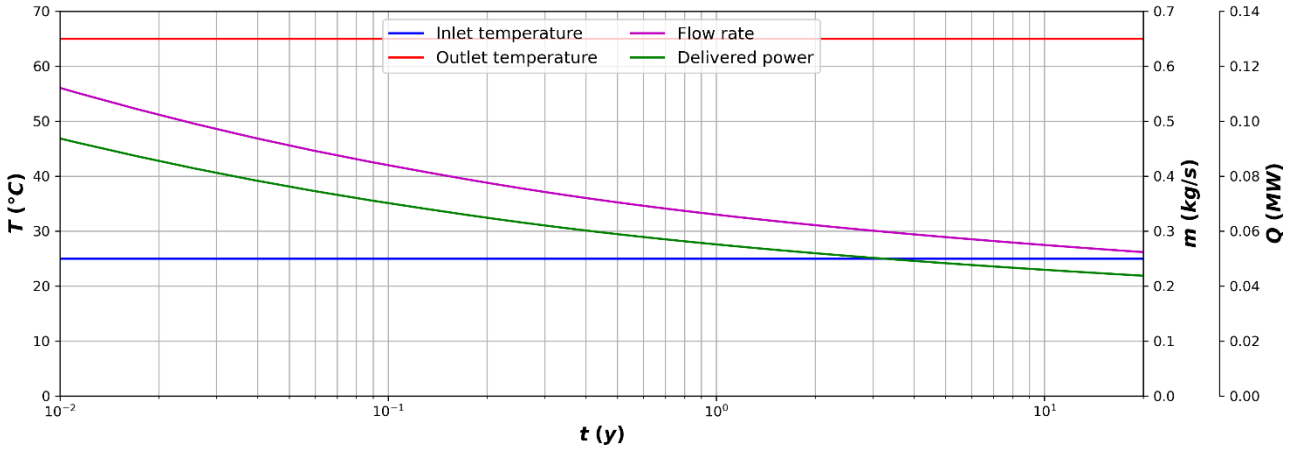

*Figure **48**. Evolution of flow rate and delivered gross thermal power for fixed inlet (25°C) and outlet (65°C) temperatures in the actual GFR-3 well of the French site.*

By considering a 2 km horizontal extension (Figure 49), the performance of the system is improved with higher flow rates for the same inlet and outlet temperatures as before. Due to the higher flow rates, the system produces more power. With a longer horizontal section (4 km), the system can deliver the same temperature as the doublet (73°C), but with much lower power output (Figure 50).

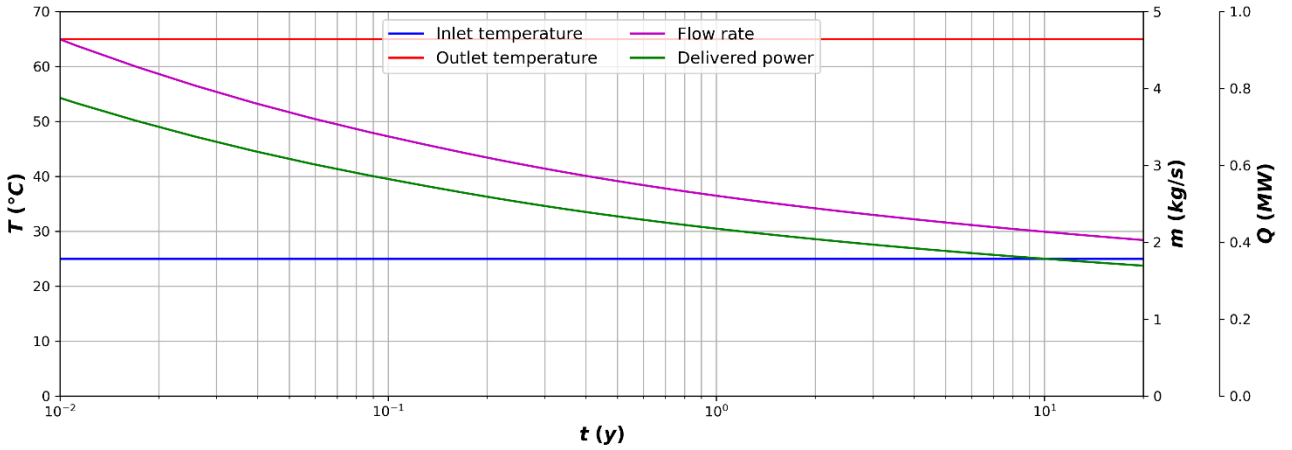

*Figure **49.** Evolution of flow rate and delivered gross thermal power for fixed inlet (25°C) and outlet temperatures (65°C) in the GFR-3 well of the French site with a 2 km horizontal extension.*

This project has received funding from the European Union's Horizon Europe research and innovation program under grant agreement No 101083558

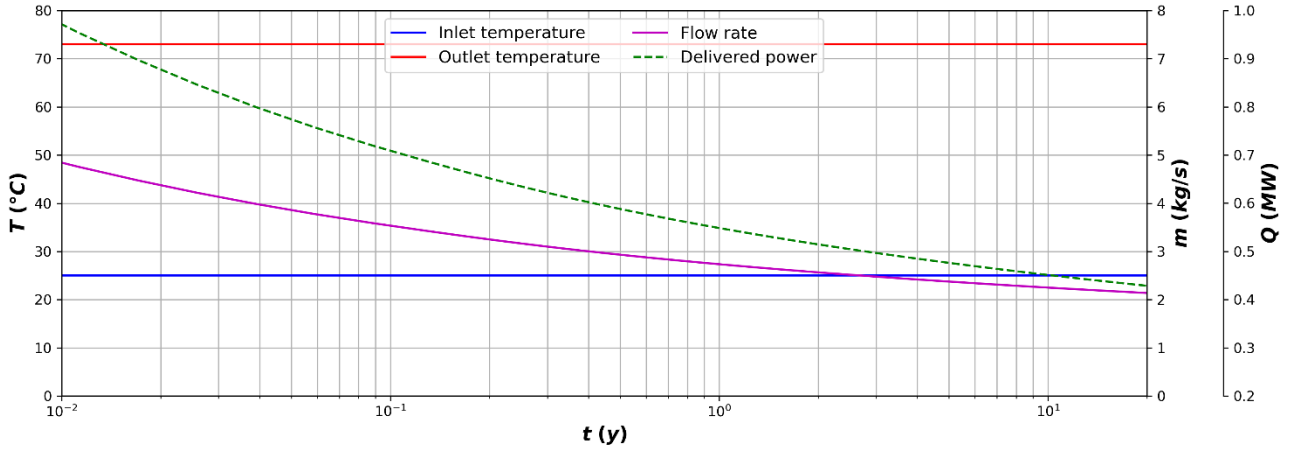

*Figure **50.** Evolution of flow rate and delivered gross thermal power for fixed inlet (25°C) and outlet (73°C) temperatures in the GFR-3 well of the French site with a 4 km horizontal extension.*

The last two cases are also simulated with a seasonal variation of the inlet temperature. For 6 months the inlet temperature is 25°C and then increases to 35°C for another period of 6 months. Increasing the inlet temperature results always in an increase of the flowrate and a corresponding decrease of the power delivered, and vice-versa when the temperature is increased.

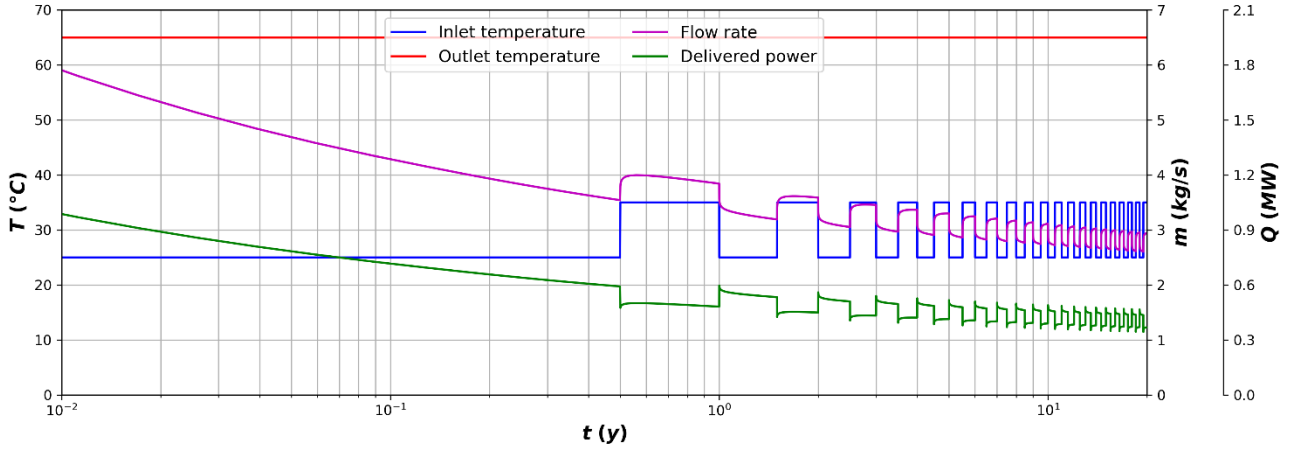

*Figure **51.** Evolution of flow rate and delivered gross thermal power with a seasonal variation of the inlet temperature and fixed outlet temperatures (65°C) in the GFR-3 well of the French site with a 4 km horizontal extension.*

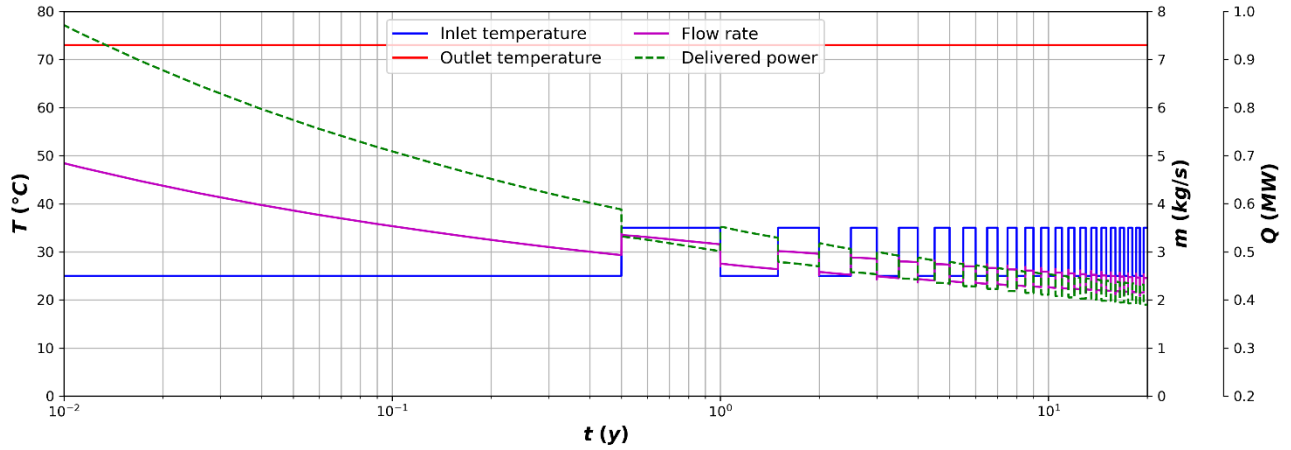

*Figure **52.** Evolution of flow rate and delivered gross thermal power with a seasonal variation of the inlet temperature and fixed outlet temperatures (73°C) in the GFR-3 well of the French site with a 4 km horizontal extension.*

This project has received funding from the European Union's Horizon Europe research and innovation program under grant agreement No 101083558

The evolution of the temperature in the rock domain for the cases without (constant inlet temperature) and with seasonal variation of the inlet temperature is slightly different. In Figure **53**, the evolution of temperature, expressed as the difference with the initial temperature (at t = 0) is shown for 4 distances from the wellbore and in 3 locations along the wellbore. In the case of the seasonal variation (solid lines), the decrease of the rocks temperature occurs at a lower rate. Also, closer to the surface, the rock temperature increases during the first months of injection with 35°C because the fluid temperature is initially higher than the rock temperature. The amplitude of the temperature change decreases with the depth and the distance from the wellbore.

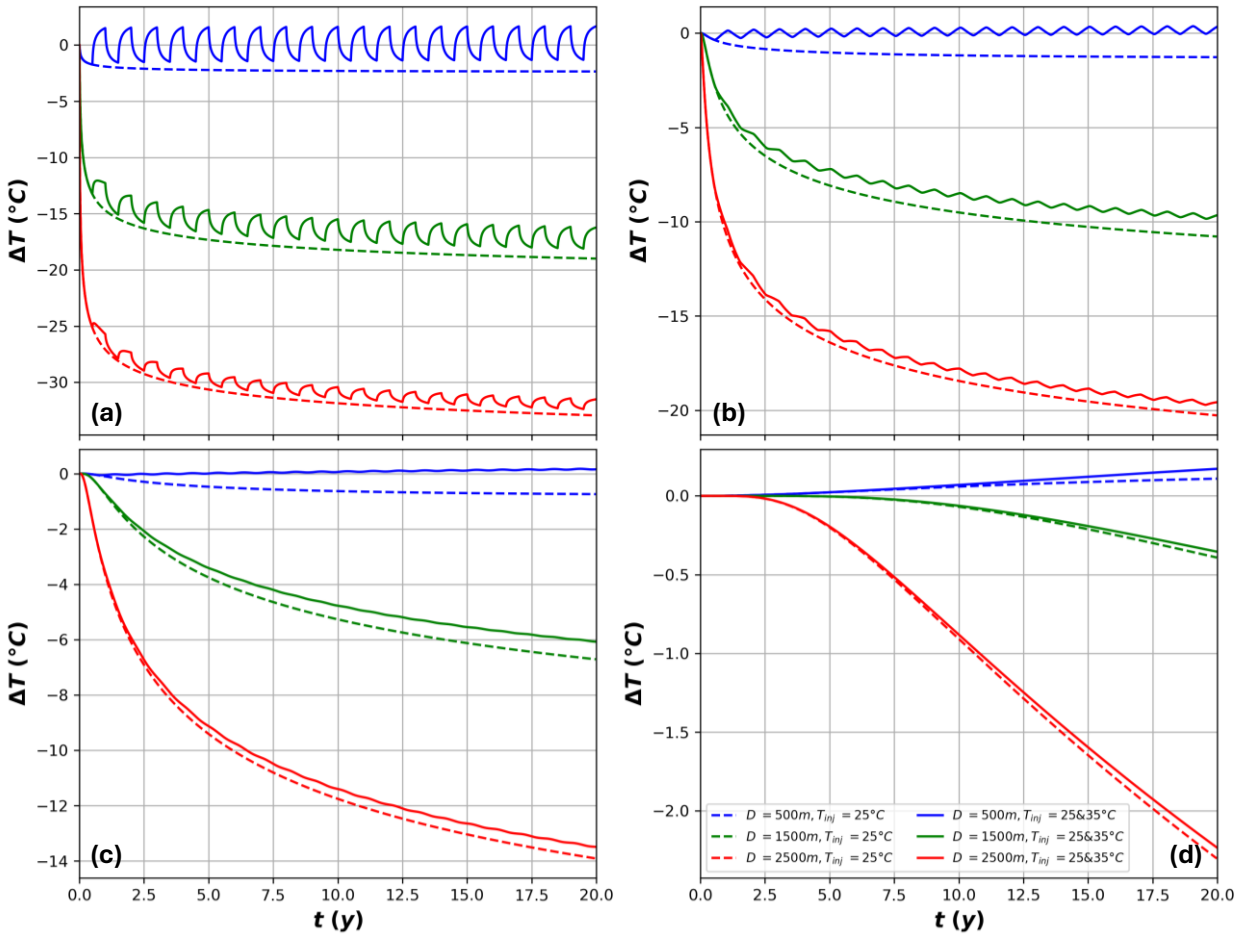

*Figure **53.** Evolution of the temperature in the rock domain at (a) 1 m, (b) 5 m, (c) 10 m and (d) 50 m distance from the wellbore and in three total lengths for the GFR-3 well of the French site with a 4 km horizontal extension, and without (dashed lines) and with seasonal variation (solid lines) of the inlet temperature.*

3.3.6. Conclusion of the French case

The evaluation of the HOCLOOP concept for a low temperature geological setting showed that its overall performance is always much lower when compared to the geothermal doublet. Even with a potential horizontal extension of the wellbore, the produced power from one closed system is four (around 0.01 MW) to three (0.1 MW) orders of magnitude lower than the actual production of the geothermal doublet (10 MW).

Due to the highly transient nature of the heat conduction transfer from the rocks to the wellbore, the outlet temperature of the fluid decreased by several degrees, with the phenomenon being more important during

This project has received funding from the European Union's Horizon Europe research and innovation program under grant agreement No 101083558

the first stages of the operation. For the system to be able to deliver to the district heating system a fluid with constant temperature, the inlet conditions must be controlled. From the two optimization procedures tested, adjusting the inlet flow rate proved to be the optimal method in comparison with the control of the inlet temperature.

3.4. Italian case study

3.4.1. Introduction

Several Italian case studies have been selected for possible application of the HOCLOOP technology, representative of the wide range of heat flux values affecting areas with different lithologies and tectonic settings.

The first case study, Gargano, south-eastern Italy (Apulia), is representative of low heat flux regions and is characterized by a heat flux value of about 40 mW/m². The area is rich in geophysical and boreholes information, permitting integration with data collected at the surface (fracture distribution and lithology) and providing the dataset for evaluating the potential location of the HOCLOOP solution, in the presence/absence of hydrothermal fluids at suitable depth, through modeling.

The second and third Italian cases, Gavorrano and Monte Amiata, are in the western side of central Italy (Tuscany) and are representative of regions with intermediate and high heat flux, as the values there are about 70 mW/m² and higher than 80 mW/m², respectively.

The Gavorrano case is an abandoned mining area, where geophysical and sub-surface data is available. Integration with the fracture distribution dataset will enable to define a clear picture of the possible water pathways, providing key information on the potential HOCLOOP solution in such a context. On the other hand, the Monte Amiata area is close to an active geothermal field where a massive dataset on the substratum is already available.

3.4.2. Collected available data

Due to the limited availability of data for the Italian case studies and, most importantly, the absence of specifically identified wells for the application of the HOCLOOP concept, the well geometry for the subsurface simulations was chosen based on the other case studies analysed in this task. Specifically, the well geometry from the French case (Figure 25) was used as a reference for all the case studies considered.

The detailed description of the geological settings of the different Italian cases, as already provided in Deliverable D4.1 of the project, are summarised in Table 25.

*Table **25.** Thermal properties of all geological layers for the three Italian cases*

Monte Amiata			
Lithology	Thickness (m)	Thermal Conductivity (W/mK)	Heat Capacity (MJ/m3K)
Oceanic Units	600	2.1	2.18
Evaporite	300	4.18	2.18

This project has received funding from the European Union's Horizon Europe research and innovation program under grant agreement No 101083558

Quartzite	350	2.7	2.18
Phyllite	1500	2.7 - 3	2.18

Gargano

Lithology	Thickness (m)	Thermal Conductivity (W/mK)	Heat Capacity (MJ/m3K)
Alluvial sediments	100	1.8	-
Limestone and dolostone	1000	2	-

Gavorrano

Lithology	Thickness (m)	Thermal Conductivity (W/mK)	Heat Capacity (MJ/m3K)
Alluvial sediments	100	1.8	2.18
Limestone and dolostone	220	2.5	2.18
Phyllite	60	3	2.18
Granite	200	2.5	2.18
Phyllite	550	2.7 – 3	2.18

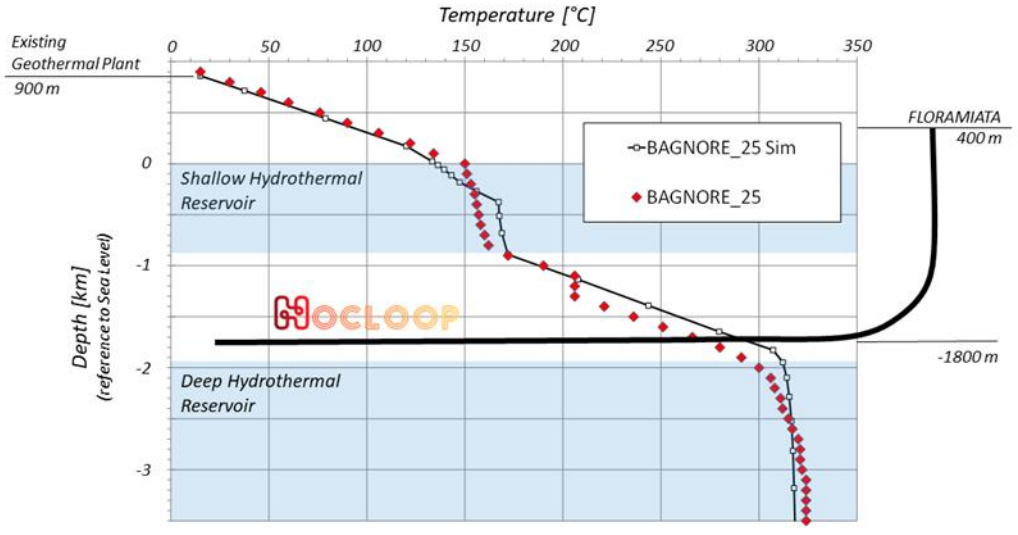

*Figure **54.** Temperature profiles of two existing geothermal wells in the Amiata area with highlighted the two hydrothermal reservoir and the possible well profile that targets the low permeability section between the two*

In the Amiata case, the HOCLOOP solution will be installed near an existing and productive hydrothermal reservoir. The primary goal of this case study is to assess the performance of HOCLOOP technology in a real geothermal setting. However, targeting either of the two reservoirs shown in Figure 52 for the

This project has received funding from the European Union's Horizon Europe research and innovation program under grant agreement No 101083558

installation of the closed-loop system is not a viable option, as such a system cannot compete with conventional geothermal solutions when a water reservoir is present. The hypothetical HOCLOOP well has thus been positioned within the low-permeability cap of the deep reservoir (1,800 m below sea level) to simulate heat extraction from a hot dry rock reservoir. This approach enables a comparative analysis with other technologies, such as those utilizing hydraulic fracturing. Furthermore, the final heat user is situated in a valley below the existing geothermal power plant. This geographical advantage allows for a reduction in the vertical well section by extending the horizontal segment to reach the area beneath the plant.

3.4.3. Simulation procedure

For the Italian case calculations, a semi-analytical model is used. The well is modeled through a quasi-stationary approach as a heat exchanger. Specifically, the internal heat transfer between the fluid in the annulus and the inner tubing is neglected as the fluid flowing in the inner tube is considered as completely insulated from the annulus. The well is discretized along its length and only the heat transfer in the radial direction is considered, while the heat propagation in the axial direction is neglected. A scheme of the proposed model is shown in **55**.

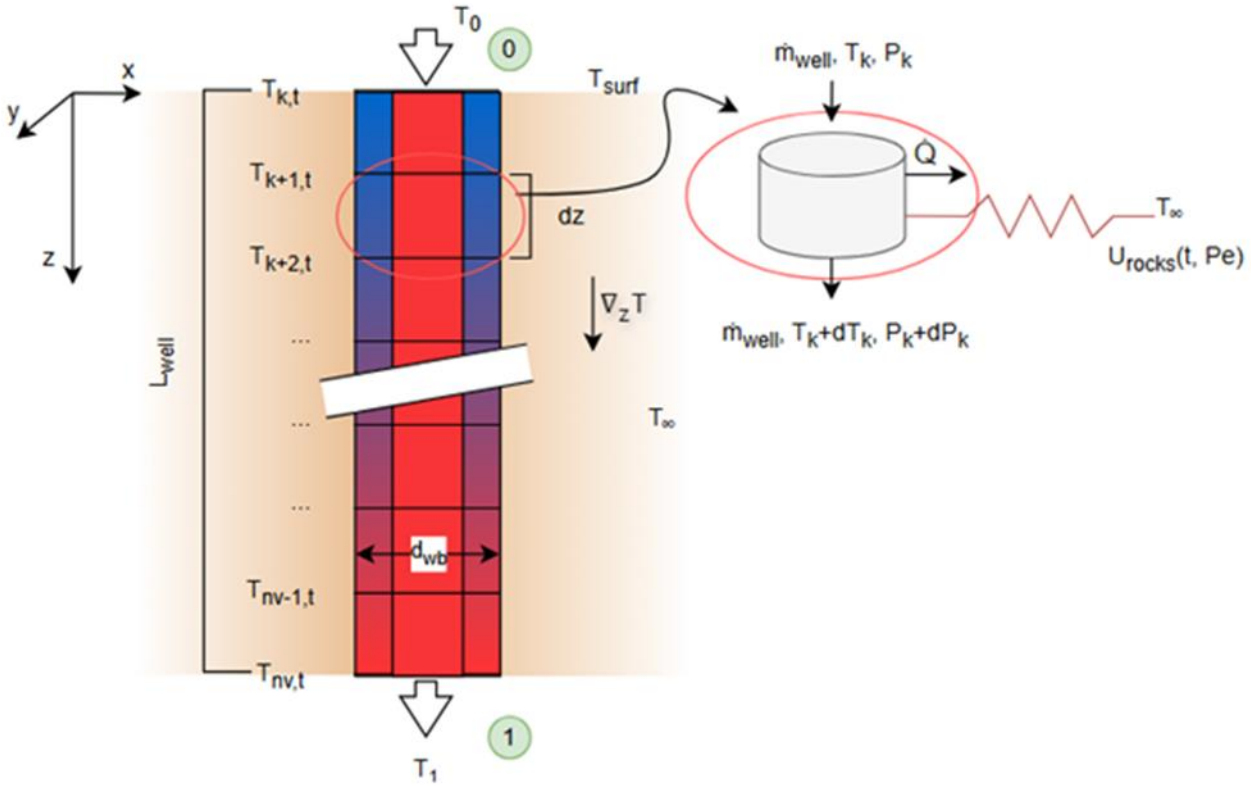

*Figure **55.** Geothermal well model: heat transfer and discretization scheme*

The problem is solved by integrating the momentum and energy balance equation along the length of the well:

$$\frac{dp}{dz} = -(\rho g cos\vartheta_i + dp_{loss}) \quad \text{Equation 7}$$

This project has received funding from the European Union's Horizon Europe research and innovation program under grant agreement No 101083558

$$\frac{dh}{dz} = \left(gcos\vartheta_i - \frac{dq_{tot}^{\cdot}}{m_{well}^{\cdot}}\right) \quad \text{Equation 8}$$

Where ϑ_i is the inclination of the well and $dq_{tot}^{\cdot}$ is the total heat transfer.

In this case, the internal heat exchange is neglected and $dq_{tot}^{\cdot}$ corresponds to the heat exchanged with the rocks, evaluated as:

$$dq_{tot}^{\cdot} = U_{rocks} A \Delta T(t_d, z) \quad \text{Equation 9}$$

Where $A=\pi d_{well}$ is the area of the well per unit length and d_{well} is the outer diameter of the well. $\Delta T(t_d, z)$ is the temperature difference between the heat transfer fluid and the undisturbed rock formation, with t_d being the dimensionless time, and $U_{rocks}(t_d, Pe)$ is the heat transfer coefficient of the rocks, defined as:

$$U_{rocks}(t_d, Pe = 0) = \frac{d_{well}}{2k_{rocks} f(t_d, Pe=0)} \quad \text{Equation 10}$$

Where $f(t_d, Pe = 0)$ is the response of the rock formation to the heat exchanged with the well over time in case of pure conduction, i.e. Peclet number equal to zero. Zhang *et al.* [11] use a formulation for $f(t_d)$ considering the case of pure conduction. In previous works [12], a correlation that considers the convective heat transfer quantified by Peclet Number has been developed and it is the one used in this analysis.

The proposed formulation of the heat transfer coefficient neglects the thermal resistances due to the conduction in the walls of the well and the convection of the fluid in the annulus.

Applying the temporal convolution approach to the heat flux between the rocks and the well allows to obtain the heat exchanged through the following equation:

$$q_{total,i} = \sum_{j=0}^{i-1} \frac{2k_{rocks}(t_{d,i} - t_{d,j})}{d_{well}} \Delta T(t_{d,j}) \quad \text{Equation 11}$$

$\Delta T(t_{di}) = T_{\{f,i\}} - T_{\{r,i-1\}}$ represents the temperature difference between the fluid and the rocks at each timestep. $f\left(t_{d_i} - t_{d_j}\right)$ is reversed to apply the convolution. The convolution approach enables the model to accurately represent heat exchange and temperature profiles over time during normal transient phase, as can be noted in the benchmarking performed in the following section.

It should be noted that neglecting internal heat exchange between the inner tube and the annulus introduces a modelling error when a sharp variation of flow rate occurs, i.e. during the transient phase following a period of stagnation or of low mass flow rate. Nevertheless, this deviation is due to the dynamics of the well and is restricted to the time interval during which the fluid "trapped" within the geothermal well is completely extracted on the surface. Based on the typical values of flow velocity inside the tubes, the duration of this phenomenon is generally lower than a couple hours, leading to this error to be marginal when the temporal window of the analysis is large enough.

3.4.3.1. Benchmarking

The correlation and convolution approach were validated against the results of Zhang et al. (2011).

Zhang proposed a vertical geothermal well of 1000m which is first subject to injection of water at 20°C. Secondly, after 100 days water is extracted from the bottom of the well at 180°C. The reference graph published by Zhang et al. illustrates the temperature trend of the fluid at three different vertical positions: the top, middle and bottom of the well. The results obtained from the developed model, shown in Figure 56, demonstrate good agreement with those from Zhang et al. (2011). Both models, which rely on time

This project has received funding from the European Union's Horizon Europe research and innovation program under grant agreement No 101083558

convolution, effectively capture the transient phases and illustrate how the fluid temperature evolves over time.

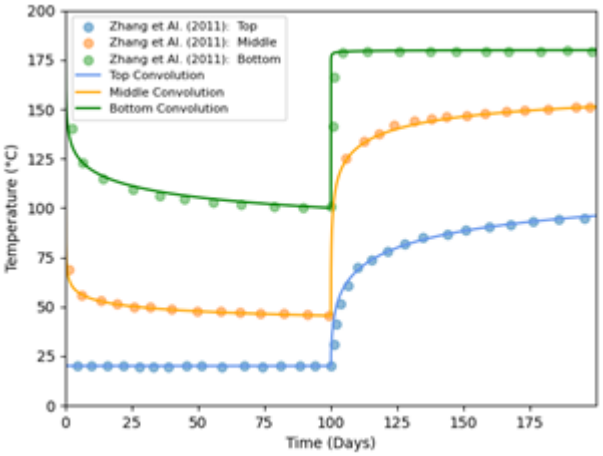

*Figure **56.** Benchmarking of time convolution and correlation*

Additionally, the overall model is benchmarked against results from the Balmatt case. Specifically, Scenario 2 has been considered. In this scenario, the VITO well is operated at a constant mass flow rate of 3 kg/s and the injection temperature is controlled to meet the monthly averaged power demand. 57 .

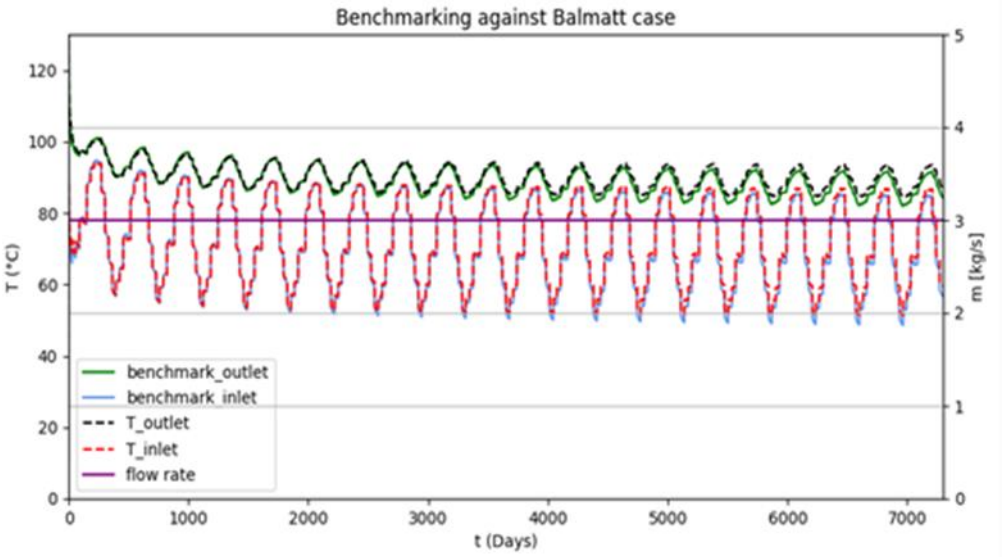

*Figure **57.** Benchmarking of the model considering off-design conditions and injection temperature control*

As observed, the proposed model demonstrates sufficient accuracy in estimating the performance and, consequently, the production of a geothermal well over time. The discrepancy noticeable in the later years arises from the correlation developed for the response of the rock formation. In fact, for high values of the dimension less time t_d, and consequently time t, the correlation tends to reach a constant value. This implies that the system reaches a state where the temperature no longer decreases over time.

3.4.3.2. Heat demand tracking – Control Strategies

Two different controls are implemented to assure that the delivered power is equal to the power demand.

This project has received funding from the European Union's Horizon Europe research and innovation program under grant agreement No 101083558

In **Control 1** the injection temperature varies inside the well while keeping the mass flow rate circulating in the geothermal well constant.

In **Control 2** the mass flow rate is adjusted, to meet the required power demand, while the injection temperature remains fixed at 40°C.

In both cases the convergence is obtained applying the bisection method. At each timestep, the heat transfer calculated through convolution is optimized to find either the Injection Temperature or Mass flow rate that guarantees the required power demand.

3.4.4. Integration scenarios

This section outlines the methodology used for the analysis of the various case studies. First, a comprehensive description of the proposed exploitation scenarios for each case study is provided, together with a description of the procedure for the heat demand estimation. Finally, the scenarios for heat demand tracking are discussed.

3.4.4.1. Gavorrano Case

3.4.4.1.1. Exploitation Scenario

Leveraging its significant geothermal resources, the proposed scenario for the Gavorrano area consists in a district heating network fuelling several small villages, highlighted in yellow in Figure 58, between the geothermal area and Follonica.

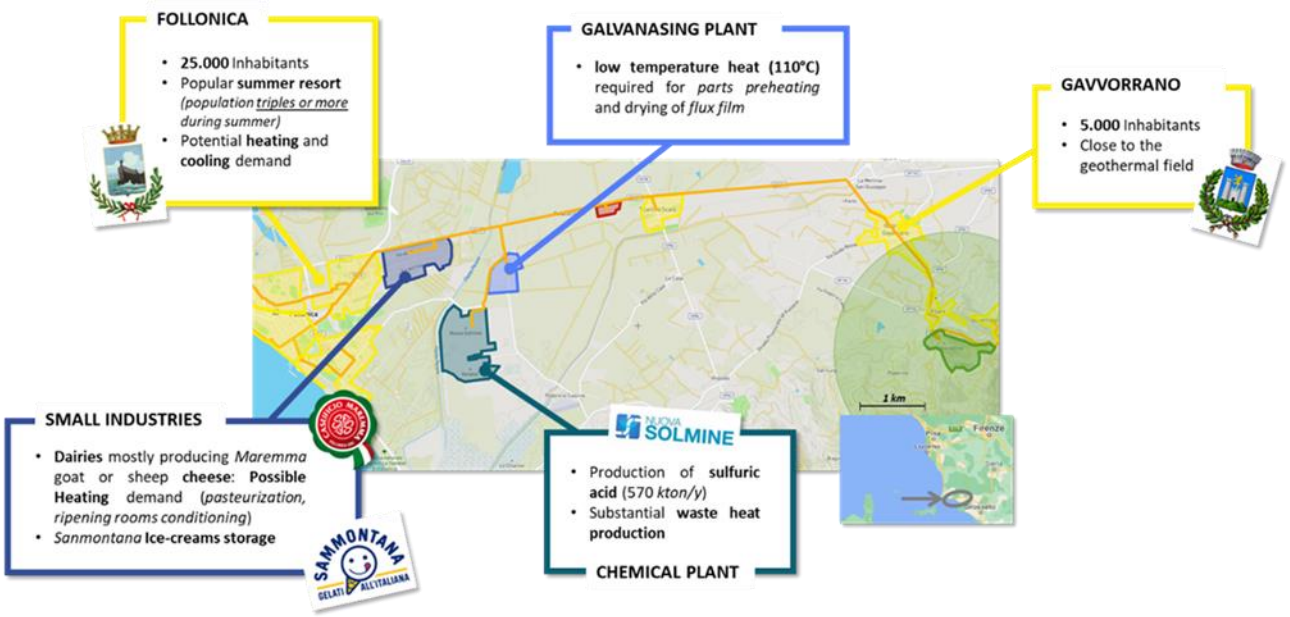

Figure 58: Area selected for the case study (yellow - municipalities, bluish - industries, green - geothermal resource, orange - DHN)

The scheme of the proposed heating networks is shown in Figure **59**. As observed, the main heating network is coupled to the geothermal borehole and feeds several sub-networks, one for each municipality. The sub-networks have been designed as medium-temperature networks, with 80°C supply temperature and 40°C return temperature [13]. Pressure losses along the main network pipes have been calculated through the Churchill correlation.

This project has received funding from the European Union's Horizon Europe research and innovation program under grant agreement No 101083558

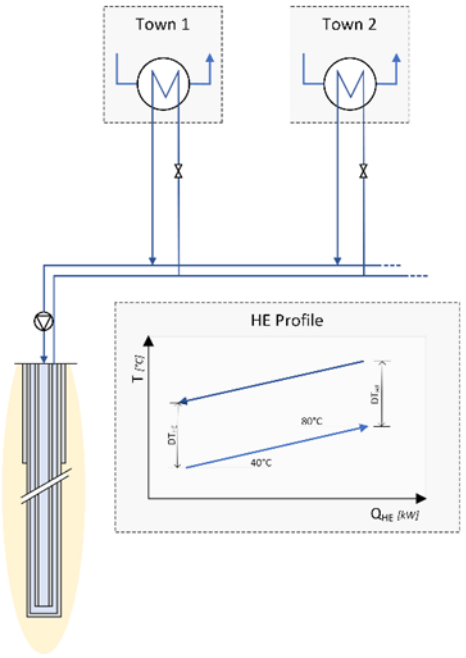

*Figure **59.** Scheme of the proposed heating network*

The pipe diameter has been defined so that the flow speed inside the pipes remains below a defined threshold value (v_{max}). The different network parameters are summarized in Table **26**:

*Table **26**. System Model Parameters*

Parameter	Value	Description
DT_{HE}	5°C	Temperature difference at main heat exchangers
V_{max}	2 m/s	Maximum water speed inside pipes
η_{pump}	85%	Pump isentropic efficiency

3.4.4.1.2. Heat demand estimation

The heating demand in the area was estimated considering the limit energy performance index of the buildings (EP_{li}, as defined by Italian legislation). This value represents the maximum allowable annual consumption per square meter of residential buildings as a function of the heating degree-days (HDD) and the building shape factor (S_f). The Italian legislation provides a table with different values for EP_{li} for a set of HDD and S_f. A continuous curve was generated by interpolating these discrete values using equation 12 with the parameters summarized in Table **27**:

$$EP_{li} = (a_1 S_f + a_2) HDD^3 + (b_1 S_f + b_2) HDD^2 + \cdots + (d_1 S_f + d_2) \quad \textit{Equation 12}$$

This project has received funding from the European Union's Horizon Europe research and innovation program under grant agreement No 101083558

*Table **27.** Interpolation parameters for EP_{li}*

	a	b	c	d
1	$6.28 \cdot 10^{-9}$	$-3.68 \cdot 10^{-5}$	$8.73 \cdot 10^{-2}$	-1.80
2	$-2.87 \cdot 10^{-9}$	$1.5 \cdot 10^{-5}$	$-1.24 \cdot 10^{-2}$	3.30

Following the relationship between EP_{li}, HDD and S_f, the annual network energy demand can be estimated from the area population using equation 13:

$$Q_{tot} = 1.5 \cdot EP_{li}(HDD, S_f) \cdot Pop \cdot A_p \quad \textit{Equation 13}$$

where Pop and A_p are the population and the required useful area in m² per person. The values of Sf and A_p are set to 0.6 and 33 m² person, according to standard Italian values. A 1.5 safety factor is considered, as, unfortunately, many Italian buildings still do not comply with the legislation because they were built before the law came into force in 2010. The calculation was performed for each municipality in the area (shown in Figure 58) and the results are presented in Table **28**.

*Table **28.** Estimated overall residential heating consumption*

Village	Distance	HDD	Population	Consumption	Power
	[km]	*[°C/day]*	*[-]*	*[GWh/y]*	*[MW]*
Gavorrano	1	1748	1,000	2.82	0.98
Bagni di Gavorrano	1.7	1748	3,000	8.47	2.95
Scarlino Scalo	5.2	1840	1,230	3.61	1.26
Follonica	12.1	1527	20,000	50.88	17.75
Tot	-	-	25,230	**65.79**	**22.95**

To better estimate the network behaviour throughout the year, data from an existing DHN in Calenzano (Ungar et Al, 2022), a small town near Florence, have been used and rescaled to identify the maximum power demand over a year (Q_{max}) and the expected capacity factor (C_f). The power demand measured in the Calenzano network over a year, shown in Figure **60**, was resized to match the demand predicted for each municipality in the Gavorrano area.

This project has received funding from the European Union's Horizon Europe research and innovation program under grant agreement No 101083558

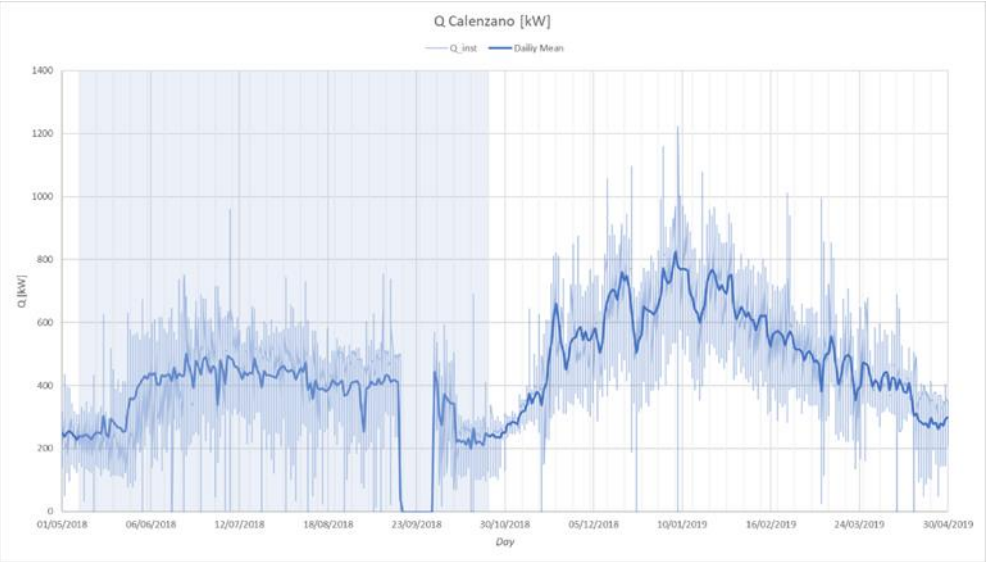

*Figure **60.** Calenzano power demand. The unshaded area, excluding summer operation for absorption refrigeration, has been considered to estimate the heating demand.*

For this purpose, only the winter months (the unshaded part of the figure, from the beginning of October to the end of April) have been considered. The Calenzano DHN is used in summer to power two refrigeration absorbers and cover the cooling needs of a nearby university campus, so it has been excluded from this analysis. Q_{max} has been calculated by designing the system to cover the requested power up to 2σ. This results in a capacity factor Cf = 33%. The system is therefore expected to integrate external burners for a maximum of 100 hours per year.

3.4.4.2. Gargano Case

Given the limited geothermal potential of this region, the proposed system for this case study is designed to utilize the thermal source without conversion into electrical energy, which would necessitate significantly higher temperature levels. In addition, due to the high average ambient temperature typical of southern Italy (Figure 61), the system has been primarily designed for cooling applications.

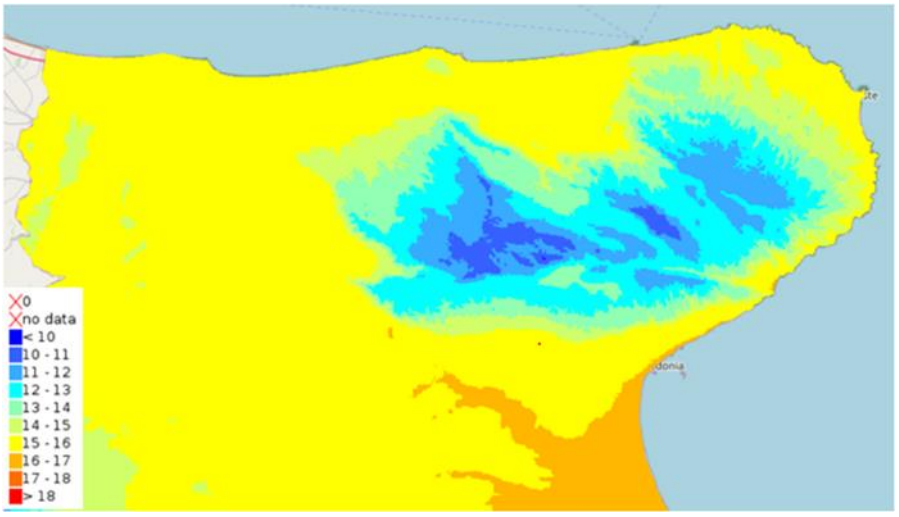

*Figure **61.** Annual average temperature in the Gargano region*

This project has received funding from the European Union's Horizon Europe research and innovation program under grant agreement No 101083558

*Figure **62.** Existing activities in the Manfredonia Area. Highlighted in the map are the targeted geothermal field (in green), residential areas (in yellow), Flat glass production plant (in blue), and Industrial fish market (in violet)*

This choice is further justified by the presence within the area of interest, shown in

Figure 62, of industrial facilities requiring high thermal power for refrigeration, such as the fish market. Moreover, waste heat from a flat glass manufacturing plant can support the geothermal system during its operation.

The proposed system consists of an injection refrigeration cycle, whose operational scheme is illustrated in Figure 63. The system's generator is powered by the fluid from the geothermal system, which transfers its heat to the tri-thermal cycle before being reinjected into the well. Given the high ambient temperatures, particularly during the summer season, the condenser is cooled using seawater, which significantly reduces the refrigerant's condensation temperature. The working fluid selected for this analysis is R152a, one of the possible drop-in replacements for R134a, offering a good balance between refrigeration performance and environmental impact.

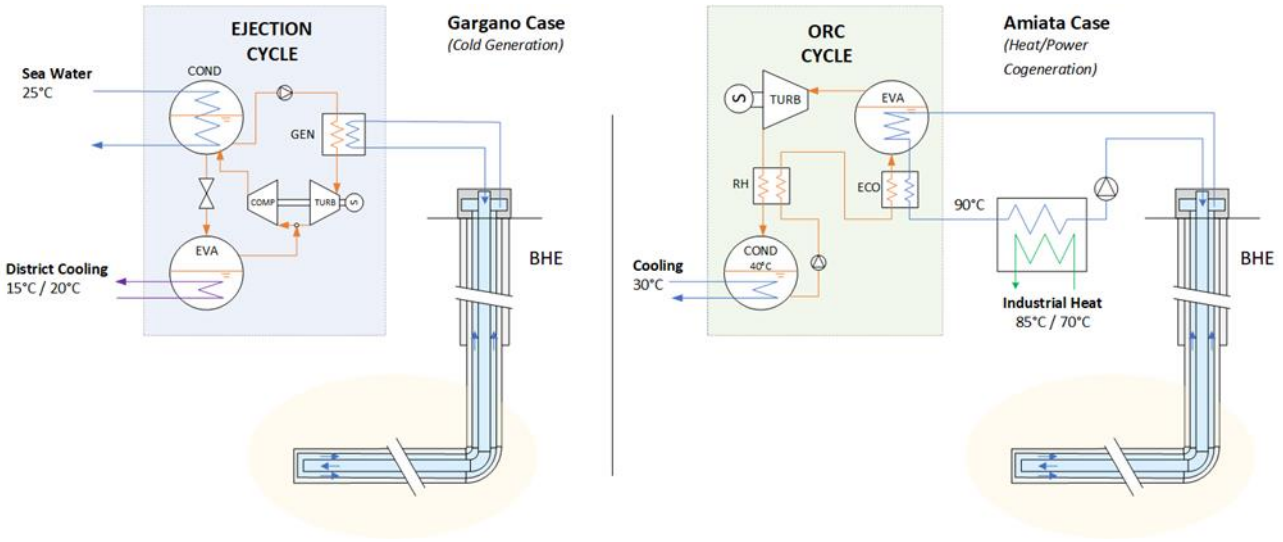

*Figure **63.** Schemes of the surface plant installation for the Gargano and Amiata Cases*

This project has received funding from the European Union's Horizon Europe research and innovation program under grant agreement No 101083558

Due to the lack of reliable off-design data from existing users in the area, this case study focuses on optimizing the system under steady-state conditions, considering the expected well output after 20 years of continuous operation. Unfortunately, the extreme low geothermal gradient in the area coupled with a very high sea temperature in the summer represents an extreme environment for this system to work, resulting in very poor overall cooling performances. Because of this, the analysis was limited to the production of 15°C water for district cooling which is expected to be a reachable goal.

3.4.4.3. Amiata Case

Due to the high geothermal gradient in the area, the Amiata case study was devoted to the analysis of a cogeneration case. The only relevant industry nearby the geothermal area is Floramiata (Figure 64), an agricultural company specialized in the production of indoor plants, which manages 200,000 m2 of greenhouses heated up with the waste heat from a nearby geothermal power plant. Floramiata average heat consumption is 114 GWht per year. Based on previous research efforts, UNIFI has got the Floramiata consumption data for the period 2017 – 2020 on a 10-mins basis. This data will be used in the evaluation of the system performances over time.

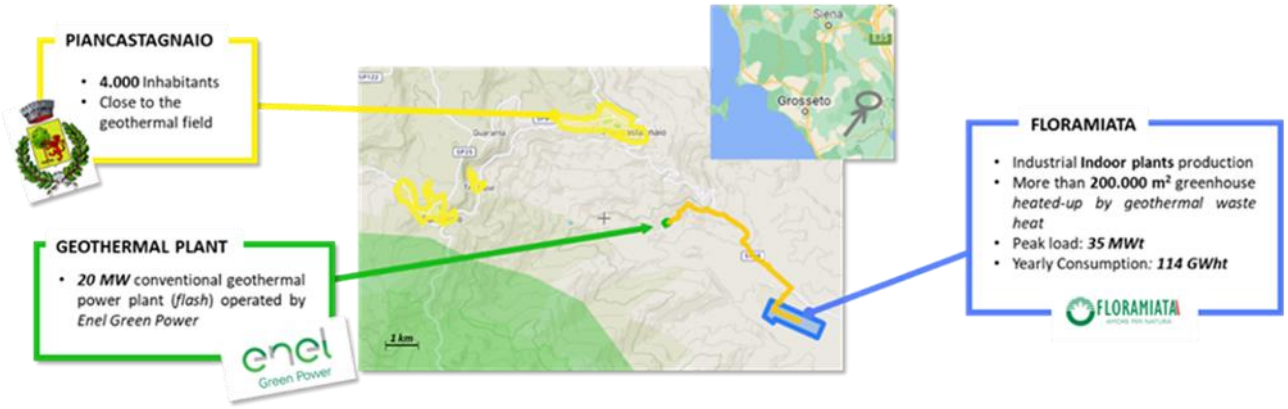

*Figure **64.** Existing activities in the monte Amiata Area. Highlighted in the map are: the targeted geothermal field (in green), residential areas (in yellow), Floramiata industrial area (in blue), and Conventional geothermal power plant (in dark green). In orange is an existing DH network that provides residual heat from the geothermal power plant to Floramiata.*

The cogeneration system shown in Figure 63 has been modelled to ensure that the ORC load will adjusts dynamically to meet the industrial plant's need. When the thermal demand of the industrial complex is low the ORC compensates by increasing power production.

To make the simulation more realistic, the control strategy s the one actually employed by the industrial complex operator that clearly emerges from the historic data (Figure 65): the flow rate of the water circulated in the well is adjusted approximately once a month according to the forecasted power requirements, dynamic adjustment to the power demand.

Note that in the existing configuration the inlet temperature in the main industrial heat exchanger is almost constant, especially on a daily / weekly basis, while the power extracted from the fluid is controlled by changing the injection temperature. As a consequence, in our analysis, the pressure in the ORC evaporator is set to keep the temperature at the inlet of the main heat exchanger stable at 90°C.

This project has received funding from the European Union's Horizon Europe research and innovation program under grant agreement No 101083558

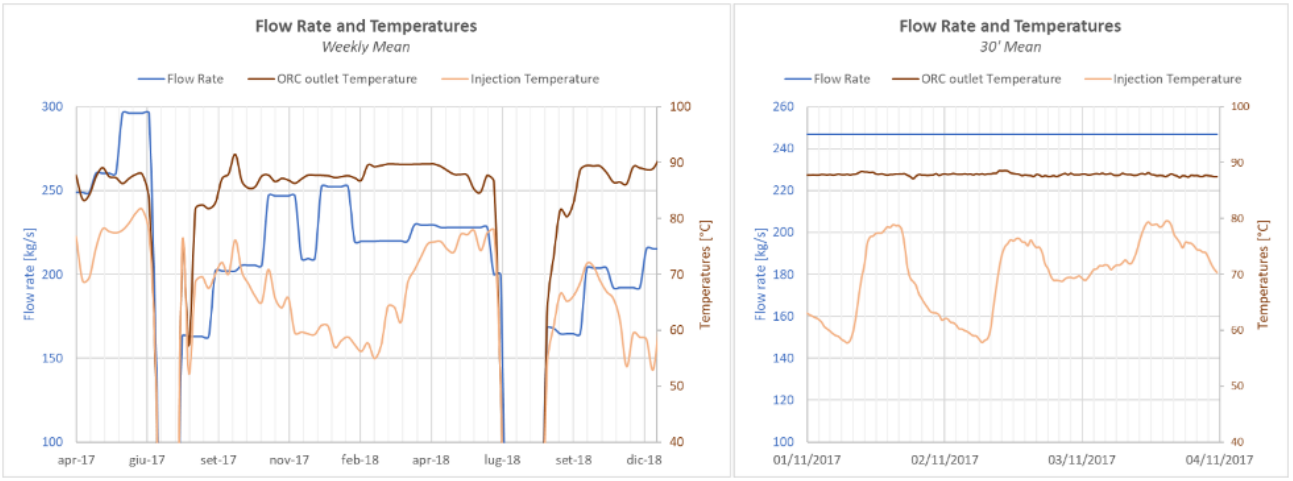

*Figure **65.** Historic temperatures and flow rates in the existing FLORAMIATA heating system. Notice that the flow rate is adjusted approximately on a monthly base while the dynamic adjustment to the power is handled by a variation of the injection temperature.*

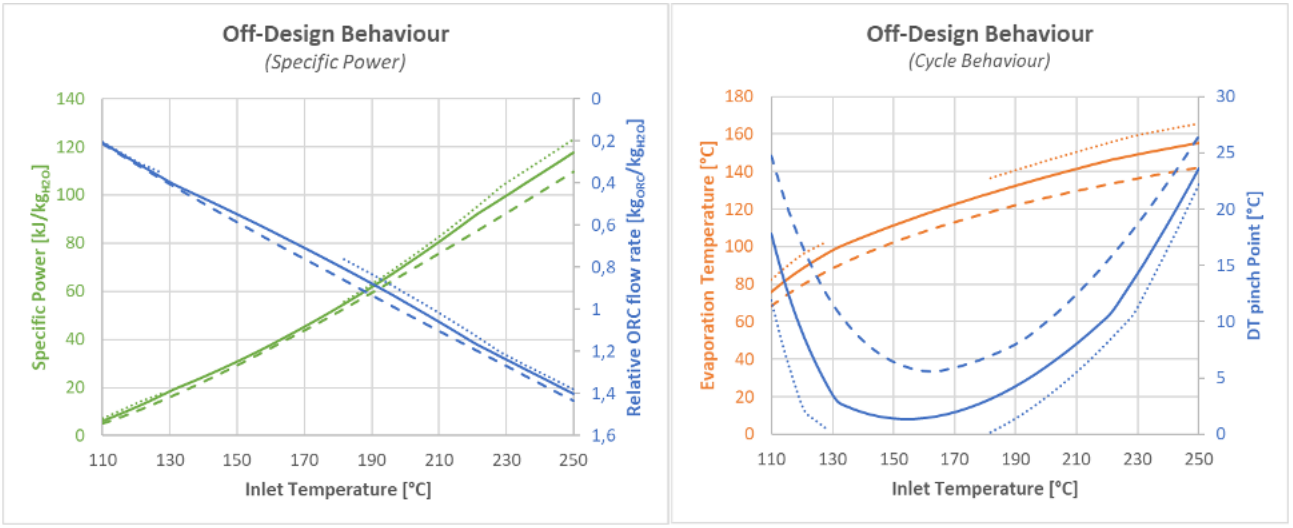

*Figure **66.** Off-design behaviour of the ORC. Dashed line represents the behaviour of the cycle with if the water flow rate drops to 0.75x of the design condition while dotted lines represent the behaviour of the cycle with water flow rate equal to 1.25x of the design.*

To evaluate exactly how the ORC should adapt, an off-design model of this subsystem has been developed in EES (Engineering Equation Solver). The main feature of this off-design model is its consideration of turbine performance under off-design conditions. As illustrated in Figure 66, when the ORC flow rate increases, the evaporation pressure (and temperature) of the ORC fluid must also rise to ensure the fluid passes through a turbine originally designed for smaller flow rates. This can lead to control issues under certain conditions, particularly when water flow rates exceed the design specifications, and the inlet temperature ranges between 130°C and 180°C. In such a case, the increase in evaporation temperature becomes too significant for the ORC to adapt, making it impossible to maintain a fixed outlet temperature at 90°C (the pinch point becomes negative). This does not happen when the water flow rate decreases. Therefore, the sizing of the turbine has been determined based on the highest flow rate recorded in the

This project has received funding from the European Union's Horizon Europe research and innovation program under grant agreement No 101083558

time-series (300kg/s from Figure 65).

The Turbine off-design model has been implemented using the classical Stodola correlation. *N-Pentane* has been considered as working fluid as it is almost an industrial standard for geothermal applications. The condenser temperature has been set to 40°C. The turbine design has been fixed for the optimized condition of the ORC for a well production temperature of 150°C.

Finally, a simple polynomial correlation has been developed starting from the prediction of off-design power output from the ORC turbine given by the EES code to be used for the evaluation of the ORC power outlet in each time step. The retrieved correlation is the following:

$$\dot{w_{ORC}} = (a_1 m_{w\%}^2 + a_2 m_{w\%} + a_3) T_{in}^2 + (b_1 m_{w\%}^2 + b_2 m_{w\%} + b_3) T_{in} + (c_1 m_{w\%}^2 + c_2 m_{w\%} + c_3)$$

Equation 14

Where w_{ORC} is the specific power outlet (kJ of energy produced by the turbine relative to kg of water circulated in the well), $m_{w\,\%}$is the relative difference between the water design flow rate and the actual flow rate circulated in the well, and T_{in} is the water inlet temperature in the ORC evaporator (the production temperature of the well). The coefficients used in the equation above are listed in Table 29.

*Table **29.** Values of the parameters used in the calculations*

Parameter	1	2	3
a	*2,58E-03*	*-2,46E-03*	*1,67E-03*
b	*-1,49E+00*	*1,97E+00*	*-3,17E-01*
c	*1,33E+02*	*-1,77E+02*	*1,18E+01*

Figure 67 illustrates how the correlation successfully predicts the ORC power outlet.

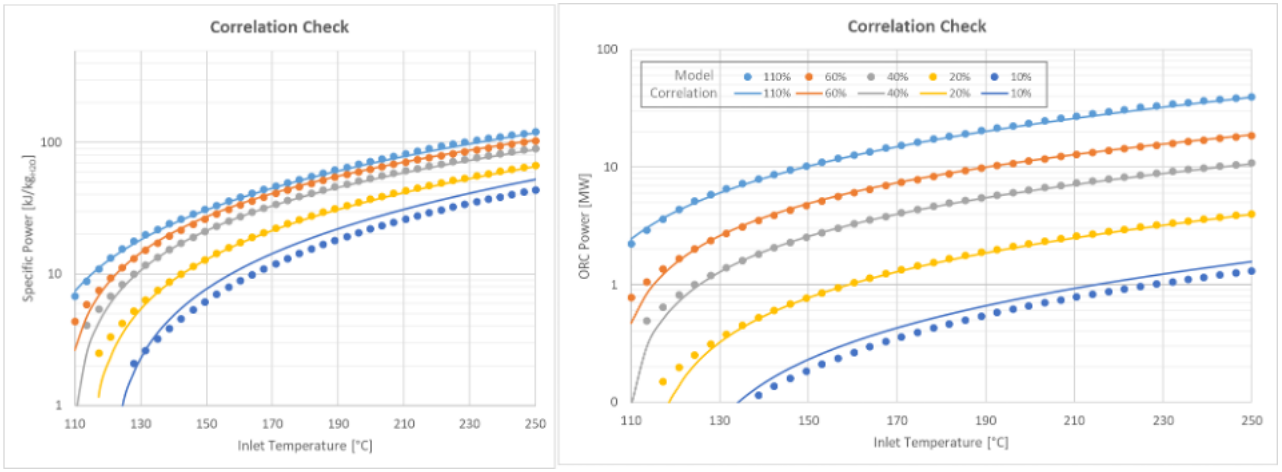

*Figure **67.** Validation of the correlation for the prediction of the ORC power output for different inlet temperatures and water flow rate percentage. The absolute power refers to a 300kg/s flow rate of water.*

This project has received funding from the European Union's Horizon Europe research and innovation program under grant agreement No 101083558

3.4.5. Simulation of the integration scenarios and results

3.4.5.1. Gavorrano Case

The proposed Gavorrano geothermal power plant has been analysed in off-design conditions operating in both control conditions. In the case of **Control 1**, the mass flow rate is taken constant and the power demand is met daily, Figure **68**Figure 68. *Control 1 results* Top *left in dashed lines are represented the injection temperature in the well while in the continuous lines are the outlet temperature, both with different number of operating wells.* Bottom *left* graph *represents the circulating mass flow rate.* On the right, the graph shows the outlet temperature over time..

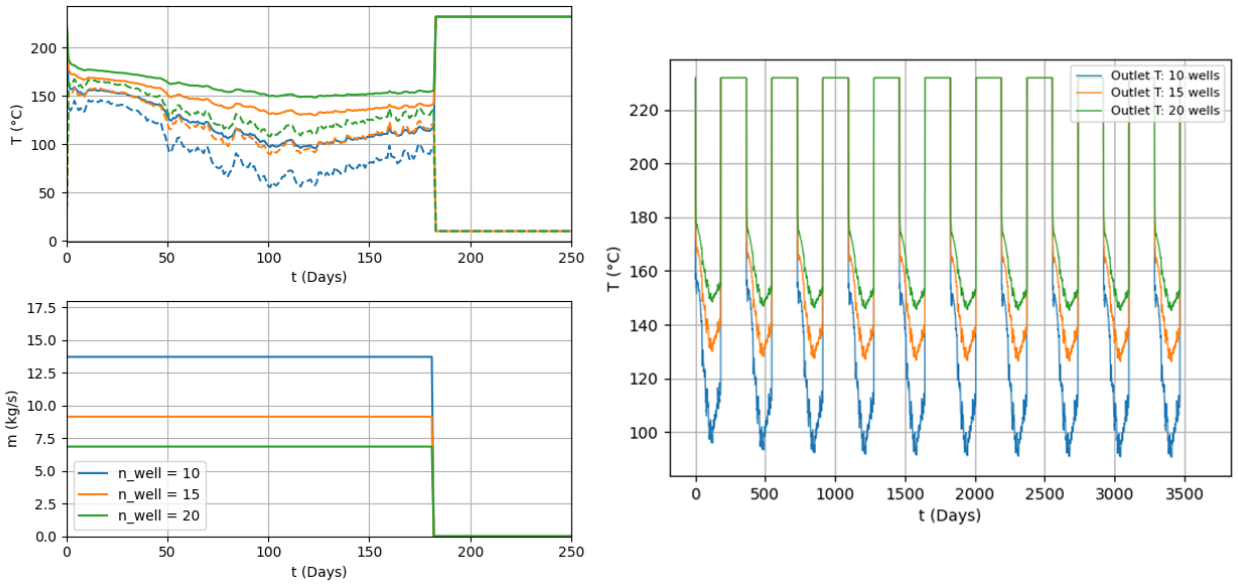

*Figure **68.** Control 1 results Top left in dashed lines are represented the injection temperature in the well while in the continuous lines are the outlet temperature, both with different number of operating wells. Bottom left graph represents the circulating mass flow rate. On the right, the graph shows the outlet temperature over time.*

In the summer periods when there is no heat demand the rocks temperature quickly reinitializes.

The results obtained show that the design configuration consisting of 10 geothermal wells can deliver the thermal power demand of the DH network without depleting the temperature of the rock formation. A small decrease in the outlet temperature of the well can be observed in the first years and more importantly during periods of time where the heat demand is higher.

Configurations with higher number of wells were also considered. Such configurations allow to reduce the mass flow circulating in each single well, reducing the pressure losses in the geothermal wells. These configurations also meet the requirements of the DH network.

For **Control 2**, the injection temperature is maintained at a constant 45°C, while the mass flow rate is adjusted at each timestep to match the weekly average power demand (

Figure 69). Keeping the injection temperature fixed at 45°C maximizes the geothermal resource by achieving a greater temperature difference between the inlet and outlet of the geothermal well, even at lower mass flow rates.

The design configuration of 10 wells is not suited for Control 2. Even though it can meet the heat demand, with 10 wells the rock formation temperature decreases steadily and falls below 85°C already during the

This project has received funding from the European Union's Horizon Europe research and innovation program under grant agreement No 101083558

first year of operation.

If this control were to be applied, a bigger number of wells should be considered. The upside is that achieving a greater temperature difference between the inlet and outlet (Figure 67), allows the system to circulate a lower mass flow, which in turn means that pressure losses will be much smaller compared to Control 1.

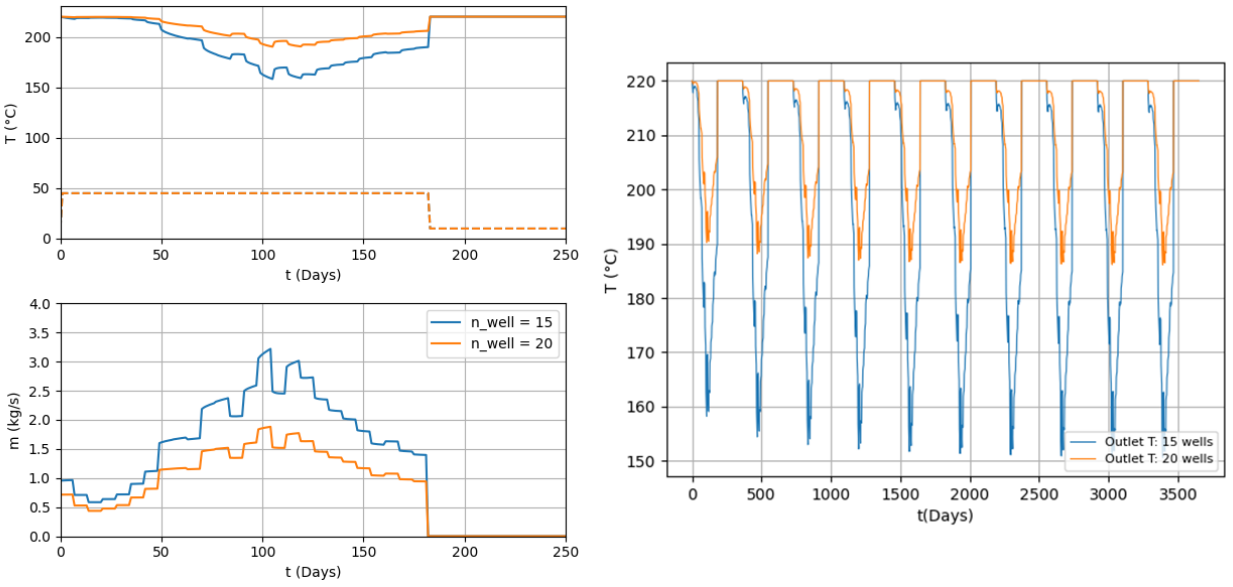

*Figure **69.** Control 2 results: On the top left in dashed lines are represented the injection temperature in the well while in the continuous lines are the outlet temperature, both with different number of operating wells. The graph on the bottom left represents the circulating mass flow rate. On the right, the graph shows the outlet temperature over time.*

3.4.5.2. Gargano Case

Unlike the other two cases, there is no existing off-design data for the surface plant in the Gargano case. Therefore, instead of analyzing a complete time series, the focus is on optimizing the plant in a steady-state configuration.

First, the outlet temperatures (

Figure 70) and the power extracted (Figure 71) from the HOCLOOP well after 20 years have been evaluated for different depths, lengths of the horizontal section of the well, and flow rates. As expected, deeper and longer wells lead to higher temperatures and greater heat extraction, while an increased flow rate enhances extracted power but lowers the temperature. Due to the extremely low geothermal gradient in the area, achieving a reasonable outlet temperature (>80°C) requires a very deep and long well with a low flow rate. This is likely to result in poor cycle performance.

The temperatures and power outputs presented must be considered alongside the performance of the surface ejection plant to evaluate the overall cooling capacity of the system. The results are shown in Figure 72. From the figure emerges that a minimum outlet temperature (around 60°C) is required for the system to work. This means that for shallower wells there's a minimum horizontal length that ensure that the system produces some cooling capacity. In addition, in the Gargano condition, should be at least 2.8 km deep otherwise the temperature of the surrounding rock is itself not enough for reaching the desired outlet

This project has received funding from the European Union's Horizon Europe research and innovation program under grant agreement No 101083558

temperature (even with an infinitely long horizontal section). In addition to that, for well depths close to that limit, even though the system is theoretically capable of producing some cooling capacity, this capacity is very low due to the low efficiency of the surface plant. For the analysed conditions, achieving consistent cold production requires very deep wells. Specifically, a 5 km deep well can generate up to 100 kW of cooling power. However, this output is extremely limited, especially considering the significant effort and cost involved in drilling to such depths. This limitation is primarily due to the area's extremely low geothermal gradient, which makes geothermal resource extraction particularly challenging.

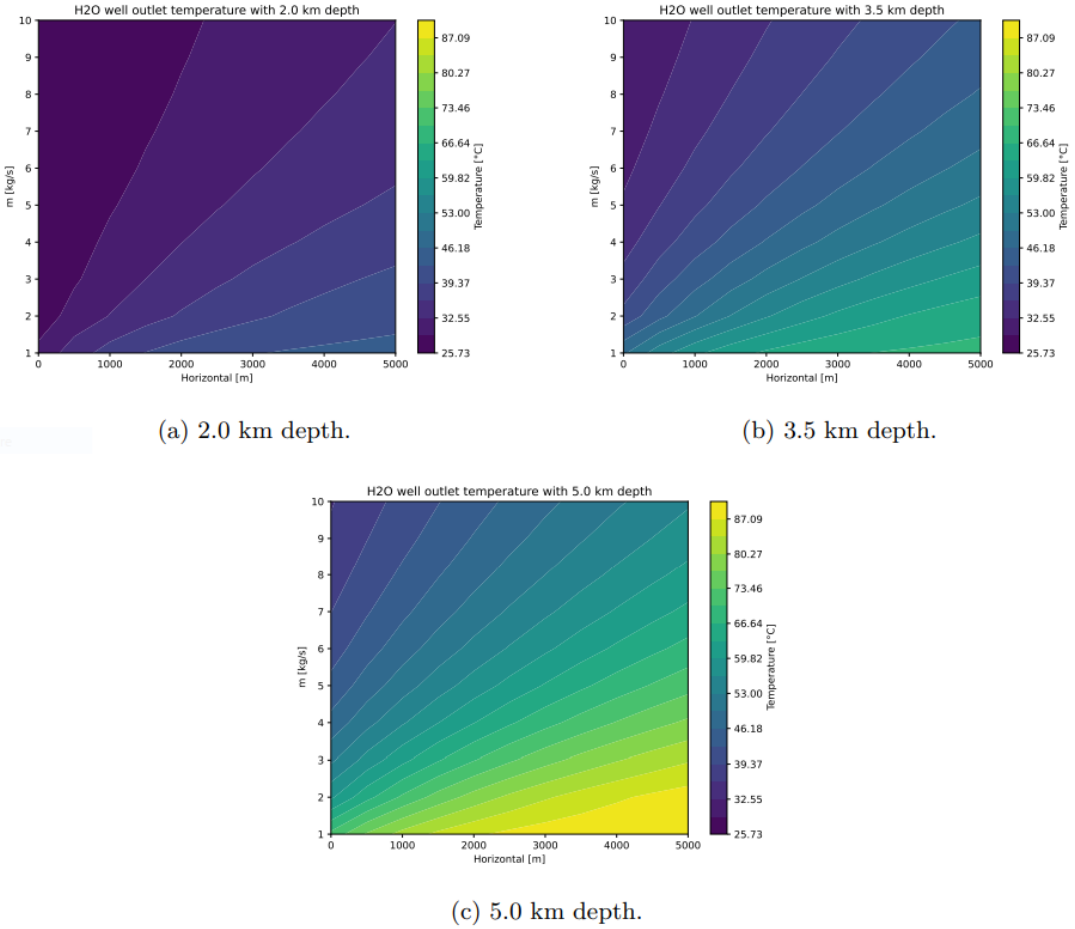

(a) 2.0 km depth.

(b) 3.5 km depth.

(c) 5.0 km depth.

*Figure **70.** Extracted power from an HOCLOOP well installed in the Gargano area for different depths, horizontal section lengths and flow rates.*

This project has received funding from the European Union's Horizon Europe research and innovation program under grant agreement No 101083558

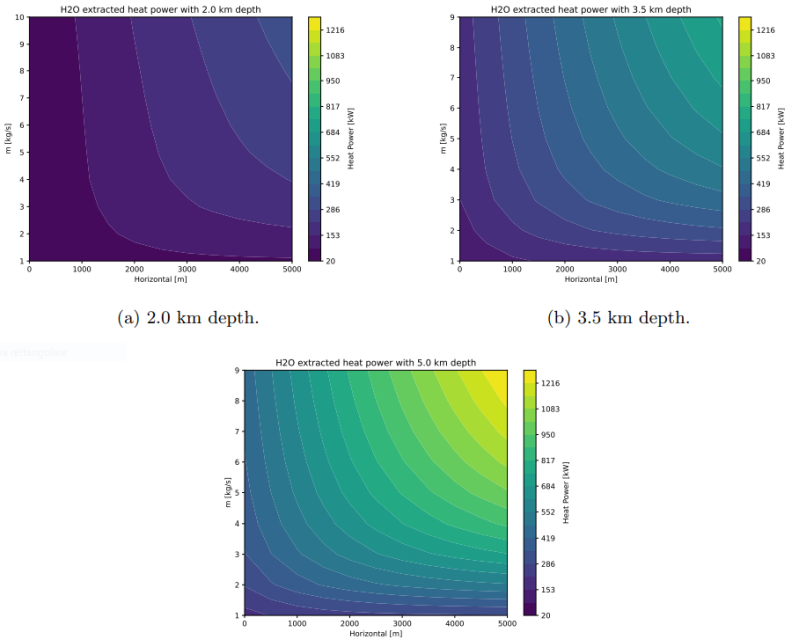

(a) 2.0 km depth.

(b) 3.5 km depth.

(c) 5.0 km depth.

*Figure **71.** Extracted power from an HOCLOOP well installed in the Gargano area for different depths, horizontal section lengths and flow rates.*

This project has received funding from the European Union's Horizon Europe research and innovation program under grant agreement No 101083558

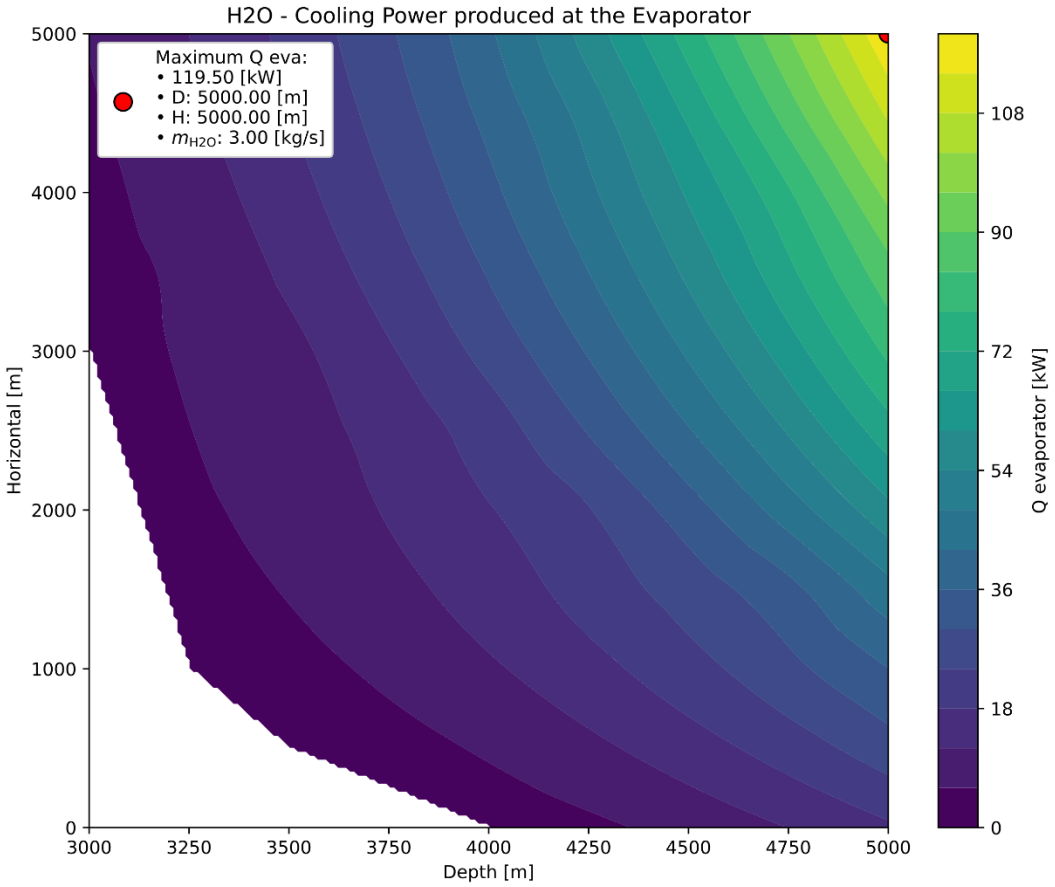

*Figure **72.** Ejection cycle cooling capacity for different depth and horizontal section (the flow rate has been chosen to maximize the cooling capacity itself)*

3.4.5.3. Amiata Case

For the Amiata case, similarly to the industry control mode, a monthly average mass flow rate was applied based on available data from FlorAmiata. Additionally, the injection temperature is not constant and fluctuates according to FlorAmiata's demand.

Currently, FlorAmiata requires hot water flow rates ranging from 150 kg/s to 260 kg/s at approximately 90°C except for the summer months when the plant is shut down. A single geothermal well is insufficient to meet these demands. Therefore, alternative solutions involve power plants with multiple wells, each handling an equal share of the original circulating mass flow rate. Two scenarios are considered, featuring 15 and 20 wells.

The peaks observed in the temperature profile result from the reinitialization of the rock temperature and the assumption of no internal heat exchange,

Figure 73.

This project has received funding from the European Union's Horizon Europe research and innovation program under grant agreement No 101083558

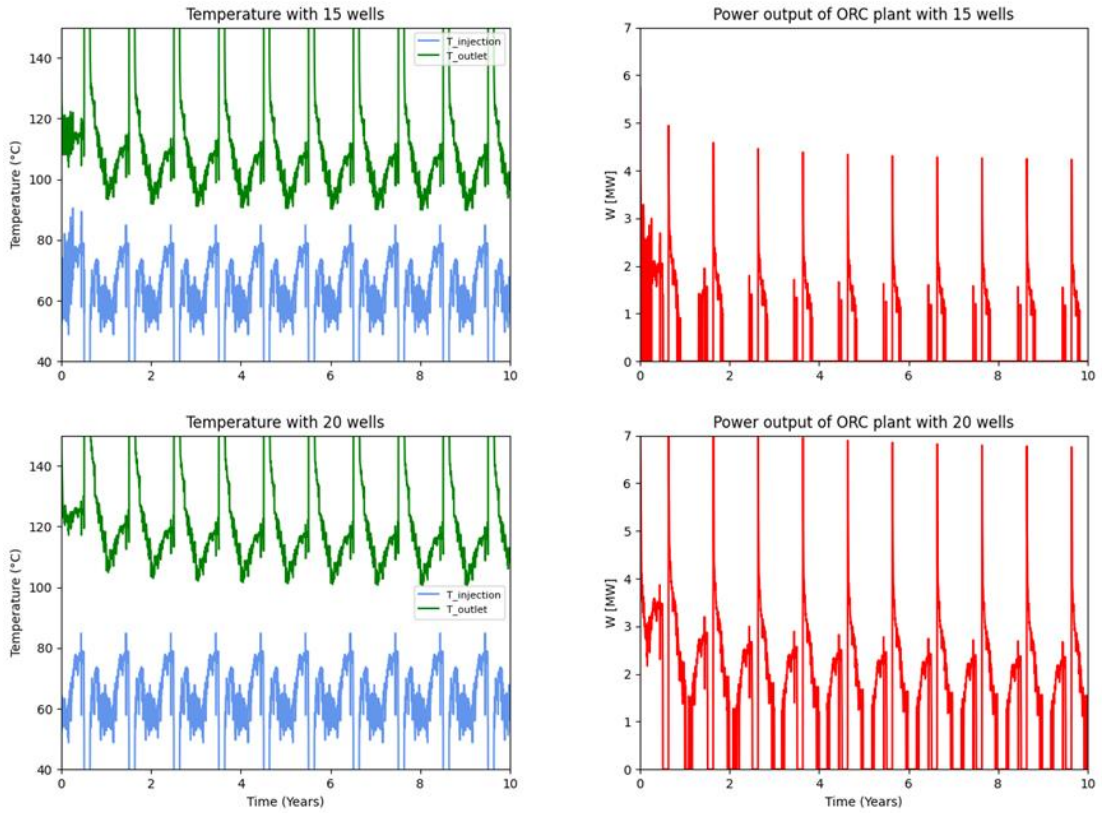

*Figure **73.** In the figure are shown the inlet and outlet temperature of the geothermal well and the electrical power output of the ORC plant with two different configurations*

With a configuration of 15 operating wells, the required circulating mass flow rate ensures that the minimum outlet temperature of 90°C is maintained at any point throughout the year and for the first ten years of operation. At the same time for specific times of the year, after the summer, the ORC power plant manages to produce electric power though it is still a small amount.

If 20 wells are considered the outlet temperature of the fluid is well above the 90°C threshold fixed by the FlorAmiata industry plant and is often above the 110°C minimum threshold of the ORC. In Figure **74** is shown the behaviour of the geothermal system. In each well flows a variable flow rate which is a twentieth of the actual requested flow rate, except for a period in July and August when the plant is closed. The geothermal systems consisting in 20 wells can consistently output the required flow rate with a temperature higher than 110°C. In the first year and at the restart of operation after the summer stop a sharp decrease in the outlet temperature of the wells can be observed. After ten years of operations the geothermal system, produces water at temperatures higher than 90°C but the time in which outlet temperature is higher than 110°C and therefore the capacity factor and the yearly energy output of the ORC decrease with time, Figure **74**.

This project has received funding from the European Union's Horizon Europe research and innovation program under grant agreement No 101083558

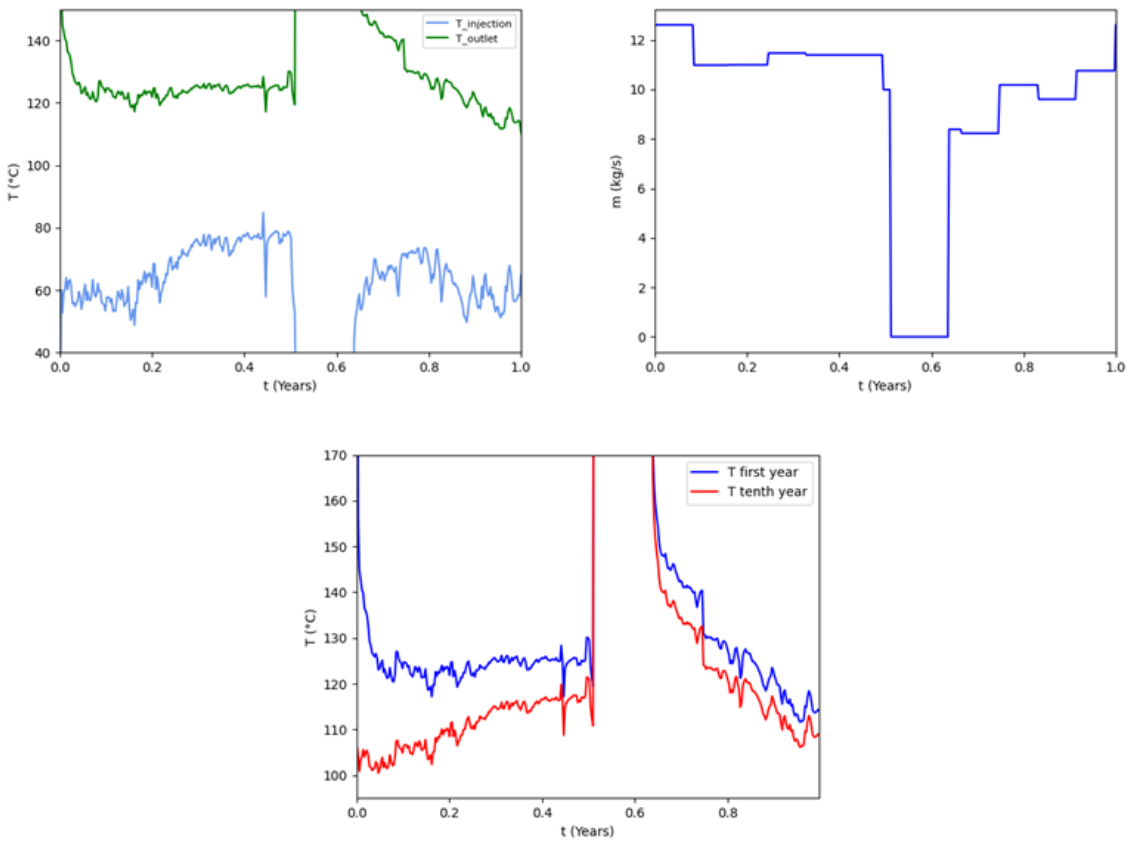

*Figure **74.** In the graphs are shown the inlet and outlet temperature of the geothermal well, the mass flow rate and the outlet temperatures of the well during the first and the tenth year of operation, respectively from the top left to the bottom*

The solution with 15 wells allows the operation of the FlorAmiata agricultural plant with a lower energy output from the ORC plant. The solution with 20 wells produces more energy during the year at the cost of an increased number of wells.

This project has received funding from the European Union's Horizon Europe research and innovation program under grant agreement No 101083558

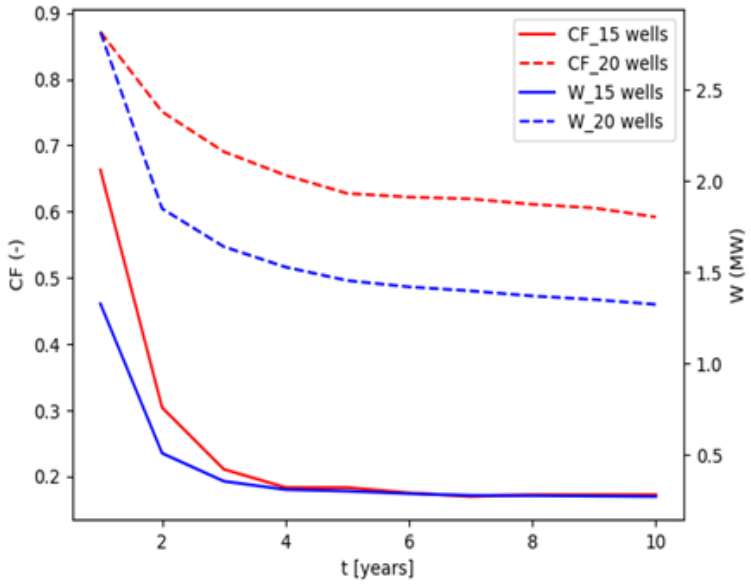

*Figure **75.** Capacity factor and average power of the ORC power plant for each year of operation*

3.4.6. Conclusions of the Italian cases

The HOCLOOP solution has shown its capablities of providing a reasonable amount of heat for the medium and high gradient areas (Gavorrano and Amiata) without interacting with the underground hydrothermal environment. In the Amiata case, the predicted outlet temperature is high enough to produce some electrical power alongside providing heat to the final user.

A comparison of the two different control modes applied to the Gavorrano case reveals distinct advantages and limitations. Control 1 experiences less temperature depletion in the surrounding rock over time. However, due to generally higher mass flow rates, it results in greater pressure losses. In contrast, Control 2 leads to lower pressure losses but is not suitable for all operating conditions. If implemented with the design systems, it would have caused the rock formation's temperature to deplete within the first year.

For the Gargano area, the extremely low gradient means that the amount of power that can be extracted from the well and, therefore the cooling capacity of the ejection cycle, is very limited (100kW cooling) especially when considering the effort needed for drilling a very deep well (5km).

3.5. Polish case study

3.5.1. Introduction

The case study in Poland evaluates salt structures, the Goleniów salt dome and salt pillow, as potential targets for applying the closed-loop technology developed in the HOCLOOP project. These structures are typically found in sedimentary basins where extensive salt deposits have formed and are one of the best geologically recognized forms. D 4.1 provides a detailed description of this region.

3.5.2. Geological and well-characteristic

The northern Goleniów salt dome along the direction NNW-SSE has dimensions of 4,5 × 2,0 km. It reaches a depth of 3649.0 m and was drilled through the evaporite series of Zechstein from 888.0 m depth to

This project has received funding from the European Union's Horizon Europe research and innovation program under grant agreement No 101083558

3649.0 m bgl, reaching a thickness of >2761.0 m. Basic information about salt domes geology in the Polish Lowlands has been presented in existing literature [14 – 16]. Figure 76 presents the location of salt structures in the Szczecin region on the tectonic map of the Zechstein-Mesozoic complex in the Polish Lowlands.

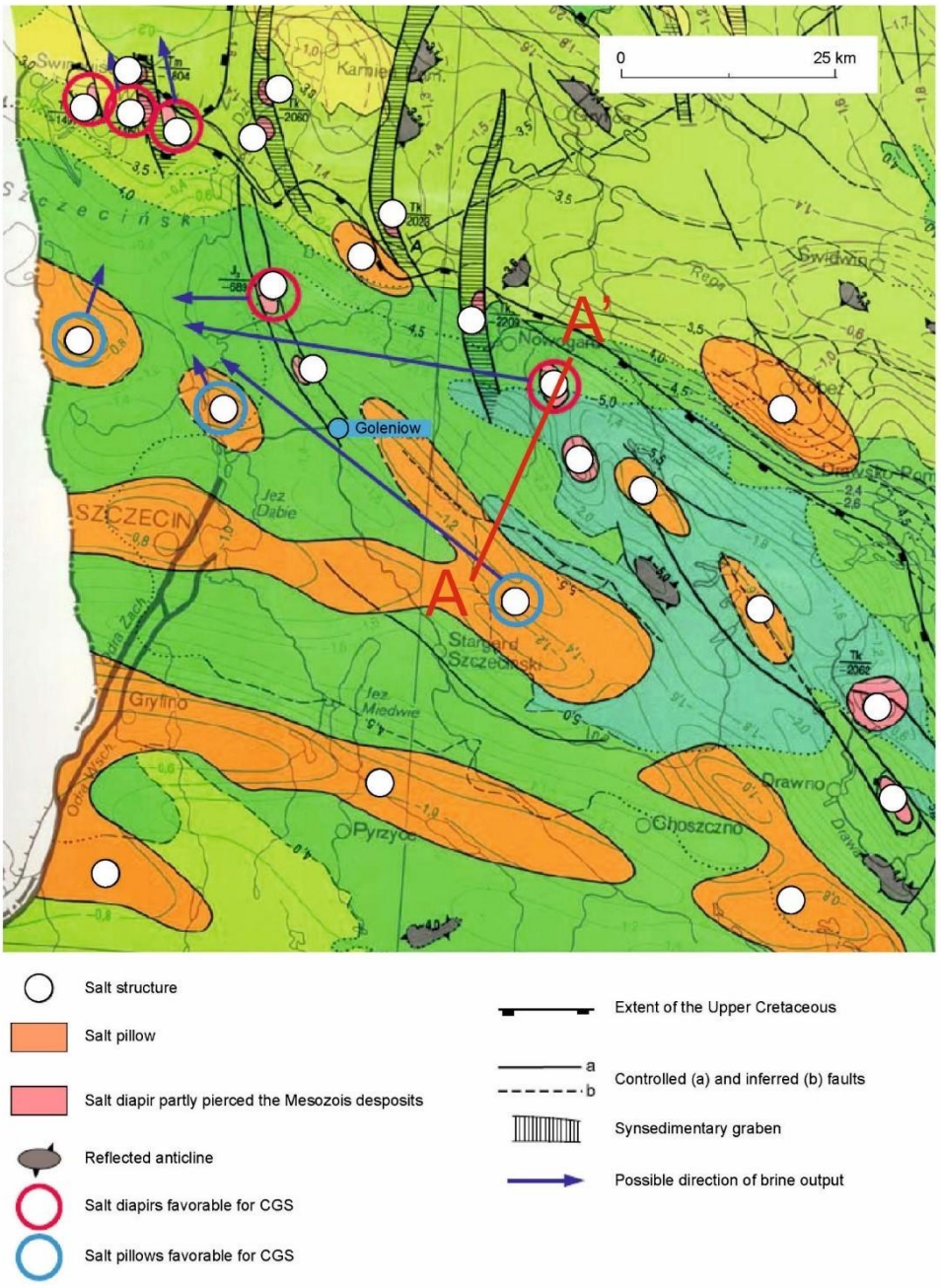

*Figure **76.** Location of salt structure in the Szczecin region on the Tectonic Map of the Zechstein-Mesozoic complex in the Polish Lowlands, 1:500000 (after Dadlez, 1998) with forms favorable for CGS (based on Czapowski & Tomassi-Morawiec, 2012, modified)*

Salt structures are composed of evaporites from the Permian (Zechstein) formations. They are surrounded and overlain by a thick complex of Mesozoic-Cenozoic sediments, ranging from several hundred meters to several kilometers in thickness, though this thickness is often reduced directly above the structures [15]. In the area of Szczecin, salt structures are formed mainly by salt domes [14] and salt pillows [16].

This project has received funding from the European Union's Horizon Europe research and innovation program under grant agreement No 101083558

In the analyzed region, surrounding the Goleniów salt dome, lies the Stargard-Maszewo salt pillow. Its estimated dimensions range from 42–70 km in length to 6–13 km in width. The deepest borehole in the region, Stargard 1, reaches a total depth of 5,444 meters, with Upper Permian salts and anhydrites occurring between 4,024 and 4,766 meters. In contrast, boreholes east of Goleniów (Maszewo 1, Grzęzno 1) encounter the salt pillow at much shallower depths, around 1.5 km, in zones where salt ridges and domes are present. Analysis of available geological data, including borehole records and geological maps [17], has helped define the geometry of the salt pillow in the Goleniów region. The top of the Permian formations lies at a depth of 3,496 meters below ground level, with Upper Permian deposits primarily composed of rock salt and anhydrites.

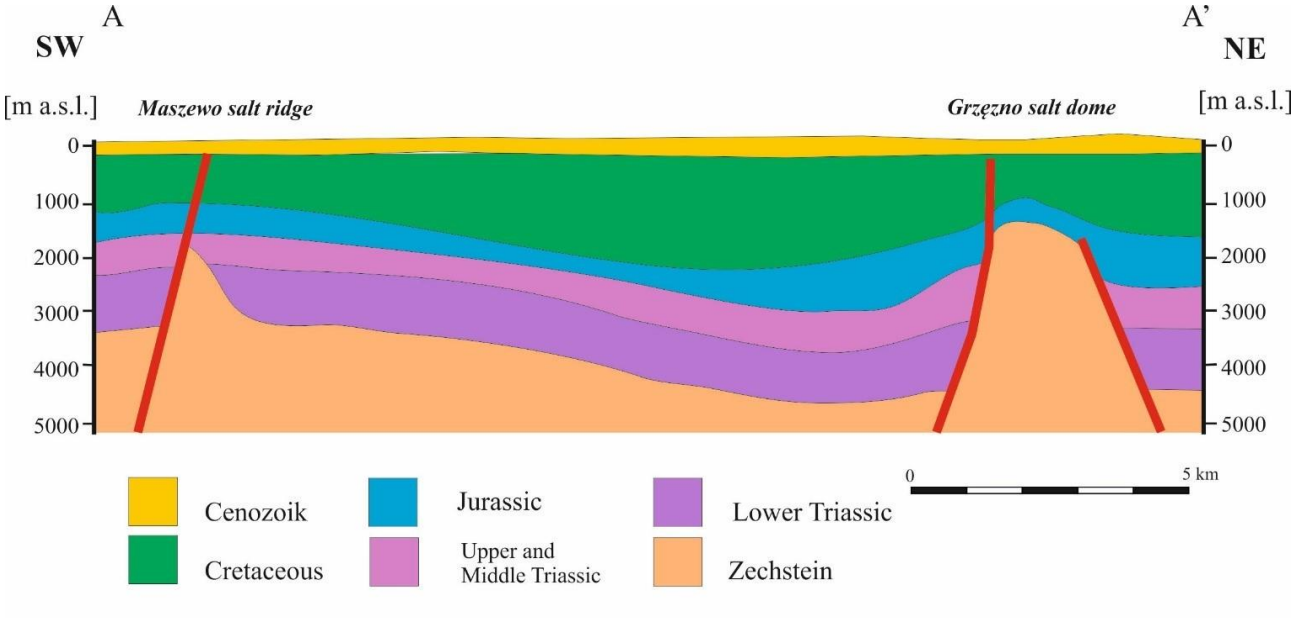

*Figure **77.** Geological cross-section through the salt structures of Maszewo and Grzęzno (Sowiżdżał, 2009). Cross-section location line in Figure **76***

The Goleniów IG-1 borehole drilled Permian formations at a depth of 702.2 m bgl, with the profile starting with salts appearing from depths 888 m bgl. Rock salts, potassium salts and anhydrites appear in the profile already to the bottom of well (3,649 m bgl).

This project has received funding from the European Union's Horizon Europe research and innovation program under grant agreement No 101083558

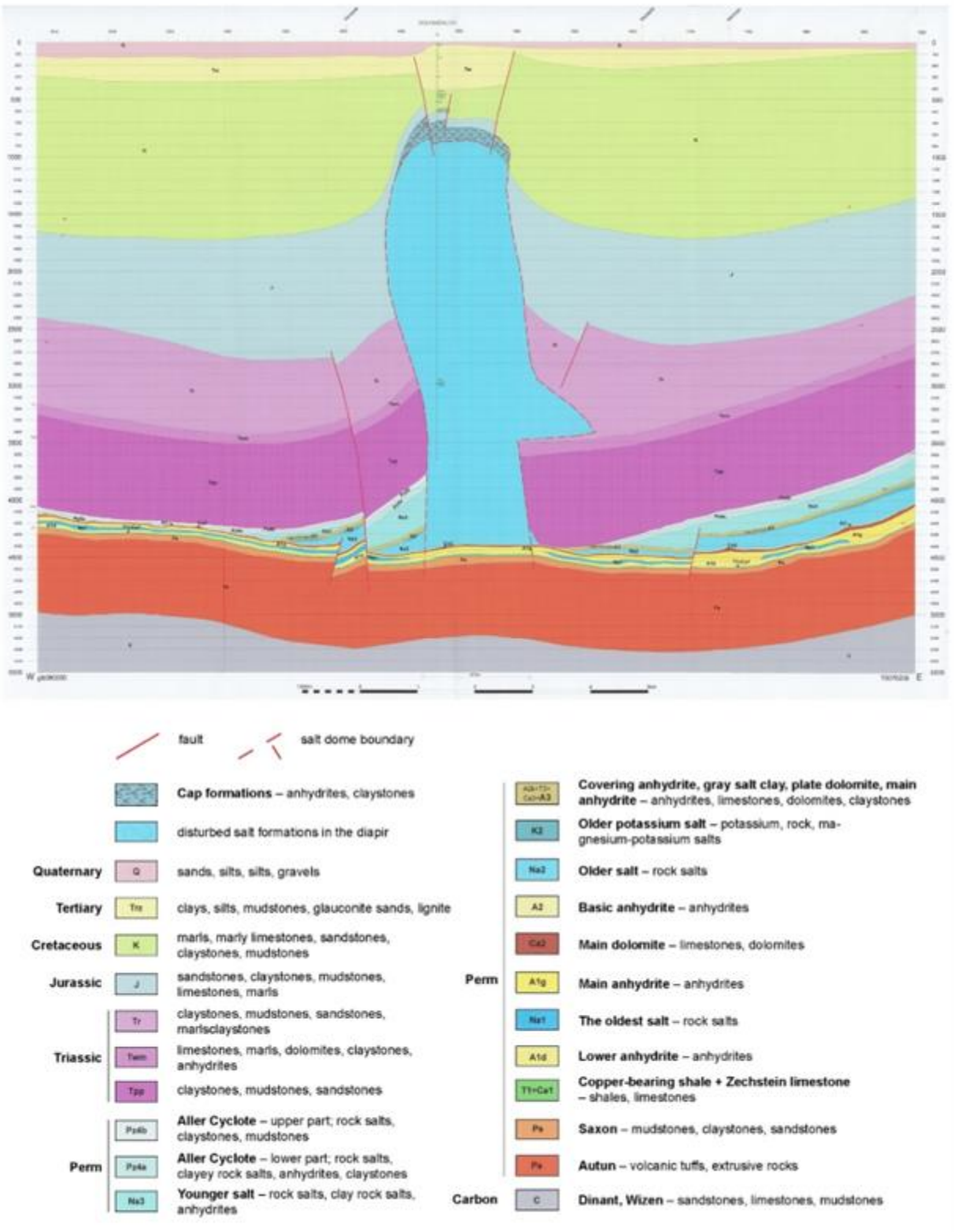

Figure ***78.*** Geological cross-section along the T0076209 seismic line passing through the Goleniów rock salt diapir deposit (based on PGI, 2014,[18])

This project has received funding from the European Union's Horizon Europe research and innovation program under grant agreement No 101083558

Well trajectory, casing and cement layers

The drilling of the Goleniów IG-1 borehole started in November 1962 and was completed in April 1963. Initially, it was supposed to reach a depth of 4,500 m; however, due to technical problems, drilling was completed at 3,649.0 m. So, finally, Goleniów IG-1 is a well with a total depth of 3,649.0 m.

Several geophysical tests were carried out in the borehole: lateral electrical sounding, gamma and neutron-gamma profiling, quernometer and microcavernometer, inclinometer, rezisivimeter, temperature measurement after cementing the pipes for the cooling effect and temperature measurement for the geothermal stage. In addition, coring was performed over a total area of 578.8 m, obtaining 345.4 m of drill core (59.6% recovery in the interval). The salt dome was drilled at a depth of 708.0 m. After drilling through 180 m of cap formations, drilling entered the Z2 – Strassfurt rock salt formations, which continued to a depth of 2,962.4 m, where 38.6 m of Z3 – Leine formations were encountered, developed in the form of anhydrite and plate dolomite. Below (2,999.0 m), the Z2 – Stassfurt formations were drilled again and developed as rock salts. Simplified choronostratigraphic and lithostratigraphic profiles are presented in Table 30 and Table 31.

*Table **30.*** Simplified chroostratigraphic profile for Goleniów IG-1 (based on CBDG, access: 12.2024)

Depth from [m bgl]	Depth to [m bgl]	Description
0	35	Quaternary
35	149	Miocene
149	318	Oligocene
318	428.6	Eocene
428.6	439	Paleocene
439	471	Maastrichtian
471	489	Upper Campanian
489	534	Lower Campanian
534	605	Turonian
605	623	Lower Cretaceous
623	702.2	Tithonian
702.2	3649	Permian

Table 31: Simplified lithostratigraphic profile Goleniów IG-1 (based on CBDG, access: 12.2024)

Depth from [m bgl]	Depth to [m bgl]	Description
702.2	888	Zechstein Group (gr)
888	2 962.4	Younger rock salt Na3

This project has received funding from the European Union's Horizon Europe research and innovation program under grant agreement No 101083558

2 962.4	2 994.7	Main anhydrite A3
2 994.7	2 999	Platy dolomite, including grey salt claystone
2 999	2 999.6	Covering anhydrite A2r
2 999.6	3 020	Older potash salt K2
3 020	3 649	Older rock salt Na2, older potash salt K2

Thermal static model

The thermal profile of the Goleniów IG-1 boreholes was developed based on the "Geological documentation of the rock salt dome deposit "Goleniów" in category D at the site of Zielonczyn, Stepnica commune, Goleniów, West Pomeranian Voivodeship, No. CBDG 1014323; Inw. 271/2014 Arch. CAG PIG, Warsaw" [19]. The digital version in 100 m intervals is presented in Figure **79**. Temperature profiling was performed in the depth interval up to 2800 m, where the temperature was measured at approx. 99°C. It should be added that the measurements were taken in unstabilized conditions and in the lower part of the profile you can see the temperature disturbance which required correction. The average geothermal gradient for Permian formations (salt dome) is at 2.5 °C /100m, while in the zone above the salt dome the geothermal gradient for Mesozoic formations is about 3.5°C /100m. The average geothermal gradient for the entire profile in this area is about 3 °C /100m.

Salt formations are characterized by significantly higher thermal conductivity than other sedimentary rocks. Such increased thermal conductivity of rock salt is not without influence on the thermal parameters of the surrounding rocks. This manifests itself in the increased value of heat flux within the salt effusion itself, as well as the surrounding rocks, which is directly reflected in the increased value of the surface heat flux above the salt effusion. Salt outcrops, due to the specific distribution of physical parameters in space, are thermal bridges that cause anomalies in temperature distribution. The heat transferred to the surroundings, accumulated in the salt structures, causes the lithological diverse rocks of the surroundings, to be characterized by higher temperatures than similar formations lying at the same depths, but occurring away from the salt outcrops [17].

The maximum value of heat flux occurs directly above the salt dome, although elevated values of this parameter are recorded in the radius of the entire salt structure. The magnitude of the anomalous heat flux values is influenced by the depth of the salt effusion and its size. The distribution of temperature with depth is very characteristic in salt effusions. The largest anomalous temperatures occur directly above and below the salt effusion. Characteristically, the magnitude of the anomalies varies between the sediments found in the upper and lower layers surrounding the salt effusion. In the upper part of the exudate, an increase in temperature values is observed in the layers surrounding the dome relative to similar formations lying at the same depths but occurring away from the dome, while negative temperature anomalies occur in the

This project has received funding from the European Union's Horizon Europe research and innovation program under grant agreement No 101083558

lower part. Such local changes are also evident in the Goleniów IG-1 thermal profile, but due to the thermal measurement under unstabilized conditions, it is uncertain whether they are not due to disturbances associated with the well drilling.

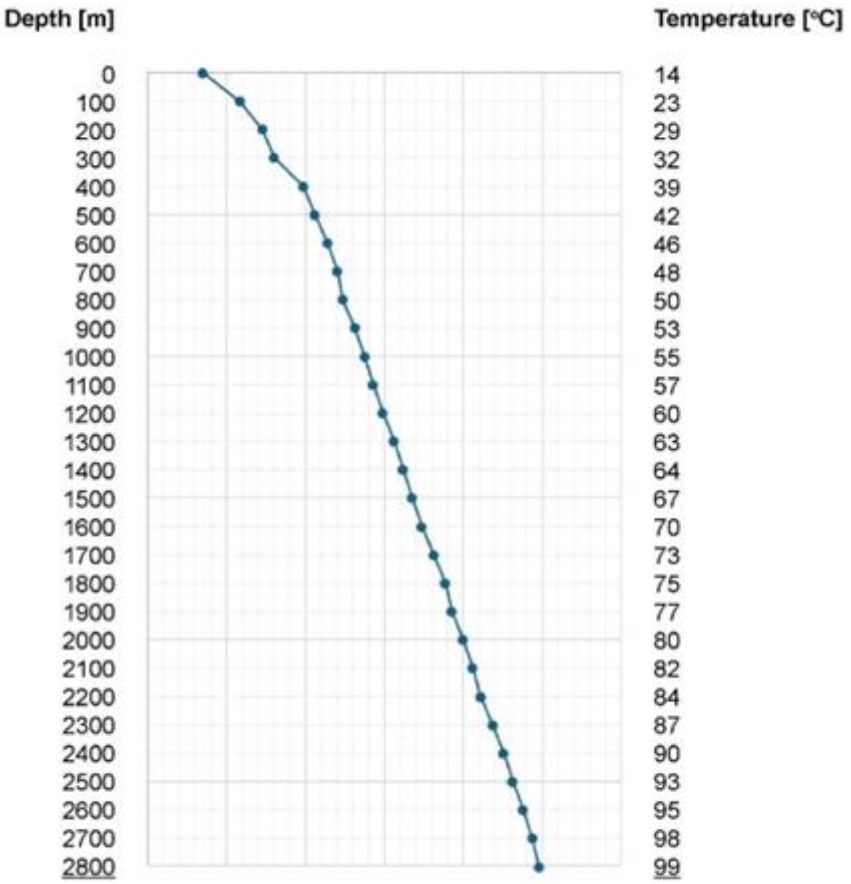

*Figure **79.*** Temperature profile for Goleniów IG-1

3.5.3. Simulation procedure

3.5.3.1. Simulation tool

GTW (Geo-Thermal-Well) is a single-phase numerical geothermal simulator in cylindrical coordinates for single well applications. This is the same tool that was used for Balmatt and benchmarked during WP2, Task 2.1 of the present project (Hernandez, Leontidis, Wangen, & Harcouët-Menou, 2023).

3.5.3.2. HOCLOOP Well conceptual design

Four configuration options for the well construction in the HOCLOOP system have been assumed in this analysis. It takes into account the use of both salt domes and salt pillows as heat sources. In addition, two different lengths of the horizontal section of the well were analyzed for each geological formation.

This project has received funding from the European Union's Horizon Europe research and innovation program under grant agreement No 101083558

3.5.3.3. Well trajectory and temperature distribution

Salt dome study.

In the case of the location on the salt domes. a 4212-meter-deep borehole was assumed. passing through the overburden rocks. the salt dome. and entering the salt deposit with a horizontal section. The vertical section was defined to a depth of 3690 meters. where the kickoff point is located. Figure 80 shows the well trajectory. The stratigraphic profile for the well estimated from the available data along with the temperatures is shown in Table 32. Figure 81 shows the temperature distribution.

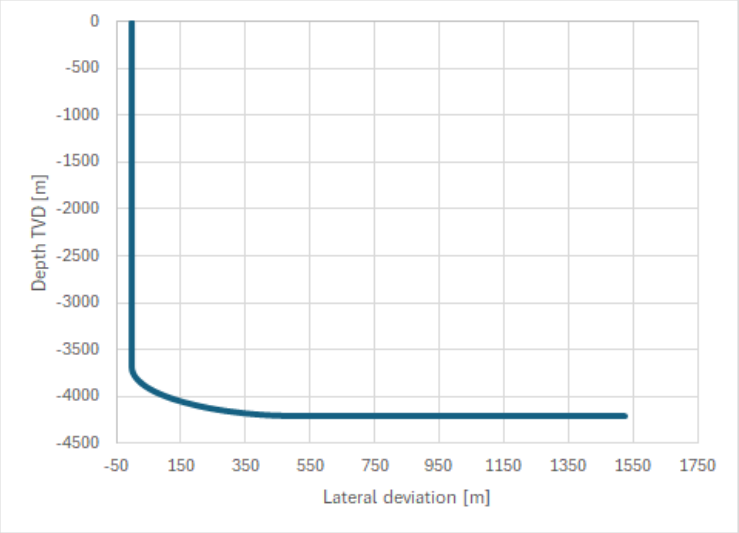

*Figure **80.** The well trajectory – salt dome case (1000 m horizontal part)*

*Table **32.*** Estimated stratigraphic profile for well – salt dome case

From [m]	Stratigraphy	Temp. [°C]
0.0	Quaternary	10
35.0	Tertiary	20
439.0	Cretaceous	40
657.6	Upper Jurassic	47
702.2	Permian	48
4300.0	Permian	126

This project has received funding from the European Union's Horizon Europe research and innovation program under grant agreement No 101083558

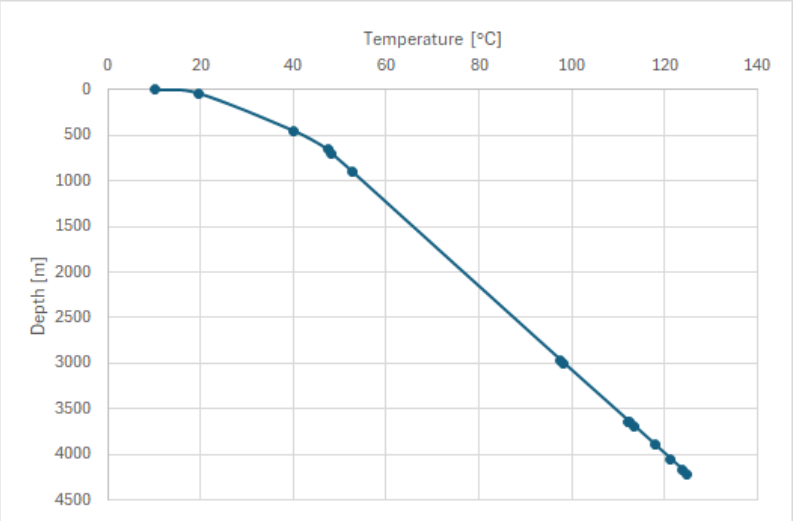

*Figure **81.*** The temperature distribution with depth – salt dome case

Salt pillow study.

In the case of the location on the salt pillow. a 4512-meter-deep borehole was assumed passing through the overburden rocks and entering the salt deposit with a horizontal section. The vertical section was defined to a depth of 3990 meters where the kickoff point is located. Figure 82 shows the well trajectory. The stratigraphic profile for the well estimated from the available data along with the temperatures is shown in Table 33. Figure 83 shows the temperature distribution with depth.

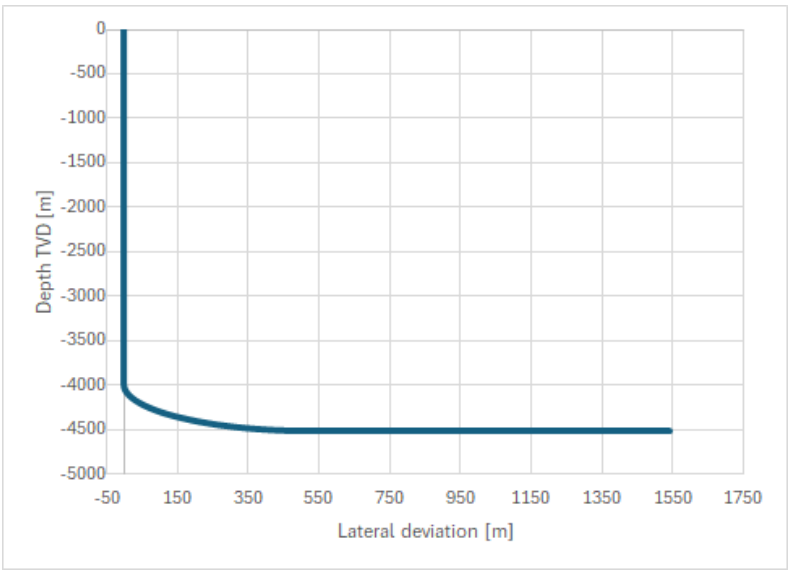

*Figure **82.*** The well trajectory – salt pillow case (1000 m horizontal part)

*Table **33.*** Well stratigraphy

From [m]	Stratigraphy	Temp. [°C]
0	Quaternary	10
138	Tertiary	20
162	Upper Cretaceous	21

This project has received funding from the European Union's Horizon Europe research and innovation program under grant agreement No 101083558

1235	Lower Cretaceous	51
1359	Upper Jurassic	54
1444	Middle Jurassic	56
1601	Lower Jurassic	60
2040	Upper Triassic	70
2448	Middle Triassic	79
2796	Lower Triassic	86
3496	Permian	102
4550	Lower Permian	130

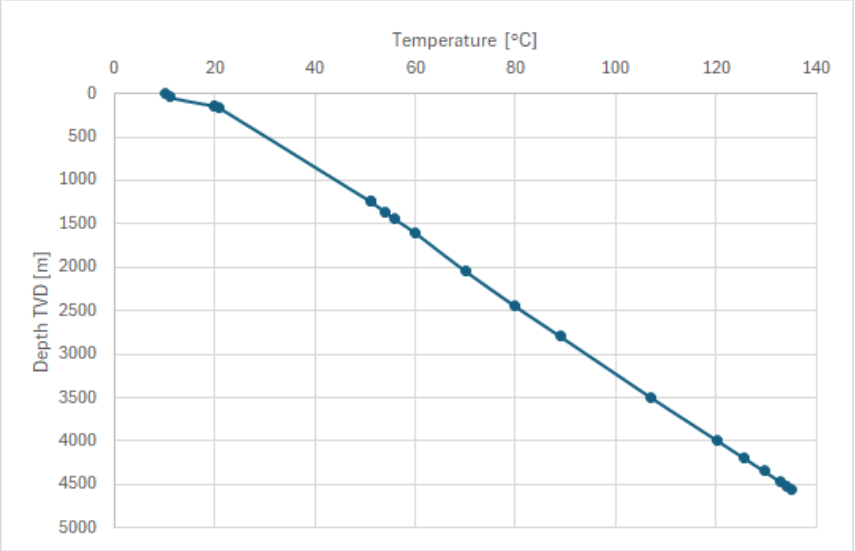

Figure ***83.*** The temperature distribution with depth – salt pillow case

3.5.3.4. Well casing and cementing

Salt dome study.

The well structure consists cased sections. from top to bottom as follows: a conductor pipe at the top. followed by four casing strings. Cementation of the casing in the overburden layers was assumed. The diameters and properties of these different sections and the corresponding cemented sections are described in Table 34 for 1000 m long horizontal section. In cases with an extended horizontal section. the last casing section is correspondingly longer. The diameters assumed refer to the casing used in the Balmat case.

Table ***34.*** Geometrical characteristics of the casings. and cemented layers - salt dome cases

Casing layers				
Well's walls	Top depth [m MD]	Bottom depth [m MD]	OD [inch]	ID [inch]
1	0	40	32	31.5
2	0	450	24	23.5

This project has received funding from the European Union's Horizon Europe research and innovation program under grant agreement No 101083558

3	0	900	18.625	17.755
4	900	4500	13.375	12.347
5	4500	5500	9.625	8.535
Cement layers				
	Top depth [m MD]	Bottom depth [m MD]	OD [inch]	ID [inch]
6	0	40	31.5	24
7	0	450	23.5	18.625
8	0	900	17.755	13.375

Salt pillow study

The well structure includes cased sections arranged from top to bottom as follows: a conductor pipe at the top, followed by four casing strings. The casing in the overburden layers is assumed to be cemented. The diameters and properties of these sections, along with the corresponding cemented intervals, are detailed in Table 35 for a 1,000 m long horizontal section. In cases with an extended horizontal section, the final casing section is increased accordingly. The assumed diameters correspond to the salt dome case.

*Table **35.*** Geometrical characteristics of the casings. and cemented layers - salt pillow cases

Casing layers				
Well's walls	Top depth [m MD]	Bottom depth [m MD]	OD [inch]	ID [inch]
1	0	40	32	31.5
2	0	140	24	23.5
3	0	1240	18.625	17.755
4	1240	4800	13.375	12.347
5	4800	5800	9.625	8.535
Cement layers				
	Top depth [m MD]	Bottom depth [m MD]	OD [inch]	ID [inch]
6	0	40	31.5	24
7	0	140	23.5	18.625
8	0	1240	17.755	13.375
9	1240	3990	12.347	9.625

3.5.3.5. The thermal properties of rock and borehole construction elements.

The thermal properties of the steel and cement were assumed to be the same as the Balmatt case. The property averaging procedure for the segments was performed according to the same methodology as the Balmatt case. For all cases analyzed, the production pipe parameters (diameters and thermal properties) were also assumed to be those of Balmatt. There are no measurements of the thermal properties of rocks

This project has received funding from the European Union's Horizon Europe research and innovation program under grant agreement No 101083558

in the Goleniów area. so data from the literature were used for simulations. The values of rock density. thermal conductivity. and heat capacity adopted for each layer are shown in Table 36 (salt domes) and Table 37 (salt pillow).

*Table **36.*** Rock properties – salt dome cases

Stratigraphy	Top trajectory MD [m]	Bottom trajectory MD [m]	Rock density [kg/m^3]	K [W/m·°C]	Cp [J/kg·K]
Quaternary	0	35	1850	1.44	2300
Tertiary	35	439	1800	2.21	850
Cretaceous	439	657.6	2475	2.25	1150
Upper Jurassic	657.6	702.2	1800	2.21	850
Permian	702.2	900	2900	4.00	1000
Permian	900	2962	2100	5.80	1095
Permian	2962	2999	2900	4.0	1000
Permian	2999	3635	2100	5.80	1095
Permian	3635	3642	2900	4.00	1000
Permian	3642	5500	2100	5.80	1095

*Table **37.*** Rock properties – salt pillow cases

Stratigraphy	Top trajectory MD [m]	Bottom trajectory MD [m]	Rock density [kg/m3]	K [W/m·°C]	Cp [J/kg·K]
Quaternary	0	140	1850	1.44	2300
Ternary	140	162	1800	2.21	850
Upper Cretaceous	162	1240	2475	2.25	1150
Lower Cretaceous	1240	1359	1800	2.21	850
Upper+Midle Jurasic	1359	1601	2475	2.25	1150
Lower Jurasic+Upper Triasic	1601	2448	1800	2.21	850
Middle Triassic	2448	2796	2900	4.00	1000
Lower Triassic	2796	3496	1800	2.21	850
Permian	3496	5800	2100	5.80	1095

3.5.3.6. Recirculating fluid properties and initialization

The recirculating fluid chosen for this HOCLOOP application in Goleniów site study is water. The properties used for modelling are shown in

Table **38**.

This project has received funding from the European Union's Horizon Europe research and innovation program under grant agreement No 101083558

*Table **38.*** Properties of the recirculating fluid for the HOCLOOP application in Goleniów site study

Fluid	Thermal conductivity [W/m- °C]	Thermal capacity [J/kg- °C]	Density [kg/m^3]	Viscosity [mPa·s]
Water	0.6	1000	4200	1

The temperature of the injected water will be analyzed in the range of occurrence in the currently operating heating plant; the injection pressure will be selected to provide an output pressure adapted to the surface plant requirements. In the case of Goleniów, this is 1.2 [MPa].

3.5.4. Integration scenarios

Two different integration options of the HOCLOOP concept at Goleniów facilities were envisaged as possible ways to provide heat to the existing heating network.

The integration scenarios considered in this deliverable are as follows:

1. Without Heat Pump – (Figure **84**), return water from a district heating is directed to the heat exchanger (or heat exchangers). It can be heated up if its temperature is lower than the temperature obtained in the HOCLOOP system. An existing heating plant supplements the lack of temperature or power.
2. With Heat Pump – (Figure **85**), return water from a district heating is directed to a heat exchanger and heated to a possible temperature level. The HOCLOOPs' working fluid is directed to the evaporators of heat pump units. It's cooled down, and the energy obtained is directed to the condensers of heat pumps. An existing heating plant supplements the lack of heat or/and temperature. Due to heat pumps, it is possible to reach lower temperatures of the HOCLOOPs working fluid, higher heating capacity and higher supply temperature. Unfortunately, using heat pumps is associated with the consumption of driving energy, which in Poland still largely comes from the combustion of fossil fuels - primarily coal.

This project has received funding from the European Union's Horizon Europe research and innovation program under grant agreement No 101083558

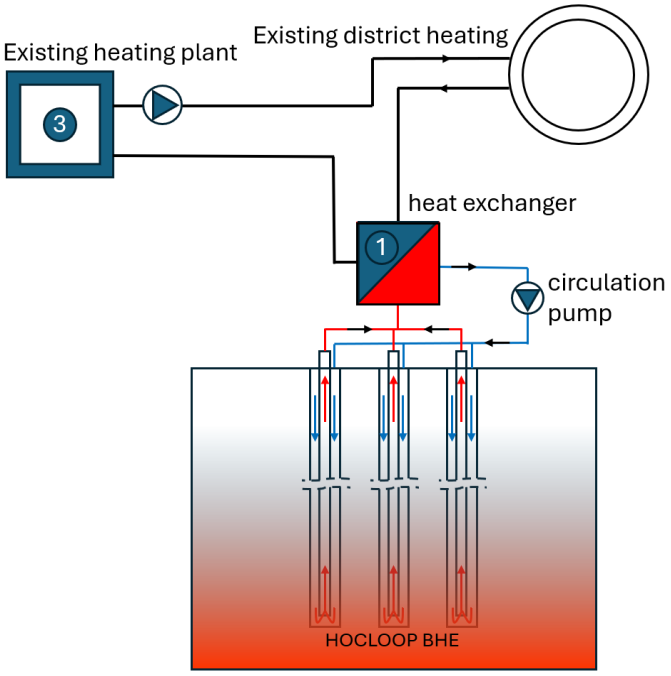

*Figure **84.*** The general scheme of the system utilized the HOCLOOP units without heat pump utilization

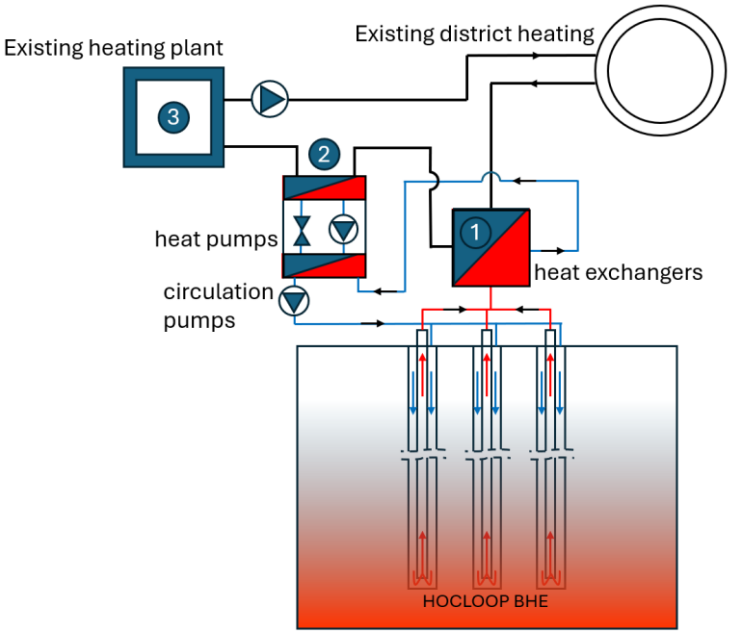

*Figure **85.*** The scheme of the HOCLOOP system supplemented by a heat pump unit

Information about district heating in Goleniów, update

The following information updates the data on the heating system in Goleniów with new information obtained directly from the operator in September 2024 Goleniów is a city with a population of about 22.5 thousand citizens (in 2017, based on the GUS National Statistic Office of Poland). A district heating and the biggest energy source operator in the case of Goleniów is Goleniowskie Przedsiębiorstwo Energetyki Cieplnej (PEC Goleniów: https://bip.pec.goleniow.pl/). The heat carrier for the mentioned energy source is hard-fine coal, and one boiler is adapted to burn biomass in the form of wood chips with a power 6 MW.

This project has received funding from the European Union's Horizon Europe research and innovation program under grant agreement No 101083558

Biomass can also be co-fired with coal. The installed capacity in the source is 29.26 MW (2 x 11.63 MW coal, boiler type WR-10 manufactured in 1981, thermal efficiency 78% + 6 MW biomass+coal, WR-6, efficiency 85%) (Atmoterm S.A., 2017) (Aktualizacja Założeń do Planu Zopatrzenia w Ciepło, Energię Elektryczną i Paliwa Gozowe dla Gminy Goleniów. Małopolska Fundacja Energii i Środowiska, 2022). The efficiency of exhaust gas dust removal is 93%. The heat carrier in the heating network is circulating water with a pressure of 1.6 MPa. The network is designed for parameters of 135/70°C (Przedsiębiorstwo Energetyki Cieplnej Spółka z o.o., 2018). The nominal flow of water is 263 Mg/hr (~263 m^3/hr). The amount of heat distributed (sold) by the district heating in Goleniów commune is estimated at 165 468 GJ/yr in 2023 (based on a request sent to PEC Goleniów in September 2024). Energy production by the source of energy at that time was 201 618 GJ/yr. The efficiency of energy delivery can be estimated at 82%. In 2023, the ordered power for heating was 18.7 MW and for hot tap water 4.1 MW. The non-renewable primary energy input factor for the PEC Goleniów installation is Wpc = 1.6056 (direct information delivered by PEC Goleniów, September 2024). Exact calculations based on a Typical Meteorological Year in the case of Goleniów suggest a bit smaller utilised power by the energy source.

The utilisation of energy obtained based on the HOCLOOP solution, assumptions

The obtained thermal power from a single HotLoop unit varies in the case of various supply temperatures, from hundreds of kW to a few MW. The number of HOCLOOP units should be the subject of optimisation. That will be the task for the next step of work in the frame of the HOCLOOP project. The present stage of work focuses on elaborating on the mathematical model, which allows us to estimate technical and economic results. Here, it is assumed that an optimal solution will probably be based on a few HOCLOOP units. Taking into account power supply and demand, it is assumed that three HOCLOOP units should be utilised under variable inlet temperature but on a constant flow of working fluid. Both system configurations are considered: direct HOCLOOP utilisation – without heat pumps and with heat pumps (the HOCLOOP supplies power directly by a heat exchanger, and heat pump units use low-temperature energy as a low-temperature heat source).

3.5.5. Simulation of the integration scenarios and results

3.5.5.1. Description of the scenarios

Since salt structures have not yet been used as a geothermal heat source in Poland, the borehole heat exchanger's behavior needed evaluation under various conditions. The analysis, conducted in different scenarios, helped determine the system's achievable operating parameters for systems targeting salt domes and the salt pillow.

To assess the impact of horizontal section length on the borehole heat exchanger's efficiency, calculations were performed for various scenarios. Consequently, the simulation cases are categorized as follows:

Case 1. Salt dome

1.1. Horizontal part – 2000 m. (MD – 6500 m. TVD – 4212 m).

1.2. Horizontal part – 2500 m. (MD – 7000 m . TVD – 4212 m).

This project has received funding from the European Union's Horizon Europe research and innovation program under grant agreement No 101083558

Case 2. Salt pillow

2.1. Horizontal part – 1000 m. (MD – 5800 m . TVD – 4512 m).

2.2. Horizontal part – 2000 m. (MD – 6800 m . TVD – 4512 m).

The exchanger's efficiency was evaluated based on the injected water temperature and flow rate. Different parameter ranges were applied to assess performance in each scenario, with each case covering a specific set of parameters.

Injection temperature:

a) 30 °C
b) 40 °C
c) 50 °C
d) 60 °C
e) 70 °C
f) Variable temperature profile according to the output temperatures of the district heating system.

Injection rate:

a) Case-X1: 10 m^3/hr
b) Case-X2: 20 m^3/hr
c) Case-X3: 30 m^3/hr
d) Case-X4: 40 m^3/hr
e) Case-X5: 50 m^3/hr
f) Case-X6: 60 m^3/hr

To maintain stable operation of the district heating system, all variants assume an output pressure of 1.2 MPa for the borehole heat exchanger in the HOCLOOP system. During the simulation, the required discharge pressures were determined based on the water flow rate to meet this condition.

3.5.5.2. Scenarios Results – constant injection temperature

For the assumed range of water circulation flow rates in the HOCLOOP system, discharge pressures were determined. Table 39 shows the results obtained.

Table 39. Injection pressure depend on flow rates

Case name	Flow rate [m^3/hr]	Injection pressure [MPa]			
		Salt dome		Salt pillow	
		Horizontal part 2000 [m]	Horizontal part 2500 [m]	Horizontal part 1000 [m]	Horizontal part 2000 [m]
Case-X1	10	1.35	1.36	1.32	1.36
Case-X2	20	1.81	1.91	1.77	1.88
Case-X3	30	2.61	2.73	2.43	2.67

This project has received funding from the European Union's Horizon Europe research and innovation program under grant agreement No 101083558

Case-X4	40	3.60	3.80	3.31	3.71
Case-X5	50	4.82	5.12	4.38	4.98
Case-X6	60	6.25	6.67	5.64	6.48

Case 1.1. Salt dome, horizontal part 2000 [m].

The output heat power of the HOCLOOP borehole heat exchanger during 20 years of heat production, calculated for *the* above assumptions, are shown in Figure **86**.

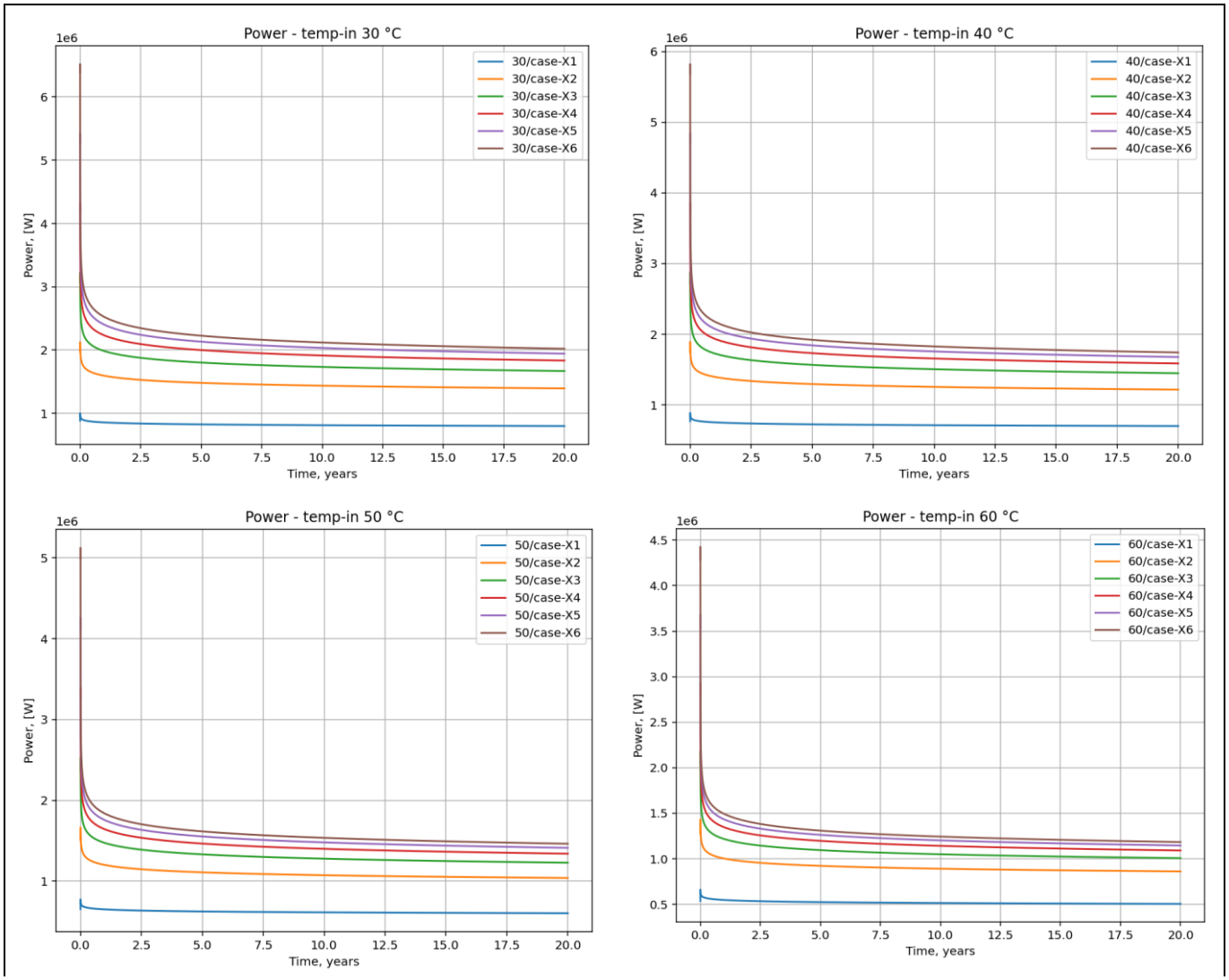

This project has received funding from the European Union's Horizon Europe research and innovation program under grant agreement No 101083558

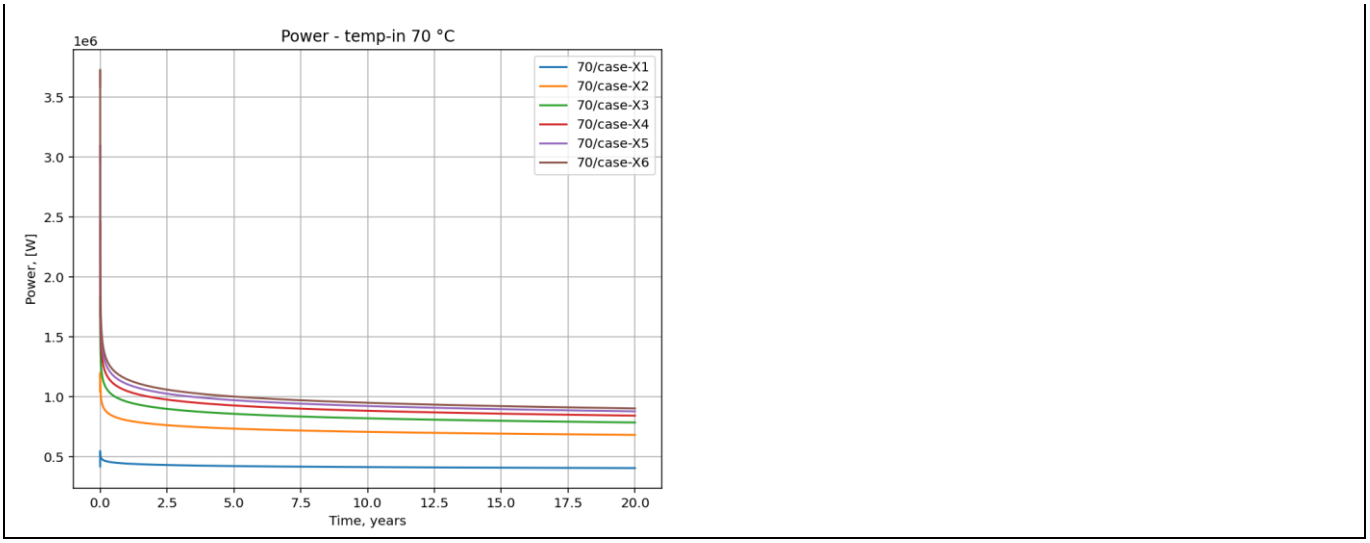

*Figure **86.** The output heat power for salt dome, horizontal part 2000 [m] case depending on the inlet temperature and flow rate*

Case 1.2. Salt dome, horizontal part 2500 [m].

The output heat power of the HOCLOOP borehole heat exchanger during 20 years of heat production, calculated for the above assumptions, are shown in Figure **87**.

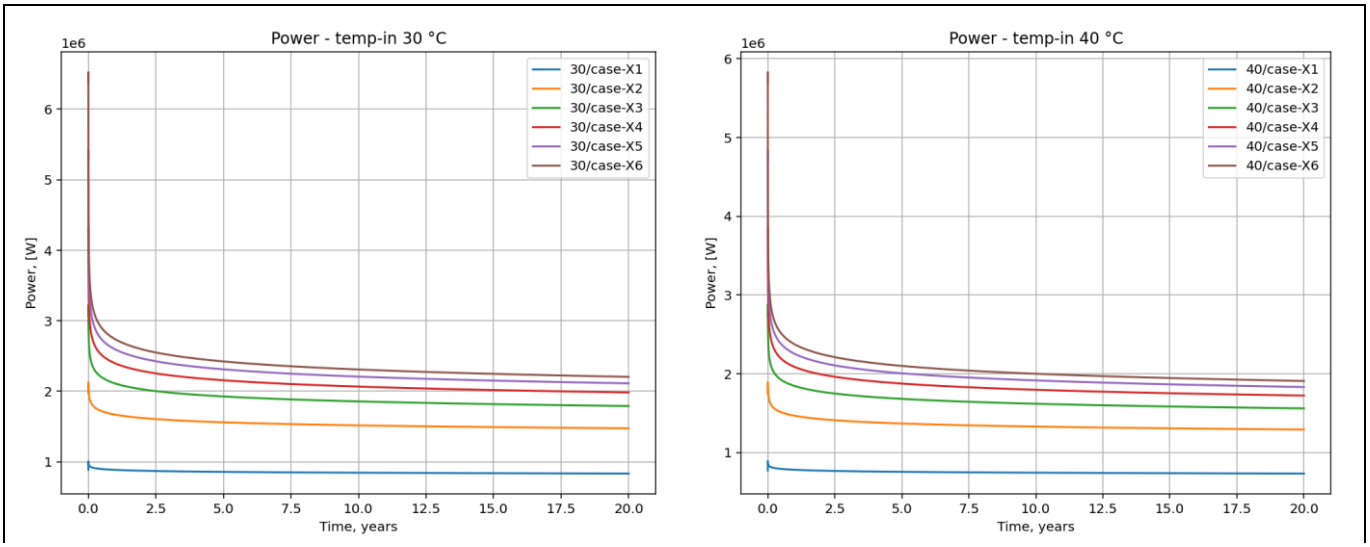

This project has received funding from the European Union's Horizon Europe research and innovation program under grant agreement No 101083558

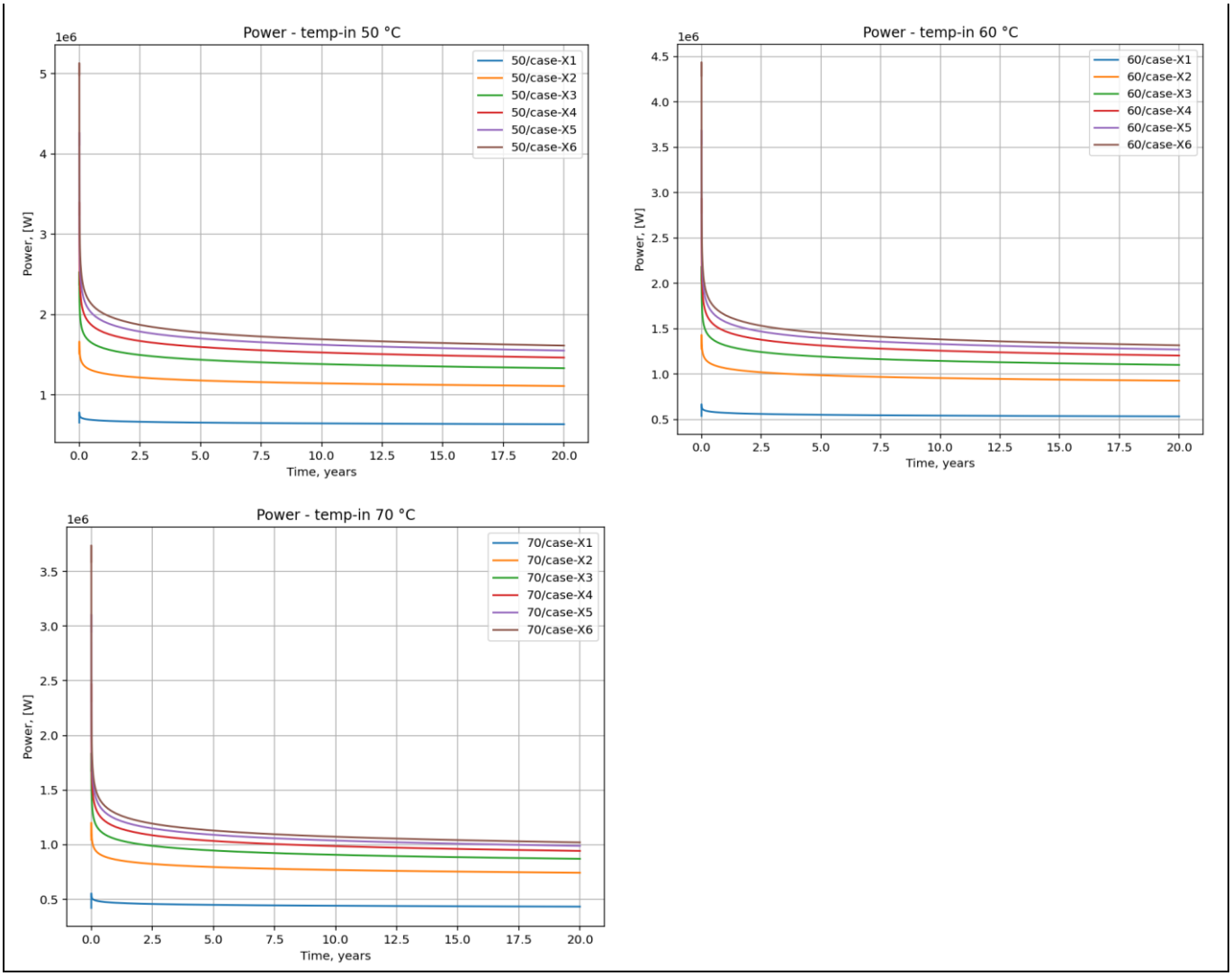

*Figure **87.** The output heat power for salt dome, horizontal part 2500 [m] case depending on the inlet temperature and flow rate*

Case 2.1. Salt pillow, horizontal part 1000 [m].

The output heat power of the HOCLOOP borehole heat exchanger during 20 years of heat production, calculated for the above assumptions, are shown in Figure **88**.

This project has received funding from the European Union's Horizon Europe research and innovation program under grant agreement No 101083558

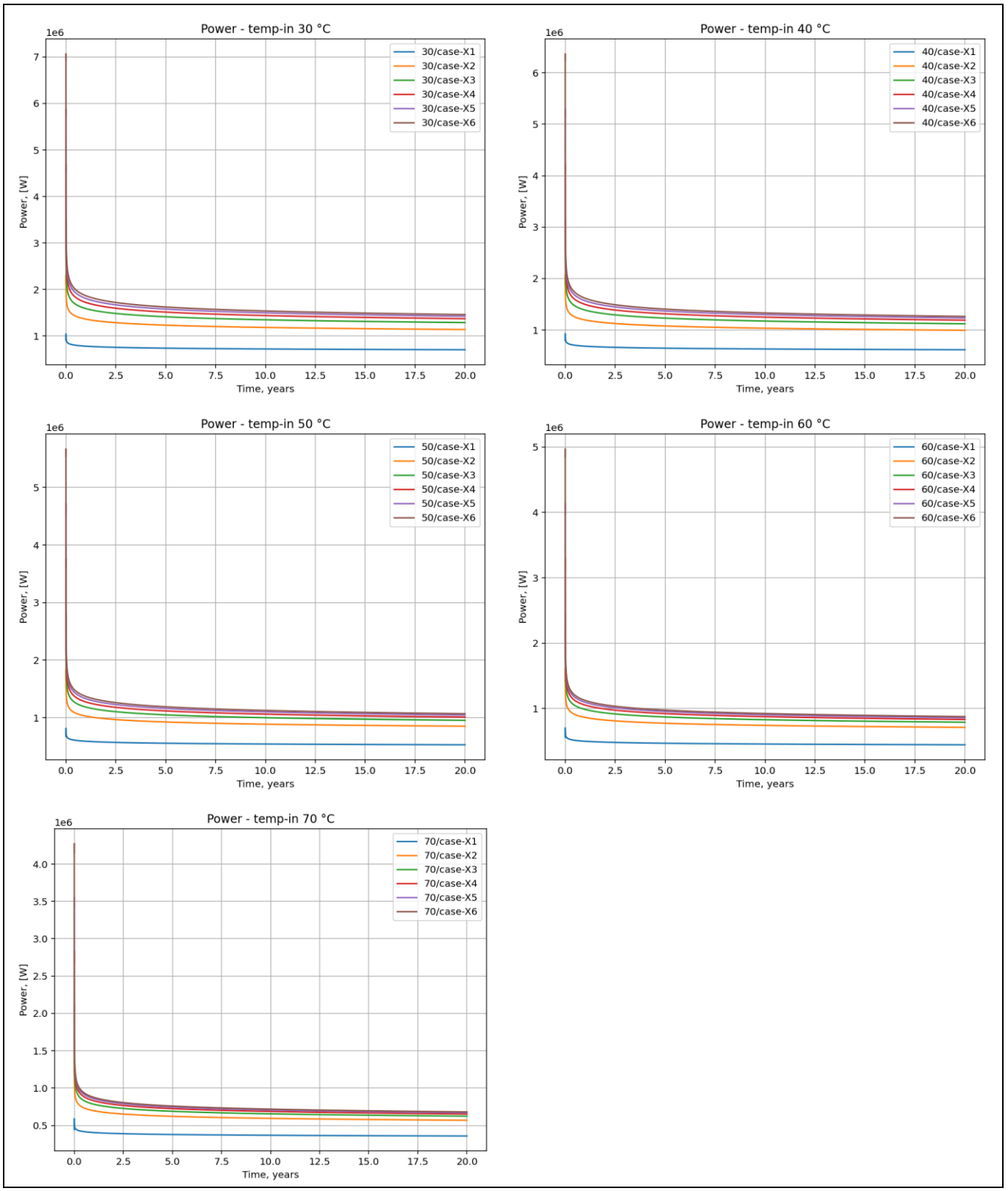

*Figure **88.** The output heat power for salt pillow, horizontal part 1000 [m] case depending on the inlet temperature and flow rate*

This project has received funding from the European Union's Horizon Europe research and innovation program under grant agreement No 101083558

Case 2.2. Salt pillow, horizontal part 2000 [m].

The output heat power of the HOCLOOP borehole heat exchanger during 20 years of heat production, calculated for the above assumptions, are shown in Figure 89.

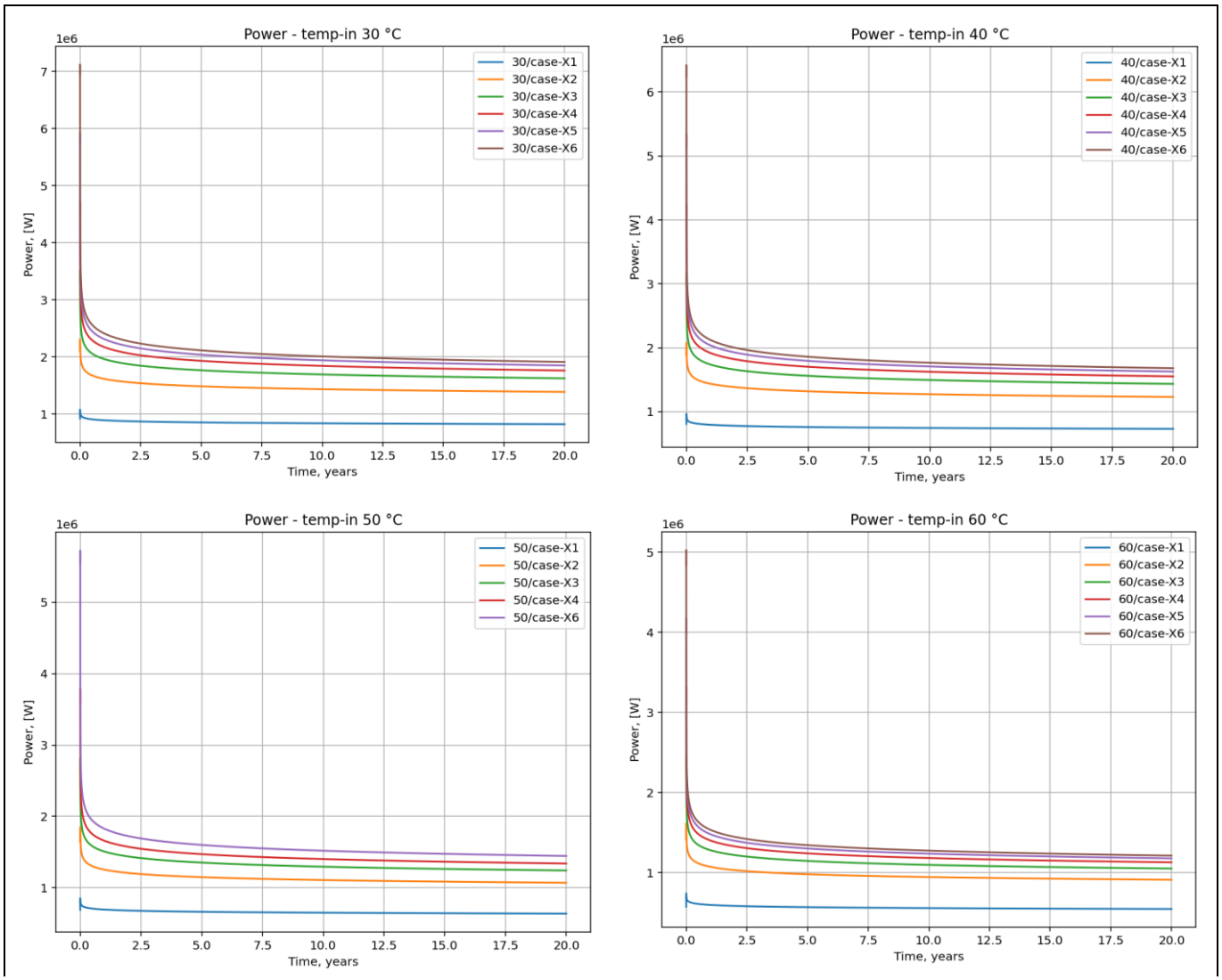

This project has received funding from the European Union's Horizon Europe research and innovation program under grant agreement No 101083558

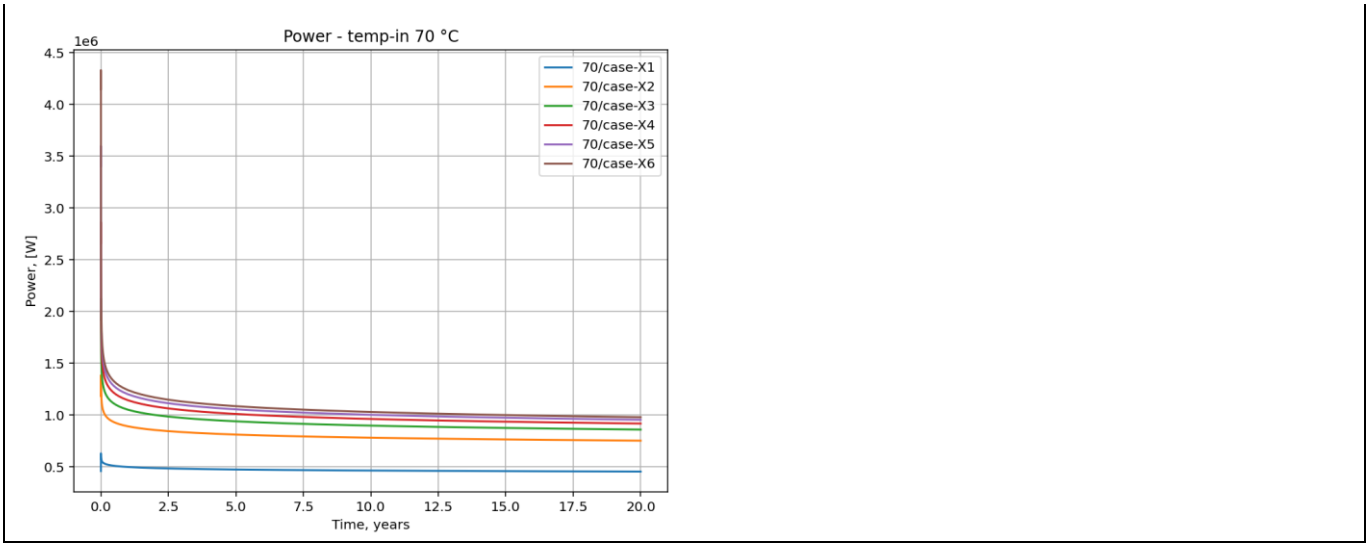

*Figure **89**. The output heat power for salt pillow, horizontal part 2000 [m] case depending on the inlet temperature and flow rate*

3.5.5.3. Scenarios Results – variable injection temperature

To determine the operating parameters of the surface plant, its output temperature profile, adjusted for seasonal load, was used as the input temperature for HOCLOOP borehole heat exchanger calculations. The district heating network temperatures in Goleniów were averaged over monthly intervals.

Simulations were performed for both proposed surface installation configurations: with and without a heat pump. Figure 90 shows the seasonal variation of the input temperature for a system without a heat pump; Figure 91 shows the input temperatures for a system with a heat pump (case 1.2).

For the system considering a heat pump, the inlet temperature profile of the underground heat exchanger varies with the injected water flow rate due to the differing operational characteristics of the heat pump in each scenario.

This project has received funding from the European Union's Horizon Europe research and innovation program under grant agreement No 101083558

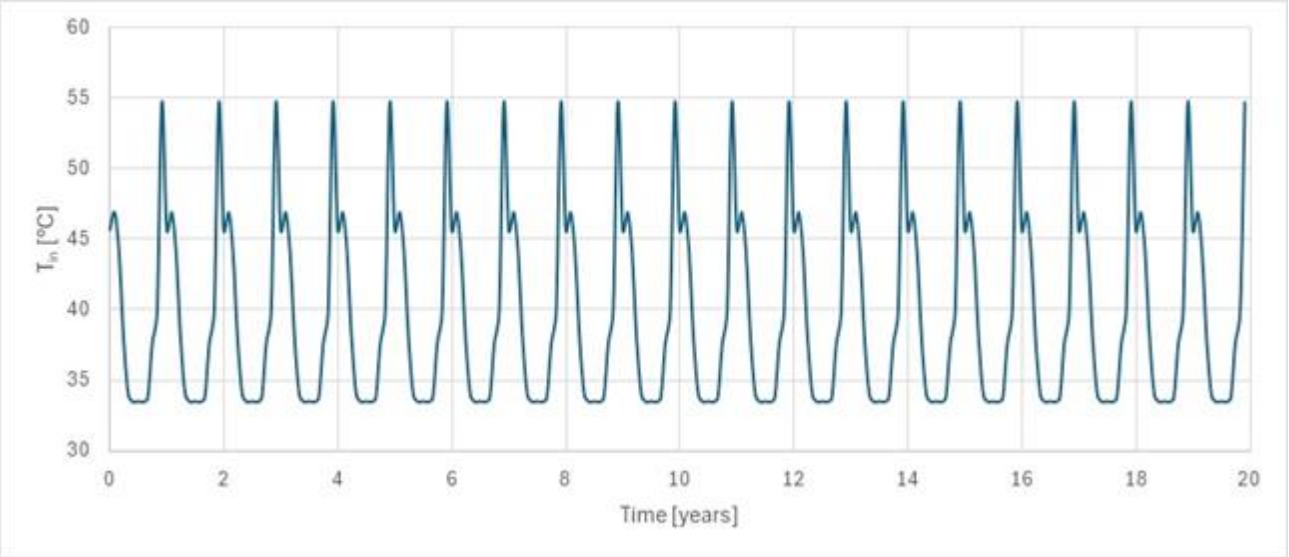

Figure ***90.*** Input temperature for HOCLOOP system – installation without Heat Pump

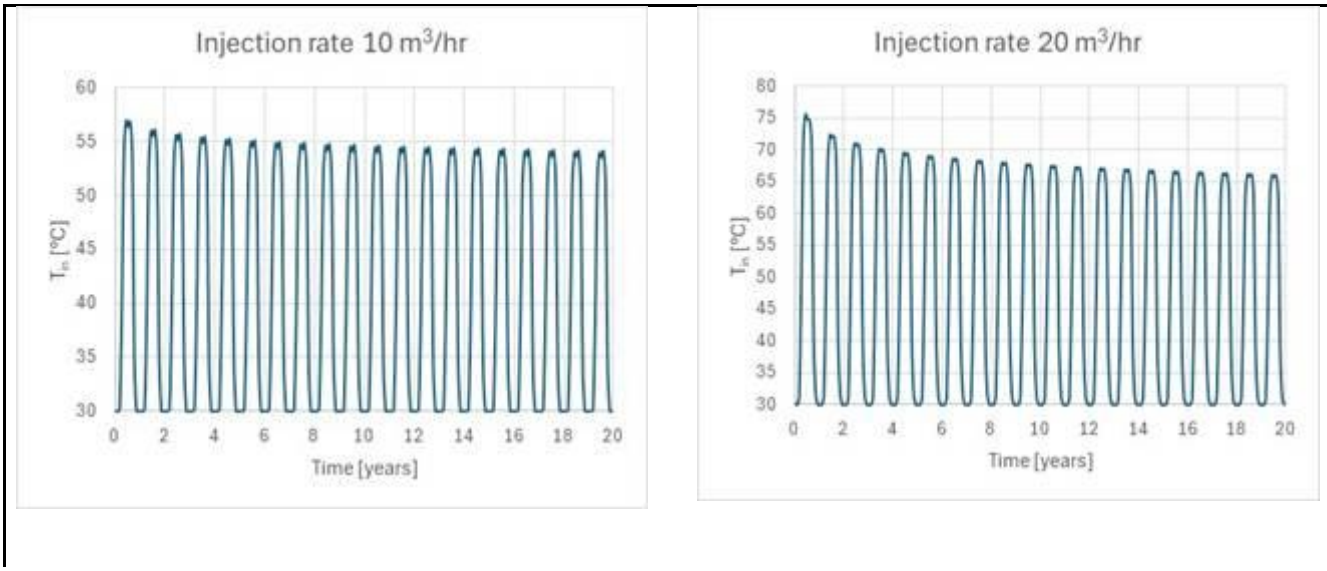

This project has received funding from the European Union's Horizon Europe research and innovation program under grant agreement No 101083558

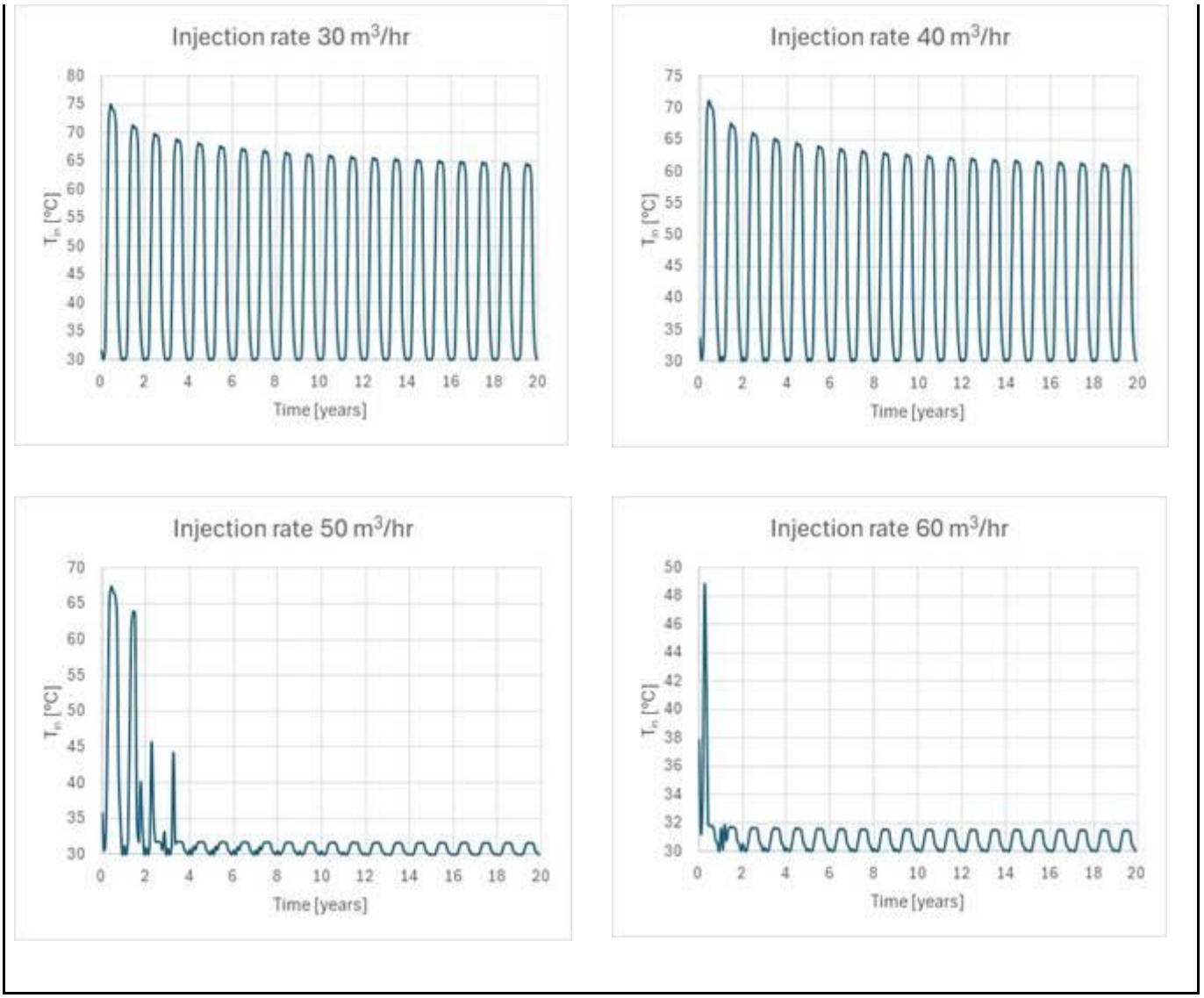

*Figure **91.** Input temperature for HOCLOOP system – installation with Heat Pump (case 1.2)*

Case 1.1. Salt dome, horizontal part 2000 [m].

The output temperatures and heat power of the HOCLOOP borehole heat exchanger during 20 years of heat production – installation without Heat Pump, are shown in Figure **92**.

This project has received funding from the European Union's Horizon Europe research and innovation program under grant agreement No 101083558

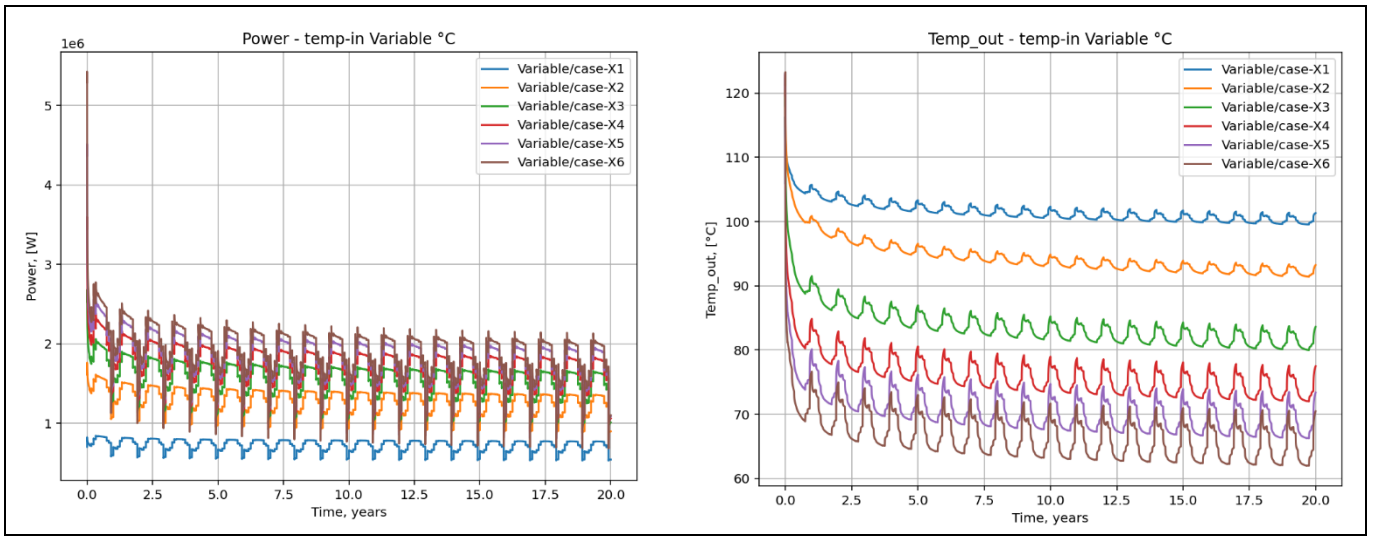

*Figure **92.*** The output temperatures and heat power for salt dome, horizontal part 2000 [m] case depending on the flow rate – without Heat Pump

The output temperatures and heat power of the HOCLOOP borehole heat exchanger during 20 years of heat production – installation with Heat Pump, are shown in Figure **93**.

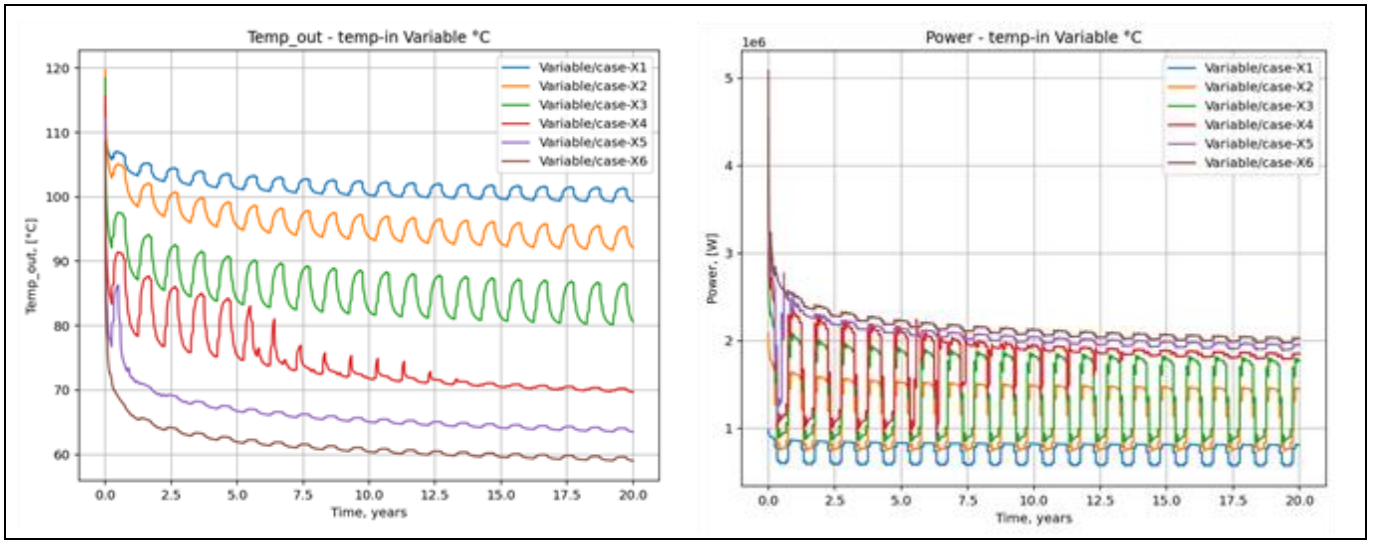

*Figure **93.** The output temperatures and heat power for salt dome, horizontal part 2000 [m] case depending on the flow rate – with Heat Pump*

Case 1.2. Salt dome, horizontal part 2500 [m].

The output temperatures and heat power of the HOCLOOP borehole heat exchanger during 20 years of heat production – installation without Heat Pump, are shown in Figure **94**.

This project has received funding from the European Union's Horizon Europe research and innovation program under grant agreement No 101083558

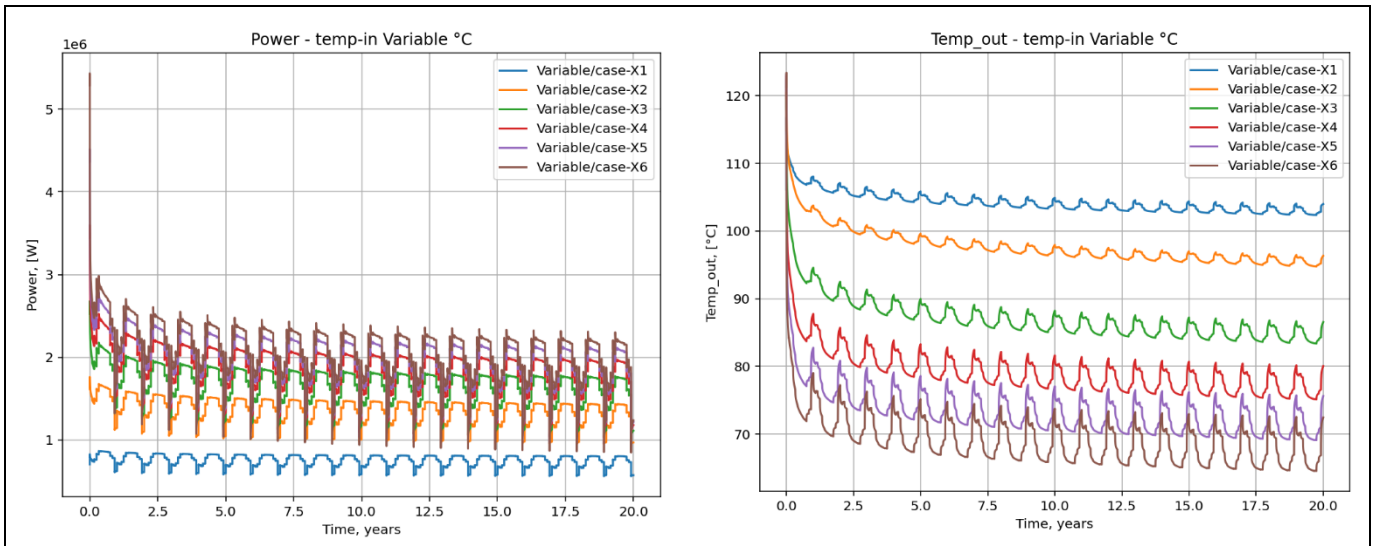

*Figure **94.** The output temperatures and heat power for salt dome, horizontal part 2500 [m] case depending on the flow rate – without Heat Pum*

The output temperatures and heat power of the HOCLOOP borehole heat exchanger during 20 years of heat production – installation with Heat Pump, are shown in Figure 95.

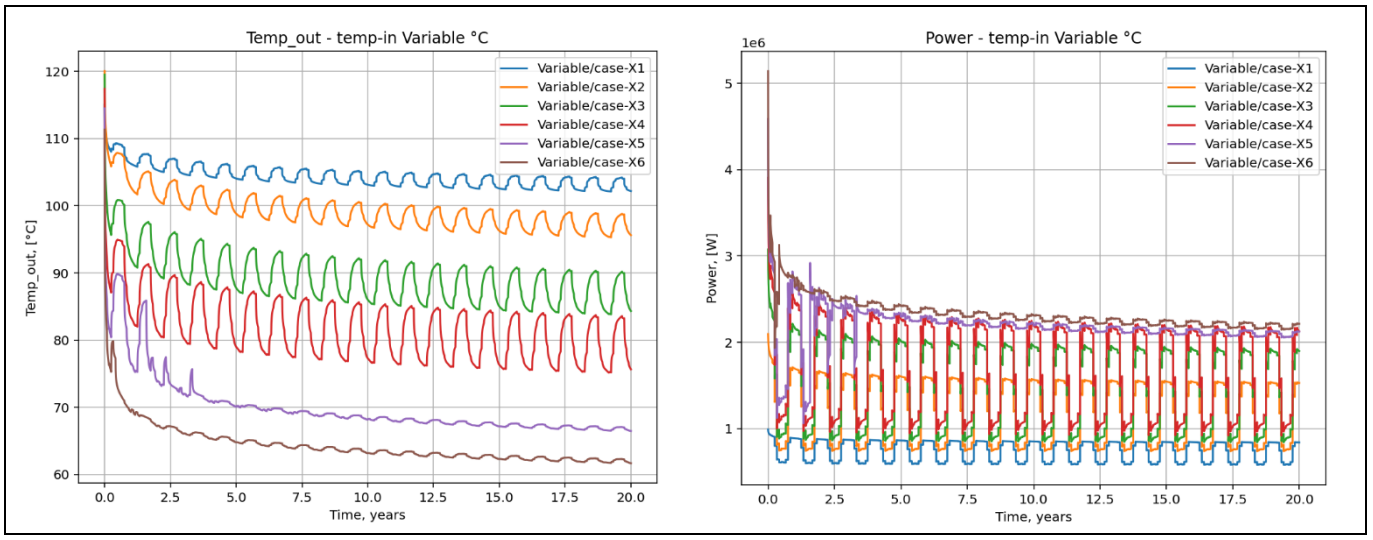

*Figure **95.** The output temperatures and heat power for salt dome, horizontal part 2500 [m] case depending on the flow rate – with Heat Pump*

Case 2.1. Salt pillow, horizontal part 1000 [m].

The output temperatures and heat power of the HOCLOOP borehole heat exchanger during 20 years of heat production – installation without Heat Pump, are shown in Figure 96.

This project has received funding from the European Union's Horizon Europe research and innovation program under grant agreement No 101083558

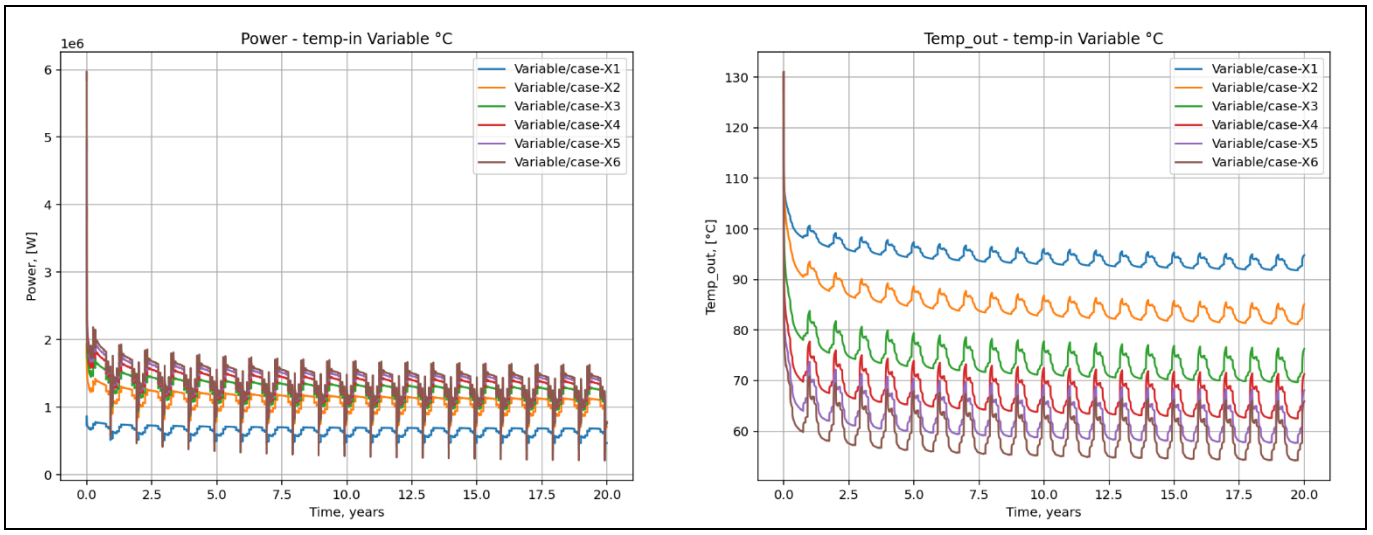

*Figure **96.** The output temperatures and heat power for salt pillow, horizontal part 1000 [m] case depending on the flow rate – without Heat Pump*

The output temperatures and heat power of the HOCLOOP borehole heat exchanger during 20 years of heat production – installation with Heat Pump, are shown in Figure **97**.

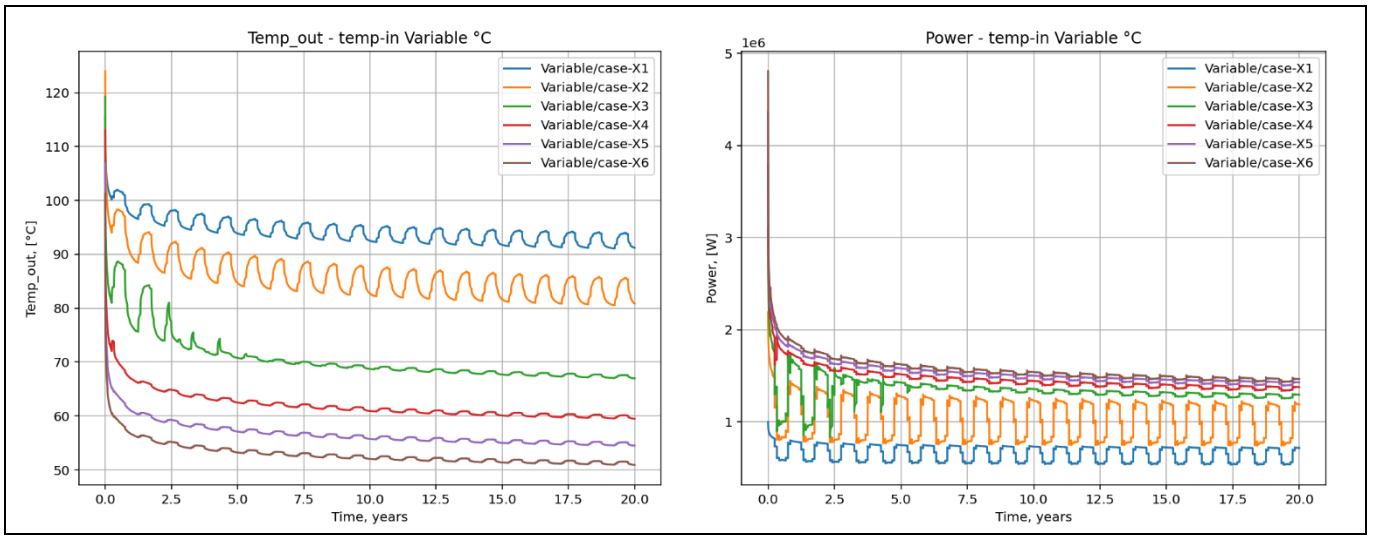

*Figure **97.** The output temperatures and heat power for salt pillow, horizontal part 1000 [m] case depending on the flow rate – with Heat Pump*

Case 2.2. Salt pillow, horizontal part 2000 [m].

The output temperatures and heat power of the HOCLOOP borehole heat exchanger during 20 years of heat production – installation without Heat Pump, are shown in Figure **98**.

This project has received funding from the European Union's Horizon Europe research and innovation program under grant agreement No 101083558

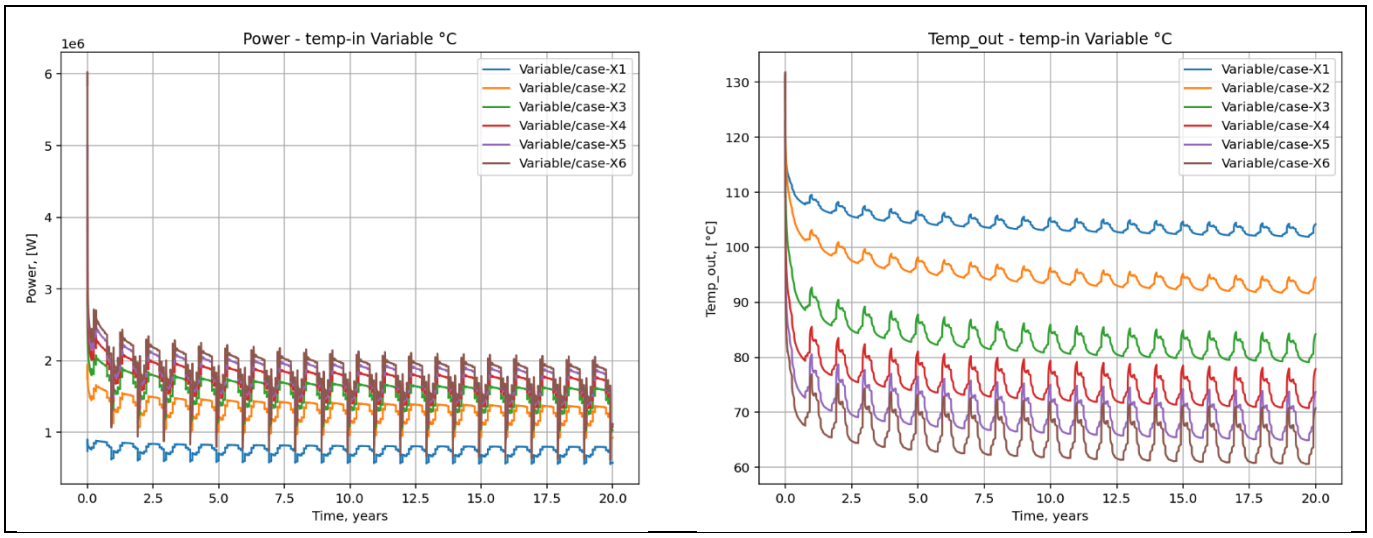

*Figure **98.** The output temperatures and heat power for salt pillow, horizontal part 2000 [m] case depending on the flow rate – without Heat Pump*

The output temperatures and heat power of the HOCLOOP borehole heat exchanger during 20 years of heat production – installation with Heat Pump, are shown in Figure **99**.

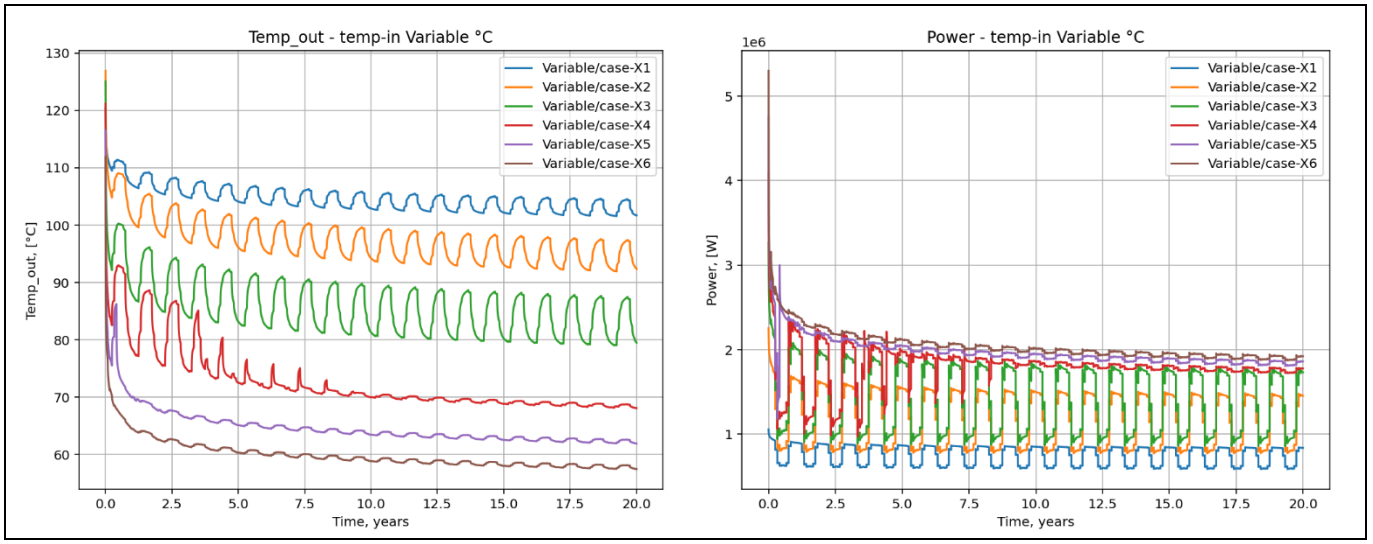

*Figure **99.** The output temperatures and heat power for salt pillow, horizontal part 2000 [m] case depending on the flow rate – with Heat Pump*

Fluid flow rate selection and optimization procedure

To determine the optimum flow rate, the variation of the plant's power in each variant was analyzed in relation to the system pressure. shows the power changes after 20 years of HOCLOOP heat exchanger operation as a function of flow rate. Figure **100** shows the changes in power divided by the pressure difference at the input and output of the heat exchanger, while Figure **101** shows the changes in power divided by the input pressure.

This project has received funding from the European Union's Horizon Europe research and innovation program under grant agreement No 101083558

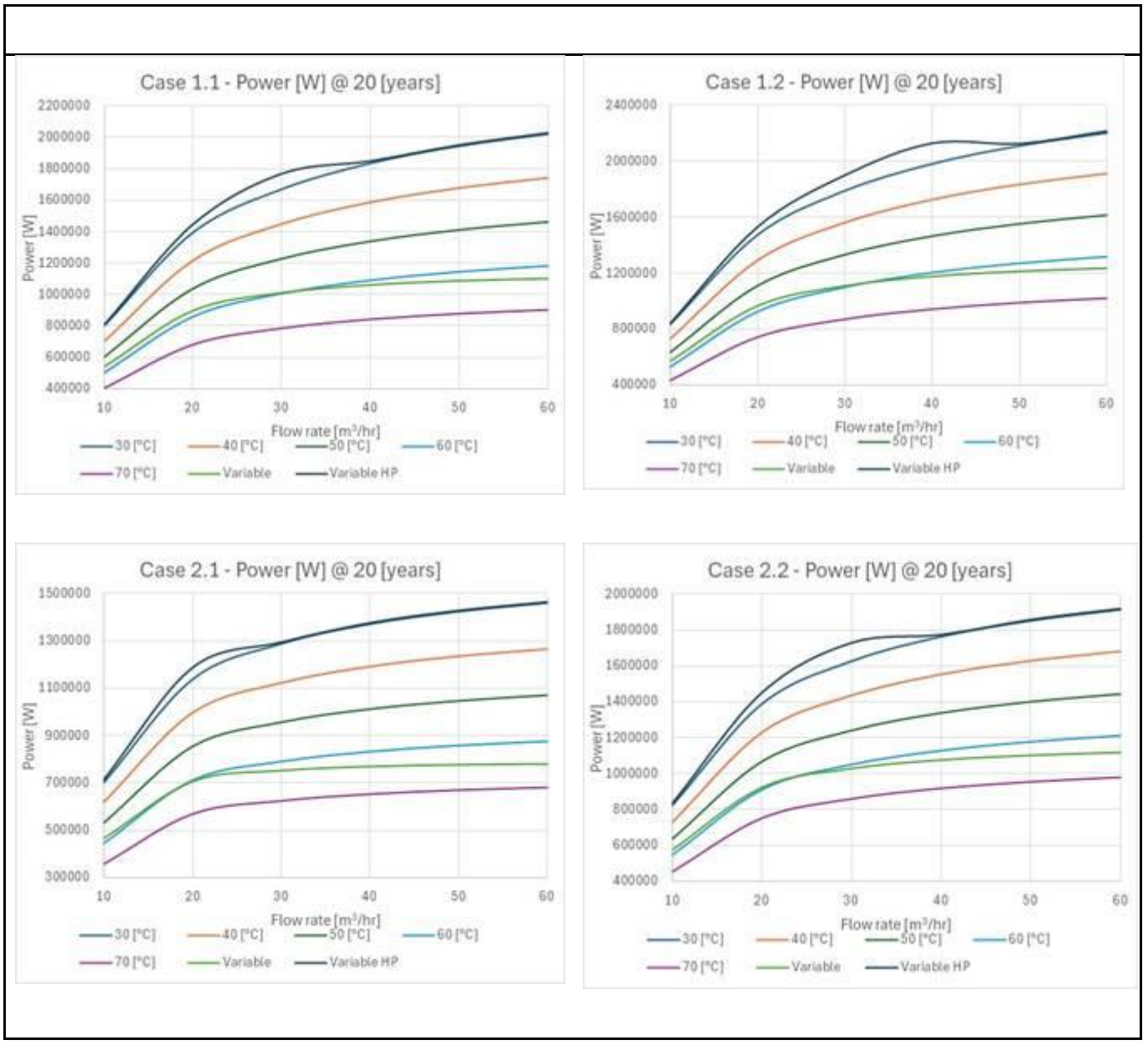

*Figure **100.** The power changes after 20 years of HOCLOOP heat exchanger operation as a function of flow rate*

This project has received funding from the European Union's Horizon Europe research and innovation program under grant agreement No 101083558

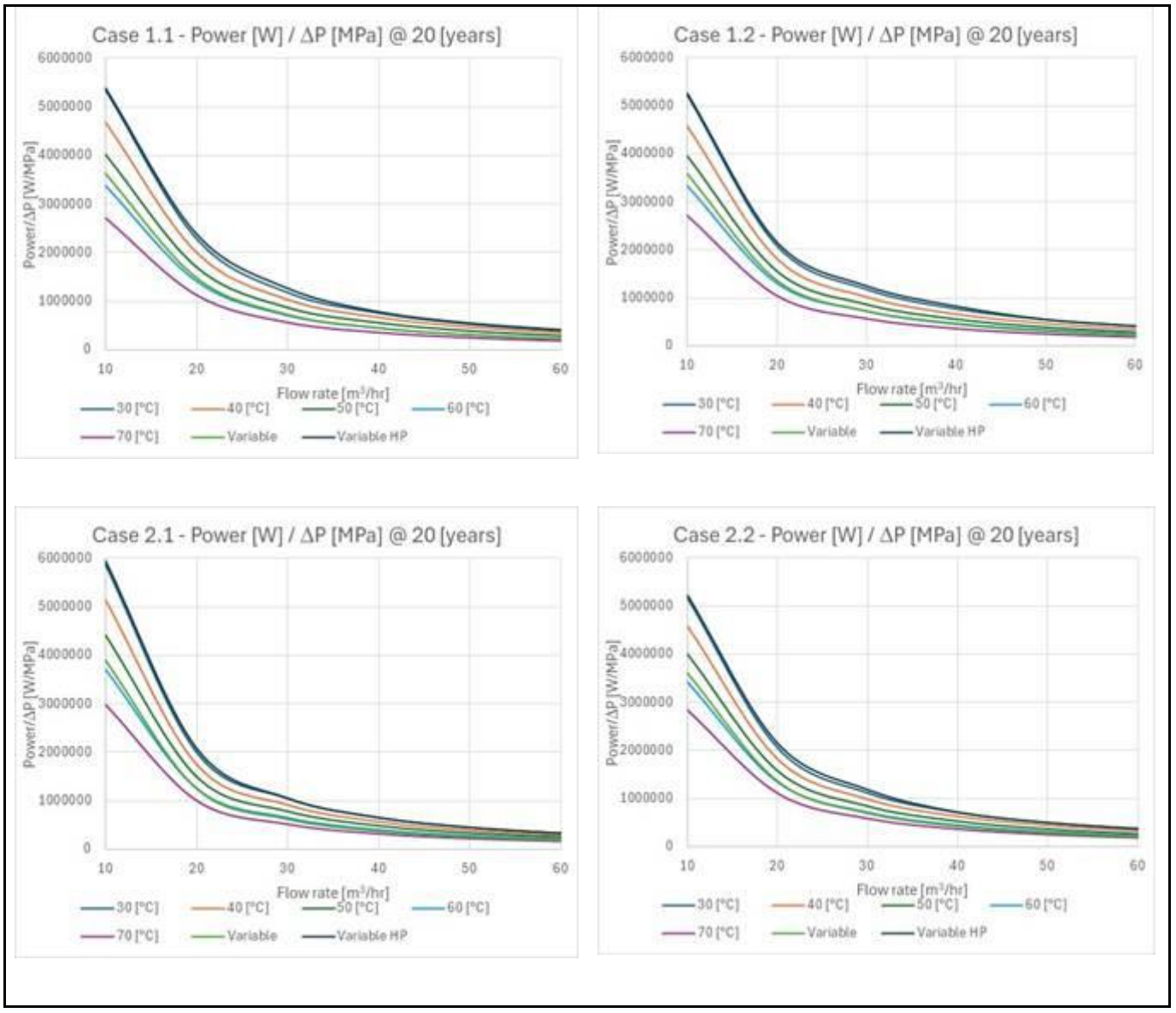

*Figure **101.** The changes in power divided by the pressure difference at the input and output of the heat exchanger*

This project has received funding from the European Union's Horizon Europe research and innovation program under grant agreement No 101083558

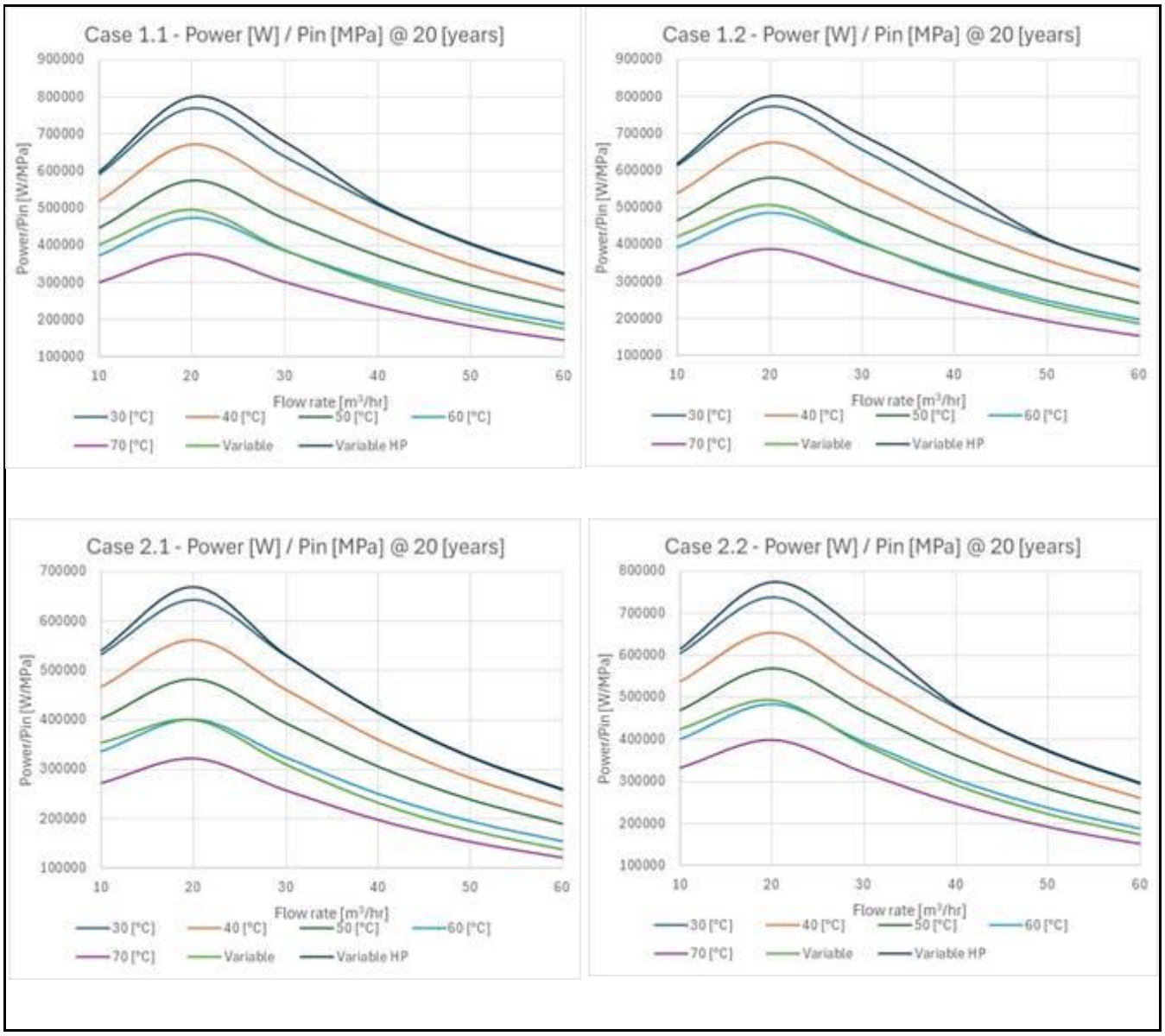

*Figure **102.** The changes in power divided by the input pressure of the heat exchanger*

In all cases, power increases are observed at lower flow rates. For flow rates above 20 m³/hr, the power gain is much smaller and decreases as the flow rate increases. This can also be seen in Figure 102, where the power is divided by the pressure difference. The largest changes are observed for flow expenses up to 20 m³/hr. Since the output pressure was the same in all cases due to surface installation adjustment, the key parameter is input pressure, which increases with flow rate. The ratio of power to input pressure reaches its maximum for a flow rate of 20 m³/hr, and this is the optimal flow rate from the point of view of system operation. Although increasing the capacity causes an increase in power, this is also associated with a much faster increase in system pressure (more pump power).

The utilisation of energy obtained based on the HOCLOOP solution results

Figure 103 and Figure 104 present the Goleniów district heating system's thermal characteristics in terms of demand for thermal power and scheme of power control (flow of energy carrier – which is water, its supply and return temperature).

This project has received funding from the European Union's Horizon Europe research and innovation program under grant agreement No 101083558

*Figure **103.** Ordered and time-dependent demand for thermal power covered by energy source*

This project has received funding from the European Union's Horizon Europe research and innovation program under grant agreement No 101083558

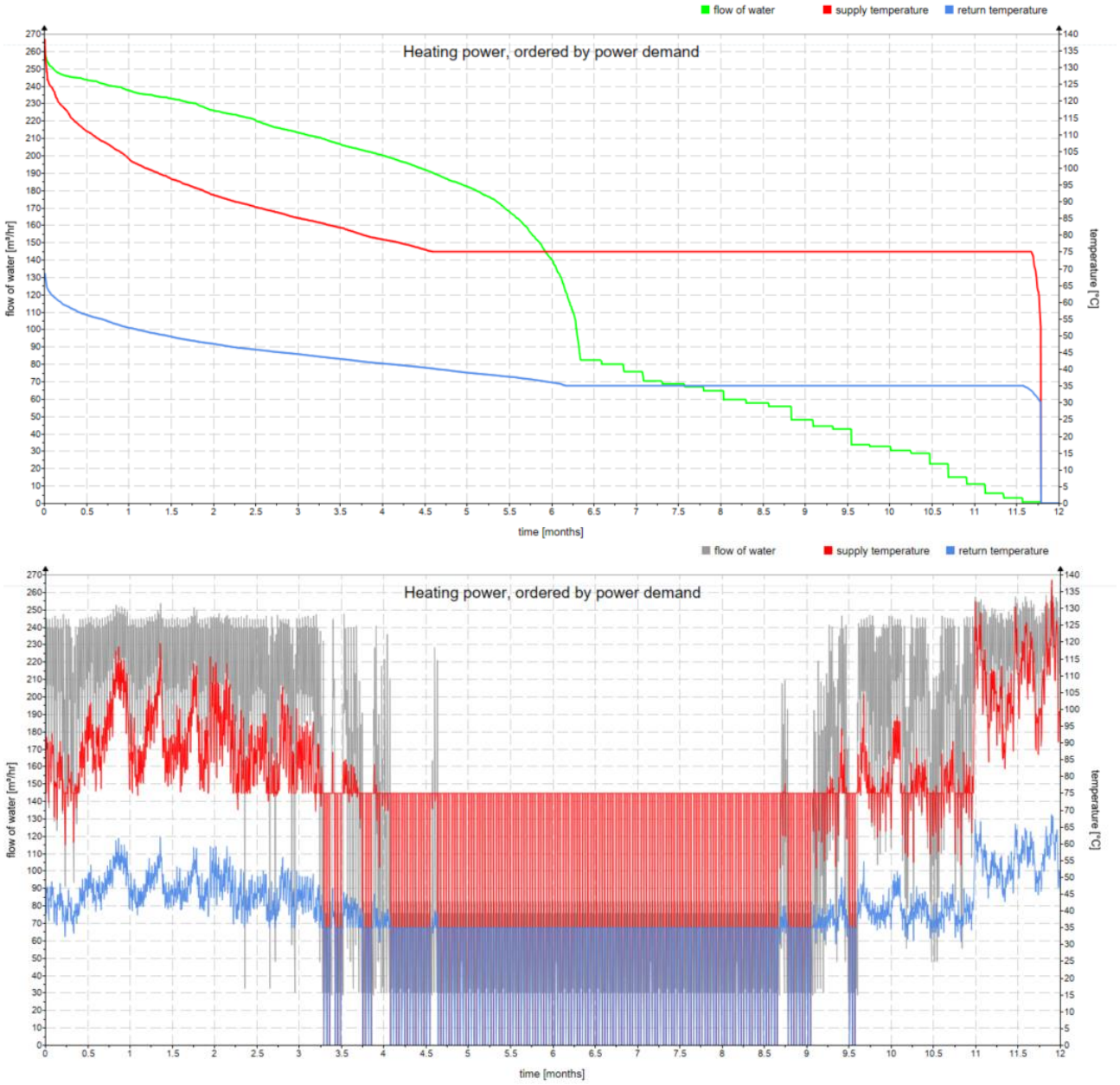

*Figure **104.** Ordered and time-dependent way of power control used in the Goleniów district heating (defined based on system design parameters and TMY – PV GIS in the location of Goleniów)*

Based on the assumptions defined above, it was possible to estimate the outcomes of the utilization of three HOCLOOP units integrated into the district heating system in Goleniów for a flow rate of 20 m³/h per unit (considered as optimal, based solely on the analysis of the underground system). The results pertain to a system targeting a salt dome as the geothermal energy source, with a 2 km horizontal section in the underground heat exchanger. Figure 105 and Figure 106 illustrate direct energy utilisation while Figure 107 and Figure 108 refer to the system supported by heat pumps.

This project has received funding from the European Union's Horizon Europe research and innovation program under grant agreement No 101083558

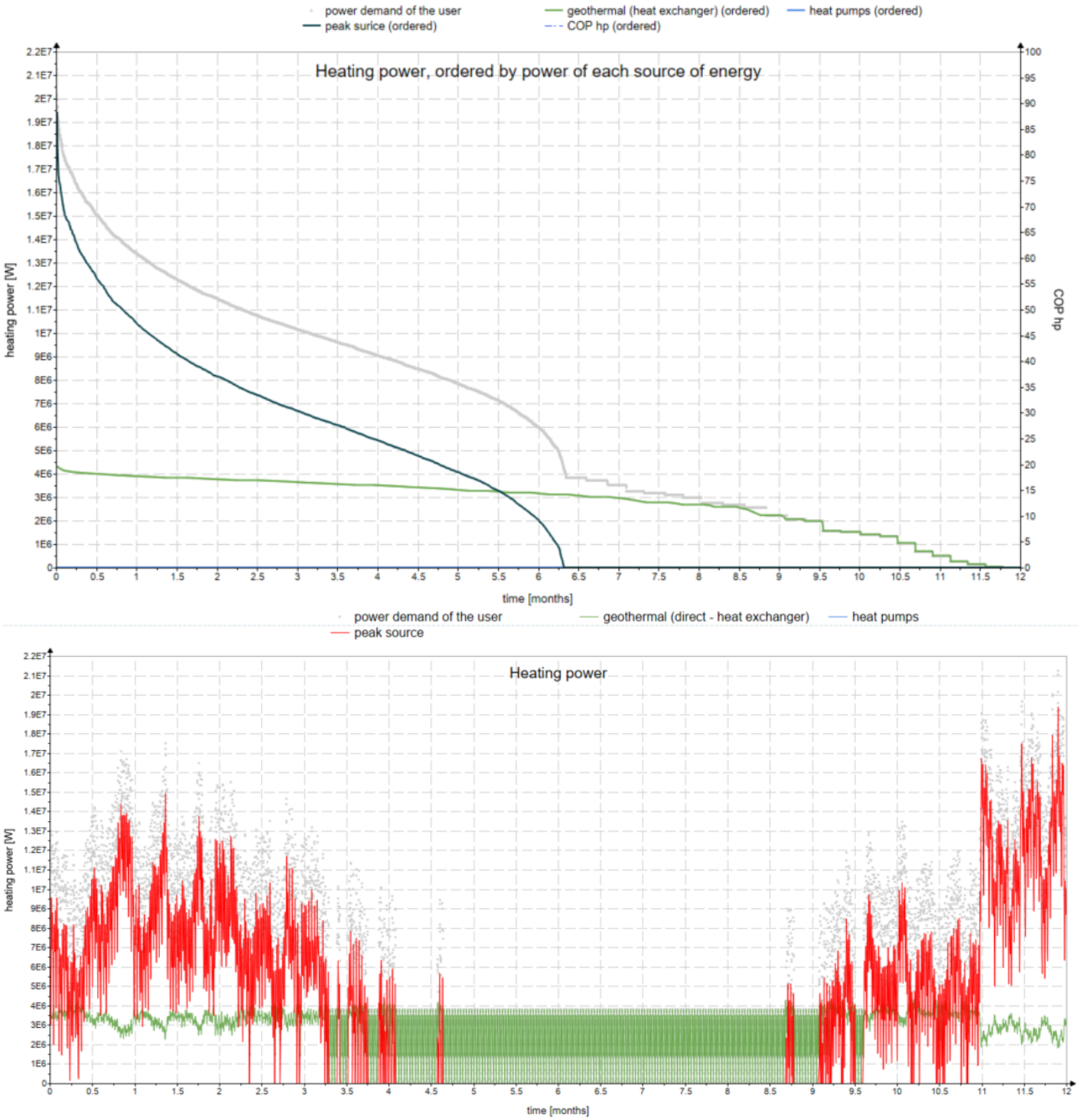

*Figure **105.** Coverage of power demand in the case of the direct HOCLOOP units utilisation (no heat pumps), in Case-X2 (20 m3/hr flow of water by each HOCLOOP unit), number of units: 3, various inlet temperatures (time and power-dependent), horizontal length of the well 2 km, location the salt dome, 10th year of the system exploitation. Ordered (top) and time-dependent curves (bottom)*

This project has received funding from the European Union's Horizon Europe research and innovation program under grant agreement No 101083558

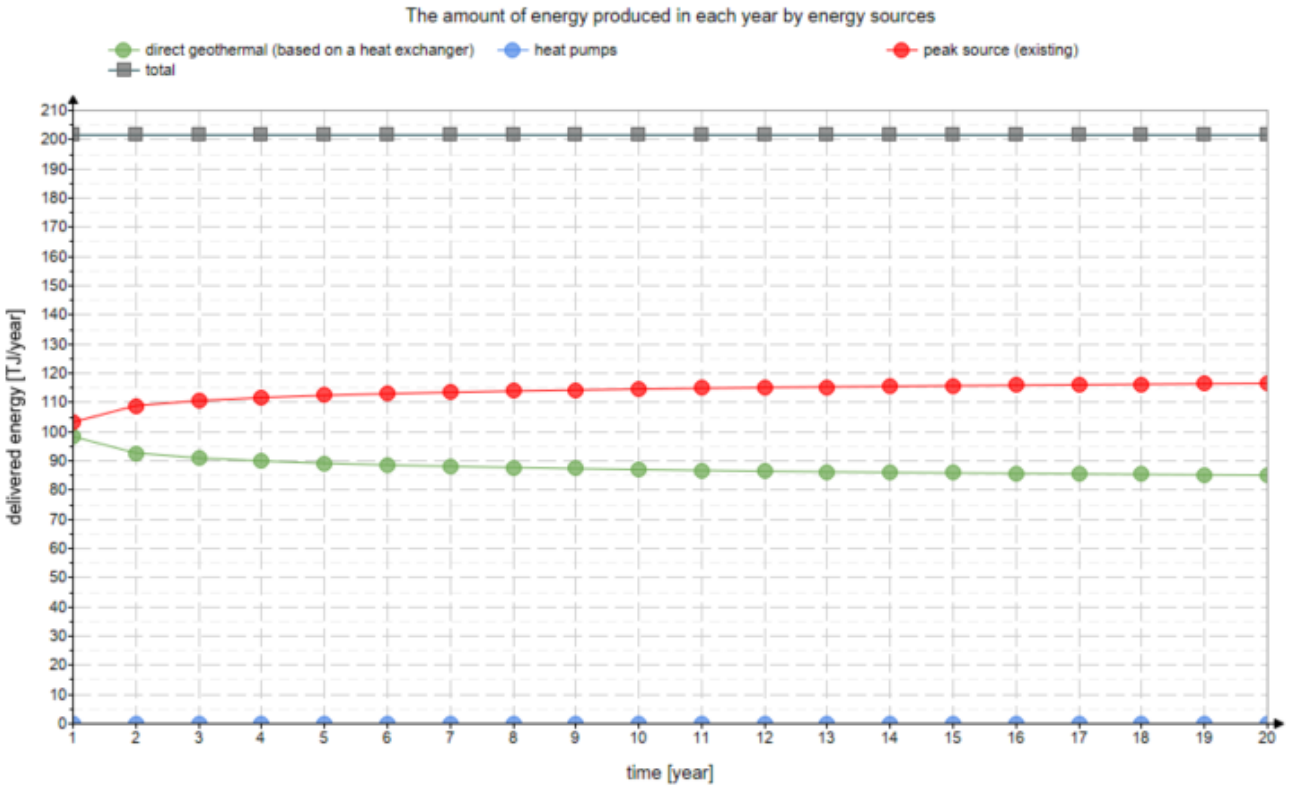

*Figure **106.** The share of energy production in lifetime of the system in the case of the direct HOCLOOP units utilisation (no heat pumps), in Case-X2 (20 m3/hr flow of water by each HOCLOOP unit), number of units: 3, various inlet temperatures (time and power-dependent), horizontal length of the well 2 km, location the salt dome (share in the lifetime: direct geothermal 43.6%, heat pumps 0.0%, peak sources 56.4%)*

This project has received funding from the European Union's Horizon Europe research and innovation program under grant agreement No 101083558

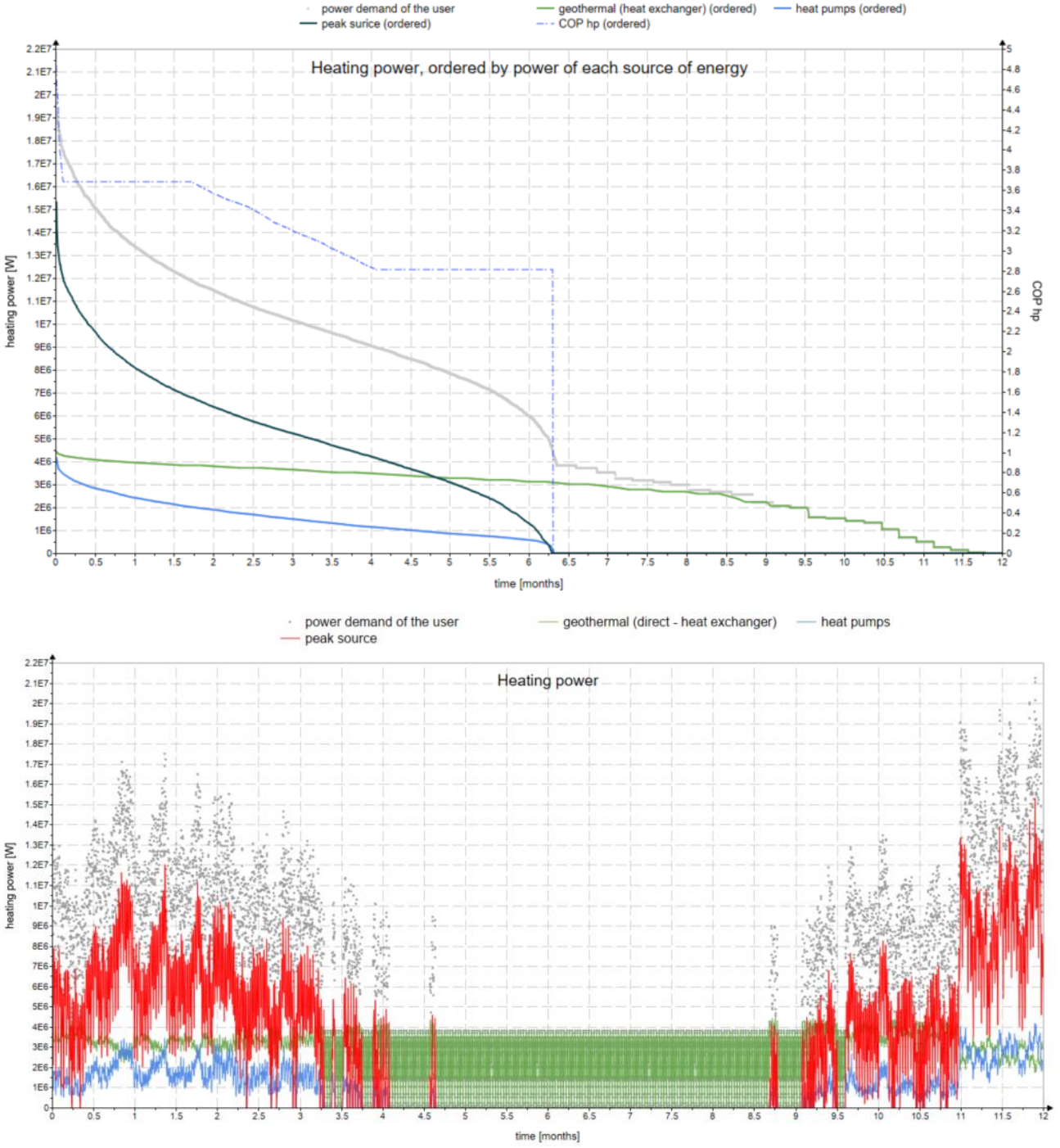

*Figure **107.** Coverage of power demand in the case of the direct HOCLOOP units utilisation supported by heat pumps, in Case-X2 (20 m3/hr flow of water by each HOCLOOP unit), number of units: 3, various inlet temperatures (time and power-dependent), horizontal length of the well 2 km, location the salt dome, 10th year of the system exploitation. Ordered (top) and time-dependent curves (bottom)*

This project has received funding from the European Union's Horizon Europe research and innovation program under grant agreement No 101083558

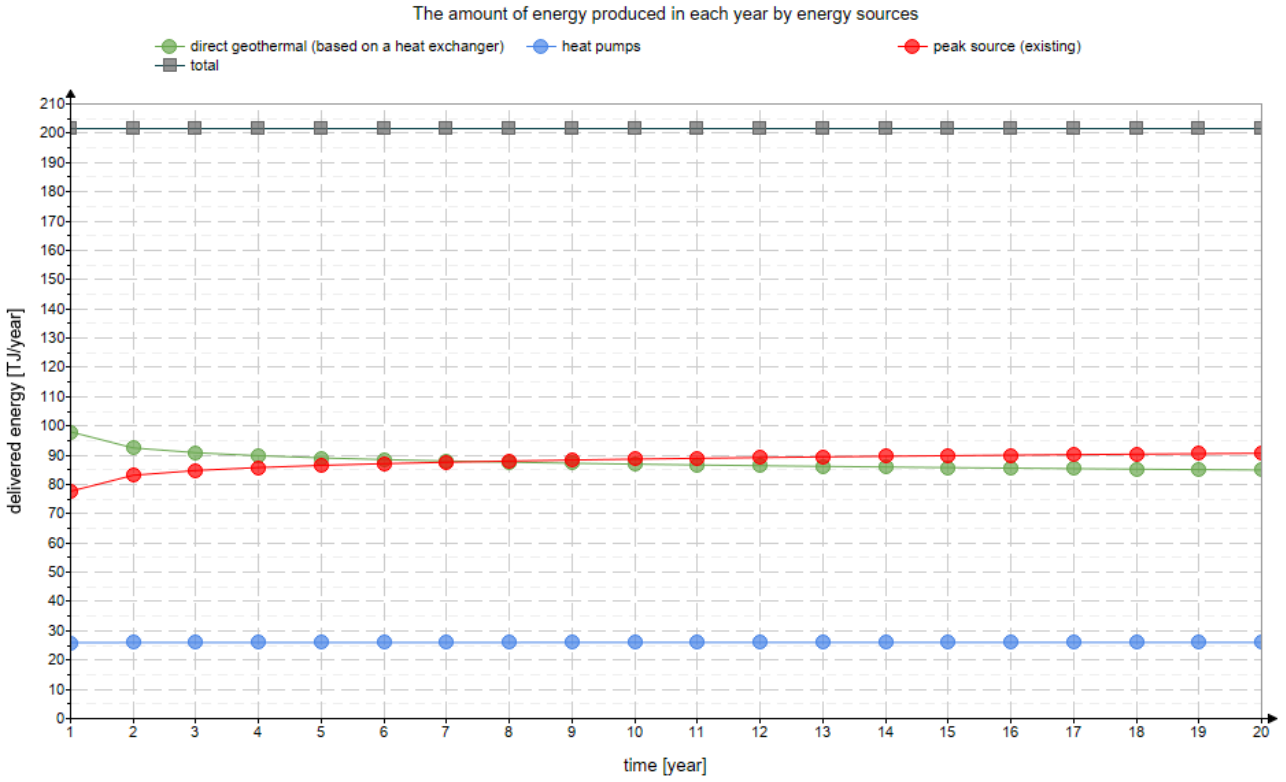

*Figure **108.** The share of energy production in the lifetime of the system in the case of the direct HOCLOOP units utilisation supported by heat pumps, in Case-X2 (20 m3/hr flow of water by each HOCLOOP unit), number of units: 3, various inlet temperatures (time and power-dependent), the horizontal length of the well 2 km, location the salt dome (share in the lifetime: direct geothermal 43.5%, heat pumps 12.9%, peak sources 43.6%. Total share of renewables, including energy obtained by heat pumps evaporators 52.4%)*

3.5.6. Conclusions of the case of Poland

For the Polish case, two integration options of the HOCLOOP concept were investigated at the Goleniów facilities to supply heat to the existing district heating network.

The simulations enable to understand the potential benefits of HOCLOOP systems in combination with heat pumps or as stand-alone systems – utilising additional heat exchangers: HOCLOOP working fluid (water)/district heating energy carrier (water) only. In both cases existing coalfired heating plant is a peak energy source, but HOCLOOP designs allows to reduce coal consumption. Both cases were equipped with three HOCLOOP units working parallel, and water was the working fluid.

The calculations show that by implementing HOCLOOP, the share of renewable energy is significant, exceeding 40% in both configurations and reaching over 50% with heat pumps. A flow rate of 20 m^3/h, as assumed in the calculations and validated by underground system analysis, ensures stable thermal power output over time, confirming the system's reliable operation. Additionally, this case study shows the promising results in terms of technical feasibility thanks to the favourable subsurface conditions. Indeed, the targeted salt structures are associated with high thermal conductivity that impacts positively the system performance.

This project has received funding from the European Union's Horizon Europe research and innovation program under grant agreement No 101083558

Defining the optimal solution requires establishing economic boundary conditions, with underground heat exchanger installation costs being a key factor. System optimization, including economic feasibility, will be addressed in later project stages, and the tools developed so far provide all necessary data for this process.

4. Conclusions

In this deliverable the conceptual closed loop systems designed specifically for each pilot as well as the different scenarios and input parameters used to assess the long-term energetic performance of the conceptual systems are presented. The results of the dynamic simulations obtained using the simulation tools developed in T2.3 or benchmarked in T2.1 are analysed and discussed. The modelling exercise contributes towards the selection of optimal combination of geological and surface conditions for the HOCLOOP concept.
The simulations performed in T4.2 unable to understand the technical feasibility of the HOCLOOP under various subsurface and surface demand conditions.

The Belgian case examined two HOCLOOP integration schemes at VITO: reusing the deep dry well (MOL-GT-03) for pre-heating the research campus's working fluid or for directly heating new buildings designed for low-temperature sources. In the first scenario, simulations show the well's power output remains low (<1 MW) even with a horizontal extension due to high injection temperatures (>60°C), causing thermal losses and reduced heat transfer. To fully evaluate the techno-economic potential of this scheme, particularly with horizontal drilling, the next step requires an economic analysis. In contrast, heating new buildings is more efficient. With the lower required temperature (≥45°C) and moderate demand (~2015 MWy), the existing well in combination with the HOCLOOP system can supply energy for over 20 years without additional drilling. This option minimizes heat losses and maximizes heat flow, whereas pre-heating the working fluid would require further drilling. Based on the technical feasibility study, direct heating appears to be the preferred solution, offering a more sustainable and cost-effective use of the well. The main advantage of reusing the dry well is that saving on drilling costs would be substantial.

The Paris case evaluated the HOCLOOP concept in a low temperature geological setting where a geothermal doublet is already installed. The simulations results showed that the overall performance of the closed-loop is always much lower when compared to the geothermal doublet. Even with a potential horizontal extension of the wellbore, the produced power from one closed system is four (around 0.01 MW) to three (0.1 MW) orders of magnitude lower than the actual production of the geothermal doublet (10 MW). For the system to be able to deliver to the district heating system a fluid with constant temperature, the inlet conditions must be controlled. From the two optimization procedures tested, adjusting the inlet flow rate proved to be the optimal method in comparison with the control of the inlet temperature.

The Darmstadt case compares the HOCLOOP solution with a medium-deep borehole thermal energy storage (MD-BTES) system. Due to the lower temperature gradient in Darmstadt, and excluding economic

This project has received funding from the European Union's Horizon Europe research and innovation program under grant agreement No 101083558

considerations, the HOCLOOP solution produces less heat than the MD-BTES system during the winter period.

The Italian case considers three different potential locations for the deployment of HOCLOOP systems, representative of the wide range of heat flux values affecting this area. Consequently, different possible integration schemes have been proposed to properly exploit the various geological conditions.In the Amiata case, due to the high geothermal gradient, a cogeneration application has been evaluated. For the Gavorrano case, where the geothermal gradient is still significant, a district heating network has been proposed. On the other hand, for the Gargano case, since the geothermal potential is limited, a cooling application has been considered. The HOCLOOP solution has demonstrated its capability to supply a substantial amount of heat in medium-high gradient areas, such as Gavorrano and Amiata, without interacting with the underground hydrothermal environment. In the case of Amiata, the predicted outlet temperature has been shown to be sufficiently high to generate electrical power in addition to providing heat to the end user. Conversely, in the Gargano area, the extremely low geothermal gradient significantly limits the amount of extractable power from the well - and consequently, the cooling capacity of the ejection cycle - to approximately 100 kW. This limitation is particularly relevant when considering the substantial effort required to drill a deep well (5 km).

For the Polish case, two integration options of the HOCLOOP concept were investigated at the Goleniów facilities to supply heat to the existing district heating network. The simulations enable to understand the potential benefits of HOCLOOP systems in combination with heat pumps or as stand-alone systems. The calculations show that by implementing HOCLOOP, the share of renewable energy is significant, exceeding 40% in both configurations and reaching over 50% with heat pumps. A flow rate of 20 m^3/h, as assumed in the calculations and validated by underground system analysis, ensures stable thermal power output over time, confirming the system's reliable operation. Additionally, this case study shows the promising results in terms of technical feasibility thanks to the favorable subsurface conditions. Indeed, the targeted salt structures are associated with high thermal conductivity that impacts positively the system performance. Defining the optimal solution requires establishing economic boundary conditions, with underground heat exchanger installation costs being a key factor. System optimization, including economic feasibility, will be addressed in later project stages, and the tools developed so far provide all necessary data for this process.

This project has received funding from the European Union's Horizon Europe research and innovation program under grant agreement No 101083558

5. References

[1] M. Singh, C. Souque, D. Liota, D. Fiasci, B. Laenen and V. Harcouët-Menou, "Pilot sites data and integration analysis D4.1," 2023.

[2] E. Robertson, "Thermal properties of rocks," USGS, 1988.

[3] D. Waples and J. Waples, "A Review and Evaluation of Specific Heat Capacities of Rocks, Minerals, and Subsurface Fluids. Part 1 Fluids and Porous Rocks," Natural Resources Research, vol. 13, 2004.

[4] E. Hernandez, V. Leontidis, M. Wangen and V. Harcouët-Menou, Benchmark cases D2.1, 2023.

[5] L. Seib, M. Frey, C. Bossennec, M. Krusemark, T. Burschil, H. Buness, L. Weydt and I. Sass, "Assessment of a medium-deep borehole thermal energy storage site in the crystalline basement: A case study of the demo site Lichtwiese Campus, Darmstadt," Geothermics, 2024.

[6] R. Al-Khoury and P. Bonnier, "Efficient finite element formulation for geothermal heating systems," International Journal of Numerical Methods in Engineering, 2006.

[7] P. Eskilson and J. Claesson, "Simulation model for thermally interacting heat extraction boreholes," Numerical Heat Transfer , 1988.

[8] Diersch, Bauer, Heidemann, Rühaak and Schätzl, "Finite element modeling of borehole heat exchanger systems," Computers and Geocsiences, 2011.

[9] V. Leontidis, N. Anand and M. Wangen, “Deliverable D2.4: Optimized design for the closed loop geothermal system,” 2023.

[10] V. Leontidis, M. Wangen, P. Ungar and D. Fiaschi, "Flow pipe model for fluid circulation D2.2," HOCLOOP Project 101083558, 2023.

[11] Y. Zhang, L. Pan, K. Pruess, S. Finsterle, A time-convolution approach for modeling heat exchange between a wellbore and surrounding formation, Geothermics 40 (4) (2011) 261–266. doi:10.1016/j.geothermics.2011.08.003.

[12] P. Ungar, Use of CO2 as working fluid in geothermal systems, Ph.D. thesis, University of Florence, Florence (3 2023).

[13] H. Li, S. Svendsen, Energy and exergy analysis of low temperature district heating network, Energy 45 (1) (2012) 237–246. doi:10.1016/j.energy.2012.03.056.

[14] Czapkowski. G. & Tarkowski. R. (2018). Geological conditions of selected salt domes in Poland and their suitability for the construction of caverns for hydrogen storage (Uwarunkowania geologiczne wybranych wysadów solnych w Polsce i ich przydatność do budowy kawern do magazynowania wodoru). Bulletin of the Polish Geological Institute (Biuletyn Państwowego Instytutu Geologicznego). 472. pp. 53-82.

This project has received funding from the European Union’s Horizon Europe research and innovation program under grant agreement No 101083558

[15] Czapkowski G., Tomassi-Morawiec H. (2012). Current geological knowledge on salt structures from the Szczecin region (NW Poland) for perspective location of cavern storages and depositories, Biuletyn Państwowego Instytutu Geologicznego 448, 145–156.

[16] Krzywiec P. (2009). Geometry and evolution of selected salt structures in the Polish Lowlands in the light of seismic data, Przegląd Geologiczny 57(9).

[17] Sowiżdżał, A. (2009). Geological analysis and evaluation of water and geothermal energy resources of the Mesozoic formation of the Szczecin Trough, PhD dissertation. Kraków: AGH Archive.

[18] PGI, 2014: Dokumentacja geologiczna złoża wysadowego soli kamiennej "Goleniów" w kat. D w miejsc. Zielonczyn, gm. Stepnica, Goleniów, woj. Zachodniopomorskie, Nr CBDG 1014323; Inw. 271/2014 Arch. CAG PIG, Warszawa.

[19] PGI, 1966: Dokumentacja wynikowa wiercenia strukturalnego Goleniów IG-1, Nr CBDG 258924; 69233,CAG PIG, Warszawa.

This project has received funding from the European Union's Horizon Europe research and innovation program under grant agreement No 101083558

Annex 1- MOL-GT-03 well trajectory

MD[m]	INC [degree]	TVD [m]	dx [m]
0	0	0	0
30	0	-30	0
60	0	-60	0
90	0	-90	0
120	0	-120	0
150	0	-150	0
180	0	-180	0
200	0	-200	0
210	0.1	-210	0
215	0.15	-215	0
240	0.4	-240	0
270	0.7	-270	1
300	1	-300	1
330	1.3	-330	2
360	1.6	-360	3
390	1.9	-390	4
400	2	-400	4
420	2	-420	5
450	2	-450	6
480	2	-480	7
510	2	-510	8
540	2	-540	9
570	2	-570	10
600	2	-600	11
630	2	-630	12
660	2	-660	13
690	2	-690	14
700	2	-700	14
720	2	-720	15
750	2	-750	16
780	2	-780	17
810	2	-810	18
840	2	-840	19
870	2	-870	20
885	2	-885	21
900	2	-900	21
930	2	-930	22
960	2	-960	24
990	2	-990	25
1020	2	-1020	26
1025	2	-1025	26
1050	2.58	-1050	27
1080	3.54	-1079	29
1110	4.63	-1109	31
1120	5	-1119	32

MD[m]	INC [degree]	TVD [m]	dx [m]
1140	5.68	-1139	34
1170	6.85	-1169	38
1200	8.13	-1199	42
1230	9.47	-1228	47
1260	10.86	-1258	52
1290	12.27	-1287	59
1320	13.7	-1316	66
1350	15.14	-1345	74
1380	16.59	-1374	82
1410	18.05	-1402	92
1440	19.52	-1431	102
1470	20.99	-1459	112
1500	22.46	-1486	124
1530	23.94	-1514	136
1560	25.42	-1541	149
1590	26.9	-1568	162
1620	28.39	-1594	177
1650	29.87	-1620	192
1680	31.36	-1646	207
1710	32.85	-1671	224
1740	34.34	-1696	240
1770	35.83	-1720	258
1800	37.32	-1744	276
1830	38.81	-1767	295
1860	40.3	-1790	314
1890	41.79	-1813	334
1894.22	42	-1816	337
1920	42	-1835	354
1950	42	-1857	375
1980	42	-1879	395
2010	42	-1902	415
2040	42	-1924	435
2070	42	-1946	455
2100	42	-1969	475
2130	42	-1991	495
2160	42	-2013	515
2190	42	-2036	535
2220	42	-2058	555
2250	42	-2080	575
2280	42	-2102	595
2310	42	-2125	615
2320	42	-2132	622
2340	42	-2147	636
2370	42	-2169	656
2400	42	-2192	676

MD[m]	INC [degree]	TVD [m]	dx [m]
2430	42	-2214	696
2460	42	-2236	716
2490	42	-2258	736
2520	42	-2281	756
2550	42	-2303	776
2580	42	-2325	796
2610	42	-2348	816
2640	42	-2370	836
2670	42	-2392	856
2700	42	-2415	876
2730	42	-2437	896
2760	42	-2459	917
2790	42	-2481	937
2820	42	-2504	957
2850	42	-2526	977
2880	42	-2548	997
2910	42	-2571	1017
2940	42	-2593	1037
2955	42	-2604	1047
2960.04	42.22	-2608	1050
2970	42.22	-2615	1057
3000	42.22	-2637	1077
3030	42.22	-2660	1097
3060	42.22	-2682	1118
3090	42.22	-2704	1138
3120	42.22	-2726	1158
3150	42.22	-2748	1178
3180	42.22	-2771	1198
3210	42.22	-2793	1218
3240	42.22	-2815	1239
3270	42.22	-2837	1259
3286.19	42.22	-2849	1270
3300	42.03	-2860	1279
3330	41.65	-2882	1299
3360	41.3	-2904	1319
3390	40.99	-2927	1338
3420	40.7	-2950	1358
3450	40.45	-2973	1377
3480	40.23	-2996	1397
3510	40.04	-3019	1416
3540	39.89	-3042	1435
3570	39.78	-3065	1454
3600	39.7	-3088	1474
3630	39.65	-3111	1493
3660	39.64	-3134	1512

MD[m]	INC [degree	TVD [m]	dx [m]
3660	39.64	-3134	1512
3690	39.67	-3157	1531
3720	39.73	-3180	1550
3750	39.83	-3203	1569
3780	39.96	-3226	1589
3800	40.07	-3241	1602
3810	40.13	-3249	1608
3840	40.33	-3272	1627
3870	40.56	-3295	1647
3900	40.83	-3317	1667
3917.07	41	-3330	1678
3930	40.5	-3340	1686
3960	39.32	-3363	1705
3990	38.15	-3387	1724
4020	36.98	-3411	1742
4050	35.81	-3435	1759
4080	34.65	-3460	1776
4110	33.48	-3485	1793
4140	32.31	-3510	1809
4170	31.14	-3536	1824
4200	29.98	-3562	1839
4230	28.81	-3588	1854
4260	27.65	-3615	1868
4290	26.49	-3642	1881
4320	25.33	-3669	1894
4350	24.17	-3696	1906
4380	23.02	-3724	1918
4410	21.86	-3752	1929
4440	20.71	-3780	1940
4470	19.56	-3808	1950
4500	18.42	-3836	1959
4530	17.28	-3865	1968
4560	16.15	-3894	1977
4590	15.02	-3923	1984
4620	13.9	-3952	1992
4644.38	13	-3976	1997
4650	13	-3981	1998
4680	13	-4010	2005
4710	13	-4040	2012
4740	13	-4069	2019
4770	13	-4098	2025
4800	13	-4127	2032
4830	13	-4157	2039
4860	13	-4186	2046
4890	13	-4215	2052
4905	13	-4230	2056

This project has received funding from the European Union's Horizon Europe research and innovation program under grant agreement No 101083558

Annex 2- Fluid flow rate optimization procedure

Python scripting was used for varying heat demand scenarios in order optimize the well flowrates. The optimization process was an iterative process where the power and temperature delivery were evaluated at the end of a flow cycle to determine if the well could deliver the required power/temperature and if so, to deliver exactly that value, without excess. So, for the 7-month yearly usage scenarios presented in Figure 18, the power and temperature delivered were evaluated at the end of the 7-month production period. If power was too low, flow rate was increased; if power was in excess, flow rate was decreased; and if temperature was too low, flow rate was decreased. If less power than the required power was predicted, but production temperature was the minimum value, then less power was delivered. So, the minimum required delivery temperature of 45°C was given priority. An initial guess at the required flowrate was made based on the flow from the previous production period. In addition, a very low value (0.01 kg/s) and a very high value (20 kg/s) were tested for the flow rate. The flow was interpolated linearly between solutions until the change in flow between iterations was less than 1e-7 kg/s. In practice, flow steps typically converged in less than 10 iterations with this procedure. The only outlier to that occurs near the laminar/turbulent flow transition, where there is a discrete change in the solution space. A pseudo-code for the iteration/optimization procedure is as follows:

```
  WHILE change_in_flow > 1e-7


new_flow_estimate FROM linear interpolation to deliver required_power

temp_estimate FROM linear interpolation from new_flow_estimate

power_estimate = required_power


IF temp_estimate < required_temp

   new_flow_estimate = linear interpolation from required_temp

   power_estimate = linear interpolation from new_flow_estimate

   temp_estimate = required_temp


RUN simulation with new_flow_estimate to determine:

                out_temp, out_power, old_flow


change_in_flow = abs(new_flow_estimate – old_flow)
```

This project has received funding from the European Union's Horizon Europe research and innovation program under grant agreement No 101083558

A graphical representation of the linear interpolation iteration scheme can be seen in

Figure 109.

First a high and low value of flow rate (W_{high}, W_{low}) and an initial guess ($W_0 \approx 2$ kg/s) were made, then values were interpolated based on the solutions and the required power. After 5 iterations, the solution converged.

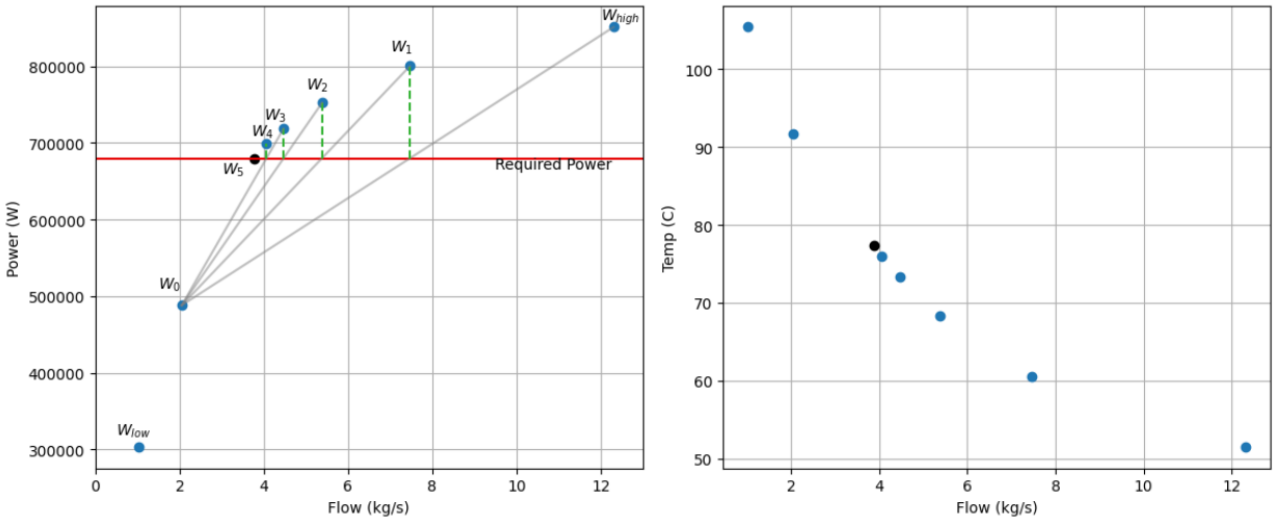

Figure 109: Example linear interpolation iteration technique to find minimum flowrate for required power.

This project has received funding from the European Union's Horizon Europe research and innovation program under grant agreement No 101083558

Annex 3- Detailed results of the simulations for the Polish case

Case 1.1. Salt dome, horizontal part 2000 [m].

The output temperatures of the HOCLOOP borehole heat exchanger during 20 years of heat production, calculated for the above assumptions, are shown in Figure 110.

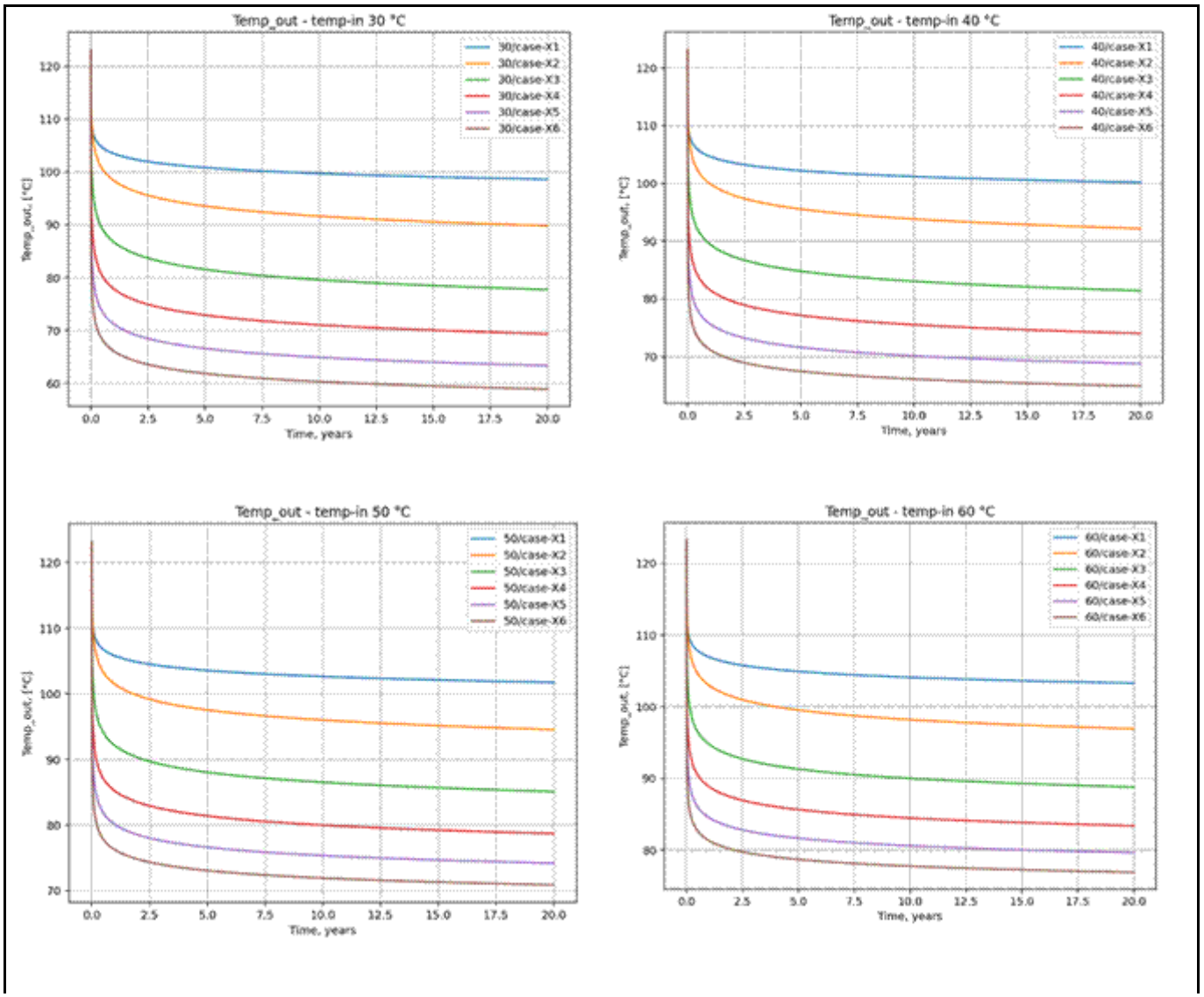

This project has received funding from the European Union's Horizon Europe research and innovation program under grant agreement No 101083558

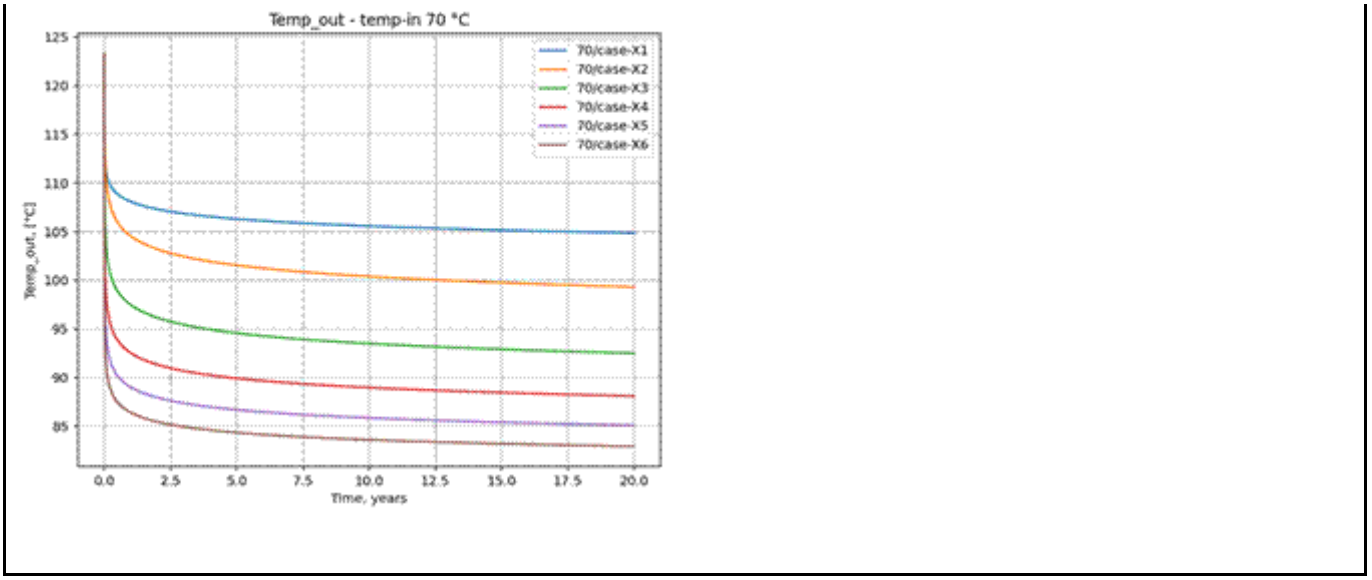

Figure 110: The output temperatures for salt dome, horizontal part 2000 [m] case depending on the inlet temperature and flow rate

The temperature distribution in the HOCLOOP borehole heat exchanger for T_{in} = 30 [°C] for analyzed flow rates is shown in Figure 111.

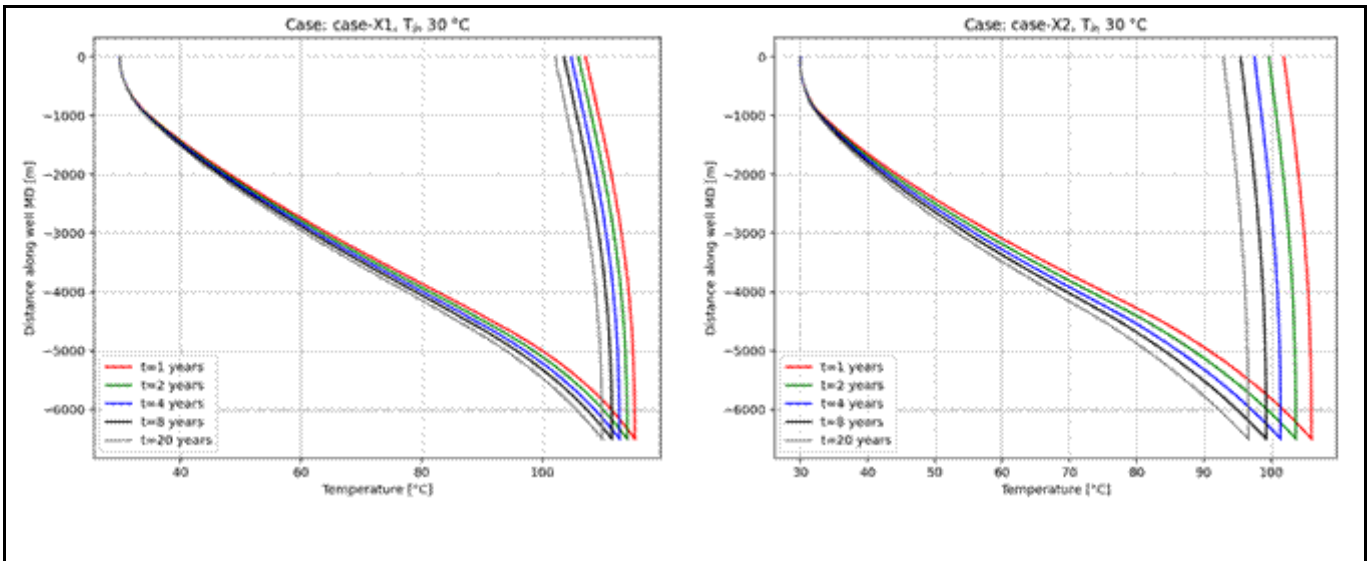

This project has received funding from the European Union's Horizon Europe research and innovation program under grant agreement No 101083558

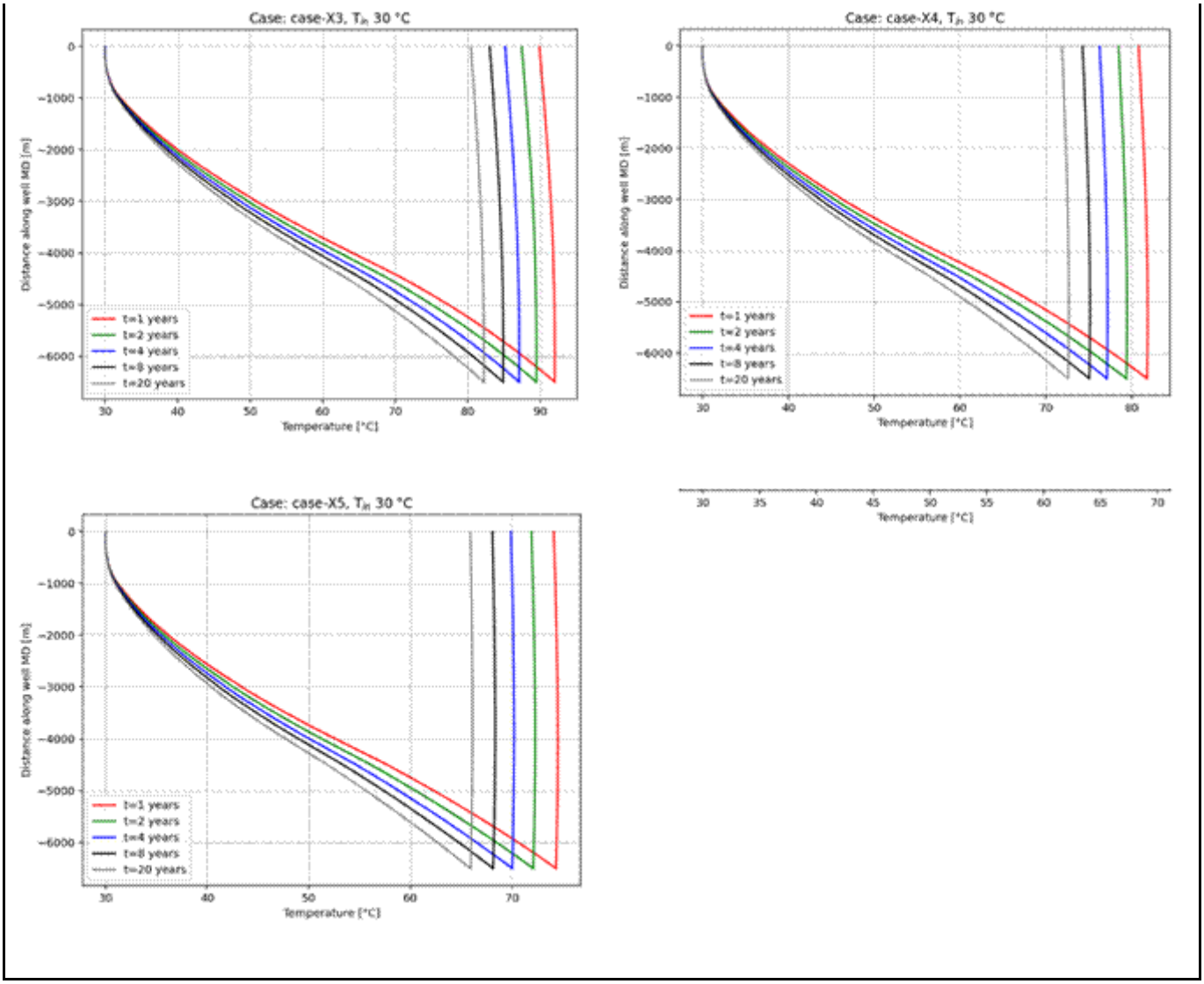

Figure 111: The temperature distribution in the HOCLOOP borehole heat exchanger for salt dome, horizontal part 2000 [m] case - T_{in} = 30 [°C]

The temperature distribution in the HOCLOOP borehole heat exchanger for T_{in} = 60 [°C] for analyzed flow rates is shown in Figure 112.

This project has received funding from the European Union's Horizon Europe research and innovation program under grant agreement No 101083558

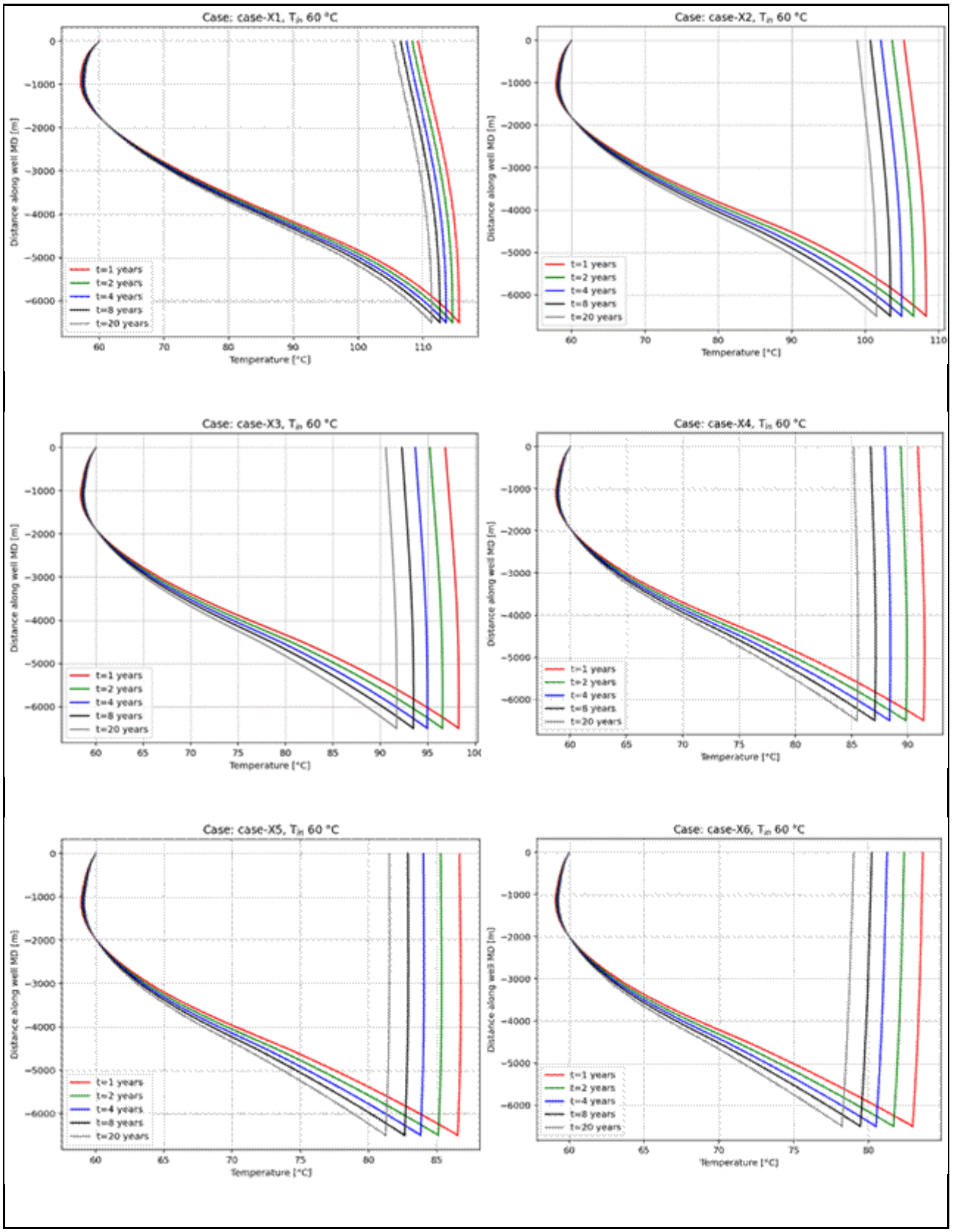

Figure 112: The temperature distribution in the HOCLOOP borehole heat exchanger for salt dome, horizontal part 2000 [m] case - T_{in} = 60 [°C]

This project has received funding from the European Union's Horizon Europe research and innovation program under grant agreement No 101083558

Case 1.2. Salt dome, horizontal part 2500 [m].

The output temperatures of the HOCLOOP borehole heat exchanger during 20 years of heat production, calculated for the above assumptions, are shown in Figure 113.

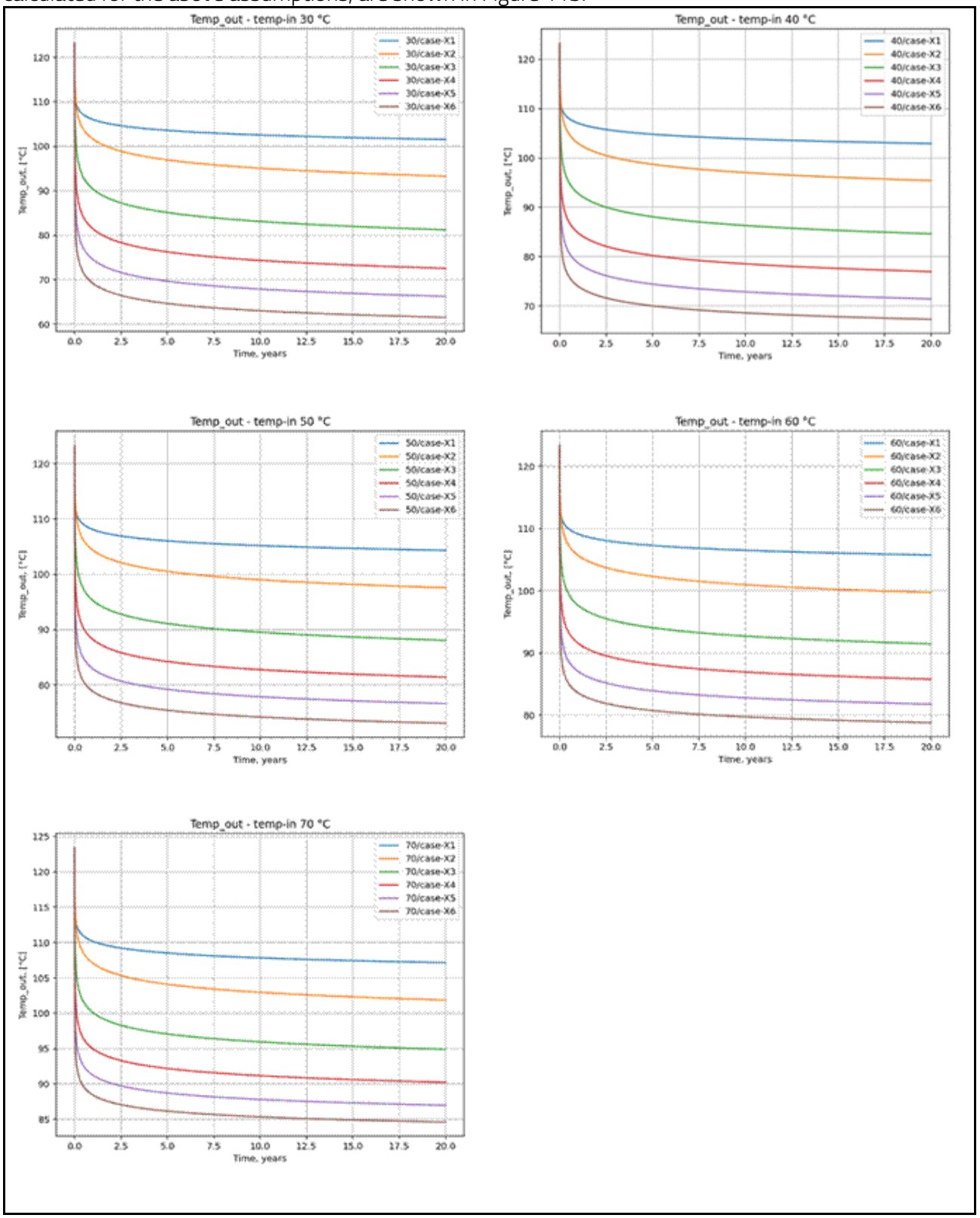

Figure 113: The output temperatures for salt dome, horizontal part 2500 [m] case depending on the inlet temperature and flow rate

This project has received funding from the European Union's Horizon Europe research and innovation program under grant agreement No 101083558

The temperature distribution in the HOCLOOP borehole heat exchanger for T_{in} = 30 [°C] for analyzed flow rates is shown in Figure 114.

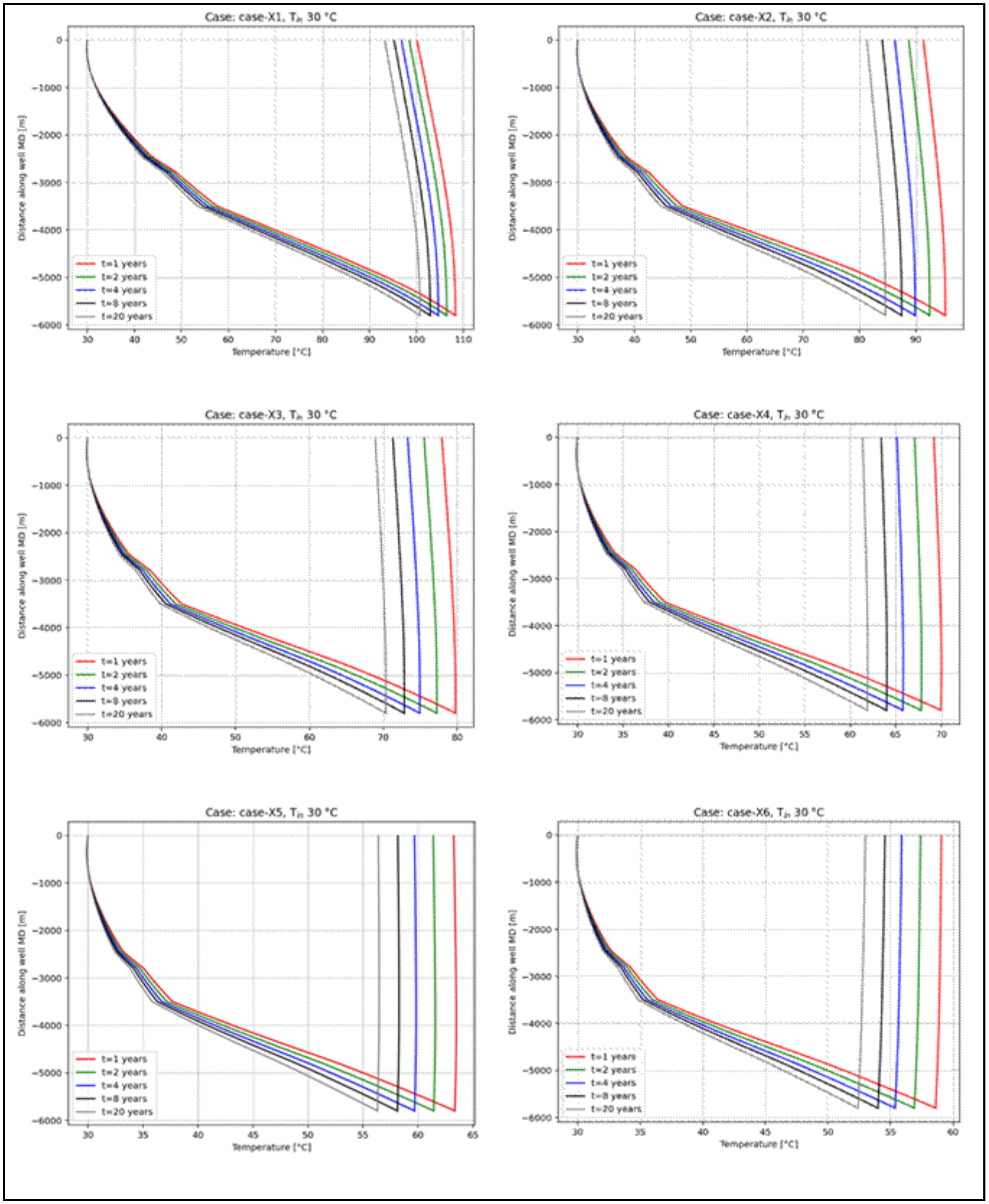

This project has received funding from the European Union's Horizon Europe research and innovation program under grant agreement No 101083558

Figure 114: The temperature distribution in the HOCLOOP borehole heat exchanger for salt pillow, horizontal part 1000 [m] case - T_{in} = 30 [°C]

The temperature distribution in the HOCLOOP borehole heat exchanger for T_{in} = 60 [°C] for analyzed flow rates is shown in Figure 115.

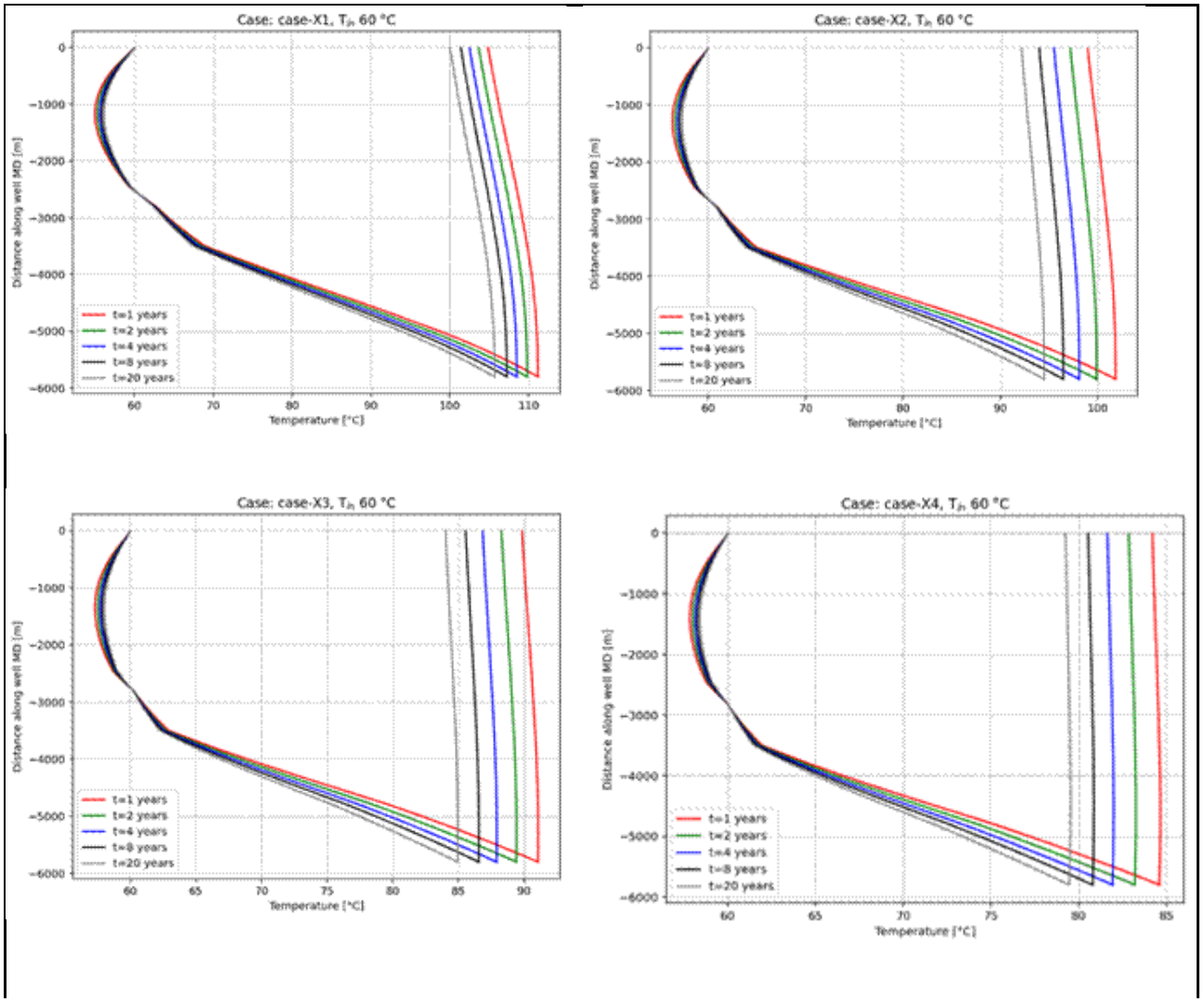

This project has received funding from the European Union's Horizon Europe research and innovation program under grant agreement No 101083558

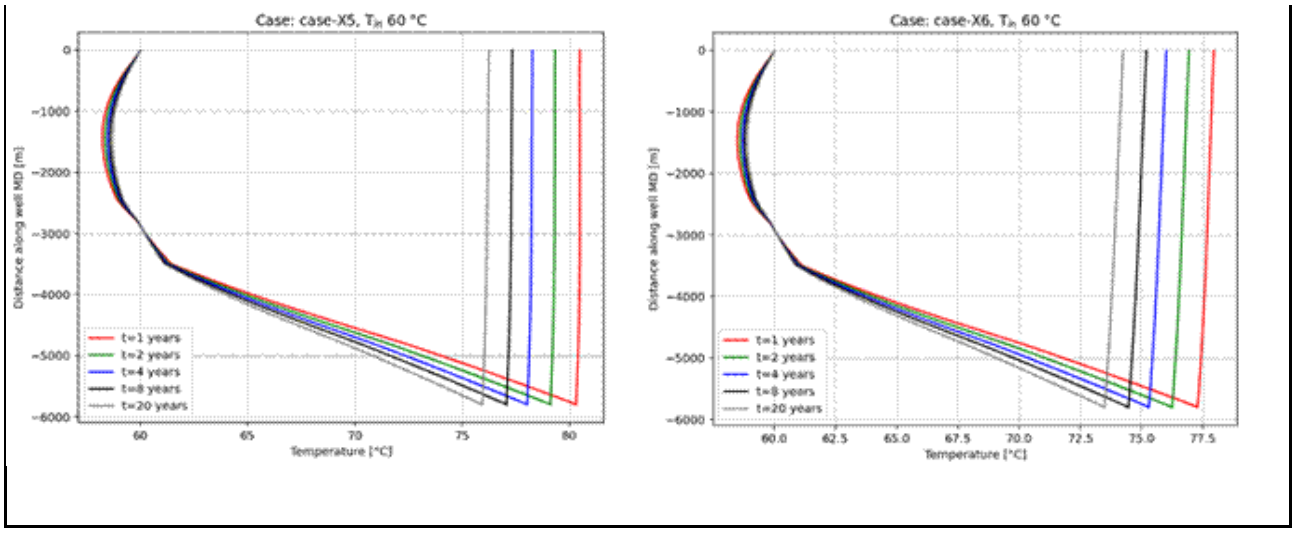

Figure 115: The temperature distribution in the HOCLOOP borehole heat exchanger for salt pillow, horizontal part 1000 [m] case - T_{in} = 60 [°C]

Case 2.2. Salt pillow, horizontal part 2000 [m].

The output temperatures of the HOCLOOP borehole heat exchanger during 20 years of heat production, calculated for the above assumptions, are shown in Figure 116.

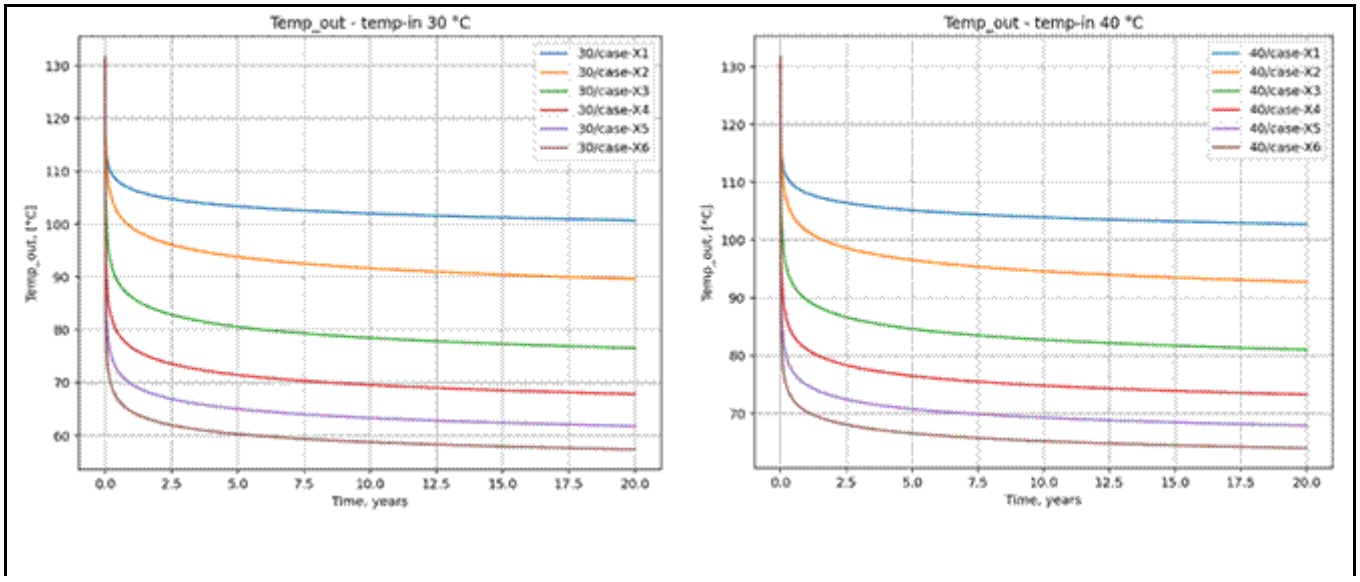

This project has received funding from the European Union's Horizon Europe research and innovation program under grant agreement No 101083558

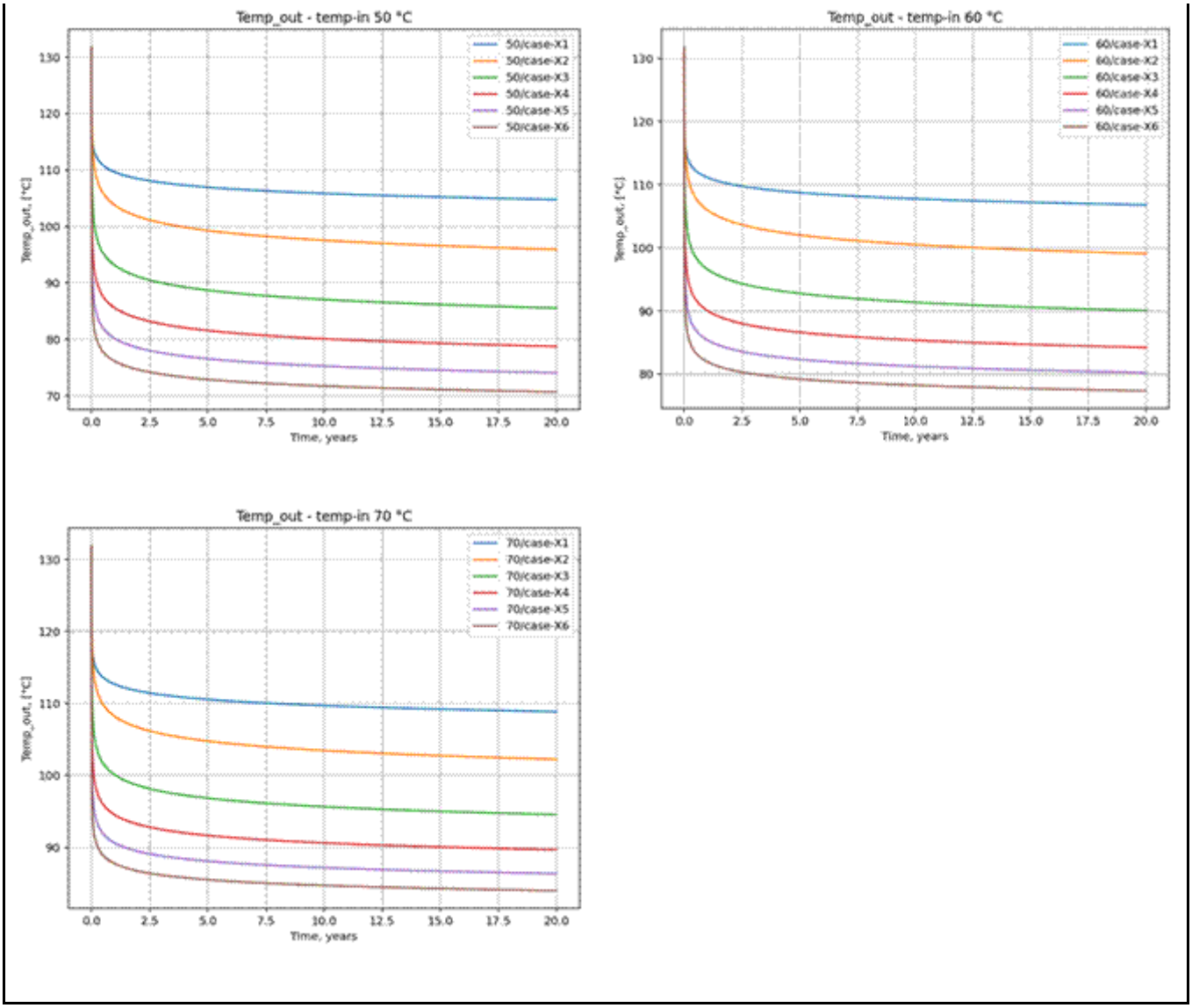

Figure 116: The output temperatures for salt pillow, horizontal part 2000 [m] case depending on the inlet temperature and flow rate

The temperature distribution in the HOCLOOP borehole heat exchanger for T_{in} = 30 [°C] for analyzed flow rates is shown in Figure 117.

This project has received funding from the European Union's Horizon Europe research and innovation program under grant agreement No 101083558

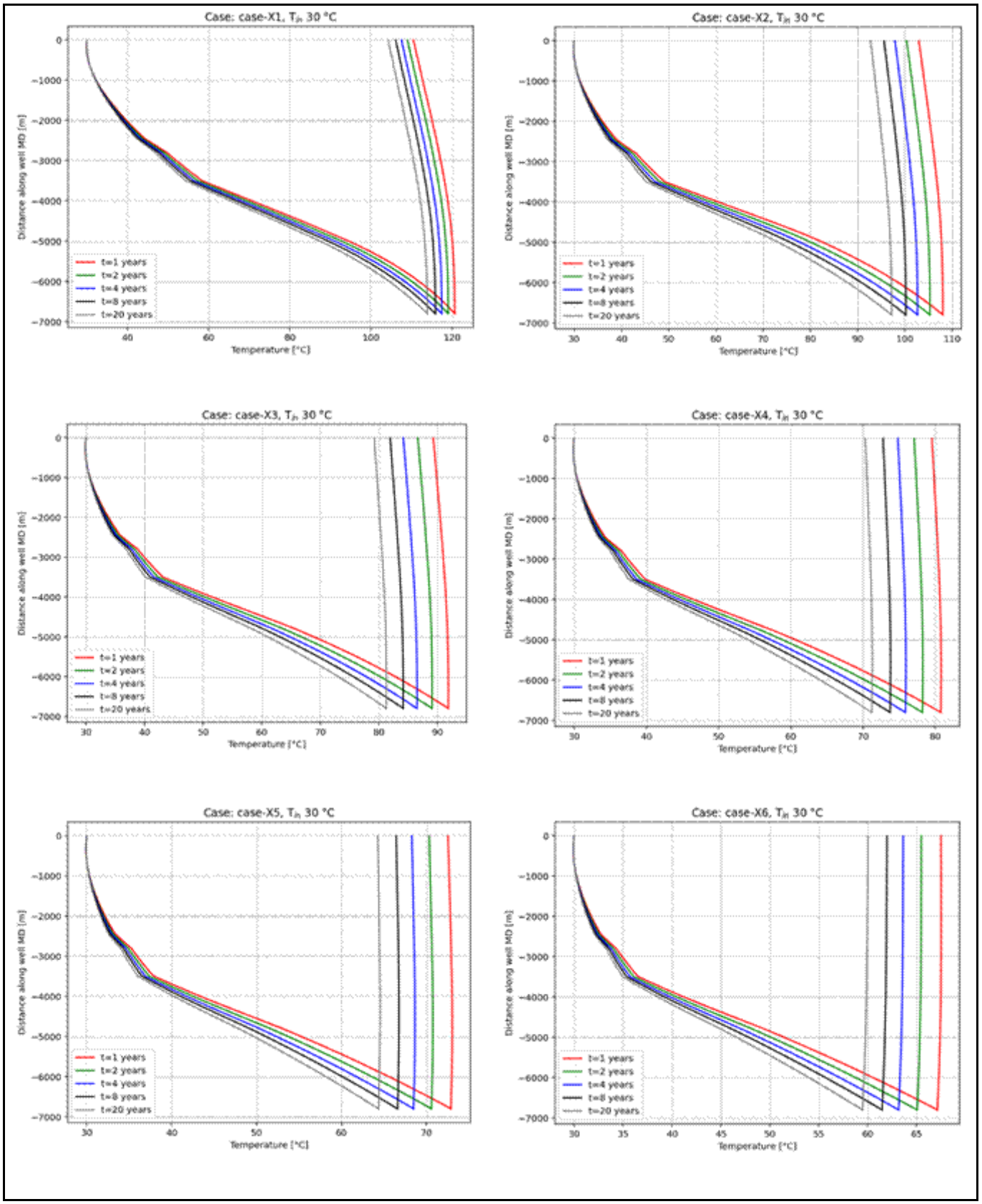

Figure 117: The temperature distribution in the HOCLOOP borehole heat exchanger for salt pillow, horizontal part 2000 [m] case - T_{in} = 30 [°C]

The temperature distribution in the HOCLOOP borehole heat exchanger for T_{in} = 60 [°C] for analyzed flow

This project has received funding from the European Union's Horizon Europe research and innovation program under grant agreement No 101083558

rates is shown in Figure 118.

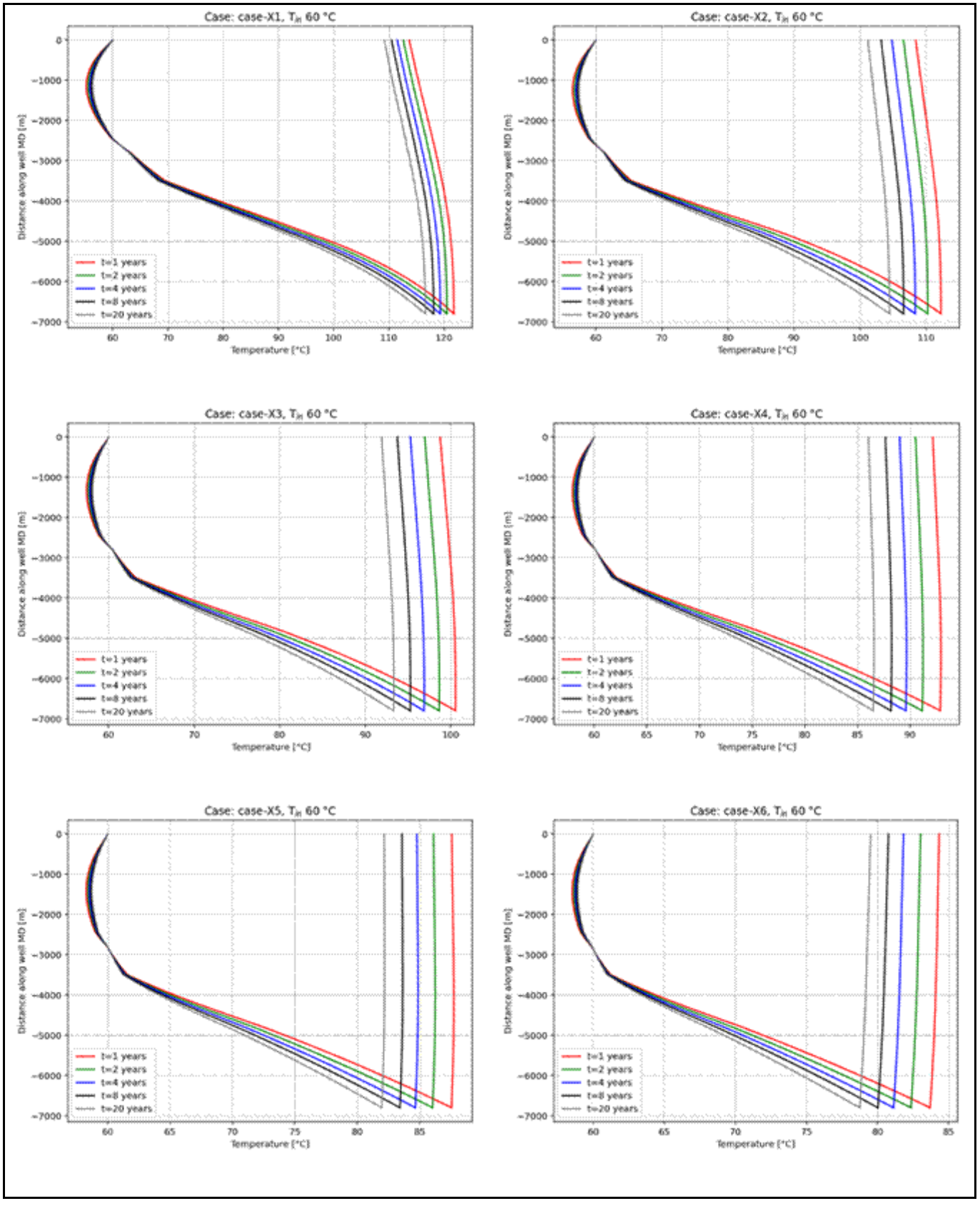

This project has received funding from the European Union's Horizon Europe research and innovation program under grant agreement No 101083558

Figure 118: The temperature distribution in the HOCLOOP borehole heat exchanger for salt pillow, horizontal part 2000 [m] case - T_{in} = 60 [°C]

Scenerios Results – variable injection temperaturure

The temperature distribution in the HOCLOOP borehole heat exchanger for variable input temperature (installation without Heat Pump) for analyzed flow rates is shown in Figure 119.

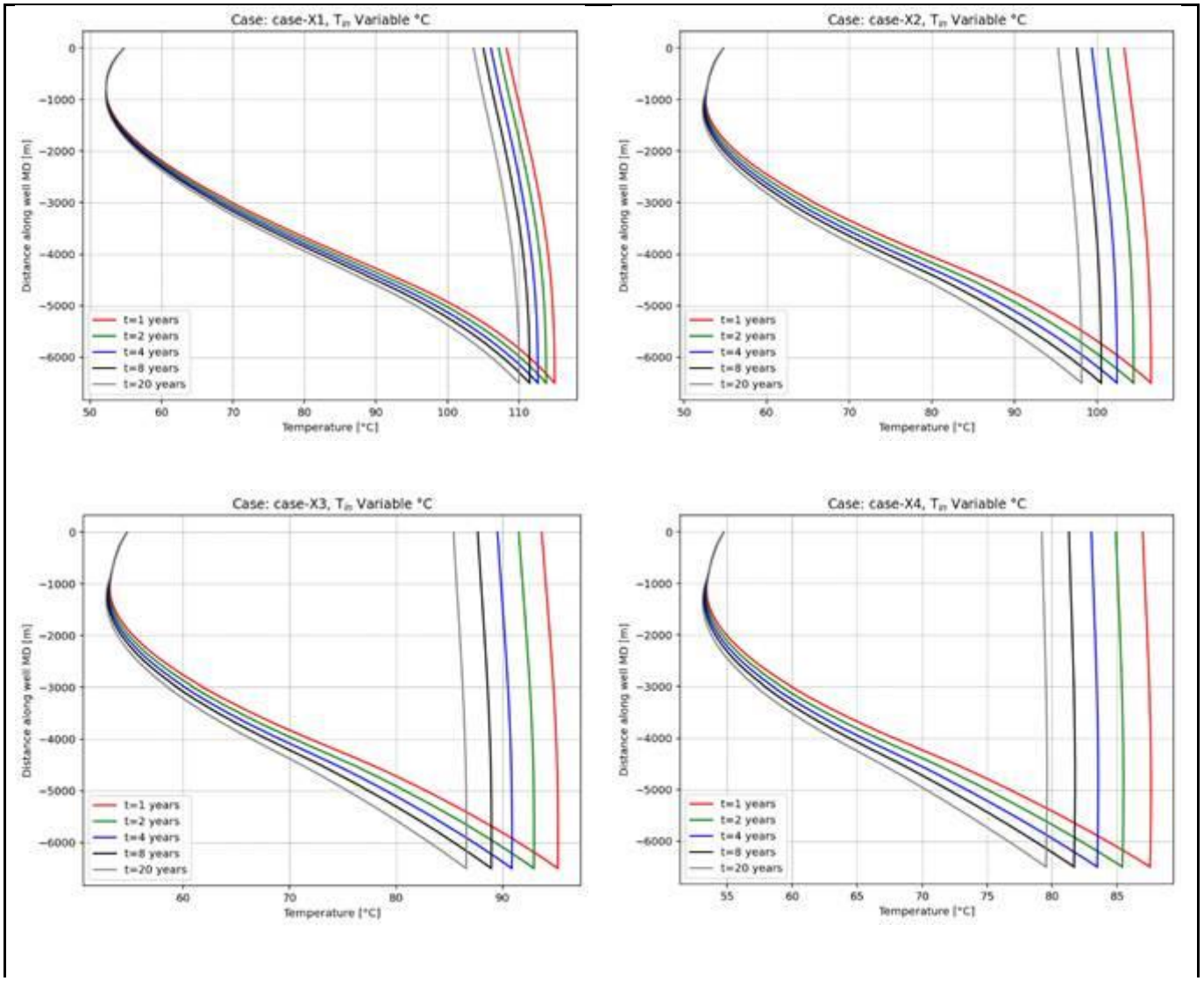

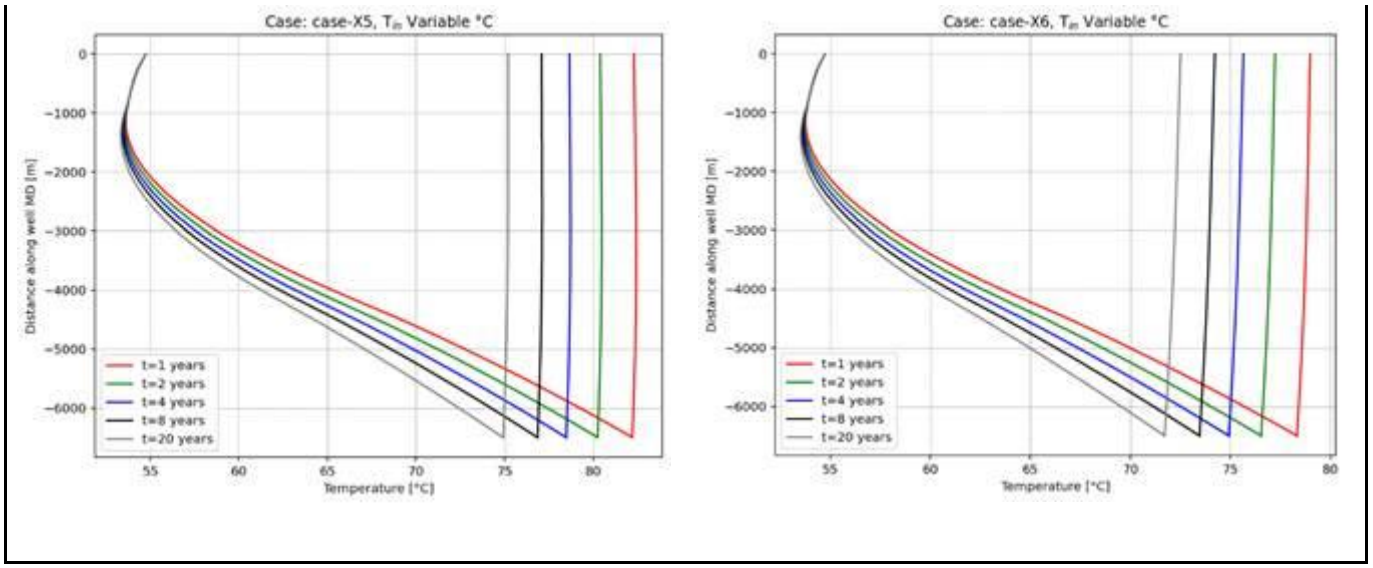

Figure 119: The temperature distribution in the HOCLOOP borehole heat exchanger for salt dome, horizontal part 2000 [m] case – variable T_{in} without Heat Pump

The temperature distribution in the HOCLOOP borehole heat exchanger for variable input temperature (installation with Heat Pump) for analyzed flow rates is shown in Figure 120.

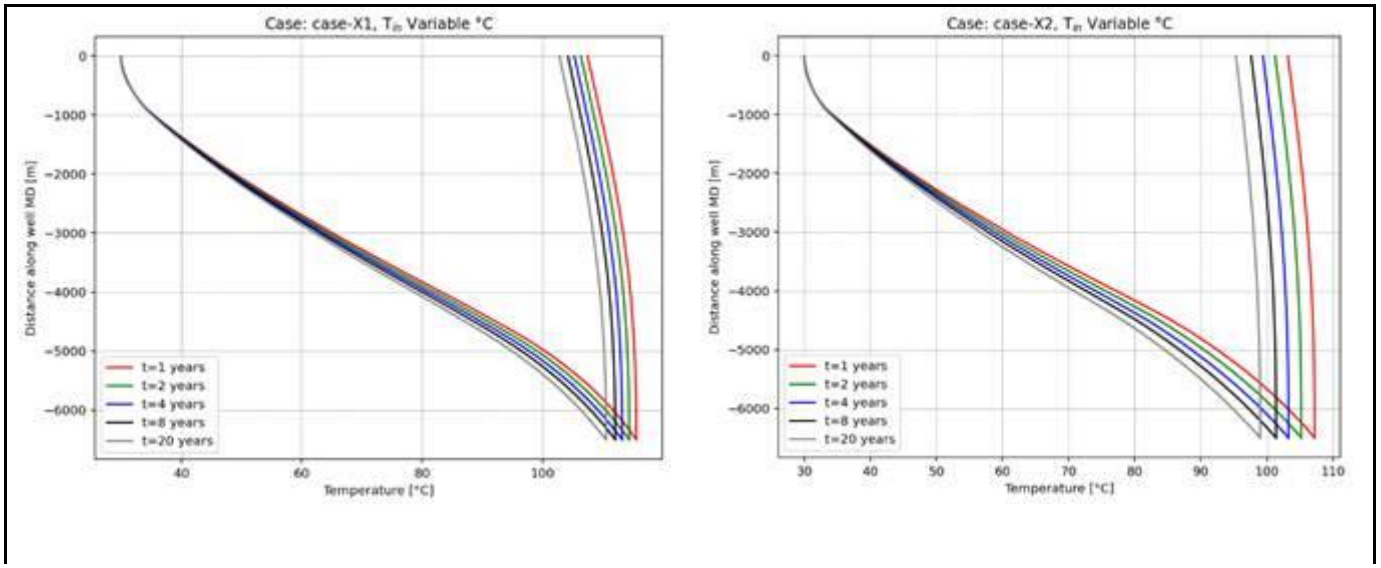

This project has received funding from the European Union's Horizon Europe research and innovation program under grant agreement No 101083558

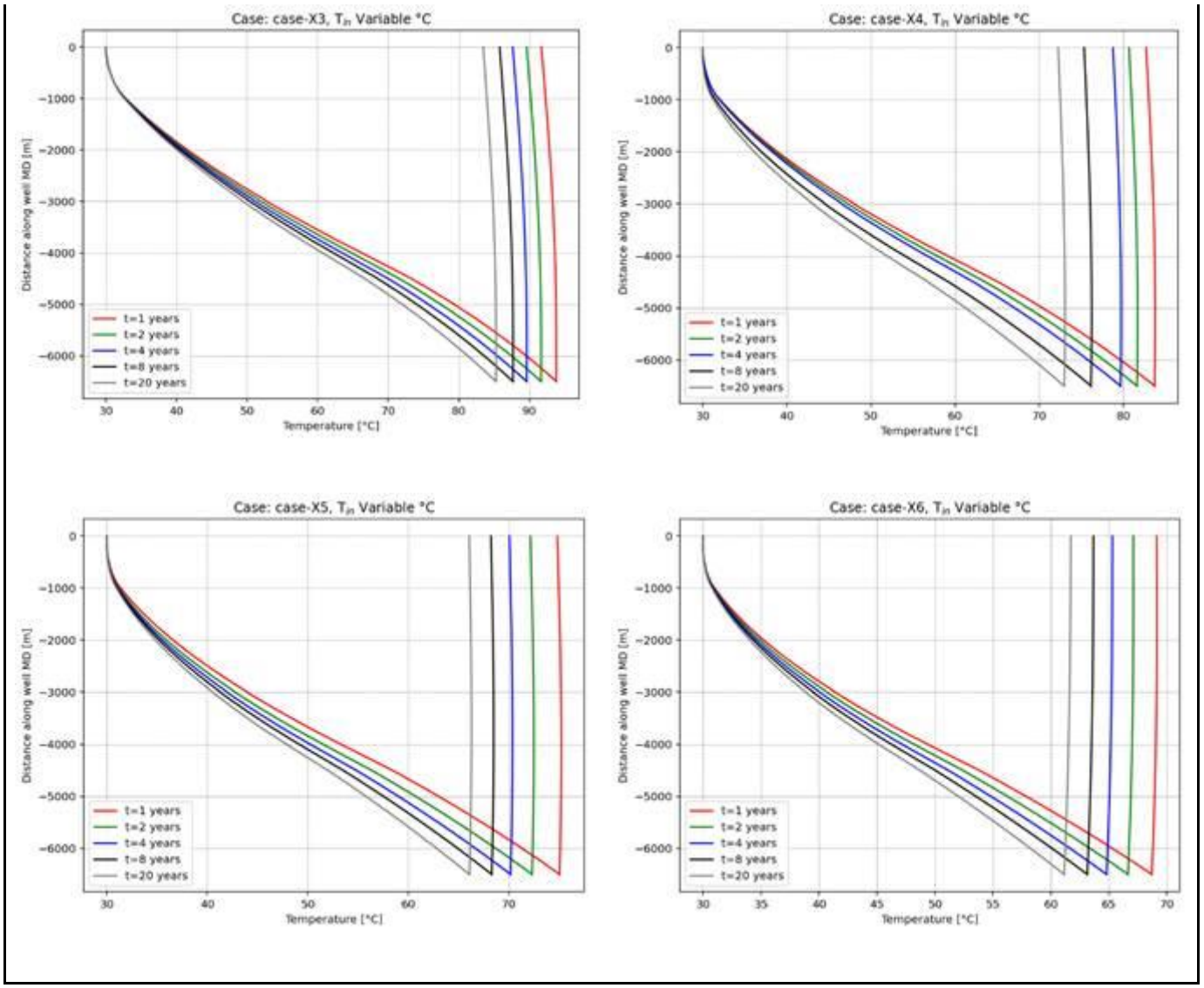

Figure 120: The temperature distribution in the HOCLOOP borehole heat exchanger for salt dome, horizontal part 2000 [m] case – variable Tin with Heat Pump

The temperature distribution in the HOCLOOP borehole heat exchanger for variable input temperature (installation without Heat Pump) for analyzed flow rates is shown in Figure 121.

This project has received funding from the European Union's Horizon Europe research and innovation program under grant agreement No 101083558

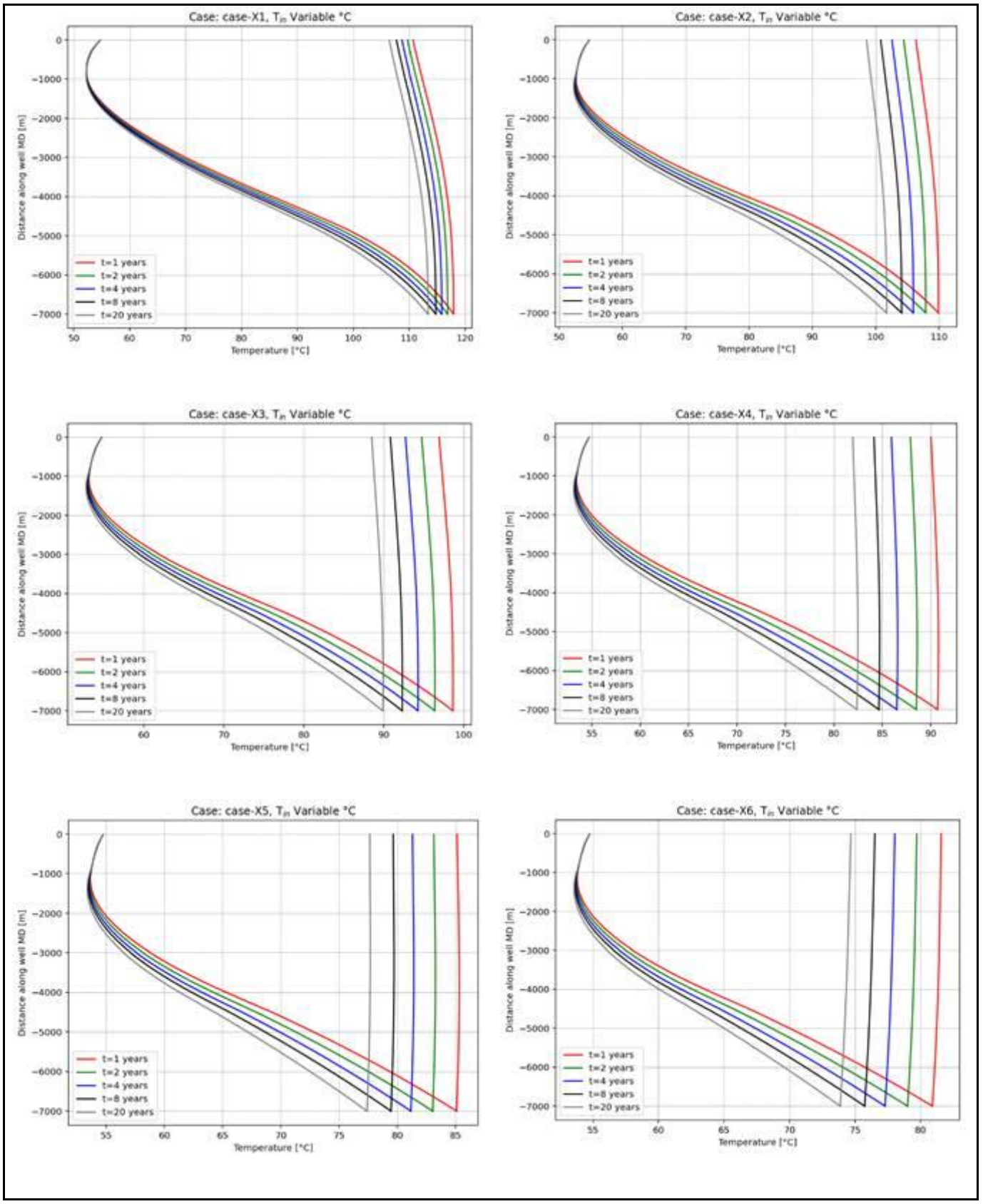

Figure 121: The temperature distribution in the HOCLOOP borehole heat exchanger for salt dome, horizontal part 2500 [m] case – variable T_{in} without Heat Pump

The temperature distribution in the HOCLOOP borehole heat exchanger for variable input temperature

This project has received funding from the European Union's Horizon Europe research and innovation program under grant agreement No 101083558

(installation with Heat Pump) for analyzed flow rates is shown in Figure 122.

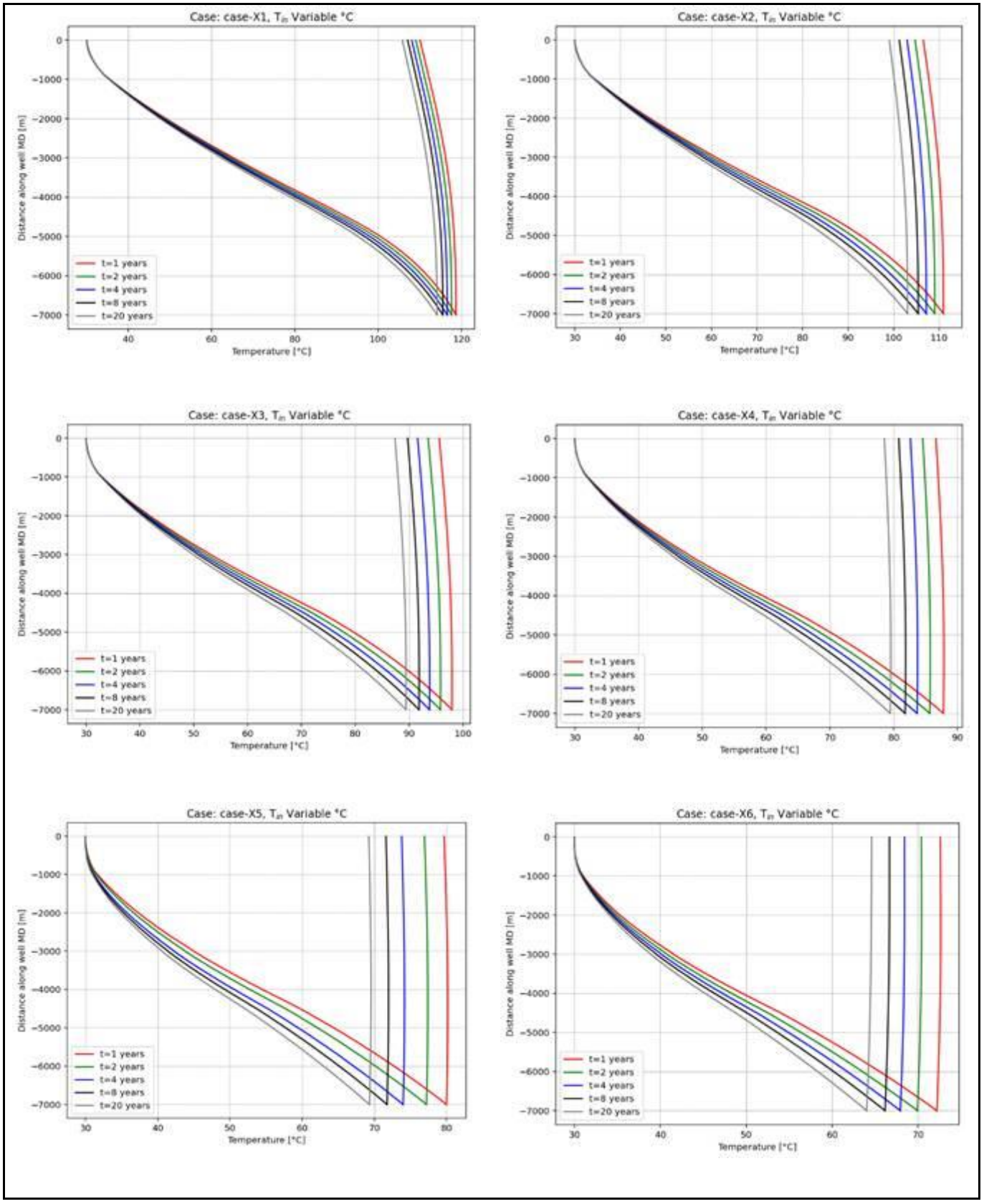

This project has received funding from the European Union's Horizon Europe research and innovation program under grant agreement No 101083558

Figure 122: The temperature distribution in the HOCLOOP borehole heat exchanger for salt dome, horizontal part 2500 [m] case – variable T_{in} with Heat Pump

The temperature distribution in the HOCLOOP borehole heat exchanger for variable input temperature (installation without Heat Pump) for analyzed flow rates is shown in Figure 123.

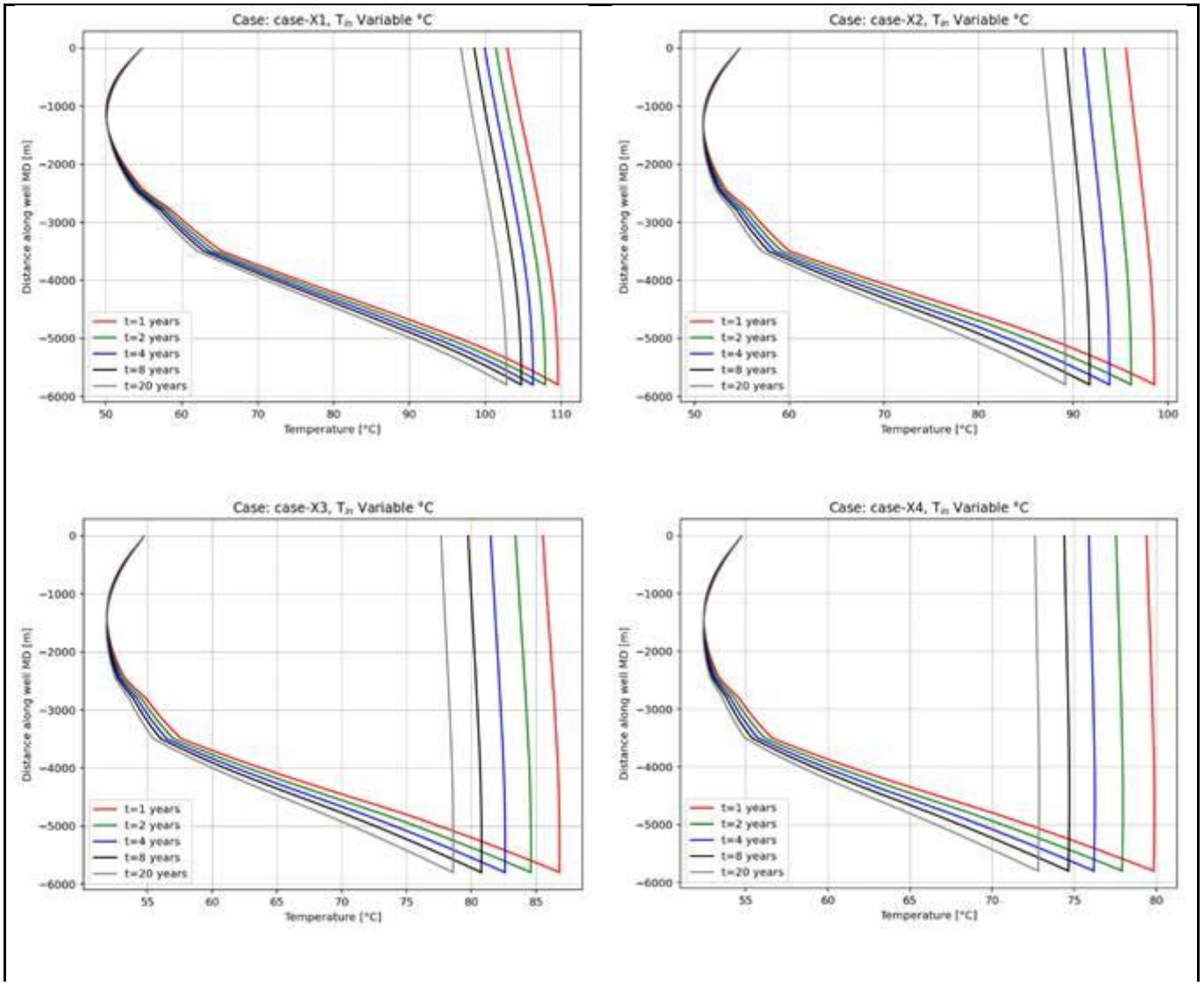

This project has received funding from the European Union's Horizon Europe research and innovation program under grant agreement No 101083558

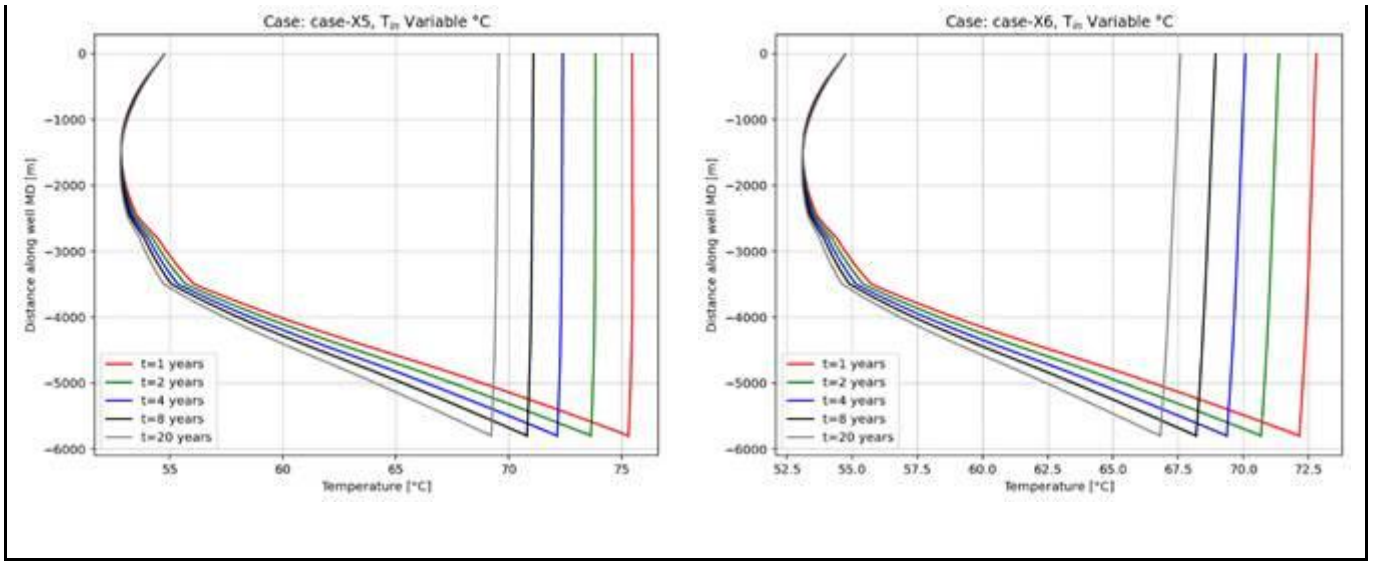

Figure 123: The temperature distribution in the HOCLOOP borehole heat exchanger for salt pillow, horizontal part 1000 [m] case – variable T_{in} without Heat Pump

The temperature distribution in the HOCLOOP borehole heat exchanger for variable input temperature (installation with Heat Pump) for analyzed flow rates is shown in Figure 124.

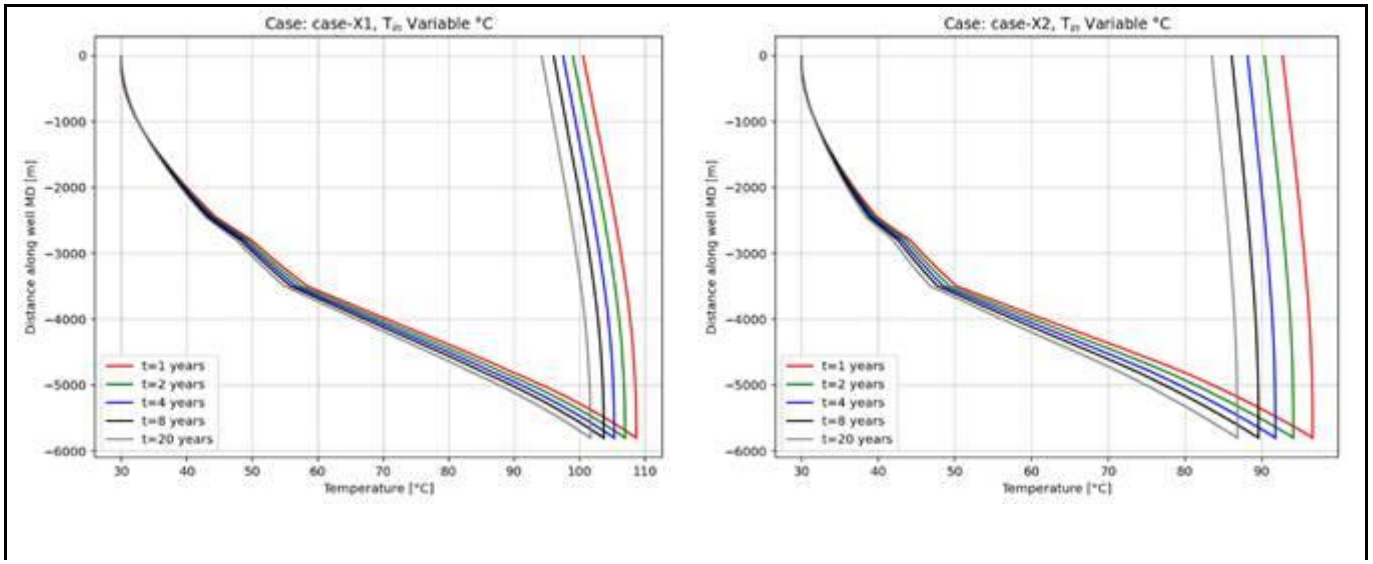

This project has received funding from the European Union's Horizon Europe research and innovation program under grant agreement No 101083558

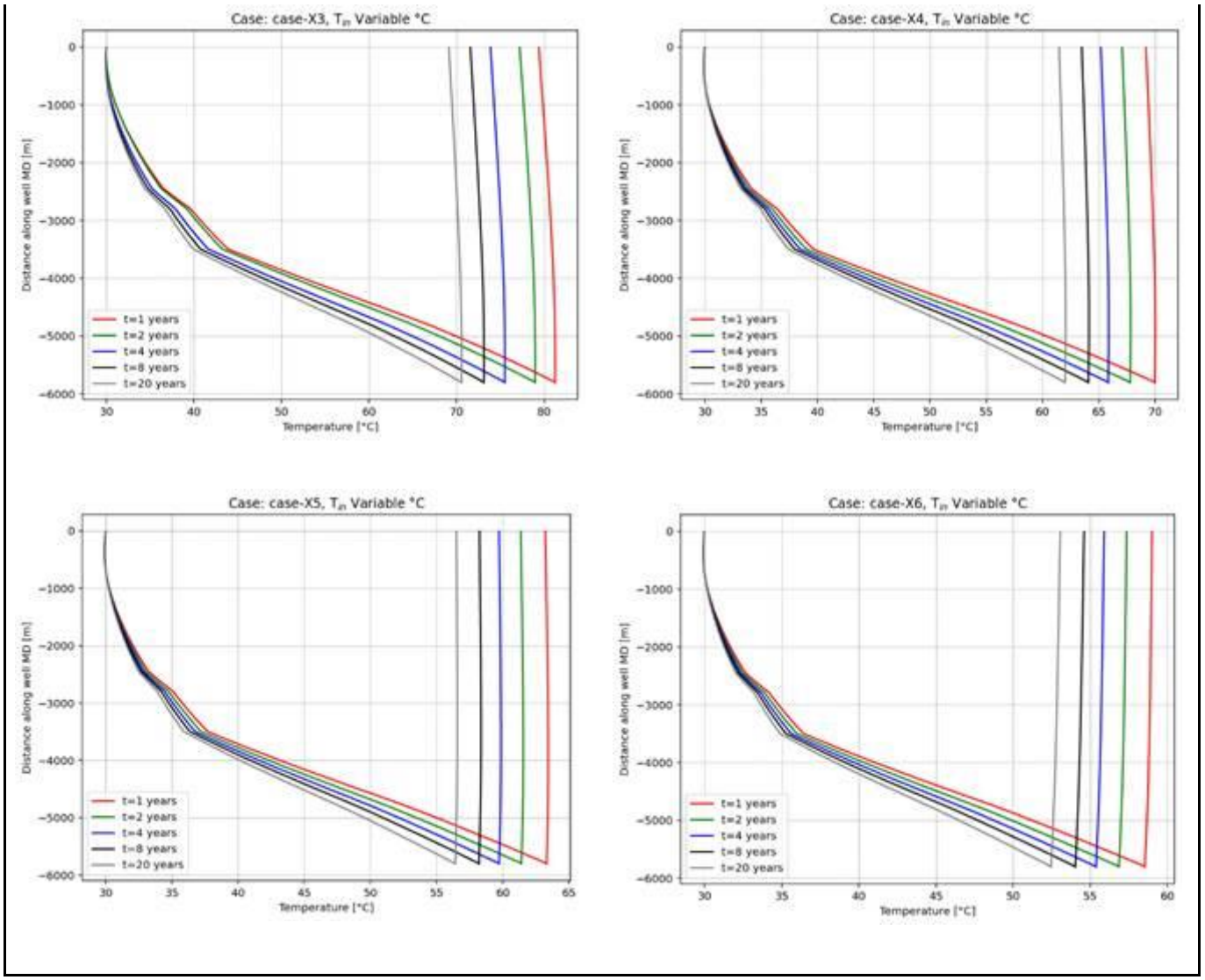

Figure 124: The temperature distribution in the HOCLOOP borehole heat exchanger for salt pillow, horizontal part 1000 [m] case – variable T_{in} with Heat Pump

The temperature distribution in the HOCLOOP borehole heat exchanger for variable input temperature (installation without Heat Pump) for analyzed flow rates is shown in Figure 125.

This project has received funding from the European Union's Horizon Europe research and innovation program under grant agreement No 101083558

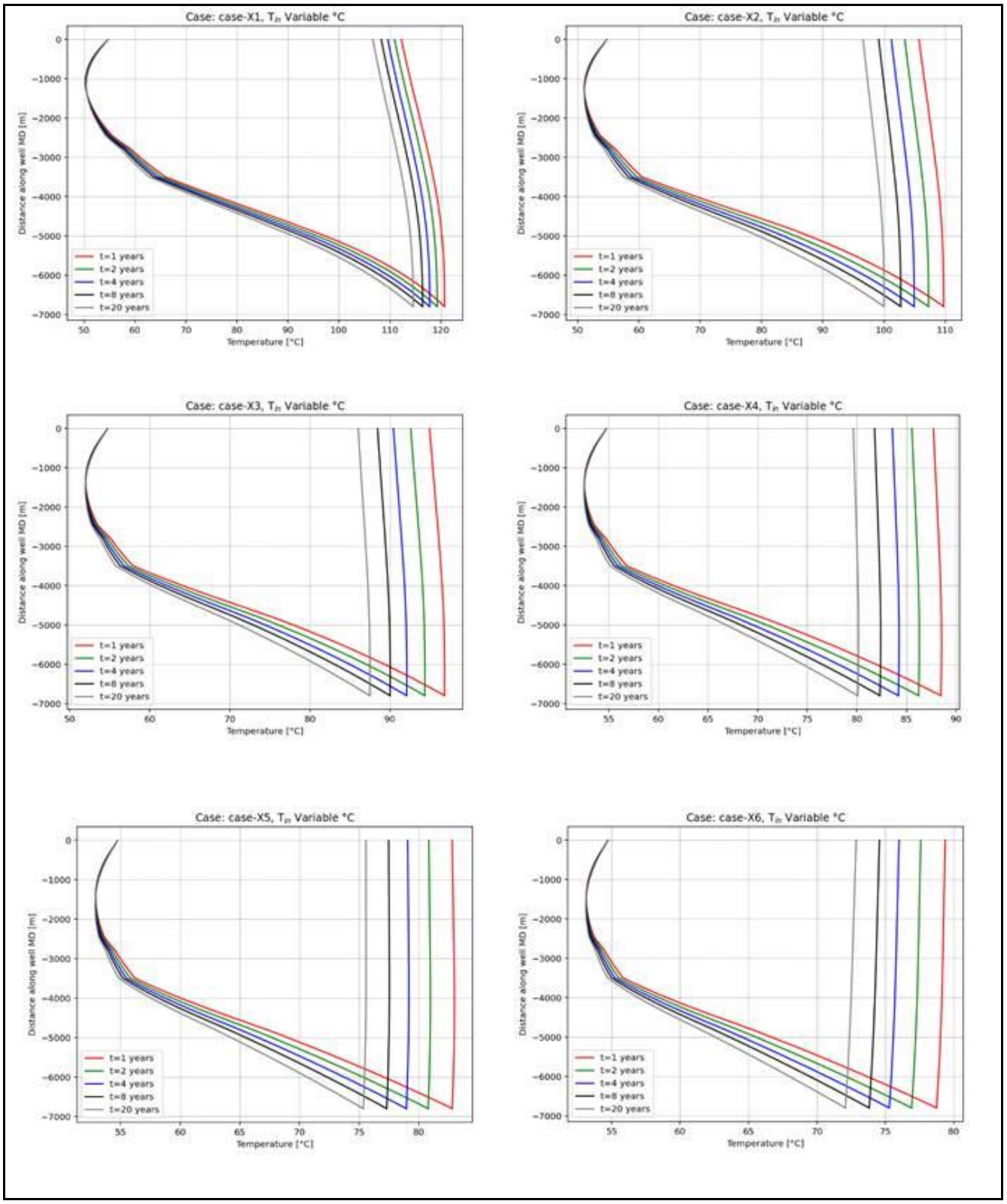

Figure 125: The temperature distribution in the HOCLOOP borehole heat exchanger for salt pillow, horizontal part 2000 [m] case – variable T_{in} without Heat Pump

The temperature distribution in the HOCLOOP borehole heat exchanger for variable input temperature (installation with Heat Pump) for analyzed flow rates is shown in Figure 126.

This project has received funding from the European Union's Horizon Europe research and innovation program under grant agreement No 101083558

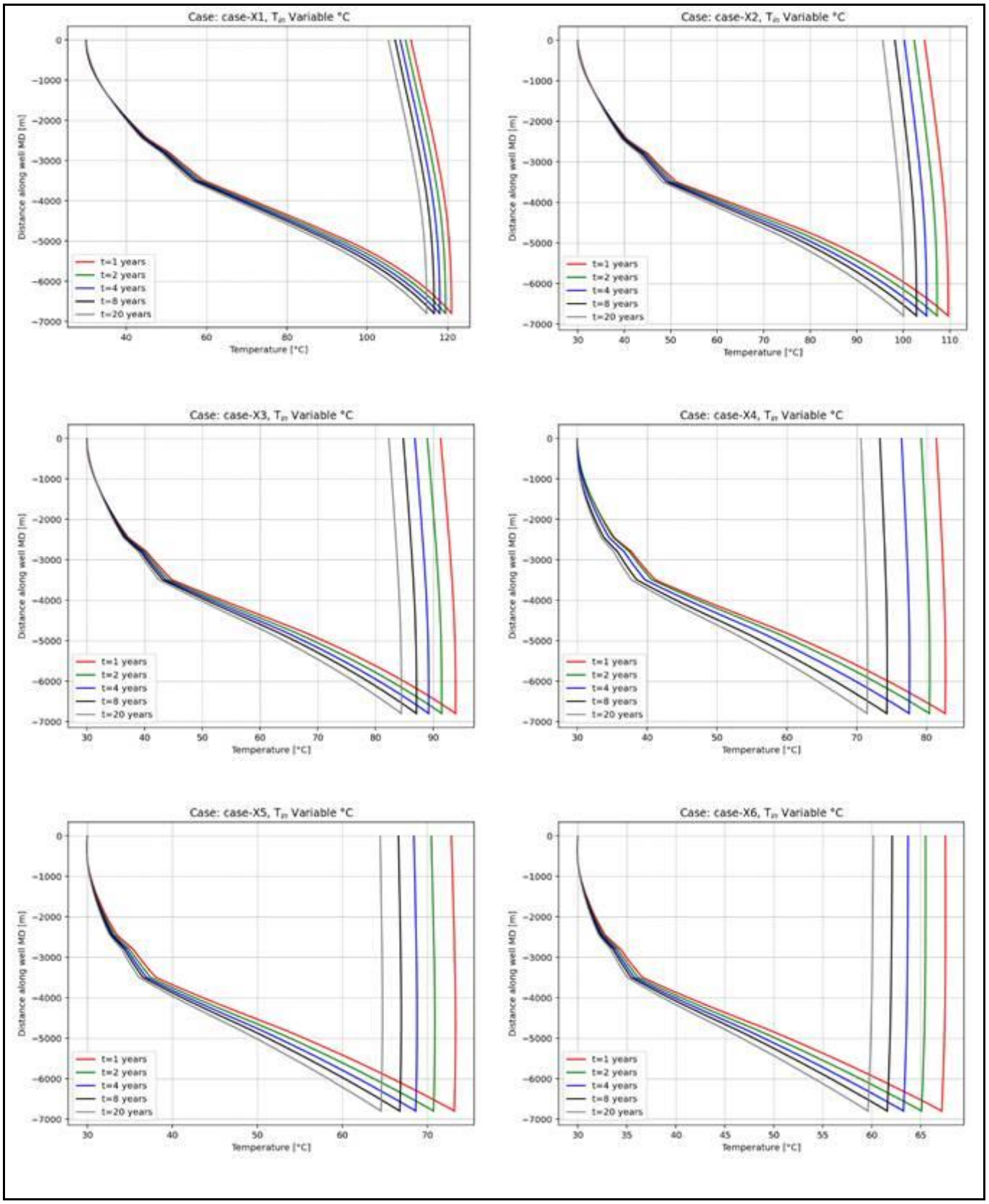

Figure 126: The temperature distribution in the HOCLOOP borehole heat exchanger for salt pillow, horizontal part 2000 [m] case – variable T_{in} with Heat Pump

This project has received funding from the European Union's Horizon Europe research and innovation program under grant agreement No 101083558